Capturing T-cell Receptors - A potential new modality for targeting hepatic tumours and Post-Transplantation Lymphoproliferative Disease (PTLD)

Nicola Dawn Ruth

A thesis submitted to the University of Birmingham for the degree of DOCTOR OF PHILOSOPHY

School of Immunity and Infection College of Medical and Dental Sciences University of Birmingham 2018

Abstract

The primary aim of this project has been to identify paediatric tumour-specific MHC class I phosphopeptide antigens on lymphoblastoid cell lines LCLs (an *in vitro* model for PTLD) as well as paediatric hepatic tumour clinical samples. Tumour specific T-cells are notoriously difficult to maintain in long-term culture and as a result it is difficult to establish an 'off the shelf' T-cell product, however the secondary aim of this project was to explore potential modalities for capturing the T-cell receptor (TCR), important in recognising tumour specific antigens and the resultant product could be used to establish a non-patient-specific, but tumour specific product. In order to achieve this we have used T-cell hybridomas as one modality and also Human Induced Pluripotent Stem Cell (hIPSc) technology to immortalise tumour specific T-cells. Following on from this we have developed a technology for expanding these and differentiating them into a T-cell of interest with potential for future clinical application in paediatric tumours, using OP9 DL1 mouse feeder cell system to support differentiation of hIPSc towards haemopoietic lineage, demonstrating functionality of the end stage 'T-cell product'.

In summary we have identified a number of novel phosphopeptide antigens *in vitro* as well as on patient tissues. This information has been used to identify potential T-cell targets and by formation of hIPSc we have established a method for expanding specific T-cell's *in vitro*. Using OP9DL1 cells we have also identified a method for differentiating these cells into lymphocyte-like cells with T-cell functionality therefore representing a possible methodology for expanding tumour-specific T-cells for clinical application.

Dedication

I dedicate this thesis to my brother Brian, who died suddenly in 2005 just as he was writing up his PhD thesis. Together we can be proud.

Acknowledgements

I have a long list of people that I owe gratitude to for helping me in various ways to complete this thesis. Firstly, Graham Anderson, Mark Cobbold and Paloma Garcia for giving me the opportunity to complete this research. Graham Anderson was an invaluable mentor when Mark Cobbold left the UK for pastures new, providing me with the expertise and enthusiasm to not give up but just keep going. To Mark Cobbold for making me an independent thinker and also for hosting me at Harvard University to enable me to once again experience life on the 'other side of the pond'.

In the Cobbold laboratory I would like to particularly thank David Millar, Oli Goodyear, Sarah Penny who were post docs in the lab and offered advice, support and most importantly friendship. I could not have got this far and would not have got this far without you. Particularly David Millar, who has supported me from day 1, shepherded me in Boston, and was never too busy to Skype or chat about the project (even though I know he was).

Extra special thanks goes to Lora Steadman, technician in the lab, and sole surviving member of the disbanded 'Cobbold group' for keeping me sane, plying me with sausage and mushroom sandwiches and sharing the trials and frustrations of lab life. Thanks to other members of the lab and 'ELG 38' including Nico Büttner (my fellow hepatologist), Punam Mistry (who taught me how to make T-cell lines), Laura Morton (who was brave enough to teach me to make PBMC's) who helped by reading my thesis with enthusiasm. To Emma Ehrlich, technician at Harvard for the giggles, knitting tips and general girl chitchat – definitely helped break up the monotony of T-ALL104! Thanks to Margaret Goodall for teaching me the 'art' of hybridoma generation. Finally, to Jennifer Heaney and John Campbell for the banter in the office and wise words when I needed them most.

Secondly, my second laboratory in the University of Birmingham, the Anderson Lab, where I

feel equally at home thanks to all the lovely people that I worked with there, who accepted this lab refugee with open arms and always made me feel welcome– Kieran James – who helped me analyse the ‘5 events’ and Andrea White particularly have supported me during my quest to master the Flow Cytometer, and the rest of the lab group including Song Baik, Emilie Cosway, Beth Lucas, Nick McCarthy, Sonia Parnell and Will Jenkinson. Thanks also to Ms Vikki Harrison for being my go to ear to bend when things were tough.

I want to thank Professor Kelly at Birmingham Children’s Hospital, for being my mentor and first taking an interest in me back in 2008 when I was a lowly ‘liver sho’, for showing me how to better myself and for reigniting my academic dream in 2012. I also have much gratitude for Mr Khalid Sharif, hepatic surgeon at Birmingham Children’s Hospital for facilitating collection of specimens, and Dr Ina Nicklaus, Consultant histopathologist for preparing the samples for transfer to the HBRC facility at Queen Elizabeth Hospital, Birmingham. My Stacy Malaker, Paisley Trantham and Prof Don Hunt at the University of Virginia for characterisation of the phosphopeptides. Of course I thank my funder – Wellcome Trust, without whom none of this would have been possible.

Most of all, thanks to my wonderful mum without whom I most certainly would not have got this far. Thanks for being my best friend and listening to all my moaning, wiping away the tears and encouraging me at every step, even though you probably had no idea what I was talking about.

Capturing T-cell receptors – a potential new modality for targeting hepatic tumours and post-transplantation lymphoproliferative disease (PTLD)

Table of Figures

Chapter 1

Chapter 2

Chapter 3

Chapter 4

Appendix

Table of tables

Chapter 1

Chapter 2

Chapter 4

Appendix

List of Abbreviations

AC Alternating current

ADCC antibody-dependent cellular cytotoxicity

AFP alphafetoprotein

AIDs Acquired immune deficiency syndrome

AKT Protein Kinase B

ALL acute lymphoblastic leukaemia

AML acute myeloid leukaemia

AMP Adenosine monophosphate

APC antigen presenting cell

ATP Adenosine triphosphate

BrdU bromodeoxyuridine

CDC complement-dependent cytotoxicity

CDR complementarity determining regions

CEA carcinoembryonic antigen

CM Central memory

CML chronic myeloid leukaemia

CMV Cytomegalovirus

CRC colorectal cancer

CTL Cytotoxic T-cell

CTLA4 cytotoxic T-lymphocyte antigen 4

DC dendritic cell

DC Direct current

DMSO Dimethyl sulfoxide

DN double negative

DNA Deoxyribonucleic acid

DP double positive

dUMP deoxyuridine monophosphate

EBNA2 EBV nuclear antigen 2

EBV Epstein-Barr virus

EFS Event Free Survival

EGFR epithelial growth factor receptor

EM Effector memory

ELISAEnzyme linked immunosorbent assay

ELISpot Enzyme-linked immunospot assay

ER endoplasmic reticulum

ER oestrogen receptor

ESc Embryonic Stem Cell

E:T Effector:Target ratio

ETD electron transfer dissociation

Fab Fragment Antigen Binding

FAS CD95

Fc Fragment crystallizable region

FACS Fluorescence-activated cell sorting

FCS Fetal calf serum

FDA US Food and Drug Administration

FGF Fibroblast Growth Factor

GI gastrointestinal

GMCSF granulocyte-macrophage colony–stimulating factor

GMP Guanosine monophosphate

GSK3-B Glycogen Synthase Kinase 3 beta

GTP Guanosine triphosphate

HAT hypoxanthine-aminopterin-thymidine medium

HB Hepatoblastoma

HBV hepatitis B virus

HCC hepatocellular carcinoma

HER2 human epidermal growth factor receptor 2

hESc human Embryonic Stem Cell

HGF Hepatocyte growth factor

HGPRT Hypoxanthine-guanine phosphoribosyltransferase

hIPSc human Induced Pluripotent Stem Cell

HIV human immunodeficiency virus

HLA human leukocyte antigen

HNPCC hereditary non-polyposis coli

HPV human papilloma virus

HTLV Human T-lymphotrophic virus

HVS Herpesvirus Saimiri

ICS Intracellular staining

IFNγ Interferon-γ

Ig immunoglobulins

IGF2 Insulin-like Growth Factor 2

IL interleukin

IMAC immobilized metal ion affinity chromatography

iNOS Inducible nitric oxide synthase

IPSc induced Pluripotent Stem Cell

ITP idiopathic thrombocytopenic purpura

J junctional gene segments

JKA Jurkat

JKA-GFP GFP-tagged jurkat line

JKA-NLV Jurkat line which has been retrovirally transduced to possess an NLV TCR

LC liquid chromatography

LCL lymphoblastoid cell lines

LDH lactate dehydrogenase

LMP low-molecular-mass protein

mAb monoclonal antibodies

MACS Magnetic-activated cell sorting

MAPK mitogen-activated kinases

MEF mouse embryonic feeder cell

MHC major histocompatibility complex

MOAC metal oxide affinity chromatography

MS mass spectrometry

MSI microsatellite instability

MUC1 mucin 1

NCI National Cancer Institute

NF-κB Nuclear Factor-κB

NICE National Institute for Health and Care Excellence

NLV or NLVPMVATV CMV-derived HLA-A2 binding epitope

NK natural killer

NSCLC non-small cell lung cancer

OEAC oesophageal adenocarcinoma

OMK Owl Monkey Kidney cell

OP9DL1 OP9 cells expressing the Notch ligand, Delta-like 1

OS Overall survival

PAMP pathogen-associated molecular patterns

PAP prostatic acid phosphatase

PBMC Peripheral blood mononuclear cell

PCR Polymerase Chain reaction

PD1 programmed cell death 1

PDGF Platelet derived growth factor

PEG Polyethylene glycol

PHA Phytohaemagglutinin

PI3K phosphoinositide-3-kinase

PID pathway interaction database

PMA Phorbol 12-myristate 13-acetate

PR progesterone receptor

PRETEXT Pretreatment extent of disease staging system

PRR pattern recognition receptors

PTLD Post-transplant lymphoproliferative disease

PVP Polyvinylpyrrolidone

qPCR quantitative PCR

RAG Recombination Activating Gene

SCID Severe Combined Immunodeficiency

SFU Spot forming unit

SIOPEL Societe Internationale d'Oncologie Pediatrique – Epithelial Liver Tumour Study Group

TCR T-cell receptor

TEMRA Terminallay differentiated effector memory

6-TG 6-thioguanine

TH helper T-cell

TIL Tumour infiltrating T-cell

TK Thymidine kinase

TMP Thymidine diphosphate

TNF-α Tumour Necrosis Factor alpha

T_{regs} Regulatory T-cell

VEGF Vascular endothelial growth factor

VSV-G Vesicular stomatitis virus

WHO World Health Organisation

Chapter 1: INTRODUCTION

1.1 Background

Cancer remains a significant challenge with current treatments being toxic and/or inefficient and therefore this is an area where research is thriving. However, cancer as a disease has multiple forms and each tumour is different therefore the mechanisms of carcinogenesis and how tumours develop and evade the immune system vary from tumour to tumour. Tumours of interest to this project are hepatoblastoma, hepatocellular carcinoma (liver tumours) and post-transplantation lymphoproliferative Disease or PTLD – a lymphoma-like process occurring following organ transplantation.

There are various mechanisms linked to the development of cancer which could form potential targets for cancer therapies. The immune system plays a somewhat pivotal role in recognising pathogens and it is now understood to play a role in preventing tumour growth. When this system is evaded, a tumour can propagate and grow, therefore this is clearly an area where much interest has been generated in attempting to identify an anti-tumour therapy. One of the primary problems in tumour immunology relates to tumours developing from 'self' cells and therefore an appropriate target needs to be sought. Phosphopeptides could be a new class of tumour-specific antigens and may therefore have potential and as a cancer immunomodulatory therapy.

Major Histocompatibility Complex (MHC) class I restricted phosphopeptides have been identified as being a likely contributor to the anti-tumour T-cell response in cancer (Zarling, Polefrone et al. 2006, Cobbold, De La Pena et al. 2013, Abelin, Trantham et al. 2015) and therefore the first aim of this project was to identify phosphopeptides on the tumour surface and their role in tumour recognition (Chapter 3).

As identified as a valuable *in vitro* human model of post-transplant lymphoproliferative disease (PTLD) by Dr Penny of this group, lymphoblastoid cell lines (LCL) have been used to determine the relative proportion of the anti-tumour $CD8^+$ T-cell responses that are thought to recognise phosphopeptides (Chapter 3). The use of phosphatases allows for discrimination of anti-tumour versus anti-viral peptide responses to be described. In Chapter 4, specific MHC class-I restricted phosphopeptides associated with hepatoblastoma were identified and analysed, and their pattern compared to adult tumours (Hepatocellular carcinoma). Following on from this, specific T-cell responses to tumour associated phosphopeptides were further explored in tumour-infiltrating lymphocytes (TILS) and peripheral blood from patients as well as in healthy donors with characterisation of healthy donor responses to target phosphopeptides identified.

The second aim of this project was to identify mechanisms for promoting longevity in culture of T-cells. T-cell hybridomas and viral transduction of T-cells were both explored as potential modalities for achieving this.

1.2 Cancer

Cancer remains the leading cause of death globally, and the World Health Organisation figures suggest that there were an estimated 12.7 million cases around the world in 2014 (WHO 2014, NIH 2015). This has been predicted to reach 21 million by the year 2030. Cancer is a collection of diseases with one thing in common – the ability of cells to multiply without any control mechanism and invade into surrounding tissues. Usually cells divide and multiply in the healthy state, but are stopped from growing further (and needlessly) by contact inhibition. Cancerous cells lose this and therefore grow uncontrolled. These cells continue to survive becoming progressively more abnormal transitioning from metaplasia to dysplasia and eventually neoplasia (malignant change). This is considered to be a dynamic process, with reversibility exhibited in the early dysplastic changes.

Cancer cells can evade programmed cell death or apoptosis via a variety of mechanisms (Evan and Vousden 2001). They are also influential on surrounding cells and blood vessels – therefore manipulating what is commonly referred to as the tumour microenvironment (Hanahan and Weinberg 2000).

Hanahan and Weinberg first described the characteristics of cancer in 2000 where they identified six processes that a cancer collectively uses to survive and metastasize (Hanahan and Weinberg 2000). In order to achieve sustained malignant change, a cancer must be able to sustain proliferative signalling, induce angiogenesis, evade growth suppressors, resist cell death, activate cell invasion and metastasis and enable replicative immortality. This original influential work was revised in 2011, and an additional two characteristics employed by cancer cells were described – the capability to modify cellular metabolism and thus effectively support neoplastic proliferation and allow cancer cell to evade immunological destruction (Hanahan and Weinberg 2011).

The authors have subsequently expanded on the concept of 'hallmark switching' by which tumour treatments targeting just one of these hallmarks can be evaded by the tumour and resistance develops, and therefore they propose therapeutic 'co-targeting' of more than one hallmark in the evolution of cancer medicine – an area of research which is ongoing (Hanahan and Coussens 2012, Hanahan 2014). This is not without controversy however. These original seminal papers were based around the concept of somatic mutation theory of carcinogenesis, which suggests successive DNA mutations in a single cell. This relies on the assumption that (1) cancer is a defect of control of proliferation and (2) The default cell state is quiescence. Two recent papers have been critical of the original manuscript and have challenged this theory, proposing an alternative paradigm, including one paper suggesting that a number of the original 'hallmarks' described by Hanahan could also be considered as being characteristic of non-cancerous tumours as well. They went on to discuss that the only true hallmark of malignant

disease is actually its ability to invade adjacent tissues and metastasize further afield via induction of angiogenesis amongst other mechanisms (Lazebnik 2010). A further critique in 2013 suggested the original data was flawed for the majority of the hallmarks as the processes described were at a cellular level and cancer itself is a tissue-level disease. They concluded that these observations were therefore misleading. They proposed an alternative mechanism following re-evaluation of the original data (Sonnenschein and Soto 2013) whereby the default state of cells is that of proliferation, and carcinogenesis is related to a defect in tissue architecture.

As a paediatric hepatology trainee working in a national tertiary transplant centre, I have chosen the focus of this PhD project to be on hepatoblastoma, hepatocellular carcinoma and PTLD. Each will be considered separately.

1.2.1 Primary Hepatic Tumours in childhood are rare. The incidence is quoted in the texts as being between 0.5-2.5 per million population. Locally within the West Midlands region, this has been noted to be in the region of 1.2 per million person years, with the incidence of hepatoblastoma and hepatocellular carcinoma being 0.77 and 0.09 per million person-years respectively (Mann JR 1990). To consider this in context, this equates to between 10-15 new diagnoses of hepatoblastoma and 1-2 new diagnoses of hepatocellular carcinoma per annum. The aetiology of hepatic tumours is well described, and summarised in table 1.1 below. In hepatoblastoma, genetics plays a key role, whereas in hepatocellular carcinoma, chronic liver disease and environmental exposures appear to play a bigger role.

HEPATOBLASTOMA	HEPATOCELLULAR CARCINOMA
GENETIC o Beckwith Wiedemann Syndrome o Simpson-Golabi-Behmel Syndrome o Hemihypertrophy o Familial adenomatous polyposis (FAP) o Gardner Syndrome o Glycogen Storage Disease type 1 o Trisomy 18	*GENETIC* o Tyrosinemia Type 1 o Progressive familial intrahepatic cholestasis type 2 o Alpha-1-antitrypsin deficiency o Glycogen storage disease type I and IV o Neurofibromatosis o Familial Adenomatous polyposis (FAP) o Fanconi Anaemia
ENVIRONMENTAL o Fetal Alcohol Syndrome o Prematurity o Low birthweight o Oral contraceptives o Gonadotrophins o Metals o Petroleum products o Paints/pigments o Meckel Diverticulum	*ENVIRONMENTAL* o Any cirrhotic liver disease o Androgens o Oral contraceptives o Methotrexate o Aflatoxins *INFECTIVE* o Hepatitis B o Hepatitis C

Table 1.1 An overview of aetiology of hepatic tumours in childhood

1.2.2 Hepatoblastoma (HB) is a rare paediatric embryonal tumour (comprising ~1% of paediatric neoplasms (Otte 2010)), often affecting patients <4 years of age (91% cases) (Allan, Parikh et al. 2013). Indeed, presentation >4y of age is considered a poor prognostic factor. There is a male preponderance of 3:2. Incidence of HB has been shown to be increasing over time, with annual incidence currently being 0-05-0.15 per 100,000 paediatric population in America (Allan, Parikh et al. 2013). Tumour cells have been shown to evolve from hepatic stem cells (HSCs).

Presentation is most commonly with a mass, as well as non-specific symptoms of anorexia, pain, vomiting and rarely jaundice. It is often associated with a raised α-fetoprotein (AFP). AFP is a glycoprotein which is 70kDa in size. It is synthesized in the foetal yolk sac, and gut (Gregory and Finlay 1999). Although it is a high plasma concentration of AFP which often signposts HB as a potential diagnosis, a low plasma concentration of AFP at diagnosis in fact confers a poor prognosis (Koh, Park et al. 2011). AFP is thought to relate to tumour burden and therefore can be used as a monitoring tool to show responsiveness to treatment (Lovvorn, Ayers et al. 2010). Histological classification of HB has recently been revised in an

international consensus group (Lopez-Terrada, Alaggio et al. 2014). Here the disease is subdivided into (a) 'Epithelial' including foetal, embryonal, macrotrabecular small-cell differentiated, cholangioblastic or (b) 'Mixed' including stromal derivative or teratoid. Treatment options include chemotherapy (cisplatin) followed by resection or transplantation dependent on the extent of disease and whether there are any residual metastases following this treatment. Although some patients present with resectable disease, the majority do not. PRETEXT is the classification given to hepatoblastoma and refers to the extent of spread of disease (table 1.2). Based on an original paper by the International Childhood Liver Tumour Strategy (SIOPEL) group, staging was interpreted using Couinaud's segmentation model (Couinaud 1999, Abdalla, Vauthey et al. 2002, Roebuck, Aronson et al. 2007, Koh, Park et al. 2011). The liver is approximately divided up into 4 sections: right posterior (segments VI and VII), right anterior (segments V and VIII), left medial (segment IV) and left lateral (segments II and III). Using this classification pre-chemotherapy, patients are divided into one of four groups. Vascular involvement is also taken into account (Roebuck, Aronson et al. 2007).

PRETEXT No.	Definition
I	One section is involved only
II	One or two sections are involved, the remaining two sections are free of disease
III	Two or three sections are involved
IV	All four sections are involved

Table 1.2 Definitions of the PRETEXT numbers, based on original definitions by the International Society of Pediatric Oncology (Societe Internationale d'Oncologie Pediatrique, SIOP).

HB had a survival rate of 20-30% in 1970's, however with the introduction of newer regimes comprising cisplatin and doxorubicin in the early 1990's, this survival rate has improved markedly with newer drugs continuing to be introduced (Ninane, Perilongo et al. 1991). Overall survival is currently in the region of ~65% (Ruth, Kelly et al. 2010). In 2000, a multi-centre study reported a 5-year event–free survival of 66% and overall survival of 75%, following the introduction of combination treatment regimens consisting of four induction cycles of combination cisplatin and doxorubicin, followed by surgical resection of the primary

tumour/liver transplantation, if amenable, followed by two further courses of chemotherapy, (Pritchard, Brown et al. 2000). They also reported that of the 150 patients included, 118 (78.7%) achieved at least a partial response to chemotherapy which is promising indeed to the overall improvement in survival rates. Following this initial data, a further multi-centre study also considered introduction of combination cisplatin/doxorubicin. This study found complete surgical resection of HB was possible in 115 patients (76.2%) either by partial hepatectomy (55.6%) or by primary liver transplantation (20.6%). As a result, an event-free (EFS) and likewise overall survival (OS) demonstrated at 3 years were found to be 65% (95% CI, 57% to 73%) and 69% (95% CI, 62% to 77%) respectively for the whole group (Zsiros, Maibach et al. 2010).

Multiple signalling pathways have been implicated in HB carcinogenesis e.g. phosphatidylinositol 3 kinase-Akt (PI3K-Akt) and the insulin-like growth factor 2 (IGF2) pathways (Tomizawa and Saisho 2006, Hartmann, Kuechler et al. 2009). More recently, β -catenin mutations (Wnt signalling pathway) have been implicated in the development of 'sporadic' hepatoblastomas, occurring in up to two thirds of patients (Chen, Kozielski et al. 2012). β-catenin is an effector of Wnt-signalling, playing a role in cell-to-cell adhesion, growth, survival and differentiation. In the healthy state, β-catenin is complexed to E-cadherin/α-catenin and found in the plasma membrane. GSK3-β and CK1 phosphorylate excess β-catenin at four cytoplasmic N-terminal serine-threonine residues. The ubiquitin-proteasome pathway is able to degrade phosphorylated β-catenin. Wnt signalling inhibits GSK3-β activity, leading to stabilisation of the β-catenin allowing for nuclear translocation and subsequent activation of transcription factors including Tcf/Lef. In cancer, there are loss of function mutations which lead to constitutive activation of β-catenin (Peifer and Polakis 2000, Polakis 2000). The Wnt/ β -catenin signalling pathway plays a pivotal role in embryonic development and has been shown to be necessary for stem cell maintenance. It has been implicated in liver

development and regeneration, and has a possible role in constitutive activation and thus the aetiology of HB (Korinek, Barker et al. 1998, Korswagen, Clevers et al. 1999, Clevers 2006). It is perhaps not surprising then that this pathway is associated with hepatoblastoma given its embryonal origins (Armengol, Cairo et al. 2011). Aberrant Wnt signalling is considered a key feature of hepatoblastoma, related to mutations in the β -catenin gene. As a result of mutational activation, HB may develop from HSCs or progenitors. Due to the finding in HB of mesenchymal derivatives a multipotent progenitor has been postulated with aberrant signalling appearing to disrupt/disturb the intricate relationship between proliferation and differentiation, resulting in the well differentiated foetal-type HBs. Fig. 1.1 demonstrates the possible mechanisms of action (Armengol, Cairo et al. 2011).

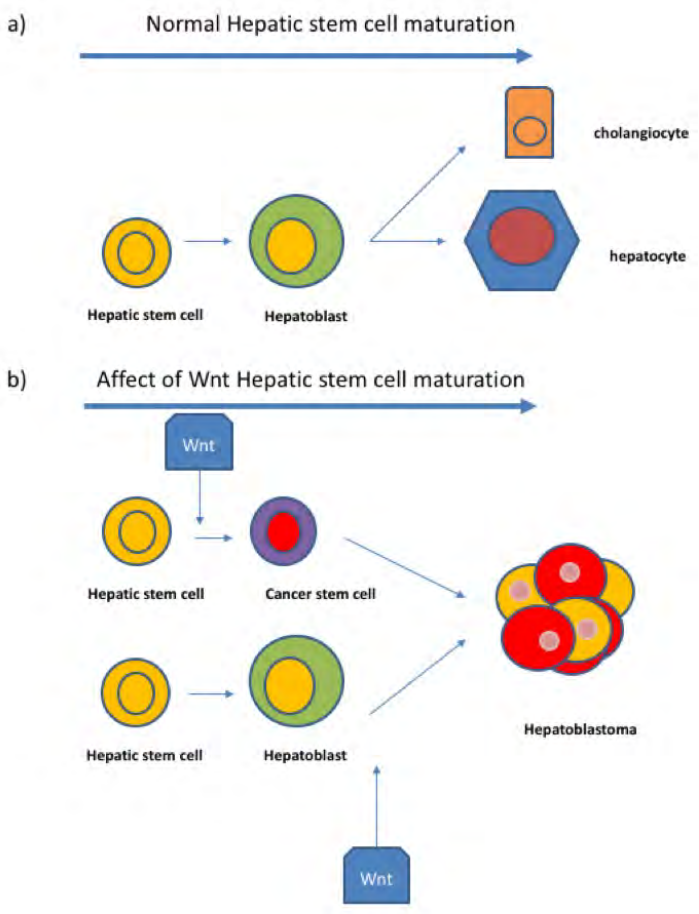

Fig. 1.1 Schematic representation of the differentiation of hepatic stem cells. (a) Normal differentiation of hepatic stem cell into cholangiocyte and hepatocyte via hepatoblast stage (b) the effect of Wnt signalling on differentiation of cells at different stages of maturation results in development of a hepatoblastoma

1.2.3 Hepatocellular carcinoma is a very rare paediatric tumour (being more common in adults). It differs from hepatoblastoma as it usually occurs in the context of chronic liver disease, rather than occurring in isolation (table 1.1). It also tends to affect the older age group. Presenting symptoms are similar to those with hepatoblastoma, although jaundice has been more commonly reported in this group of patients. The mechanism of development is scarring and regenerative nodules which have the potential to become malignant due to progressive dysplastic change. It can also be found in association with hepatitis infection (fig. 1.2). Treatment is resection with adjuvant chemotherapy or liver transplantation in the absence of distant metastases. Survival is ~50% with death occurring due to tumour recurrence (Thorgeirsson and Grisham 2002).

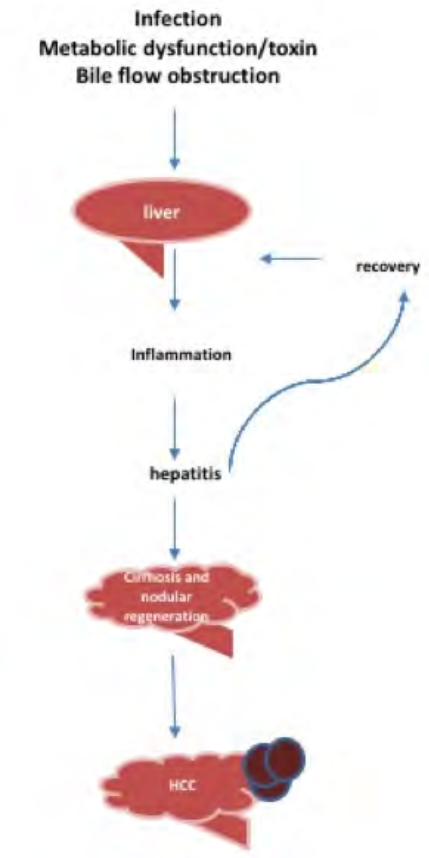

Fig. 1.2 The transformation of healthy liver into hepatocellular carcinoma. Liver is exposed to inflammatory processes such as chronic hepatitis B or C infection, metabolic dysfunction e.g. tyrosinemia, obstruction of bile flow. This leads to inflammation of the liver (hepatitis) which if left will progress to cirrhosis and regenerative nodules. This process can be reversible if the inflammatory trigger is removed, however ongoing inflammation will eventually lead to progressive dysplasia and eventual evolution into a hepatocellular carcinoma (HCC).

During the course of chronic liver disease several mutations are predicted to occur which subsequently accumulate in liver cells, resulting in a profound dysregulation of major signalling pathways that have been found to be important for malignant transformation. As a result, these pathways have become a major target for cancer treatments in hepatocellular carcinoma (HCC). For instance, the perceived survival benefits achieved with sorafenib, a kinase inhibitor, have been previously unheard of and serve to highlight the importance of understanding how signalling differs in malignant transformation. A number of key signalling pathways have become dysregulated in HCC, in particular those implicated in growth factor signalling, cell differentiation and angiogenesis – all of the pathways which have been implicated in other tumours, and those which are intimately related to the mechanisms described by Hanahan (Hanahan and Weinberg 2000, Hanahan and Weinberg 2011). RAS and AKT/MTOR have also been identified as possible key pathways which could have a role in the development of HCC. A number of mechanisms have shown disordered pathway activation including point mutations, chromosomal aberrations, and down-regulation. Novel technologies such as next-generation sequencing (NGS) in HCC research identified a number of pathways which had not previously been associated with the development of HCC e.g. autophagy. Investing research time and effort into these newer pathways could potentially lead to alternative drug/therapeutic targets.

Phenotypically altered hepatocytes have been demonstrated to have high epidermal growth factor receptor (EGFR) expression and also possess a number of potential epigenetic changes which are considered non-committal. These may go on to become dysplastic and show more committed genetic changes, e.g., increased telomerase activity. This may ultimately result in development of an HCC with additional genetic changes, e.g., an increase in c-myc and decrease in p16 expression, amongst others (Moeini, Cornella et al. 2012).

1.2.4 Post-transplant lymphoproliferative Disease (PTLD) is caused by B-cell proliferation resulting from necessary therapeutic immunosuppression after organ transplantation; with infection by Epstein-Barr virus (EBV) implicated as the trigger (fig. 1.3). EBV interacts with its host in three ways: (i) EBV infects B-lymphocytes leading to proliferation of infected cells, (ii) subsequently, it enters a latent phase *in vivo*. (iii) Finally, it can be reactivated leading to a rise in the production of infectious material leading to infection of cells of the same cell type or transmission to another individual.

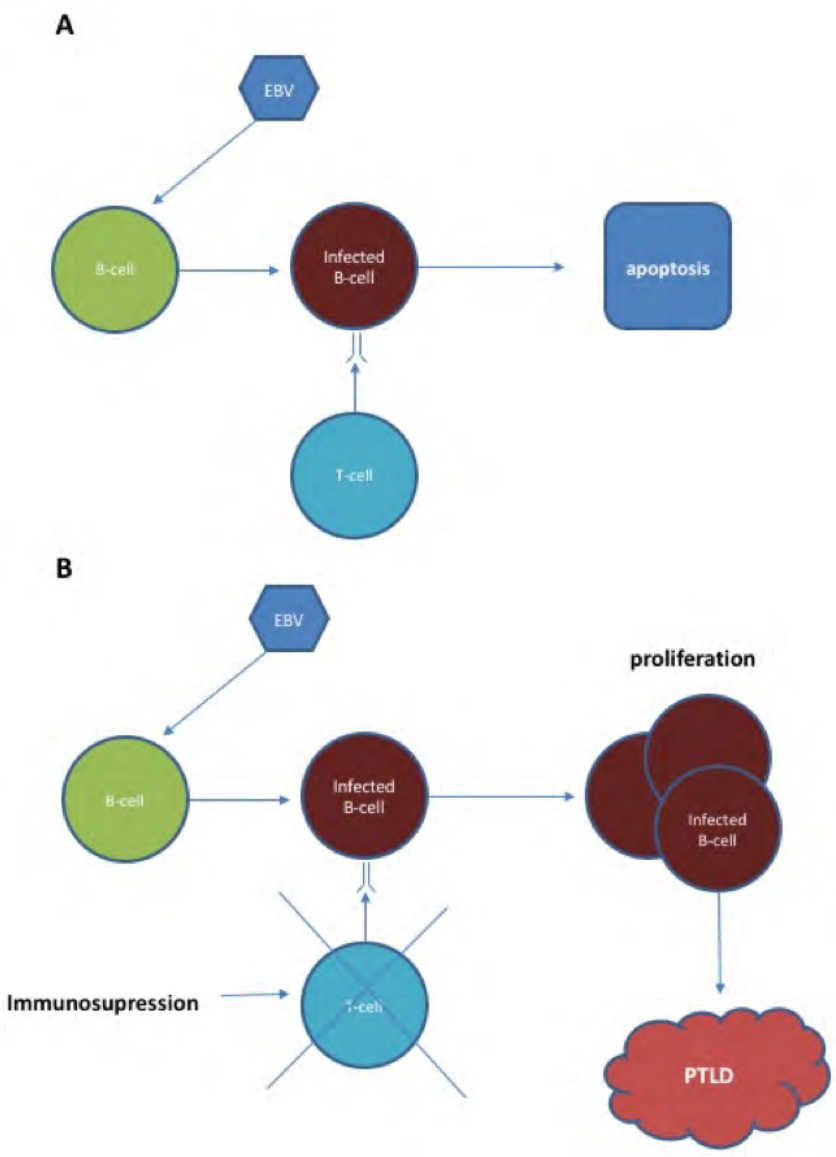

Fig. 1.3. Schematic representation to show effect of immunosuppressive agents on development of PTLD. (A) shows normal situation, where T-cells recognise transformed B-cells and eradicate them. (B) shows the situation when immunosuppression is used such as calcineurin inhibitors, which work by reducing the number of circulating T-cells thus allowing for transformed B-cells to proliferate, leading to possibility of PTLD formation

B-cell immortalization and the lytic cycle leads to production of infectious particles. Polymerase chain reaction (PCR) analyses used in conjunction with fluorescent-activated cell sorting (FACS) has delineated the virus-host interaction in peripheral blood cells *in vivo*.

It has been identified that in some patients, a malignant cell clone becomes the dominant cell type, and its proliferation results in development of B cell lymphomas (fig. 1.8). This was first described by Henle and colleagues in the 1960's (Henle, Diehl et al. 1967, Diehl, Henle et al. 1968). They identified that B-cells were induced by EBV to rapidly divide and proliferate in an exponential manner leading to an immortal B-cell clone and establishment thereof of a lymphoblastoid cell lines (LCL) *in vitro*. Based on this observation they established that these cells would form an ideal model to study EBV infection viral-induced tumour development (Keiff E 2001). This process is intimately controlled by an intracellular transcription factor EBV nuclear antigen 2 (EBNA-2), which expresses its influence over 9 separate latent viral proteins and is driven by 'The Growth Programme' which refers to the pattern of gene expression seen in this process (Thorley-Lawson 2001).

Healthy carrier individuals possess EBV-infected B-cells, but they are all memory B-cells which are considered latent or 'resting' and thus do not express viral protein (Miyashita, Yang et al. 1997, Babcock, Hochberg et al. 2000). Only those cells which possess the 'Growth Programme' have potential for tumour development and these cells are only found in the lymph nodes (Babcock, Hochberg et al. 2000, Joseph, Babcock et al. 2000). This pattern of B-cell viral segregation appears to be maintained in all individuals, including those who are immunocompromised. It has been noted that the number of EBV-infected B-cells in an immunocompromised patient can be at least 50 times more than in a healthy individual with competent immune system. EBV has been postulated to be able to transform latently infected cells into actively proliferating blast cells, allowing for the conversion thereof of these cells into memory B-cells thus making them non-pathogenic.

EBV has been found to be associated with a number of diseases including autoimmune disease and cancer (Cohen 2000, Crawford 2001, Keiff E 2001). There is strong evidence for an association between EBV and cancer. For instance, immunosuppressed patients are at an increased risk for B-cell lymphoproliferative diseases, e.g. PTLD (Thomas, Hotchin et al. 1990). Impaired cytotoxic T-cell response (due to immunosuppressive agents) allows for the unchecked growth of EBV-infected cells. Two events must occur to allow for expression of the growth program evolution of lymphoma (i) firstly the EBV-infected cell is not allowed to exit the cell cycle and therefore fails to transform into a resting memory B cell, resulting in continuous, unchecked proliferation due to a lack of effective T-cell immunity, and (ii) the cytotoxic T-cell response is prevented from destruction of lymphoblasts, proposed as resulting in the heterogeneity seen in this disease (Timms, Bell et al. 2003). Even in those patients who are immunocompromised, this transformation has to be a rare event as very few actually develop a tumour. This bolsters the view that EBV-driven *in vivo* proliferation must be a closely regulated process.

The incidence of PTLD is between 1% to 25% of solid organ transplant patients and it is 4 times higher in paediatric transplant patients versus adults (due to their likelihood of being EBV seronegative pre-transplant compared to adult recipients). It has been shown to occur in 3% of liver transplant recipients and 18% of intestinal transplant recipients. Prognosis is poor with overall 5 year survival between 25-65% (Haque, McAulay et al. 2011, Wistinghausen, Gross et al. 2013, Lee 2015, Dharnidharka, Webster et al. 2016).

Cells possessing the oncogenic protein LMP-1 (which induces expression of BCL2 leading to inhibition of apoptosis) are kept in check by cytotoxic T lymphocytes (CTL's) and Natural Killer (NK) cells, whereas cells without LMP-1 persist leading to latent infection with the potential for reactivation. Following immunosuppression, cells which express the oncogenic protein LMP-1 are allowed to grow uninhibited due to reduction in circulating CTLs (as a result

of the immunosuppressive agents) and there is the potential for malignant transformation and resultant PTLD (Jacobson and LaCasce 2010).

Tacrolimus and cyclosporin are calcineurin inhibitor agents used post-transplant as part of the immunosuppressant regimen to prevent organ rejection, by inhibiting T-cell function, therefore leading to unchecked B-cell proliferation. Anti-T cell antibodies (such as basiliximab, daclizumab) leads to T-cell depletion, and is often used in conjunction with standard immunosuppression protocols to prevent or treat organ transplant rejection, but at the expense of increased risk for the development of PTLD. The level of immunosuppression needed to prevent rejection is directly proportional to the risk of developing PTLD, i.e. in small bowel transplant trough tacrolimus levels are 3-4 fold higher than those needed in liver transplant for instance. PTLD can spontaneously regress simply by reducing or stopping immunosuppressive agents. It could also be treated with anti-viral agents, however in some cases it will continue to progress resulting in non-Hodgkin's lymphoma which can be fatal (Jacobson and LaCasce 2010).

1.2.5 Summary

Cancer results in major morbidity and mortality, and although the cellular basis to each tumour type is varied as is its location, it has a number of common mechanisms for evading the immune system all of which can be potential targets for cancer immunotherapy (Hanahan and Weinberg 2011). By understanding the pathways involved potential targets may be identified.

1.3 The Basics of Immune System

The immune system has evolved in order to provide protection from a growing number of pathogens, who themselves are likewise evolving. It is broadly split into two specific parts (Dranoff 2004) – the Innate and Adaptive Immune Systems (Table 1.3).

Innate Immunity	Adaptive Immunity
Macrophage	B-cell → antibodies
Mast cell	T-cell → CD4, CD8 cells
Dendritic cells	
Granulocytes →Natural killer (NK) cells, basophil, eosinophil, neutrophil	
Γδ T-cells	
NK T-cells	

Table 1.3 Table to show the division of immune systems as described by Dranoff, 2004. There is interplay between both systems with crossover demonstrated by γδ T-cells and NK T-cells, playing a role in both.

1.3.1 Innate immunity is the first line of defence comprising the physical barriers to prevent infection e.g. tight junctions and mucus layers. It also comprises a variety of immune cells such as eosinophils, phagocytes and Natural Killer (NK) cells, all of which can produce proteinaceous materials which aid in the defence of the host against pathogen e.g. ficolins or complement. The innate immune response does not generate memory.

1.3.2 Adaptive immunity comprises the responses resulting from somatic gene rearrangement. It comprises specialised B and T-cells. Memory recall is the main feature of this type of immune response i.e. cells that persist in an apparently dormant state but have the ability to re-express effector functions when challenged with the same antigen again in the future. T and B

lymphocytes express antigen-specific receptors on their cell surfaces. Selection and expansion of these receptors can take up to 7 days. Two classes of response exist: B-cell antibody responses and the T-cell mediated responses.

B-cells secrete immunoglobulins (antibodies) in response to antigen. The antibodies circulate and bind to the specific foreign antigen (that had initially stimulated their production). There are three main mechanisms of action: (1) opsonisation, (2) neutralization and (3) complement activation. These antibodies are made up of heavy and light chains comprised of highly variable domains and constant domains denoted as Fab and Fc respectively (Delves P 2006), allowing complex interactions with other effector cells and immune system molecules. Light chains comprise both a single constant and a single variable immunoglobulin (Ig) fold domain which will be either κ or λ chains. Heavy chains are made up of a single variable and three or four constant domains. Heavy chains are responsible for determining the class and therefore function of the antibody (IgA, IgD, IgE, IgG or IgM). As a result of Ig rearrangements, antibody diversity can be generated. This can be achieved in a variety of ways for example (i) different combinations of heavy and light chains; (ii) recombination of different variable (V) gene segments on the heavy or light chains, diversity (D) segments or Junctional (J) segments; (iii) addition or loss of nucleotides at the VDJ junction or (iv) mutation of the variable regions of either heavy or light chains. It is the hinge region between variable and constant domains which allows for flexibility to bind with the antigen.

1.3.3 T-cell ontogeny Haematopoietic stem cells are generated in the bone marrow and go on to form B-cells which are maintained there; whereas T-cells mature in the thymus, where they begin to express antigen receptors.

Upon being released from the thymus, these cells are considered naïve due to no previous antigen exposure. However, once they recognise their cognate antigen in the secondary

lymphoid organs (spleen and lymph nodes) they mature to become potent effector cells capable of clearing infections. It is likely development of an immune profile relates to environmental exposure. There are 3 processes of lymphocyte development:

(1) Proliferation of immature cells

(2) Expression of antigen receptor genes

(3) Selection of lymphocytes that express useful antigen receptors.

The Nuclear factor-kappaB (NFKB) family of transcription factors has remained essentially unchanged throughout evolution, and they are thought to play a significant role in host immune responses to pathogen. Studies of NFKB deficient mice have identified its role in the development of T-cells and B-cells, ensuring lymphocyte survival at various developmental stages. In autoimmune disease, this function is bypassed leading to, for example, survival of self-reactive lymphocytes or tumour cells (Siebenlist, Brown et al. 2005).

$CD4^-CD8^-$ double negative (DN) thymocytes evolve into $CD4^+CD8^+$ double positive (DP) cells within the thymus and eventually to progress further to either $CD4^+$ or $CD8^+$ single positive (SP) thymocytes, which exit the thymus entering the peripheral circulation (fig 1.10). Double negative thymocytes progress through four stages of development: DN stage 1, at which they are $CD25^-CD44^+$; DN stage 2, $CD25^+CD44^+$; DN stage 3, $CD25^+$CD44-; and DN stage 4, $CD25^-CD44^-$. DN cells in early stage 3 undergo TCR beta-chain gene rearrangement and expression. NF-kappaB appears to be important for this transition between DN stage 3 and DN stage 4. To investigate T-cell ontogeny further extra-uterine CD4 T-cell development was considered. Previous studies have shown that the immune system develops rapidly in the first year of life and this is proposed to be due to extrauterine triggers (Kotiranta-Ainamo, Apajasalo et al. 1999, de Vries, de Bruin-Versteeg et al. 2000, Berrington, Barge et al. 2005). During this early post-natal period, the development of immune phenotypes predict the risk of development of infective illnesses or an immune-related disorder (Shearer, Rosenblatt et al. 2003, Zhu and

Paul 2008, Romero, Stolberg et al. 2013). The relative proportions of basic lymphocyte subsets have been shown in a number of studies to vary with age. Although data exists relating to this transition from birth to adolescence, there is a lack of longer term data to support the ongoing transition through older age (Rellahan and Cone 1990, Kozyrskyj, Bahreinian et al. 2011).

T-cells comprise half the circulating lymphocytes in the early newborn period. These cells have derived from precursors having undergone selection, and possess a low affinity for self-peptides. The CD4-cells comprise two subsets: T helper cells and T regulatory cells (T_{reg}). These T-cells tend to be naïve on the whole, however this population of naïve cells reduces during early infancy so that by age 6 months the memory $CD4^+$ T-cells increase in numbers as immune challenges occur. Gender differences also occur which persist throughout the first year of life (Tsao, Chiang et al. 2002, Surh and Sprent 2008, Zhu and Paul 2008).

1.3.4 T-cell responses – T-cells play a pivotal role in both humoral and cell mediated immune responses. T-cells recognise antigen presented to them via the T-cell receptor (TCR). The TCR is similar in structure to immunoglobulin, however rather than recognising native protein, it recognises peptides complexed to major histocompatibility complex (MHC) molecules of the cell surfaces. These antigens are presented by Antigen Presenting Cells (APC). Variation of the TCR is generated in a similar fashion to a single antibody Fab fragment. It is encoded by α and β polypeptide chains, each containing a single constant and variable region. TCR gene rearrangement initially relies on rearrangement of the β polypeptide chain, with Dβ to Jβ, followed by Vβ to DJβ. This is then followed by α chain rearrangement. In addition to αβ T-cells, there is a distinct subset of T-cells possessing γδ chains instead of α and β polypeptide chains, thus called γδ T-cells.

Following TCR rearrangement, T-cell selection occurs in the thymus. Selection occurs in order to remove T-cells with non-desirable characteristics – i.e. to eliminate those T-cells which are

either harmful or ineffective. The first stage is positive selection. Here, TCRs are tested against self-peptide/HLA complexes which are expressed on the cortical epithelial cells. Those TCRs which have moderate affinity for self-peptide receive a positive signal to continue growing and maturing. Lack of interaction results in cell death. Co-receptor expression is then modified to match MHC restriction. The next stage is negative selection. During negative selection, potentially autoreactive cells expressing TCRs with high affinity for self-peptide/HLA complexes are removed by apoptosis. Cells surviving this second stage of selection then enter the circulation as mature naïve T-cells, waiting to be activated by professional APCs, such as dendritic cells (DC) to become functional. DCs work in three ways: (1) a signal is delivered by TCR engagement with the peptide/HLA complex and CD4 or CD8 ligation, (2) co-stimulatory molecules deliver a further signal to the complex (3) cytokines cause the differentiation of the T-cell into a specific type.

One of the best characterised co-stimulatory molecules involved in the second stage signalling as described above are the B7 molecules. These are homodimeric molecules of the Ig superfamily, specifically expressed on APCs. Two of the founding members of the B7 family, CD80 (B7-1) and CD86 (B7-2), each bind to the activating receptor, CD28, or the counter-regulatory inhibitory receptor, cytotoxic T-lymphocyte antigen 4 (CTLA4). Ligation of CD28 by B7 molecules is necessary for the clonal expansion of naïve T cells and induction of IL-2 receptor expression. CTLA-4 is upregulated on T cells to dampen responses after activation, and reduce inflammation.

Several tumour necrosis factor (TNF) family members that are expressed by APCs can co-stimulate T-cell activation, by binding to specific TNF receptor family members expressed on T-cells. Most of these TNF receptor family members are upregulated on T-cell activation, indicating that the role of this family might be to amplify responses once initial T-cell activation has occurred. TNF receptors include: 4-1BB, which binds 4-1BB ligand; CD27, which binds

CD27 ligand (CD70); OX40, which binds OX40 ligand; and Light-R, which binds Light. The third signal varies between the different types of T-cells. For cytotoxic T cells, this can be IL-2 provided by the T-cells themselves, but may also be IL-12 or type-I interferon (IFN) produced by other cells in the local environment. CD4 T-cells are capable of a much more diverse range of functions, and stimulation to differentiate into the different types of CD4 cells are provided by different cytokine profiles (Table 1.4).

T-cell type	Function	Target	Differentiation Profile	Cell marker	Cytokine profile
Cytotoxic	Kills infected cells	Virus Bacteria Tumour	IL-2, IL-12, IFN, T-bet TF, Eomes	CD8	MIP-3α, TNFα, IFNγ, IL-2
T_H1	Cellular Immune Response	Bacteria Blood-borne parasites	IL-2, IL-12, IL-18, IL-27, T-bet, IFNγ	CD4	IL-2, IL-10, IFNγ, TNFα, TNFβ/LTα
T_H2	Support of B-cells	Extracellular parasites and toxins	IL-2, IL-4, IL-6, IL-25, IL-31, IL-33, GATA3		IL-3, IL-4, IL-5, IL-6, IL-10, IL- 13, IL-25, IL-31
T_H9	Intestinal protection	Parasite	IL-4, PU.1/IRF-4, TGFβ		IL-9, IL-10
T_H17	Defence against extracellular microorganisms	Bacteria/fungi	RORγt, TGFβ, IL-1β, IL-6, IL-21, IL-23		IL-17A, IL-17F, IL-17AF, IL-21, IL-22, IL-26, GM-CSF, MIP- 3α, TNFα
T_H22	Tissue repair	Skin/gut/lung	IL-6, TNFα		CCL15, CCL17, FGF family, IL- 22, TNFα
T_{Reg}	Response suppression		FoxP3, IL-2, TGFβ	CD4, CD25	IL-10, IL-35, TGFβ

Table 1.4: Different T-cell subsets can be defined by their differentiation, cell marker and cytokine profiles, which thus determined their functions and targets. Table modified from original by Dr S Penny, with permission.

T-cells exert their effect through the production of effector molecules, such as perforin and granzymes, Fas-Ligand (FasL), and cytokines that induce activation of other cells. There are several classes of T-cells, defined by their stimuli, effector function, accessory molecule expression, and the type of MHC complex that they recognise (table 1.4). This thesis will focus mainly on cytotoxic ($CD8^+$) T-cells.

In the peripheral circulation, two thirds of T-cells are $CD4^+$, the remainder being $CD8^+$. It is the $CD4^+$ T-cells which have the ability to activate both humoral and cellular responses. $CD8^+$ cells recognise and show cytotoxic activity towards intracellular pathogens or malignant transformed cells, they also have a suppressor cell subset which can down-regulate these immune responses. In response to antigen exposure and recognition, both $CD4^+$ and $CD8^+$ T-cells are able to differentiate in order to mount a suitable response to target. For instance, resting naïve $CD4^+$ cells will only release limited amounts of cytokine prior to antigen stimulation however after stimulus IL2 is released and the cells progress from TH0 to TH1, TH2 and TH17 depending on the cytokines present. TH1 cells release IL-2, IFN-γ, and lymphotoxin. TH2 cells release IL-4, IL-5, IL-9, IL-13, and GM-CSF as well as expressing the transcription factor GATA3. In general, TH1 cells can be considered to relate to cell-mediated immune responses, and TH2 cells are considered more the humoral and allergic responses. Cytotoxic $CD8^+$ T cells also have discrete type 1 and type 2 cytokine responses, designated cytotoxic T cell type 1 and cytotoxic T cell type 2.

Approximately 5% to 10% of T-cells in the peripheral blood, and secondary lymphoid organs are DN ($CD4^-CD8^-$). These cells use either αβ TCRs or γδ TCRs. These cells do not recognize antigen in the context of MHC class I or II directly, however some can recognize related antigen for example the MHC-class I–related protein CD1 which has been adapted to present the respective glycolipid components of various pathogens. A further example relates to the DN subset of γδ T-cells which recognizes the MHC class I chain–related proteins or MIC.

Antigen-specific T-cells have proven clinical utility in a range of diseases from targeting tumours such as melanoma and leukaemia to the control of viral disease such as Epstein Barr virus (EBV), adenovirus, influenza (Flu) and Cytomegalovirus (CMV). However, highly expanded disease-specific T-cell populations are not very effective, which can in part be

explained by their gradual loss of function as a result of *ex vivo* processing of the patient autologous T-cells.

In response to this limitation a number of techniques have been employed to try to establish a T-cell line which is stable and retains its features such as cytotoxicity and IFNγ release. This has generated a vast amount of recent research interest in stem cells as a potential source of cells which despite controversy is a clear target for possible future investment.

1.3.5 Major Histocompatibility Complex (MHC) - MHC molecules, also known as Human Leukocyte Antigens (HLA) present peptide antigen to T-cells. The major histocompatibility complex (MHC) locus, also known as the human leukocyte antigen (HLA) locus, spans around 4 Mbp on the short arm of chromosome 6 (6p21.3). MHC-I molecules comprise a 45kDa heavy chain of three extracellular domains, covalently linked to beta-2-microglobulin (12kDa). There is a peptide binding groove which can accommodate a peptide between 8 and 13 amino acids in length. MHC-II molecules are similar but consist of an alpha (30kDa) and beta (33kDa) chain and possess an open ended binding groove with the ability to accommodate peptides of longer length. Class I genes are expressed on all nucleated cells, whereas class-II associated genes are only expressed on the surface of antigen presenting cells (e.g. B cells or macrophages). This study focusses primarily on MHC Class-I therefore class-II will not be discussed further at this stage.

There are three major antigens of the human class I MHC system: HLA-A, HLA-B and HLA-C. The MHC heavy chains are located on chromosome 6 at 3 different loci named human leukocyte antigen (HLA) -A, -B and -C. They are highly polymorphic, as there are well over 1500 different heavy chains which have been identified, and each individual expresses six HLA alleles, two from each locus. The peptide-binding domain is responsible for the polymorphism seen, as is the domain interacting with the TCR. This TCR will be peptide specific and domain

specific. Each HLA molecule has its own set of peptides to which it will bind, which is controlled by the physical shape of the peptide-binding groove. Molecules encoded by this region are involved in antigen presentation, inflammation regulation, the complement system, and the innate and adaptive immune responses, indicating the MHC's importance in immune-mediated, autoimmune, and infectious diseases.

MHC-restricted antigen recognition, or **MHC restriction**, refers to the fact that a given T-cell can interact with both the self-major histocompatibility complex molecule and the foreign peptide that is bound to it, but will recognize and respond to the antigen, only when it is bound to a particular MHC molecule. Foreign particles enter a cell and are broken down to smaller particles (peptides). These peptides are then presented on the surface of the infected cell by MHC. MHC restriction is important for self-tolerance. As described previously, due to a process of selection in the thymus T-cells die by apoptosis if they express high affinity for self-antigens presented by an MHC molecule or express too low an affinity for self MHC. MHC restriction allows TCRs to detect host cells that are infected by pathogens, contains non-self proteins or foreign DNA. However, MHC restriction is also involved in presenting peptide to T cells in chronic autoimmune diseases and type IV hypersensitivity.

Two models have been proposed to explain the imposition of MHC restriction. **The Germline model** proposes that MHC restriction results from co-evolution of TCR and MHC to interact with each other. **The Selection model** suggests that MHC restriction is imposed on TCRs by CD4 and CD8 co-receptors during positive selection. Supporting the selection model argument is the observation that T cells genetically modified to not possess CD4 and CD8 co-receptors express MHC-independent TCRs (Tikhonova, Van Laethem et al. 2012, Van Laethem, Tikhonova et al. 2012).

Of direct relevance to the current project is the concept of antigen cross-presentation by dendritic cells. The presentation of exogenous antigens on MHC class I molecules, known as

cross-presentation, is essential for the initiation of $CD8^+$ T-cell responses. Naive antigen-specific $CD8^+$ T-cells, however, cannot directly eliminate transformed or infected cells. To become effector cytotoxic T lymphocytes (CTLs), naive $CD8^+$ T cells need first to be activated by 'professional' antigen-presenting cells (APCs). When the APCs are not directly infected, they need to acquire exogenous antigens from the infectious agent and present them on MHC class I molecules, by a mechanism known as cross-presentation. **Cross-presentation** is the ability of certain antigen-presenting cells to take up, process and present extracellular antigens with MHC class I molecules to CD8 T cells is required in order for immunity to viruses and tumours to develop (Bevan 1976). It is also implicated in cancer vaccines where protein antigens are introduced to allow host immunity to develop.

Cross-presentation allows the presentation of these exogenous antigens, which are normally presented by MHC II on the surface of infected dendritic cells to be also presented by MHC I without infecting the dendritic cell. Cross-presentation allows the dendritic cell to avoid using the endogenous proteasomal processing pathway. Although this process primarily involves dendritic cells, macrophages, B-lymphocytes and sinusoidal endothelial cells have also been implicated.

Two main intracellular pathways for the cross presentation of exogenous antigens have been described (1) the ‘cytosolic’ and (2) ‘vacuolar’ pathways. The cytosolic pathway is sensitive to proteasome inhibitors. The Proteasome-generated peptides are able to feed into the classical MHC class I mediated antigen presentation pathway. This has been previously described as involving the transport of peptides into the endoplasmic reticulum (ER) by transporter associated with antigen processing 1 (TAP1) and TAP2 for loading on newly formed MHC class I molecules. This contrasts with the vacuolar pathway, which has previously been shown to be resistant to proteasome inhibitors and generally independent of TAP, but is sensitive to inhibitors of lysosomal proteolysis (Joffre, Segura et al. 2012).

1.4 The role of the immune system in tumour suppression The concept of immune surveillance was first described by Frank MacFarlane Burnet nearly 60 years ago where he described a process thus 'in large long-lived animals, like most of the warm-blooded vertebrates, inheritable genetic changes must be common in somatic cells and a proportion of these changes will represent a step toward malignancy. It is an evolutionary necessity that there should be some mechanism for eliminating or inactivating such potentially dangerous mutant cells and it is postulated that this mechanism is of immunological character' (Burnet 1957, Burnet 1957). Since this first observation, there has been much debate as to this statement's validity (Fuchs and Matzinger 1996, Smyth, Godfrey et al. 2001, Willimsky and Blankenstein 2005, Senovilla, Vitale et al. 2012). In 2001, in stark contrast to the theory of immunosurveillance it was proposed that cancer may even be promoted by inflammation – a concept introduced by Balkwill and further expanded over the succeeding years (Balkwill and Mantovani 2001, Mantovani, Allavena et al. 2008, Balkwill and Mantovani 2012).

1.4.1 The role of the immune system in tumour suppression – evidence in mouse models

Burnet wrote in relation to the theory of immunosurveillance that cancer should be more common in the face of immunodeficiency, a concept that can be explored in an array of mouse models for both primary and secondary immunodeficiency (Burnet 1957). There is compelling evidence that this prediction is true with a link between severe immunodeficiency and susceptibility to cancerous processes being demonstrated by a number of authors (Gatti and Good 1971, Smyth, Godfrey et al. 2001, Swann and Smyth 2007, Salavoura, Kolialexi et al. 2008, Senovilla, Vitale et al. 2012).

Schreiber's work on the cancer immunoediting hypothesis has helped develop the concept that the immune system can not only recognise and remove cancers, but it can also drive them into

a dormant state, which in some cases, leads to enhanced malignant potential. The focus of Schreiber's research work was the concept of immunosurveillance in cancer pathogenesis. The original 'immune surveillance' hypothesis proposed that tumour cells arise naturally and are normally eradicated by the immune system (Burnet 1957). Tumours would, therefore, only arise if evasion of the immune system were possible, or if the immune system were compromised. This theory was tested by Stutman assessing whether athymic, nude mice which lack an adaptive immune system have an increased incidence of tumours (Stutman 1974). He found no difference between nude mice and wildtype, which inevitably led to the theory that the immune system played no role in preventing the initiation or the prevention of tumours. With the knowledge that the innate immune system was intact in the nude mice that Stutman had used, Schreiber repeated these experiments using a strain of mice he bred to lack both innate and adaptive immunity. These mice lacked the recombination activating gene (RAG) required for adaptive immune responses and the STAT1 gene that is required for innate responses (Meraz, White et al. 1996). In 2001, it was reported that RAG2 knockout mice, i.e. those which lack an appropriate adaptive immune system (T and B cells), had a far higher rate of development of malignancy compared to immunocompetent wildtype mice (Shankaran, Ikeda et al. 2001). This led to the revival of the original hypothesis that the immune system somehow played a pivotal role in tumour surveillance and led to the proposed concept of 'cancer immunoediting' the means by which tumours are able to escape the immune system recognition by losing their antigenicity (Dunn, Old et al. 2004, Dunn, Old et al. 2004, Dunn, Bruce et al. 2005, Dunn, Koebel et al. 2006).

These studies have been critical in forming the scientific basis of many of the immune mediated strategies currently being tested in patients as anti-tumour regimens. Not only do these studies confirm that the immune system plays a hugely important role in tumour cell destruction, but they support the idea that better understanding of immunological recognition and regulation

will lead to breakthroughs in our ability to eradicate tumors using the immune system. Mice which have been genetically modified to lack certain components of the immune system such as RAG2 mice (which lack T and B-cells due to deficiency in the RAG2 - Recombination-activating gene 2) are more susceptible to carcinogen-induced carcinomatosis. Cytokines have also been demonstrated to be protective (in particular interferon α/β and γ) (Kaplan, Shankaran et al. 1998, Dunn, Bruce et al. 2005, Dunn, Koebel et al. 2006). But are mice a good proxy for what happens in humans? It is notable that in humans, they manage largely to avoid cancer until after the fifth decade of life on the whole, despite more than 1,000-fold greater cellularity and more than 20-fold longer life spans than mice. This would suggest that the mechanisms in human are perhaps more sophisticated or at least more efficient than those in mice.

1.4.2 The role of the immune system in tumour suppression – evidence in humans As is demonstrated in immunocompromised mice, immunodeficiency can be speculated to be responsible for development of tumours in humans also. This is clearly demonstrated in patients with HIV for instance and PTLD. It is well described that patients with HIV are several thousand times more susceptible to Kaposi's sarcoma (secondary to Human Herpesvirus 8 infection) and at least 70 times more likely to acquire Non-Hodgkin lymphoma (due to EBV infection) – and it can be postulated that this may be due to a deficiency in the immune regulation and monitoring for disease. Patients who have received an organ transplant and are prescribed immunosuppression are far more susceptible than their healthy counterparts to developing PTLD secondary to B-cell proliferation in response to viral infection (EBV). It may therefore be postulated that these malignancies are secondary to an exaggerated viral response. Although this may well be the case – it is also notable that these subsets of immunocompromised patients are in general more susceptible to tumours than the general population without a virus being implicated, which would suggest that it is not solely due to

viral responses (Cadranel, Garfield et al. 2006, Grulich, van Leeuwen et al. 2007). The latter paper was a meta-analysis of a number of studies and found that there was an increased risk in patients who were post-transplant or with HIV/AIDS for certain types of epithelial tumour including lung. In patients with immunodeficiency such as HIV/AIDs and those patients on immunosuppressive agents post-transplant for instance, increased rates of malignancy have been noted such as myeloma, renal, leukaemias and melanoma (Grulich, van Leeuwen et al. 2007) – fig. 1.4.

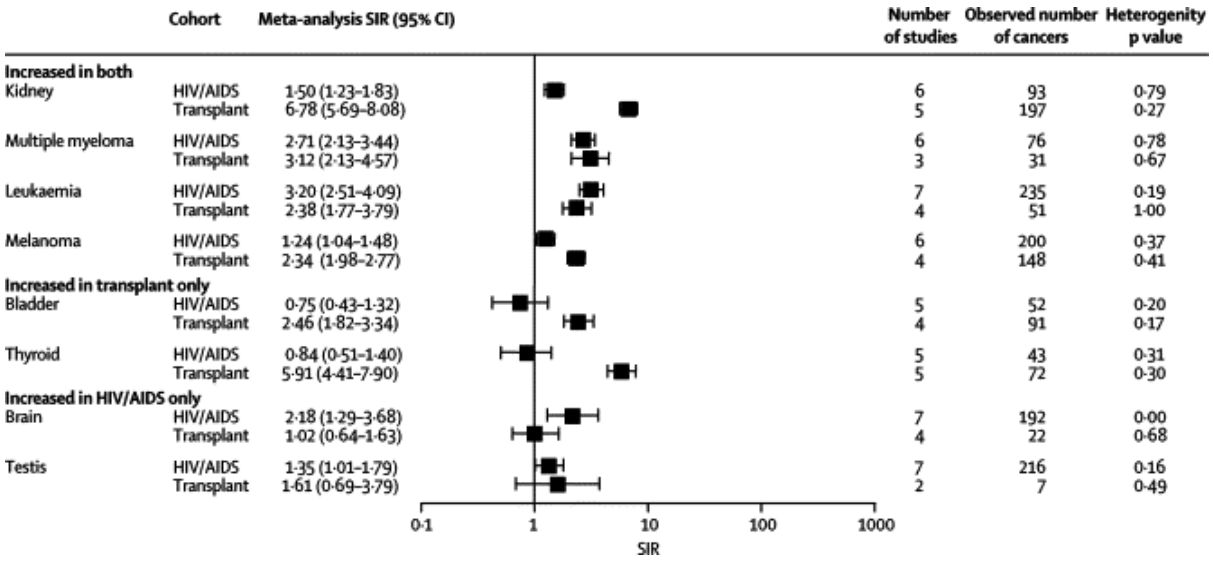

Fig. 1.4: Standardised incidence ratios for development of cancers occurring at increased rates in HIV/AIDs or post-organ transplant – This demonstrates patients who are immunosuppressed increased risk of development of malignancy, suggesting an intact immune system will protect a patient from development of malignancy (Grulich, van Leeuwen et al. 2007) .

1.4.3 The role of the Immune System in tumour suppression – Tumour Immune Evasion

The fact that tumours have the ability to evade the host immune response makes designing any anti-cancer therapy challenging. The mechanisms of immune evasion have been known about for a number of years, and they do indeed form the basis of Hanahan's hallmarks of cancer (Hanahan and Weinberg 2011).

Two broad categories have been described as to how the developing tumour can evade the immune system: (1) tolerance induction by the developing tumour and (2) resistance to killing by activated immune effector cells. These categories can be further subdivided:

a) Downregulation of tumour antigen presentation

Delineation of tumour from self, results from antigen recognition by T-cells. Carcinogenesis is characterised by genetic instability which is believed to result from inactivation of p53 for instance. Neoantigens result from this genetic instability leading to tumour growth and progression (Stronen, Toebes et al. 2016). As a result of deletion of b2-microgobulin genes, global loss of MHC I has also been noted, together with downregulation of Transporter associated with Antigen Processing (TAP) genes and components of the immunoproteosome such as the immunoproteosome subunit LMP-2. Downregulation of MHC class-I pathway has been identified in a number of solid tumours including lung, breast and prostate (Salmaninejad, Zamani et al. 2016, Seliger 2016, Dunn and Rao 2017, Garrido, Perea et al. 2017, Reeves and James 2017). In the majority of cases, where the MHC class I processing machinery is downmodulated, it is usually rapidly upregulated by IFNγ, suggesting that the diminished expression is epigenetic in origin and reversible. Downregulation of tumour antigen presentation affecting the MHC I pathways has been described as a way that tumours are able to evade immune regulation (Johnsen, Templeton et al. 1999). This downregulation leads to tumour expansion and metastasis due to non-recognition by $CD8^+$ cytotoxic T-cells (CTLs). In addition to this, other suppressive cytokines such as TGFβ, VEGF, CCL21 and IL-10 can also lead to reduced CTL functionality. These factors can recruit or promote differentiation or expansion of suppressive immune cells such as Tregs, immature dendritic cells and tumour-associated macrophages.

b) Immunologic barriers within the tumour microenvironment

One definition of a tumour is its ability to invade normal tissue and metastasize. Immune cells have an important role in inhibiting or promoting cancer through immune surveillance of tumours by the mechanism of immunoediting, immunoprocessing, and immunoevasion. Immunoevasion is one of the hallmarks associated for a tumour progression. Stromal cells in the tumour microenvironment can also actively hinder anti-tumour immunity by several mechanisms such as expression of inhibitory receptors, the production of immunosuppressive cytokines, production of molecules which induce T cell apoptosis or loss of HLA class 1, and costimulatory molecules.

In both healthy tissues and solid tumours there are two distinct regions: the parenchyma (the tumour bed in the context of solid tumours) and a stromal region (part of the tumour microenvironment in tumours). The basal lamina, which normally separates these two regions in healthy tissues, is typically incomplete in solid tumours, which allows for interaction between the tumour and tumour microenvironment resulting in a range of processes such as microenvironment-derived factors can influence tumour cell survival, invasiveness and metastatic dissemination, as well as access and responsiveness to therapeutics.

Evidence supports the idea that tumours actively inhibit the release and detection of specific ‘danger’ signals in order to invade tissues and metastasize without evoking anti-tumour immune responses that would otherwise inhibit their growth, thereby converting inflammatory responses to those that could instead potentiate tumour growth. An example of where this occurs is the Stat-3 oncogenic signalling pathway. It is constitutively activated in a number of tumours resulting in enhanced tumour cell proliferation and an anti-apoptotic effect (Ok and Young 2017, Ok and Young 2017, Shrihari 2017). In cancer, the Stat3 signalling pathway has been shown to inhibit the production of these pro-inflammatory signals and induces expression of factors that inhibit functional maturation of dendritic cells (DCs). This observation makes Stat-3 a target for blockade and thus enhancement of the anti-tumour response.

c) ‘Disabled’ antigen presenting cells (DC’s)

Some tumour-derived factors, including IL-10, IL-6, and VEGF, can induce Stat3 activation in DCs. This may directly inhibit NFkB signalling, with additional oncogenic signalling in tumours which may contribute to inhibition of DC activation within the tumour microenvironment as a whole.

d) T-cell immune tolerance in carcinogenesis

The immune system has evolved to avoid a CD4-mediated autoimmune reaction by means of thymic selection (Van Laethem, Tikhonova et al. 2012). T cells are the master regulators of adaptive immune responses and maintenance of their tolerance is critical to prevent autoimmunity. However, in the case of carcinogenesis, the tumour microenvironment aids T-cell tolerance, which contributes to uncontrolled tumour growth. The primary mechanism of self-tolerance is central deletion in which self-reactive T cells are eliminated in the thymus by negative selection. This process is incomplete however, and as a result further mechanisms of peripheral tolerance have evolved, divided broadly into two types: those that regulate the responding state of T cells intrinsically (anergy, apoptosis and phenotype skewing) and those that provide extrinsic control (Tregs and tolerogenic dendritic cells).

Tumours can induce anergy by lacking expression of co-stimulatory signals – thereby engaging with the T-cell receptor but failing to stimulate it therefore leading to tolerance (Staveley-O'Carroll, Sotomayor et al. 1998) i.e. failing to activate the CTL.

e) Coinhibition

T-cell activation and effector function is thought to potentially be controlled by a fine balance between costimulatory signals such as CD28 and co-inhibitory molecules (Chen 2004, Luo, Chapoval et al. 2004, Wang and Chen 2004). This modulates TCR signals. Ultimately this results in promotion or suppression of T-cell activation. Timing and location of these molecules leads to positive or negative control of a number of functions including growth and

differentiation as well as functional maturation of a T-cell response. These co-stimulatory and co-inhibitory molecules are termed receptors/ligands. A ligand can be a co-stimulator or co-inhibitor which results from which receptor it interacts with. A well described example is CD80/CD86 which following binding with CD28 is co-stimulatory for T-cell responses, but can also be a co-inhibitor by interacting with Cytotoxic T-lymphocyte antigen 4 (CTL4a). A ligand also has the ability to become a receptor in certain circumstances if the appropriate co-inhibitory or co-stimulatory signal is received (Chen 2004).

f) Regulatory T-cells (Treg)

CD4 T-cells that are also $CD25^+$ have previously been shown to prevent autoimmunity, and infection (Yokokawa, Remondo et al. 2008). These Tregs induce and maintain self-tolerance and immune homeostasis. Tregs prevent autoimmunity and infection, but have also been shown to promote tumours.

There are two broad subsets of Treg (1) natural (nTreg) and (2) induced (iTreg). Treg present in cancer is distinct from that which is thymus derived. As a result, cancer-induced suppressor cells are also referred to as adaptive or inducible Treg (iTreg) and are believed to arise and differentiate in the periphery in response to environmental signals such as cytokines. These iTreg have a number of functions including downregulation of anti-tumour immune cells or inhibition of tumour progression by reduction in inflammation (Whiteside, Schuler et al. 2012). Natural Treg (nTreg) was first described in the early 1990's as representing a subset of $CD4^+$ cells which were also $CD25^+$ and capable of inhibition of immune responses to self and non-self-antigen (Sakaguchi, Sakaguchi et al. 1995, Miyara and Sakaguchi 2011). FOXP3 was identified as playing a role, as absence of $FOXP3^+$ Treg results in autoimmunity (Miyara and Sakaguchi 2011). It is crucial for the development and function of Tregs. In the healthy donor, whenever $CD8^+$ effector and $CD4^+$ helper Treg accumulate in response to local signals, the homeostatic balance is maintained by accumulation of $FOXP3^+$ nTreg thus preventing potential

tissue damage. In contrast to this, as is seen in tumours, iTreg occurs, which results in generation of a pool of highly activated and indiscriminately suppressive inducible Treg, which results in the interruption of functions of anti-tumour effector T cells (Whiteside, Schuler et al. 2012).

Regulatory T-cells are known to decrease the activity of the immune system through direct and indirect interactions. In a study looking in ascitic fluid of women with advanced ovarian tumours, the presence of Tregs was associated with reduced survival (Curiel, Coukos et al. 2004). Tumour-associated Treg have also been found in a number of other solid tumours including lung, prostate, pancreatic, ovarian and breast (Yamamoto, Zou et al. 1995, Liyanage, Moore et al. 2002, Curiel, Coukos et al. 2004, Viehl, Liyanage et al. 2004, Zou, Chen et al. 2004, Barnett, Kryczek et al. 2005). Tregs express chemokine receptors CCR4, CCR5 and CXCR1 which allows for migration into tumour sites. In addition to this, TGFβ in the tumour microenvironment has been shown to promote the conversion of naïve conventional $CD4^+$ T-cells to iTregs in tumour mass. Through cell contact-dependent suppression, competitive IL-2 deprivation and secretion of immunosuppressive cytokines (e.g. IL-1,TGFβ, Tregs are able to supress the functions of CD4 and $CD8^+$ T-cells, NK cells, NKT cells, macrophages and dendritic cells.

g) Immune editing

Immune editing has been identified as one strategy by which tumours can evade immune surveillance/recognition allowing tumours to be present but inactive (and thus often undetectable) in patients for years through “equilibrium” and “senescence” before re-emerging. In addition, tumours exploit several immunological processes including regulatory T-cells, antigen presenting cells and the concept of immune tolerance is also exploited. To date a number of anti-cancer medications exploit the underlying immune surveillance mechanisms

with some success including increased production of NK cell, γδ T cell responses or inhibiting functionality (Johnsen, Templeton et al. 1999, Swann and Smyth 2007). These are thought to counter the genetic instability caused by tumours and promote anti-growth signalling – ultimately leading to tumour rejection.

The concept of immune editing essentially describes how cancers can evade the immune system by virtue of the fact that the immune system is only able to recognise certain cancer cells due to their possession of tumour antigens, however as a result of genetic instability not all cells will possess these in equal amounts and results in a heterogeneous mix of cells not all as immunogenic as each other. This results in clearance of the most active cells and the rest being in a state of equilibrium, dividing and accumulating further mutational variations (Swann and Smyth 2007). There are three phases of immunoediting which describe the fine balance between tumour and the immune system: elimination, equilibrium and escape. During the elimination phase, immune cells of the innate and adaptive immune system recognize and destroy tumour cells. If the immune system cannot fully eliminate the tumour, the equilibrium phase occurs, during which cells remain dormant and the immune system is not only sufficient to control growth, but also shapes the immunogenicity of tumour cells. This stage will remain or evolve to the elimination or escape phase. In the escape phase, tumour cells have acquired various strategies to evade the immune system and establish the dominant tumour immune tolerance.

1.5 The role of the Immune System in tumour progression The "progression model" is a well-recognised model which predicts cancers can develop and propagate as a result of a series of domino-like mutational events resulting in a number of these cells possessing metastatic potential (Nowell 1976, Fidler and Kripke 1977, Minn, Kang et al. 2005). Angiogenesis and tumour seeding/metastasis is propagated by Vascular endothelial growth factor (VEGF) and

inducible nitric oxide synthase (iNOS). Control of cell survival, cycling and division is largely due to Nuclear Factor-κB (NF-κB) and its production of the pro-inflammatory cytokine TNF-∝ (also a promoter of angiogenesis) (Yamamoto, Zou et al. 1995). This production of cytokines and chemokines allows for the progression of tumours, often at distant sites to the original primary tumour.

1.6 Immunotherapies have been a major development in the effective treatment of cancer and reduction in morbidity and mortality. It is clearly well established that the host immune system can recognise pathogens/microbes such as bacteria/viruses due to their producing foreign protein. However, tumour cells differ only marginally from host cells. Mutated protein expression may account for some of this recognition, but essentially these tumour cells would normally use established biochemical pathways as normal cells would.

1.6.1 The history of Immunotherapy and its possible role in cancer treatment

Immunotherapy first came into existence in the 18th century when scientists explored the immune system's role in fighting infection – most notable is the use of small pox vaccine by Edward Jenner. By 1970's the first biological agents had been used in humans for the treatment of breast cancer (Tamoxifen) (Kiang and Kennedy 1977).

In 1987, researchers identified cytotoxic T-lymphocyte antigen 4 (CTLA-4) as playing a part in preventing T-cells from attacking tumour cells. It was proposed that blocking this could result in the immune system being able to actually target these tumours instead. This study found that patients with metastatic melanoma lived an average of 10 months whilst being treated with the antibody, versus 6 months without it. This randomised controlled trial was the first demonstration of enhanced life potential for patients with metastatic melanoma as a result of a new cancer treatment (Couzin-Frankel 2013).

It had previously been noted that dying T-cells expressed a molecule that was called programmed death 1, or PD-1 which was proposed as a blocker of anti-tumour T-cells therefore it was hypothesized that an antibody that targeted PD-1 should produce remission. In 2013, Couzin-Frankel et al reported that across the 300 cancer patients tumours included in their study, cancers had been demonstrated to have shrunk by at least half in 31% of those with skin cancer (melanoma), 29% with renal tumours and 17% with lung cancer (Couzin-Frankel 2013). In the mid 1990's, the FDA approved rituximab as the first monoclonal antibody treatment for the treatment of follicular lymphoma, following extensive clinical trials (Coiffier, Haioun et al. 1998, Davis, White et al. 1998). Following on from this, a further 11 antibodies have now been approved as adjuvant cancer therapies including alemtuzumab (2001), ofatumumab (2009) and ipilimumab (2011). In 2003 IL-2-activated NK cells were administered together with IL-2 with a good response noted in metastatic lesions (Yang, Hokland et al. 2003). They concluded that adoptively transferred activated-NK cells were able to eliminate even well-established metastases. To overcome the adverse effects of intravenously administered cytokines, *in vitro* expansion of cells against a tumour antigen, and reinjection of these cells with appropriate stimulatory cytokines was tried instead (Egawa 2004, Li, Li et al. 2005). Sipuleucel-T, was approved in 2010 as the first cell-based immunotherapy licensed for the treatment of prostate cancer (Waldmann 2003, Strebhardt and Ullrich 2008). Sipuleucel-T is considered to be a personalised treatment for prostate cancer. It allows the patient's immune system to seek out cancer cells, acting as a therapeutic vaccine. The treatment cycle has 3 stages: (1) APCs are extracted from the patient's blood and (2) incubated with antigen prostatic acid phosphatase (PAP) – present in 95% of prostate tumours, as well as granulocyte-macrophage colony stimulating factor (GM-CSF) which aids APC maturation. Finally, (3) the activated blood product is reinfused into the patient.

After noting the success from harvesting T-cells from tumours, expanding them *in vitro* prior to re-infusion and the observation of reduction in tumour mass, the idea of redirecting the specificity of T-cells through genetic engineering was explored. This was first introduced by Zelig Eshhar, and has been further developed over time (Gross, Gorochov et al. 1989, Gross, Waks et al. 1989, Eshhar and Gross 1990, Eshhar, Waks et al. 1993, Hwu, Yang et al. 1995, Eshhar, Waks et al. 1996). Two approaches to improve the potency of the anti-tumour T-cell response have been devised; 1) TCR-engineered T-cells where the cells expressing the TCR αβ heterodimers are modified and transferred and 2) Chimeric antigen receptor therapy, or CAR engineered T-cells where the cells are composed of antibody-binding domains fused to T-cell signalling domains. With T-cell receptor (TCR) engineering, T-cells are made more potent in their recognition of tumour specific antigens by incorporating TCR constructs which activate and co-stimulate T cells in a coordinated immune response against tumour cells. The TCRs are engineered to recognise a tumour-specific peptide/MHC combination. With CAR-T cell engineering, T-cells are transfected with a CAR construct that combine the specificity of an antibody with the cytotoxicity properties of killer T cells. CARs are recombinant receptor constructs composed of an extracellular single-chain variable fragment (scFv) derived from an antibody, joined to a hinge/spacer peptide and a transmembrane domain, which is further linked to the intracellular T cell signalling domains of the T cell receptor. Both these strategies represent a shift in patient treatments and we are now entering an era where the drug is a cell product designed and repurposed through ex vivo genetic modification (Sadelain et al. Nature 2017).

CAR-T and TCR therapies are currently attracting vast amount of investment following encouraging clinical trial results and the first CAR-T cell therapy to treat adults with certain types of large B-cell lymphoma was FDA approved in October 2017. The basis of both these therapies involves the isolation of patient's T cells, genetically modifying the T cell, expanding

them and then infusing the modified T cells back into the patient. The main challenges that lay ahead are how to manufacture these treatments in a cost effective and consistent way and how to manage some of the severe side effects that can occur.

CAR-T therapy has until recently primarily focussed on B-cell malignancy as there is a clear target (CD19). However, solid tumours possess overall lesser sensitivity to T-cell mediated cytotoxicity and a tumour microenvironment with an array of immunosuppressive mechanisms which vary from tumour to tumour, thus leading to a relative paucity of suitable target antigens with a profile as favourable as that seen in CD19. With advances in genomic screening, new tumour-specific targets are being discovered which will lead to these treatments being tailored for solid tumours (e.g. Sorronto Therpaeutics Autologous Anti-CEA CAR-T Cell Therapy for Liver Metastases Demonstrate Therpaeutic Activity in Stage IV Pancreas Cancer in a Phase 1b HITM-SURE Trial). Furthermore, combinational approaches to treatment such as combining a check-point inhibitor with a CAR-T/TCR therapy, are being considered to overcome this challenge.

1.6.2 Immuno-oncology and its role in cancer treatment Based on the knowledge that tumour cells can avoid immune detection, the concept of immuno-oncology as an anticancer treatment was introduced. A raft of evidence has been gathered related to PD-1 and PD-L1 antagonists in patients with a variety of cancers, identifying immune interventions in cancer treatment as invaluable. Data accumulated from agents that block checkpoint proteins such as CTLA-4 and PD-1, have provided a therapeutic level to which other therapies can be quantitatively and qualitatively compared. Key features include broad activity, rapid onset of response, relatively low toxicity and the possibility of T-cell memory resulting in durable responses differentiate this third generation of immuno-oncology agents from the preceding ones. However, these agents are still toxic, are very expensive, and are not currently curative.

In 2010, initial outcome data following use of Nivolumab, an IgG4 PD1 antibody became available (Ascierto, Simeone et al. 2010) and it was subsequently FDA-approved to treat melanoma, lung cancer, kidney cancer and Hodgkin's lymphoma in 2014. Pembrolizumab (Keytruda) is another PD1 inhibitor that was approved to treat melanoma and lung cancer by the FDA in 2014 (2010, Kline and Gajewski 2010, Pardoll 2012, Reichert 2014, Barbee, Ogunniyi et al. 2015, Bex 2016, Cattrini, Dellepiane et al. 2016, Shreders, Joseph et al. 2016, Shukuya and Carbone 2016, Weber, Gibney et al. 2016).

1.6.3 Identification of tumour antigens T-cell clones can recognise and lyse specific target cells and cloning techniques exist to propagate these. Peptide can be eluted from MHC molecules on tumour cells. Tumour antigens should ideally only be expressed by tumour cells (and not healthy tissues) in order to be efficiently recognised by the host's immune system. The reality is that they are overexpressed in tumour cells compared with healthy cells. Tumour cells have the ability to employ 'escape mechanisms' allowing immune evasion. An example of how a tumour can evade the immune system is for instance by altering production/sequence of a protein that contains an immunogenic peptide so that the epitope is no longer presented at the cell surface and hence not recognised by host immune cells. Furthermore, MHC can be down-regulated in various tumours and as a result the tumour antigens are not recognised by CTLs.

1.6.4 Cancer Vaccines act in a variety of ways. Vaccines deliver proteins into the body. These proteins may be derived from infective materials such as viruses or from cancer cells themselves – but they are inactivated meaning they will not cause disease in the recipient. As a result of introduction of these foreign proteins the immune system will generate antibodies and/or T-cells against them, allowing clearance of the vaccine particles, but also inducing

'memory', so that if there is a second interaction with the protein again, the immune system will react and clear this more efficiently. This is essentially how vaccines against infections work.

In cancer, two types of vaccine exist: 1) vaccines to prevent cancer 2) vaccines to treat cancer. An example of a cancer preventative vaccine would be the vaccine against human papilloma virus (HPV), implicated in cervical cancer. Other vaccines are currently being investigated for similar infective causes of cancer. The second form of vaccine, works by allowing the immune system to recognise cancer cells and form an appropriate response towards them, preventing growth and recurrence. There are a number of sub-category of vaccine including: Antigen vaccines, Whole cell (autologous) vaccines, dendritic cell vaccines, DNA vaccines and anti-idiotype vaccines which relates to which part of the immune system is targeted in effecting tumour clearance. As a result of this new form of vaccine a number of FDA approved trials have been attempted or are ongoing (Gilboa 2004, Goldman and DeFrancesco 2009). In regards to the whole cell (autologous) vaccines The FDA has recently approved a license for Sipuleucel-t (Provenge®) which is an autologous immune cell prostate cancer vaccine, shown to extend life for patients with otherwise untreatable prostate cancer by up to 4 months (Higano, Schellhammer et al. 2009, Higano, Small et al. 2010, Cheever and Higano 2011, Higano 2012, Higano, Sartor et al. 2015).

Tumour-induced immune suppression is thought to be responsible for the failure of cell-based cancer vaccine attempts (Schabowsky, Madireddi et al. 2007). Furthermore vaccination has been shown to induce antigen-specific Tregs (Curiel, Coukos et al. 2004, Curiel 2007, Curiel 2007). It has been predicted that the clinical response induced by some cancer vaccines may well be due to rapid induction of CTLs which overwhelm the deleterious effects of simultaneously generated Tregs, however these CTLs will apoptose with time and disappear leading to domination by Treg (Curiel 2007).

It has been proposed that $CD4^+$ Treg is a prognostic factor for survival in a number of tumours including ovarian (Wolf, Wolf et al. 2005), which would support the idea that depletion of tumour-associated Treg could be beneficial with tumour-specific immunotherapy. Conventional depletion of Treg with anti-CD25 antibodies, have been shown to eliminate only around 70% of Treg, which has failed to significantly reduce the growth of established tumours (Gu, Guo et al. 2015). Using an animal model (Foxp3.LuciDTR-4 mice), the authors demonstrated an impressive 90–95% Treg depletion resulting in complete regression of large established tumours (Li, Kostareli et al. 2010).

Recently, Th17 T-cell infiltration has also attracted attention. It has been shown to confer a more favourable outcome. These cells have been positively associated with effector cells and negatively associated with Treg infiltration. This has inevitably led to the question, could Th17 be therapeutically induced or expanded by tumour vaccine or adoptive immunotherapy (Munn 2009)? There has been much study of this in recent years with conflicting evidence available in both support and against, as there have been a number of studies implicating IL-17 in promoting tumour growth and invasion (Murugaiyan and Saha 2009, Wang, Yi et al. 2009). It is difficult in the face of conflicting evidence to adopt a rational opinion as to how to take this therapy forward as a potential cancer immunotherapy. One viewpoint as to how these apparently conflicting observations may be reconciled is related to the important fact that like more immune responses, Th17 responses are unlikely to be homogeneous. The new challenge therefore is to identify those responses which are anti-tumour and develop a mechanism for supporting and expanding these.

1.6.5 Monoclonal Antibodies (mABs) In the quest to understand how antibodies work, early work by Milstein looked at the antibodies made by myeloma cells, and the observation was made that these appeared to be clonal – i.e. from one cell and lacked the diversity seen in other

cells (Milstein, Harrison et al. 1972, Kohler and Milstein 1975). The American immunologist Klunkel has been credited for this observation. Using mice as a model, Milstein further hypothesized that somatic mutation resulted in antibody diversity (Milstein, Harrison et al. 1972). Milstein was joined by the German scientist Kohler and together they sought to investigate somatic mutation of antibodies, in order to identify a means with which to create an antibody with the desired specificity. In order to achieve this a normal spleen-derived B-cell was fused with a mouse myeloma cell. The normal B-cell was obtained from a mouse immunised with a known antigen, thus resulting in antibody production. By fusing these cells, this would lead to creation of a hybridoma, with the aim being to transfer the immortality from the myeloma cell to the antibody producing cell. This resultant 'hybridoma' technology created a cell line capable of producing a seemingly limitless supply of highly specific antibody 'the monoclonal antibody' having been derived from a single hybrid cell (Kohler and Milstein 1975).

As a result, monoclonal antibodies have become invaluable to a large number of clinical laboratory diagnostic tests such as ELISA. Following on from this, in cancer, a number of mAbs have been developed and work in different ways. Some mAbs recognise and attach to antigens on cancer cells. Others work by interrupting cancer cell signalling, thus putting a halt to cell division e.g. trastuzumab (Herceptin®) which blocks the Her2/neu receptor in breast cancers. Conjugated mAbs are a subdivision of mAbs which are linked to a radioactive or chemotherapeutic agent, allowing delivery of said agent to the cancer cell in a targetted manner. Another example, and potentially most well-known of mAb is Rituximab, which recognises CD20 antigens expressed on lymphoma cells. Rituximab is probably one of the more well established monoclonal antibodies. It is a chimeric anti-CD20 monoclonal antibody. It comprises human-derived IgG1 and κ light chain constant regions with murine-derived variable regions. Rituximab is used for treatment of a number of tumours. In a phase II clinical

trial of patients with B-cell lymphomas, rituximab was demonstrated to induce a response in half of the patients with low grade B-cell and follicular tumours (Maloney, GrilloLopez et al. 1997). In high grade tumours, rituximab had less well defined success, although remained better than conventional therapies with response rates of 37% and 33% in patients with high grade diffuse large B cell lymphoma and mantle cell lymphoma, respectively (Coiffier, Haioun et al. 1998). The mechanism of action is as a result of complement and antibody dependent cell mediated cytotoxicity, inhibition of cell proliferation, and induction of apoptosis (Coiffier, Haioun et al. 1998).

1.6.6 Cytokine based immunotherapy Cytokine therapy is an adjuvant chemotherapeutic, synthetically made. There are 3 main types: 1) Interleukin boosts T- cell growth and division. IL-2 is an example of this. It is essential for cytotoxic T-cell proliferation and differentiation, thus increasing responsiveness to tumours. 2) Interferon can suppress cancer cell growth. 3) Granulocyte-macrophage colony-stimulating factor (GMCSF) boosts T-cell growth, allowing for increased effector cells to be present to target tumours (Dranoff 2004). There are a number of adjuvant cancer therapies available for use in the UK including Aldesleukin (IL-2) used in metastatic tumours including melanomas. It has been shown to halt disease progression (Bhatia, Tykodi et al. 2009).

As was the case in cancer vaccines, Tregs also play a role in the failure of these types of therapies also. IL-2 for instance, expands and activates CTLs leading to an early clinic response to tumour, however it also boosts human Treg function in vivo which ultimately can inhibit the anti-tumour CTL response (Curiel 2007).

1.6.7 Neoantigens Many tumours express mutations. These mutations potentially create new targetable antigens (neoantigens) for use in T-cell immunotherapy. The relative number of

$CD8^+$ T cells in cancer lesions, as identified using RNA sequencing data, is higher in tumours with a high mutational burden. The level of transcripts associated with cytolytic activity is positively correlated with mutational load as represented by NK cells and T-cells. For example, in non–small cell lung cancer patients who were treated with lambrolizumab (Domingues, Turner et al. 2014, Dang, Ogunniyi et al. 2016, Shukuya and Carbone 2016), mutational load shows a strong correlation with eventual clinical outcome. In melanoma patients who were treated with ipilimumab, any long-term benefit is also associated with a higher mutational load, although less significantly (Champiat, Ferte et al. 2014, Campesato, Barroso-Sousa et al. 2015, Van Allen, Miao et al. 2015, Marmarelis, Davis et al. 2016). The predicted MHC binding neoantigens in patients with a long-term clinical benefit were enriched for a series of tetrapeptide motifs that were not found in tumours of patients with no or minimal clinical benefit (Snyder, Makarov et al. 2014). However, human neoantigens identified in other studies do not show the bias toward tetrapeptide signatures (Schumacher and Schreiber 2015, Stronen, Toebes et al. 2016).

1.7 Phosphoproteins in Cancer If phosphorylation is so important to cellular control mechanisms, then it stands to reason that a loss of this control could be implicated in cancer. Entire pathways could be altered, many of which could be implicated in tumorigenesis. Hannahan described the many hallmarks of cancer, which when considered – phosphorylation plays a role in all of them (Hanahan and Weinberg 2000, Hanahan and Weinberg 2011, Hanahan and Coussens 2012).

1.7.1 Phosphoproteins as immune targets As already alluded to, immunotherapies are an attractive anti-cancer therapy, however until now, a lack of tumour-specific targets has hampered their potential use. Members of this group, based on Hanahan's basic principles,

have identified MHC class I-associated phosphopeptides as representing a potential new class of tumour-specific targets (Hanahan and Weinberg 2000, Hanahan and Weinberg 2011, Hanahan and Coussens 2012, Penny, Abelin et al. 2012, Cobbold, De La Pena et al. 2013, Hanahan 2014, Abelin, Trantham et al. 2015). Posttranslationally modified antigens are increasingly being shown to play important roles in human disease. Phosphopeptide neoantigens have been identified on primary human malignant tissue and would be considered to be immunogenic in healthy donors or patients with cancer. MHC-I displayed phosphopeptides have been found to be over-represented on multiple leukemic malignancies. More aggressive malignancies display a greater diversity of phosphopeptides (Cobbold, De La Pena et al. 2013). Many of these tumour-associated phosphopeptides were found to be derived from oncogenes linked to leukemogenesis, making these of particular interest as immunotherapeutic targets. Dr Penny and Dr Cobbold found that by using the well-established autologous model of cancer in healthy individuals (LCL as an *in vitro* surrogate for PTLD), it can be demonstrated that phosphopeptides are the target of a significant proportion of all anti-tumour cytotoxic memory T-cell responses. They showed that MHC class-I and class-II phosphorylated peptides derived from phosphoproteins are abundant on the surface of tumours (Penny, Abelin et al. 2012, Cobbold, De La Pena et al. 2013, Abelin, Trantham et al. 2015). These antigens exhibit differential expression between healthy and malignant tissue with aggressive tumours displaying the most phosphopeptides. Memory-like $CD8^+$ T-cells against phosphoantigens are present in healthy donors, but are thought to be reduced in patients with cancer. We propose that this may be the case for paediatric liver tumours and also PTLD. To date no post-translationally modified tumour antigens have been identified from paediatric tumour samples. Thus the discovery of phosphopeptides in the paediatric tumours would incorporate novelty in addition to providing a translational output for this project.

Many phosphorylated peptide antigens have previously been discovered in haematological malignancies, breast tumours, melanomas and colorectal tumours (Syka, Coon et al. 2004, Cobbold, Polefrone et al. 2007, Mohammed, Cobbold et al. 2008, Depontieu, Qian et al. 2009, Penny, Abelin et al. 2012, Cobbold, De La Pena et al. 2013, Abelin, Trantham et al. 2015). Mass spectroscopy analysis of surface MHC-bound phosphopeptide display of EBV transformed B-cells (LCLs) has been performed with over 50 phosphopeptides identified. One particularly interesting antigen is derived from the cytoplasmic tail of CD19 (pCD19, DPTRRFFKVpTPPPGSGPQ) which the Cobbold lab have shown to be highly immunogenic in healthy individuals. pCD19-specific $CD4^+$ cells can be expanded *ex vivo* and can target human lymphoma both *in vitro* and *in vivo*.

1.7.2 Studying phosphorylation Sites High throughput studies have advanced with the advent of mass spectrometry. Precise localization of specific phosphorylation sites was made possible with the introduction of electron transfer dissociation (ETD) in the early 2000's. Enrichment of phosphopeptides by immobilised metal ion affinity chromatography or IMAC have allowed batch processing to become a reality (Syka, Coon et al. 2004, Abelin, Trantham et al. 2015).

1.8 Summary

The disease burden from cancer is largely underestimated. Morbidity from the disease and its treatment options together with mortality associated with disease spread and recurrence has led to an identified need for development of new cancer therapies. In paediatric hepatology key tumours of interest remain most commonly hepatoblastoma, more rarely hepatocellular carcinoma and the PTLD's following organ transplantation. Although over time survival has improved, mortality rates remain relatively high, with overall survival from hepatoblastoma for instance being ~65%. Traditional treatment options have been chemotherapy and organ

transplantation, which is not itself without risk of side effects which are often difficult to tolerate.

Cancers have developed a number of mechanisms for overcoming immune recognition. This was described in the seminal paper by Hannahan in 2000, and updated in 2011 to include newly identified mechanisms for evading immune surveillance. This has even included the concept of hallmark switching where tumours change from one mechanism of evasion to another in order to avoid recognition which has fed into the idea of chemotherapy resistance (Hanahan and Weinberg 2000, Hanahan and Weinberg 2011, Hanahan and Coussens 2012, Hanahan 2014). This so called 'Somatic Mutation Theory of Carcinogenesis' has been debated by a number of authors, who appeared critical of the original data analysis, suggesting that the original 'hallmarks' were also characteristic of benign tumours (Lazebnik 2010). Furthermore another review of the hallmarks proposed that cancer is perhaps a tissue based disease and the concept of 'Tissue Organisation Field Theory' was envisaged, where proliferation and motility are the default state of all cells, but it is the cell:cell interaction and cell:extracellular matrix interaction which has bearing on cancer development – i.e. cancer could be considered as disordered development 'development gone awry' (Sonnenschein and Soto 2013).

Clearly there are a number of potential signalling pathways which may be involved in cancer development and propagation. Hence identification of proteins involved in these pathways could potentially result in identifying a target for cancer therapy. The immune system plays a key role in tumour recognition - in particular the adaptive immune system cell response to cancer. MHC is also thought to play a pivotal role in this tumour recognition, resulting from cortical selection in the thymus, with those cells selected on MHC class I molecules becoming $CD4^{-}CD8^{+}$ cells and MHC class-II becoming $CD4^{+}CD8^{-}$ cells.

Immune surveillance was a concept initially proposed in the 1950's, where it was suggested that as cells became older they would inherit more changes which may be a step towards

malignancy and the authors proposed that there was a mechanism for recognising and eliminating such cells in order to prevent tumour development (Burnet 1957). However this theory has been questioned and more recently it has been proposed that inflammation may in fact be a cancer promoter (Balkwill and Mantovani 2001, Mantovani, Allavena et al. 2008, Balkwill and Mantovani 2012). Perhaps evidence to support this is seen in mouse models where if Burnet's initial theory were to be true, then we would expect immunodeficient mice to be more susceptible to cancer development. A number of studies have demonstrated this and therefore would suggest that immunosurveillance was at least partially responsible for recognition and elimination of malignant change (Gatti and Good 1971, Smyth, Godfrey et al. 2001, Swann and Smyth 2007, Senovilla, Vitale et al. 2012). It is not just adaptive immunity however that plays a role and this was tested by Stutman looking at nude mice and comparing them to wildtype mice. He found that there was no difference in cancer occurrence but this was proposed to be due to intact innate immune system – when tested again in RAG2 mice (which lacked the recombination activating gene (RAG) required for adaptive immune responses and the STAT1 gene that is required for innate immune responses) there was a large increase in tumour occurrence (Stutman 1974, Meraz, White et al. 1996, Shankaran, Ikeda et al. 2001), leading to a revival in the concept of immune surveillance being pivotal to tumour recognition and elimination.

Further evidence is demonstrated in humans with immunodeficiency, who go on to develop malignancy e.g. Kaposi sarcoma in HIV/AIDs secondary to viral infection – although this may well be an exaggerated response to infection, patients with immunodeficiencies are significantly more likely to develop malignancy compared to the normal population with or without viral infection being implicated (Cadranel, Garfield et al. 2006, Grulich, van Leeuwen et al. 2007).

Immunotherapies have been a significant development in cancer treatment resulting in development of vaccines, monoclonal antibodies, cytokine treatments and the identification and targeting of neoantigens expressed on tumour surfaces (Coiffier, Haioun et al. 1998, Davis, White et al. 1998, Barnett, Kryczek et al. 2005, Curiel 2007, Curiel 2007, Bhatia, Tykodi et al. 2009, Domingues, Turner et al. 2014, Marmarelis, Davis et al. 2016).

Ultimately, the importance of identifying mechanisms by which a multitude of cancers can avoid immune mediated recognition and destruction, could lead to identification of potential targets for immunotherapy. This therefore forms the basis for this PhD.

1.9 Project Aims

The primary aim of this project was to assess the relative contribution of phosphopeptide-specific T-cells to anti-tumour immunity. Initially, a well-established *in vitro* surrogate model of PTLD (LCLs) was used to assess the proportion of T-cell responses that are directed against phosphopeptides identified on these cells, and more importantly differentiate between tumour-specific and non-specific phosphopeptides. We hypothesized CTLs recognised phosphopeptide expressed on tumour surfaces leading to T-cell activation and tumour recognition/destruction.

The second aim of this project was to identify tumour-specific MHC class I-associated phosphopeptides displayed on hepatic tumours and PTLD. Phosphopeptides were extracted from patient samples and their counterpart normal tissue, or from established cell lines (HepG2) or LCL lines generated from healthy donors. Our collaborators in Virginia assisted in characterising these phosphopeptides, using their well-established nano-scale mass spectrometry techniques. Synthetic phosphopeptides were manufactured based on the phopshopeptide analyses of the tumour samples in order to determine if immunity targets phosphopeptides in cancer. We proposed phosphopeptides as an immune target, and therefore sought to identify tumour specific phosphopeptides involved in key cancer pathways. We also hypothesised that certain phosphopeptides may be organ specific based on the observation that certain phosphopeptides were common to a number of tumour groups – e,g, the crossover between HB, HCC and hepatic secondary tumours identified by other members of this group. In order to reduce the risk of potential autoimmunity, phosphopeptide responses were also tested in healthy individuals, to allow for identification of potential targets. This is based on the assumption that if healthy donors already have responses there should be a reduced risk of autoimmunity should these phosphopeptides be used in a clinical environment as a cancer chemotherapeutic for example.

The third aim of this project was to identify a process for immortalising tumour-specific/phosphopeptide-specific T-cells to provide a constant supply of re-agents to study responses to specifically phosphopeptides and more generally other tumour specific targets. This is of particular importance when investigating the specificity and function of anti-tumour T cells as T-cells grown in culture long term lose specificity and function, preventing further understanding of their function in vitro. Therefore, we proposed the use of Human Induced Pluripotent Stem Cell Technology (hIPSc) as a potential technique for overcoming this challenge. This is a technique described previously by groups attempting to study T-cells specific to disease to prevent disease progression in AIDS and Malignant melanoma (Nishimura, Kaneko et al. 2013, Vizcardo, Masuda et al. 2013) and we therefore proposed this as a viable technique for expanding T-cells *in vitro.* A future application of this technology could be to have a source of tumour-specific iPSCs that could be used to re-differentiate into effector cells that could be infused into a patient as a cell therapy. As this is a relatively new technique requiring some optimisation in experimental protocols, we sought to explore some older more well established techniques in order to probe the expression of antigen and phoshopeptides on both normal and transformed cell types *in vitro* including T-cell hybridoma technology (Taniguchi and Miller 1978) and the use of HVS (Biesinger, Mullerfleckenstein et al. 1992, Meinl, Hohlfeld et al. 1995, Fickenscher, Biesinger et al. 1996) to attain T-cell immortality.

Chapter 2: MATERIALS AND METHODS

It should be noted that a number of protocols included here are standard, well established protocols used within the Cobbold Group laboratory. In particular protocols 2.1-2.2, 2.4-2.14, 2.16-2.17 are common protocols shared and incorporated by the group, including Dr L Morton and Dr S Penny.

2.1 Cell Culture

Cell lines were grown from commercially available stocks originating from the European Collection of Cell Cultures (ECACC, HPA, UK) and the American Type Culture Collection (ATCC, LGC, USA). All cells were stored in foetal bovine serum (FBS, obtained from Sigma UK) with 10% DMSO (Sigma, UK) at -80°C or in liquid nitrogen. The cells were managed in sterile conditions in a laminar airflow tissue culture hood, at all times, and incubated at 37°C with 5% CO_2. For adherent cells (except iPS clones and OP9 mouse feeder cells), the media used was D-MEM (Dulbecco's Modified Eagle Medium (1X) liquid (High Glucose) (Gibco, UK), 10% FBS, 1% penicillin/streptomycin (Sigma, UK) and the cells were grown in 25cm^2, 75cm^2, 175cm^2 and 1720cm^2 vented tissue culture flasks, or sterile plates, with 20 mM HEPES (Gibco, UK) buffer added.

For IPSc clones, the following medias were used (tables 2.1a and b):

Table 2.1a: hIPSc media components

iPSCs Medium - (KSR) 500ml	Stock conc	Final conc	Volume
DMEM/F12 (Life Technologies, UK)			400ml
Knockout Serum Replacement (KOSR) Life Technologies, UK		20% v/v	100ml
L-Glutamine (Sigma, UK)	100x	2mM	5ml
MEM-Non Essential AminoAcids (MEM-NEAA) (Sigma, UK)	100x	1%	5ml
2-Mercaptoethanol (Sigma, UK)	98%	0.007%	3.5µl
Penicillin/Streptomycin (Sigma, UK)	100x	1%	5ml
bFGF (FGF2) (Life Technologies, UK)	4µg/ml	4ng/ml	500µl

Table. 2.1b: mIPSc/ESc media components

Component	Stock concentration	Final concentration	amount
Knockout-DMEM (Sigma, UK)			425ml
Knockout serum replacement (KOSR) Sigma, UK		15%	75ml
L-glutamine (Sigma, UK)	100mM	1mM	5ml
B-mercaptoethanol (Sigma, UK)	14.3M	0.1mM	3.5µl
Penicillin/streptomycin (Sigma, UK)	100x	1x	5ml
Leukaemia Inhibitory Factor (LIF) (Millipore, UK)	10^7unit/ml	1000u/ml	50µl
Non-essential amino acids	10mM	0.1mM	5ml
GSK inhibitor	10mM	3µM	15µl
MEK inhibitor	10mM	1µM	50µl

For all suspension cells (except T-ALL 104), the media used was RPMI-1640 (high glucose) (Gibco, UK), 10% heat inactivated Foetal bovine serum (FBS, Sigma UK) (equivalent to 10ml in every 100ml complete media), 1% penicillin/streptomycin (Sigma, UK equivalent to 1ml of stock Penicillin/streptomycin (100x) every 100ml complete media), and the cells were grown in vented tissue culture flasks, or sterile plates.

OP9 cells (obtained from Prof Anderson group, and recovered from -80c storage) were cultured in the following 'OP9 media'. Minimum Essential Medium- Alpha (α-MEM) powdered media is used (Gibco, Life Technologies, Paisley, UK). The powder is added to 900ml of sterile distilled water while stirring. The package is rinsed out at least twice. Once the powder has dissolved the following were added: 2.2g of Sodium Bicarbonate (Tissue culture tested) (Sigma, UK), 6ml of L-glutamine (200mM stock, Sigma, UK, 6ml of diluted ß –mercaptoethanol (Sigma, UK). Diluted 2-mercaptoethanol is made by adding 70µl of 2-mercaptoethanol (Sigma, UK) to 100ml of sterile PBS or water. 5ml of penicillin\streptomycin solution (Sigma, UK, 50µg/ml final conc.) Top up to 1L with sterile dH_2O Filter-sterilize using a 0.22µm bottle top filter. Before use add 100ml of FBS to the 500ml bottle.

T-ALL 104 cells were cultured in Iscove's Modified Dulbecco's medium (IMDM, Gibco, UK), 20% FBS (equivalent to 20ml in every 100ml complete medium), 1% penicillin/streptomycin (equivalent of 1ml of stock 100x Penicillin/streptomycin).

Cell counts and viability were determined by the exclusion of Trypan blue dye (Sigma, UK) by light microscopy. All cell lines were tested for mycoplasma infection using the Lonza MycoAlert Mycoplasma Kit (Lonza, ME, USA). Cells infected with Mycoplasma infections were discarded.

2.2 Plasma and cell preparation from whole blood

Fresh blood samples were collected from healthy donors (as per agreed local ethics – see appendix). 50 ml of blood was collected using vacutainers containing lithium heparin (BD, UK) – fig. 2.1. In order to obtain peripheral blood mononuclear cells (PBMCs), the blood was mixed with an equal volume of plain 1640 RPMI, layered onto ficoll-paque (Sigma, UK) and centrifuged at 500 x *g* for 20 min, without a brake. The PBMCs were collected from the interface, washed twice in plain 1640 RPMI (500 x *g*, low brake), counted and resuspended in RPMI 10% FBS for use in experimental studies, or FBS 10 % DMSO at 1 x 10^7 cells/ml for storage at -80 C.

Fig 2.1: Preparation of PBMC's from whole blood. Blood was obtained from subjects (50-60ml). Equal volumes of warmed plain RPMI were added. Fresh 50ml tubes were prepared with a base layer of 15ml of FicollPaque. The Blood/RPMI mix was then carefully layered on top of the FicollPaque, being careful not to shake the samples. They were then spun initially with no brake for 20 mins at 500 *g*. The PBMC's were collected from the interface layer, and transferred to fresh tubes. These were topped up with more warmed RPMI and washed x2 at 500 *g* for 10 minutes on a low brake. Finally the resulting pellet was resuspended in T-cell media and used for experimentation or frozen at -20c.

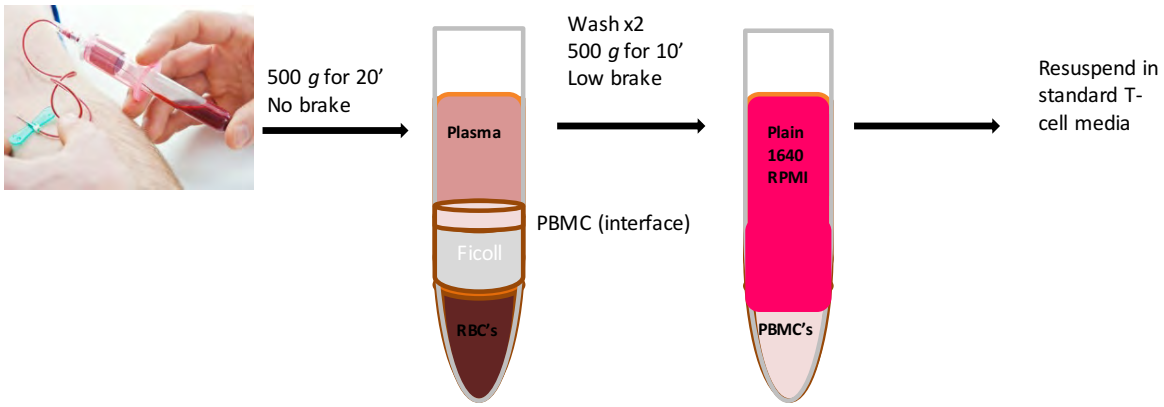

2.3 Immortalization of human B cells using EBV

EBV-transformed B95-8 marmoset cell line was procured from ATCC, USA and the EBV stock prepared (with the assistance of Dr C Shannon-Lowe). $0.5x10^6$ cells/ml were seeded in RPMI-1640, 15% FCS (Invitrogen, Carlsbad, CA), 200mM L-glutamine (Sigma, UK) and 1% penicillin/streptomycin (equivalent of 1ml of stock 100x Penicillin/streptomycin in 100ml complete media) (Sigma, UK). After 3 days, cells were spun down and the supernatant collected and passed through a 0.45µM filter. This was subsequently aliquoted and frozen at -80°C.

PBMC's were prepared as described previously and were seeded in a sterile 24 well plate at a density of $1.5\text{-}2x10^6$ cells/ml in Dulbecco's modified eagles medium (DMEM) (Gibco, UK) containing 15% FCS (Sigma, UK), 200 mM L-glutamine (Sigma, UK) and 1% penicillin/streptomycin (equivalent of 1ml of stock 100x Penicillin/streptomycin) per 100ml complete media (Sigma, UK).

EBV virus was added to PBMCs at 1:1 ratio (V/V) and placed in an incubator maintained at 37°C with 5% CO_2. After 2 hours, 5ml of complete medium was added containing cyclosporin A (final concentration of 0.5ug/ml). Media was changed twice weekly and cells cultivated for

a further 4 weeks. Cells were mixed thoroughly to break clumps before splitting to ensure multiclonal population (Neitzel 1986) – fig 2.2.

Fig 2.2: Generation of LCL's from PBMC's using EBV. PBMC were generated using standard methods as previously described. Cells were infected with EBV and incubated for 2 hours at 37c. Following this media was changed and supplemented daily with cyclosporin to remove any T-cells which would otherwise target infected B-cells for destruction. Media was changed twice weekly for 4 weeks, resulting in pure growth of LCL's.

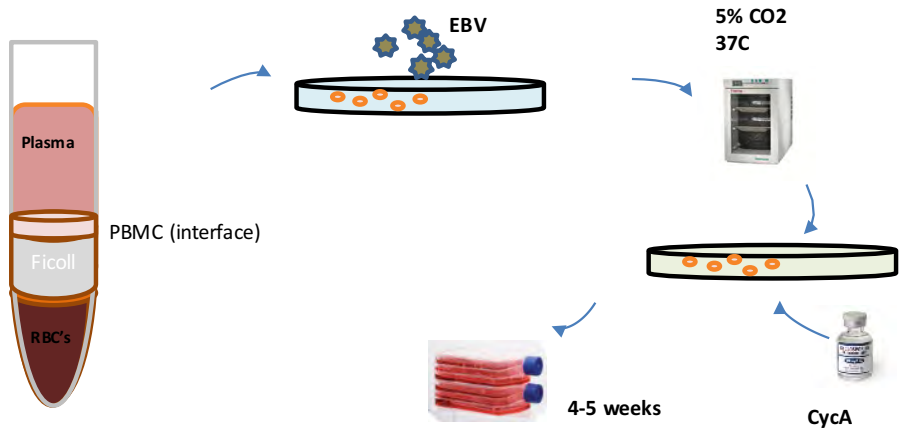

2.4 Flow cytometric analysis of T cell populations

Flow cytometry provides quantitative multiparameter analyses on single cells based on the measurement of visible and fluorescent light emission. The cells to be tested were placed into a 5ml FACS tube and the relevant antibodies added (e.g. anti-CD3-APC and anti-CD4-FITC were added at 1:100 dilution (BD Biosciences, CA, USA)) and the mixture incubated for 20 min at room temperature in the dark. The cells were then washed twice in 2 ml MACS buffer (Miltenyi, USA) (PBS, 2 mM EDTA, 2% FCS) and isolated by centrifugation at 500 x *g* for 10 min. The cells were then resuspended in 200 µl MACS buffer and analysed on the flow cytometer (Fortessa20, BD, NJ, USA) using the BD FACSDiva software (BD, NJ, USA). The exported files were then analysed using FlowJo (FlowJo LLC, CA, USA) software.

2.5 Magnetic activated cell sorting

Magnetic activated cell sorting (MACS) involves labelling cells with magnetic MicroBeads conjugated to the desired antibodies. The cells are then passed through a magnet via a plastic

column, and the magnetically labelled cells are thus separated from the unlabelled cells as the labelled cells remain in the column and the unlabelled flow out. The labelled cells are then eluted from the column by removing the magnet and applying kinetic energy, as per manufacturer guidelines (Miltenyi Biotec, Bisley, UK). The beads remain on the surface of the cell and are eventually endocytosed and degraded (they are non-toxic, biodegradable and biologically inactive) - fig. 2.3.

Fig 2.3: Schematic describing magnetic bead separation of T-cells.
PBMCs were obtained using standard methods as described previously. Magnetic beads are coated/labelled with CD8 antibody and mixed with the PBMC's. PBMC's were then applied to a column set within a magnetic field. The $CD8^+$ cells remain in the column and can be eluted out with kinetic force after the mixture has run through the column. The non $CD8^+$ cells will run through the column and are collected in a tube for either experimentation or to be discarded.

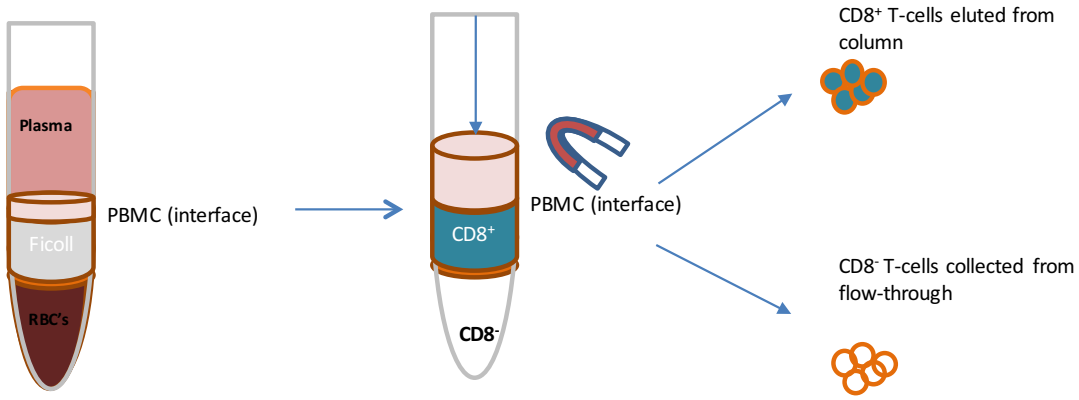

2.6 Enzyme-linked immunospot (ELISpot) assay

ELISpot assay is used for the detection of individual cells secreting specific cytokines/antigens (Czerkinsky, Tarkowski et al. 1984). The ELISpot PRO for human IFNγ kit (Mabtech, Sweden) was used for these experiments. Polyvinylidene difluoriden (PVDF)-backed 96 well plates were coated with a monoclonal antibody specific for human IFNγ were washed five times with sterile PBS (200 µl/well). The wells were then blocked by incubation with RPMI 10% FBS for 30 min at room temperature. The medium was removed and a cell suspension of the PBMCs (5 x 10^5/well) or T-cells (1 x 10^5/well) of interest, in RPMI 10% FBS, or T-cell medium, added. The stimulating peptides were then added to the test wells, 1% 1x DMSO to

the negative control (as this was the solvent used to dissolve the peptides) or 10µg/ml phytohaemagglutinin (PHA) (Sigma, UK), as the positive control. The plate was incubated for 16-24 hours at 37C. The cells were then removed and the plate washed five times with PBS (Sigma, UK) (200 µl/well). The one-step detection reagent (mAb 7-B6-1) was diluted 1:200 in 1x PBS 0.5 % FBS and 100 µl added to each well and incubated at room temperature for 2 hours. The plate was again washed five times with PBS (200 µl/well). Steptavidin-ALP was diluted 1:1000 in PBS 0.5% FBS and 100µl was added to each well and the plate incubated for a further hour. The plate was again washed 5 times with PBS (200µl/well). The ready to use substrate solution (BCIP/NBT-plus) was filtered through a sterile 0.45 µm filter and 100 µl added to each well. When spots started to appear the plate was extensively washed with tap water and dried. Once dry, the spots representing individual IFNγ secreting cells were counted using an ELISpot reader (AID ELISpot Reader HR XL, Advanced Imaging Devices GmbH, Germany)) and images captured using the AID ELISpot Software 4.0 (AID GmbH, Germany) fig. 2.4.

Fig 2.4: Schematic describing the processes involved with EliSpot.
Pre-coated 96w plates were washed with sterile PBS and blocked using the same growth media that the cells to be tested were being cultured in e.g. RPMI/10% FCS for half an hour. Plates were washed thoroughly with PBS again and required number of cells added. Plates were transferred to an incubator for 16-24hours 5%CO_2 37c. Following this, plates were thoroughly washed with PBS x2 and a detection reagent added as per ELISpot kit used. Plates were incubated at room temperature for 2 hours and washed again in PBS. Then a pre-made substrate (from the kit used) was filtered using 45µM filter and this was added to the plates to enable detection of spots within the wells equating to cell activation i.e. detection of IFNγ. Plates were washed with PBS then distilled water and dried, and read on an appropriate plate reader as per manufacturer's recommendations.

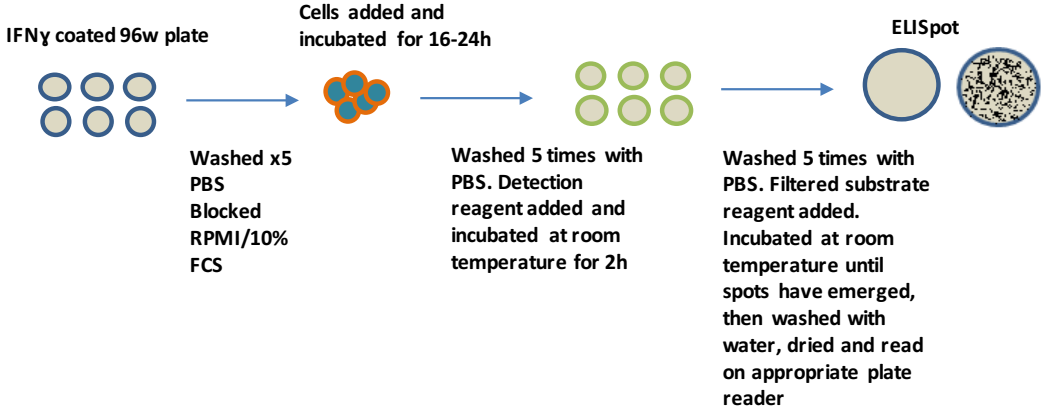

2.7 Europium Killing assay (Perkin Elmer, via Fisher Scientific, USA)

A fluorescence assay to study the loss of membrane integrity was used. In this assay, target cells are loaded with fluorescence enhancing ligand, BATDA, which penetrates the cell membrane quickly and is hydrolysed to form a hydrophilic ligand (TDA) that is released from cells only after cytolysis. In the presence of a solution containing $Eu3^{+}$, the released TDA forms a highly fluorescent and stable chelate (EuTDA), whose levels are measured using time-resolved fluorescence. Target cells were washed in the relevant medium and resuspended to 1 million cells/ml. 2.5 µl/ml of the BATDA fluorescence enhancing ligand was added and the cells incubated for 30 minutes at 37 °C, humidified 5 % CO_2. The cells were washed five times in excess medium. 10,000 target cells were added to each well of a V-bottomed 96-well plate. T cells at varying effector to target (E:T) ratios were added to the test wells. Lysis buffer was added to the wells. All well volumes were made up to 200µl. The plate was incubated for 2-5 hours in a humidified 5 % CO_2 at 37 °C. 20µl of each supernatant was transferred to a flat-bottomed, white, 96-well plate and 200 µl of Europium solution was added. This was incubated for 15 minutes, shaking, at room temperature. The fluorescence was measured in a time-resolved fluorometer (Tecan Infinite 200 PRO; Tecan, Switzerland).

2.8 Fluorescence-activated cell sorting

Fluorescence-activated cell sorting (FACS) was used to separate $CD8^{+}$ T cells into cellular memory compartment. MACS selected $CD8^{+}$ T cells were sorted into naïve ($CD27^{+}$, $CD45RA^{+}$), central memory ($CD27^{+}$, $CD45RA^{-}$), effector memory ($CD27^{-}$, $CD45RA^{-}$) and terminal effector memory compartments ($CD27^{-}$, $CD45RA^{+}$) using antibodies CD45RA-PerCP and CD27-FITC (Becton Dickinson (BD), CA, USA). These cells were sorted slowly using the FACS Aria II to ensure accurate sorting (BD, NJ, USA).

2.9 Phosphatase treatment of LCLs

LCLs were washed and phosphatase treated using Shrimp alkaline phosphatase (SAP) - (Sigma-Aldrich, Gillingham, UK). The reaction was performed in T-cell medium containing 50 mM Tris-HCl and 5 mM $MgCl_2$, with 10 units/ml of SAP, at 37 °C, for one hour (all components obtained from Sigma, UK). The LCLs for ELISpot were washed, then lightly fixed by a ten minute incubation in 1 % paraformaldehyde (Sigma, UK), which was quenched using 0.2 M glycine (in house stock). The cells for use in the killing assay were washed and loaded with BATDA solution (as described in section 2.7).

2.10 Isolation of HLA-associated Peptides

MHC class I molecules were immunoaffinity purified and their associated peptides were extracted as previously described (Zarling, Ficarro et al. 2000) – fig 2.5. A billion cells were lysed in 10 ml CHAPS buffer (20 mM Tris-HCl pH 8.0/ 150 mM NaCl with 1 % 3-[(3-cholamidopropyl) dimethylammonio]-1-propane sulfonate (CHAPS)/ 1 mM PMSF/ 5 µg/ml aprotinin/10 µg/ml leupeptin/10 µg/ml pepstatin A/ and 1:100 dilutions of phosphatase inhibitor cocktails II and III (to prevent potential dephosphorylation of peptides during extraction) (all components obtained from Sigma, UK)). The lysate was subject to centrifugation at 100,000 x *g*, for 1 hour, at 4 ºC, in an ultra-centrifuge (Optima LE-8K (Ti70 rotor), Beckman-Coulter, UK). Supernatants were incubated with W6/32 antibody-bound NHS sepharose beads, specific for MHC class I molecules (Amersham Pharmacia Biotech). The beads were washed in lysis buffer, TBS (20mM Tris-HCl/ 150 mM NaCl pH 8), TBS2 (20 mM Tris-HCl/ 1 M NaCl pH 8), and 20 mM Tris-HCl pH 8. Peptides were eluted from the MHC class I molecules with 10% acetic acid and separated using a 5,000-dalton cut-off ULTRAFREE-MC filter (Millipore, MA, USA). Extracted peptides were stored at −80°C and shipped to Virginia, USA, on dry ice, for analysis.

Fig 2.5: Schematic describing work-flow for tumour-specific, MHC class I-associated phosphopeptide discovery from patient samples

Tumour and adjacent normal liver tissue were obtained from the same patient at tumour resection/explant. These solid tissue samples were each lysed and the MHC class-I complexes affinity purified using the pan class-I antibody, W6/32. The MHC class I-associated peptides were eluted in acid as per standard protocol at University of Birmingham within the Cobbold laboratory. Our collaborators at University of Virginia enriched the phosphopeptides using IMAC. These phosphopeptides were then characterised using CAD and ETD LC-MS/MS and the sequences manually assigned.

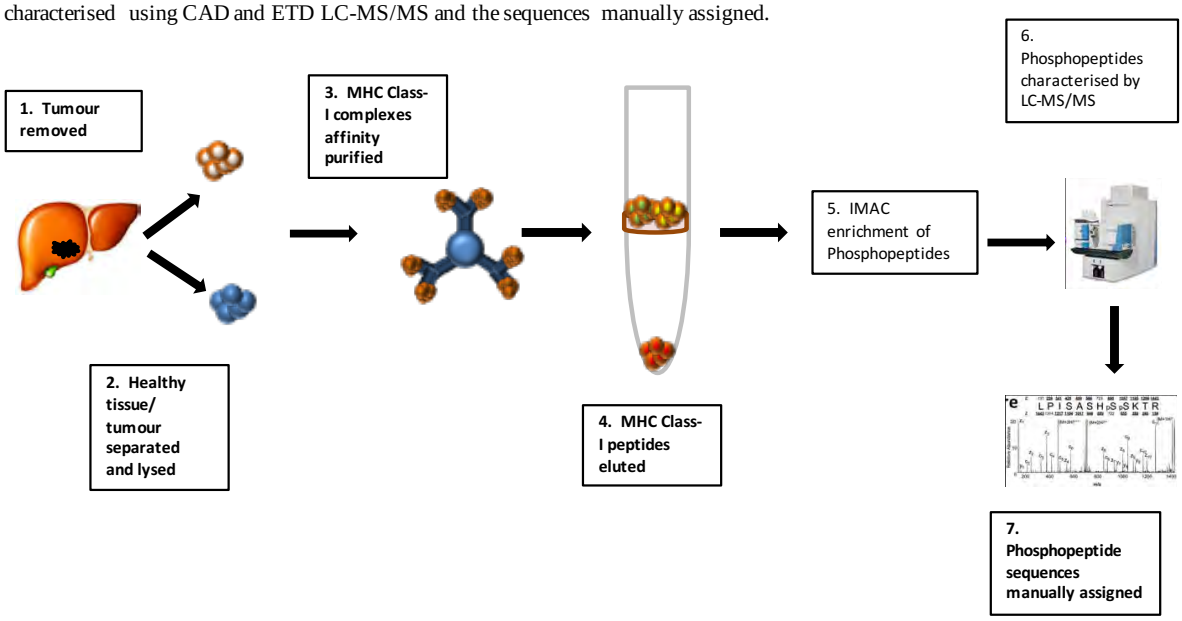

2.11 Mass spectrometric analysis of phosphopeptides

(Performed by Paisley Trantham/Stacy Malaker, VA, USA)

HLA-associated peptide mixtures were dried to completion in a Centrivap and reconstituted in 0.1 M acetic acid to a final concentration of $1x10^7$ cell equivalents per microlitre. For tissue samples, it was assumed that 1 gram of tissue contained $1x10^9$ cell equivalents.

Samples were initially screened to assess peptide levels. The data from these screens was used in the plasma biomarker analysis. For phosphopeptide analysis, samples were standardised to similar peptide levels, using peptides identified in the JY cell line. A portion of each sample containing $1x10^7$ cell equivalents with 100 fmol of two internal standard peptides, HSDAVFTDNYTR (vaso) and DRVYIHPFHL (angio), was pressure loaded onto a C18 microcapillary pre-column (packed with 7 cm of C18 reversed-phase packing material (5-20 µm diameter, 120 Å pore size)) and connected to an analytical column packed with an irregular C18 packing material (5-20 µm diameter, 120 Å pore size).

Peptides were gradient eluted at a flow rate of 60 nl/minute, using an LC gradient of 0-60 % solvent B in 40 minutes (solvent A: 0.1 M AcOH in H_2O; solvent B: 70% ACN, 0.1 M AcOH in H_2O), through an electrospray tip directly into a LTQ-FT-ion cyclotron resonance mass spectrometer. MS data was acquired in the high-resolution Fourier transform mass analyser, and the MS2 data was acquired in the linear ion trap of the LTQ-FT-ion cyclotron resonance instrument using CAD and front-end ETD.

Data analysis was performed using the Xcalibur software (Thermo Electron Corporation). The data file generated was searched against the RefSeq database using OMSSA (version 2.1.1). Searches of CAD and ETD data used the following parameters: no enzyme specificity, E-value cut-off of "1", variable modifications oxidation of Met, phosphorylation of Ser, Thr, and Tyr, and ±0.1 Da and ±0.35 Da for precursor and product ion masses, respectively. OMSSA results were used to guide the analysis, but all peptide sequences were determined by accurate mass measurement and manual interpretation of the MS2 spectra.

A normalised amount of sample was then cleaned, using another C18 column, prior to phosphopeptide enrichment. One hundred fmol of phosphopeptide standards DRVyIHPF (angio II phosphate (AIIP)) and STsLVEGR (STS) were added at the beginning and end of this process, respectively, to allow measurement of phosphopeptide recovery. These samples were then washed in methanol and dried to completion, thrice. The dried clean-up elutions were then esterified using methanolic HCl. This converts the carboxylic acid side chain of Asp and Glu to esters, to prevent the non-specific binding of peptides containing these amino acids to the IMAC column.

An IMAC column packed with 5 cm of POROS® MC 20 imidodiacetate packing material was used to enrich for phosphopeptides. The IMAC column was activated using filtered 100 mM $FeCl_3$. The column was equilibrated with 0.01% acetic acid, the sample loaded and the column rinsed in the same acid. Phosphopeptides were then eluted onto a C18 precolumn (5-20 µm

diameter, 120 Å pore size) with a pressure load of 250 mM ascorbic acid in water (pH 2) at a flow rate of 1 µl/min for 25 minutes followed by a 10 minute 0.01% acetic acid rinse at the same flow rate. As for the screen, the precolumn was connected to a C18 analytical column and the peptides eluted into the MS, using similar parameters.

Data analysis was performed by using the Xcalibur software (Thermo Electron Corporation). The data file generated was searched against the RefSeq database using OMSSA (version 2.1.1). Searches of CAD and ETD data used the following parameters: no enzyme specificity, E-value cut-off of "1", fixed modifications methyl ester of Asp, Glu, and C-term, variable modifications oxidation of Met, phosphorylation of Ser, Thr, and Tyr, and ±0.1 Da and ±0.35 Da for precursor and product ion masses, respectively. The data file was also searched using an in house program developed by Dina Bai called "Neutral Loss Finder" that identifies MS2 CAD spectra with the neutral loss of phosphoric acid (98 Da) characteristic of phosphopeptides. OMSSA and neutral loss search results were used to guide the analysis, but all peptide sequences were determined by accurate mass measurement and manual interpretation of the MS2 spectra. Manual interpretation of spectra was aided by another in house program developed by Dina Bai called "Fragment Calculator". Fragment Calculator allows the user to calculate the b-, y-, c-, and z-type ions of hypothetical peptides so that spectra can be manually validated.

2.12 Tumour Infiltrating Lymphocyte (TILs) isolation and expansion

Tumour was obtained fresh from the Queen Elizabeth Hospital (QEH) Pathology laboratory and Birmingham Children's Hospital (BCH) Clinical Histology, which was processed fresh in sterile saline, and shipped to the HBRC biobank based at the Queen Elizabeth Hospital, Birmingham for annonymisation and logging. In a laminar flow hood, the tumour was sliced into small (2 mm x 2 mm) chunks and each one placed into 2 ml T-cell medium, containing

extra antibiotics to eliminate gut bacteria and yeast (AIM-V/ 10 % Human serum/ 25 mM HEPES/ 6000 IU/ml IL-2/ 50 µg/ml neomycin/ 2 µg/ml micofungin/ 55 µM β-mercaptoethanol/ 15 µg/ml metronidazole/ 20 µg/ml vancomycin) (all tissue culture reagents obtained from Sigma, UK). The TILs were maintained at $1x10^6$ cells/ml in T-cell medium in a 24-well plate for 14-21 days. The cells were subsequently FACS analysed to determine the proportion of $CD8^+$ TILs and aliquots frozen.

TILs were rapidly expanded using a standard rapid expansion protocol (REP) (Dudley, Wunderlich et al. 2003). A million thawed TILs were added to REP medium (200 million irradiated buffies/ 30 ng/ml OKT3/ 6000 IU/ml IL-2/ 50 ml RPMI 10% HS/ 50 ml AIM-V/ 50 µg/ml neomycin/ 2 µg/ml micofungin/ 55 µM β-mercaptoethanol/ 25 mM HEPES). Half of the medium was exchanged on day 5. On day 7 the TILs were counted and their density reduced to 0.5 million/ml. Cells were maintained at 0.5 million/ml until day 14 when aliquots of up to 30 million TILs were frozen, in FCS 10 % DMSO.

2.13 Intracellular cytokine staining

Cytokine production in response to specific stimuli can be measured using intracellular cytokine staining. Golgi inhibitors are used to prevent cytokine release from the cells and the cells fixed and permeablised to allow antibodies to access the intracellular compartments. The expanded TILs were thawed and plated at 200,000 per well of a 96-well plate, in TIL medium containing 5 µg/ml of Brefeldin A and monensin and 0.5 µg anti-human CD107a-FITC antibody (eBioscience, CA, USA), and stimulated with 50 µg/ml peptide. Unstimulated TILs were used as a negative control and TILs stimulated with PMA (5 ng/ml) and Ionomycin (400 ng/ml) (Sigma, UK) were used as a positive control. The cultures were incubated for 5 hours at 37° C, 5% CO_2 in a humidified environment. They were then harvested, washed with PBS and stained with a fixable viability dye (APC-Cy7) and the surface antibodies, anti-CD3 (APC)

and anti-CD8 (PerCP) (BD, Oxford, UK). The cells were then washed in MACS buffer, fixed, using 2 % paraformaldehyde, washed, permeablised, using 0.5 % saponin, and stained with anti-IFNγ (PE), anti-IL-2 (Pacific blue) and anti-TNFα (PE-Cy5.5) (BioLegend, Cambridge, UK) for 30 minutes at room temperature. Cells were washed again with MACS buffer and lightly fixed until they could be analysed on the FACS Canto flow cytometer (BD, Oxford, UK).

TIL responses were expanded over 7 days, by incubating 200,000 TILs/well of a 48-well plate in T-cell medium supplemented with 6000 IU/ml of IL-2. TILs were rested overnight, and stimulated the following day with 10 μg/ml peptide. The positive control was stimulated with 1 μg/ml PHA. On day 6 the TILs were all washed twice in RPMI 10 % FCS and resuspended in T-cell medium supplemented with 6000 IU/ml IL-2 and 5 μg/ml each of Brefeldin A and monensin. Each well was restimulated with 10 μg/ml of the relevant peptide overnight. They were then harvested, washed with PBS and stained with a fixable viability dye (APC-Cy7) and the surface antibodies, anti-CD3 (APC) and anti-CD8 (PerCP) (BD, Oxford, UK). The cells were then washed in MACS buffer, fixed, using 2 % paraformaldehyde, washed, permeablised, using 0.5 % saponin, and stained with anti-IFNγ (PE), anti-IL-2 (Pacific blue) and anti-TNFα (PE-Cy5.5) (BioLegend, Cambridge, UK) for 30 minutes at room temperature. Cells were washed again with MACS buffer and lightly fixed until they could be analysed on the FACSCanto II flow cytometer (BD, Oxford, UK).

2.14 Enzyme-linked immunosorbent assay

An enzyme-linked immunosorbent assay (ELISA) was used to assess the production of IFNγ by activated T-cells. Multisorb 96-well plates (Thermo- Fisher Scientific, Hereford, UK) were incubated at 4°C overnight with IFNγ as a capture antibody, and then washed 5 times with PBS. The wells were then blocked with a RPMI/10% FCS for 1 hour at room temperature and

washed, as before. The sample was incubated in the wells for 2 hours and then washed off. The primary antibody, was incubated for 2 hours at room temperature and washed. The alkaline-phosphatase (ALP) linked streptavidin was then incubated for 1 hour at RT and washed. The chromogenic substrate, 3,3',5,5'-Tetramethylbenzidine (TMB) (10 ml phosphate citrate buffer (pH5)/ TMB tablet/ 2 µl Hydrogen peroxide) (Sigma, UK) was added to the wells and positive wells turned blue. After 15 minutes, the reaction was stopped with 10% HCl and the plate read at 450 nm in a GloMax microplate reader (Promega, UK).

2.15 Hybridomas

Various techniques are described for the generation of a T-cell hybridoma, and these are explored below, using the basic concept of fusing a target cell to a fusion partner.

2.15.1 Hybridomas – creation of fusion partner

Jurkat-GFP cells were obtained from Dr Millar cultured as per standard conditions. 5-20x10^6 were then taken to the irradiator and irradiated at 600 rads. Following this the cells were washed twice in RPMI and resuspended at a concentration of 20 million cells per well in a 12 well plate (Corning, USA) in RPMI + 10% FCS with IL-2 at 100units/ml. Fresh media was exchanged daily for the first 3 days. Following this, cells were put on 6-thioguanine (Sigma-Aldrich, USA) selection at either 1uM or 10uM made as per manufacturer's instruction in fresh media. Cells were put on selection for 1 week, at which point they were centrifuged at 500 x *g* for 15 minutes with Ficoll-paque (Sigma, UK) to remove the dead cells and then media exchanged for fresh RPMI + FCS (without 6-thioguanine) for 7 days before being put back on 6-thioguanine selection again. Following a second week on selection, media was again exchanged for fresh RPMI + FCS (without 6-thioguanine). This pulsing of 6-Thioguanine

continued for a further 2 rounds, following which cells were cultured in fresh RPMI + FCS and allowed to expand (fig. 2.6).

Fig 2.6: Schematic describing creation of a fusion partner for T-cell hybridomas.
A malignant partner cell line was identified for use to generate T-cell hybridoma. This partner cell line was irradiated and resuspended in fresh 1640 RPMI. On Day 3 following irradiation 6-Thioguanine was added at a concentration of 10µM. Cells were incubated at 5%CO_2/37c. Media changes were performed every 7days alternating between RPMI + IL2, or RPMI + IL2 + 6-thioguanine for 35 days in total, allowing for selection of HPRT-enzyme deficient cells which are the cells which are resistant to 6-thioguanine.

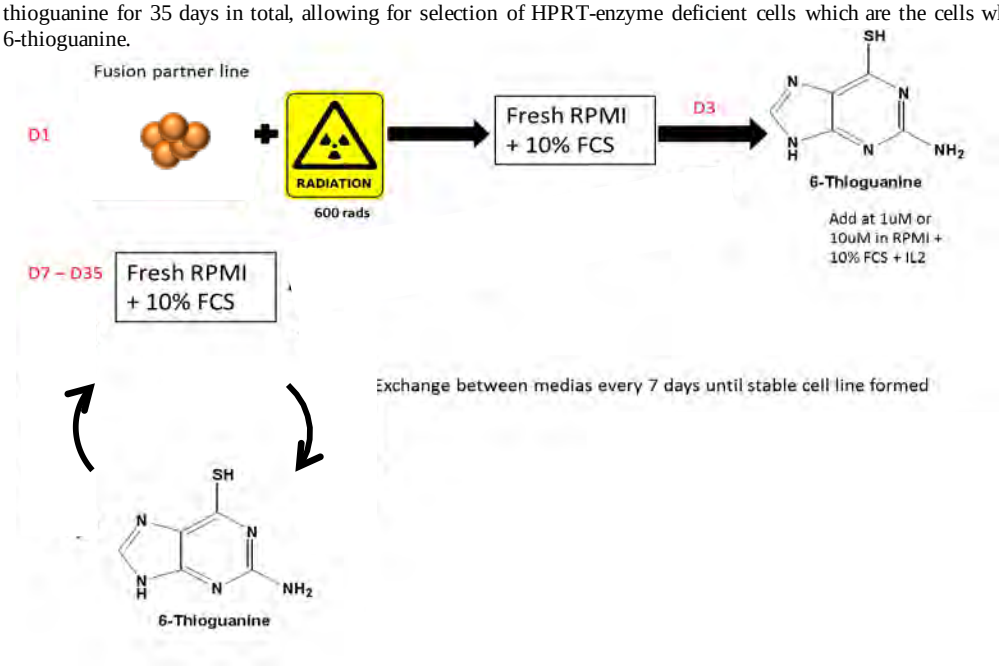

2.15.2 Hybridomas – creation using PEG/DMSO (protocol described by Dr M Goodall, Clinical Immunology, University of Birmingham)

Three days prior to fusion cells were optimised to a final density of $2x10^6$/ml. On day of fusion, cells were counted and plated into a 24-well plate at a density depending on experimental conditions. Controls set up in triplicate: fusion partner, target cell line, mixture of fusion partner and target cell line. Cells were suspended in suitable growth media (RPMI/10% FCS is a standard, however where using PEG (obtained from Dr Goodall) or PEG/DMSO, FCS should be omitted until cells washed).

$1x10^7$ fusion partner cells were added to equal number of target cells in a 50ml falcon. Cells were washed 3 times in RPMI (No FCS), 500 x *g* for 5 minutes. Falcon was placed in water bath at 37°C. PEG (or PEG/10% DMSO) was preheated in the same water bath. 200µl of

PEG was slowly added to the pellet using a transfer pipette over 1 minute, mixed by gentle shaking and incubated for 10mins. The mixture was gently mixed for a further 2 minutes, and then 20ml of plain RPMI was added over the following 5 minutes. The mixture was then placed in the water bath and left for 5 minutes prior to centrifuging at 500 x *g* for 5 minutes. The supernatant was aspirated and the pellet was gently resuspended in RPMI/20% FCS and transferred to a T25 flask. Selection with Hypoxanthine-aminopterin-thymidine (HAT) media (obtained from Dr Goodall) (100µM, 0.4µM, 16µM final concentration in DMEM respectively) was performed after 48hours. (Kohler and Milstein 1975) – fig. 2.7.

Fig 2.7: Schematic describing formation of T-cell hybridoma.
Fusion partner cell line created as previously described and fused with target T-cell using standard protocols. Cells remained in culture and had selection pressures applied HAT/6-thioguanine to remove any un-fused cells, leaving a pure population of fused hybridoma cells.

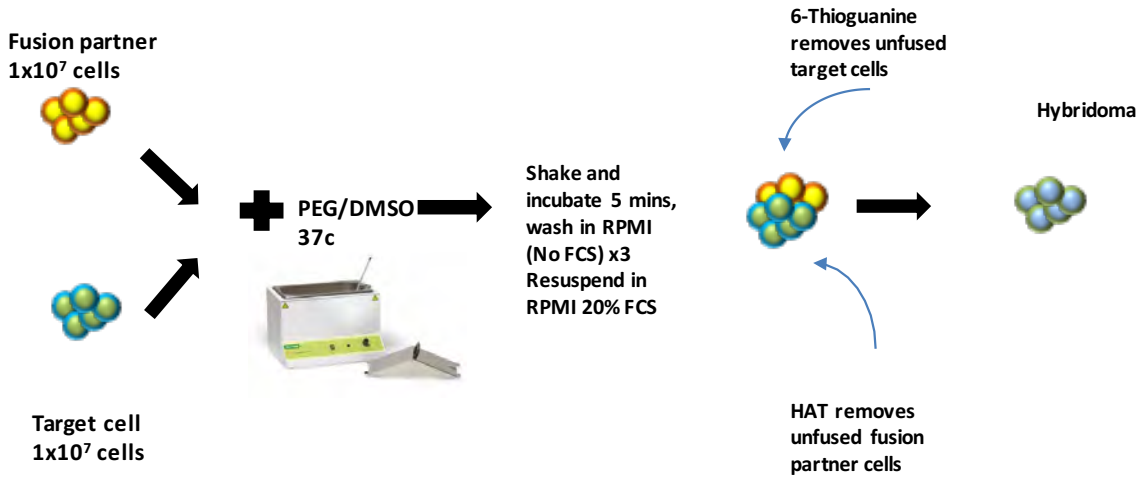

2.15.3 Use of polycations and plant lectins

Prior to hybridisation, polycation concentrations were calculated from stock. Polyvinylpyrrolidone (PVP, Sigma, UK) of various molecular weights (10,000, 40,000, and 360,000) were dissolved in the autoclaved 1640 RPMI to prepare 9 g/l stock solutions, which were then filter-sterilized using a cellulose acetate membrane syringe filter (0.2µm). The optimum dose of PVP was found to be 0.75g/l. If the experiment was using PVP then this was added 40 minutes prior to polycation in each well. Cells were not washed but polycation was added at desired concentration for 20 minutes. Cells were washed in plain RPMI and protocol

followed as per standard protocol above (Matsuya and Yamane 1985, Matsuya and Yamane 1985).

2.15.4 Transfection of hybridoma cells

Equal numbers of target:fusion cells were set up as per experimental design ($5x10^5$ – $2x10^6$ unless stated otherwise). Lonza nucleofection solution (Lonza, UK) was added to the appropriate supplement as per manufacturer instruction (Kit-V was used as designed for jurkats). Cells were centrifuged in 1.5ml microtubes, 90 x *g* for 10 minutes. Pellet was resuspended in the nucleofection solution and transferred into manufacturer's cuvette. Target DNA was added at suitable concentration (3ug VSV-G obtained in house). Cuvettes were nucleofected using Amaxa Nucleofector 2d (Lonza, UK) using programmes X-001 and X-005 - this machine was kindly loaned by Professor Murray, Cancer Studies, University of Birmingham. Cells were transferred back into 24 well plates and media was added (RPMI/10% FCS) to a final volume of 2ml and cells incubated at 37°C.

2.15.5 Use of electroporation

The ECM1000 (Harvard Apparatus, Boston, USA) allowed for the use of AC and DC current to achieve cell fusion. AC current allows for cells to line up in chains due to electrokinetic energy. A DC pulse then causes cell membrane pores to form and fuse.

Equal numbers of T-cell population and fusion partner were mixed and resuspended in BTXpress Cytofusion media (Harvard Apparatus, Boston, USA). Cells were washed twice (500 x *g*, 10 minutes). Each reaction was then resuspended in 2ml of cytofusion media and loaded into the fusion chamber. Electrodes were attached and programme set as per required parameters (e.g. AC 65v for 30 seconds, 9 second pause, followed by a DC pulse of 2000v for

25µs). Cells were then left in the electroporation chamber for 10 minutes prior to being transferred to cell culture plate and topped up with regular cell media – fig. 2.8.

Fig 2.8: Simplified schematic describing formation of T-cell hybridoma using the ECM1000 electroporator.
Fusion partner cells and target cells were washed x2 using manufacturer provided BTXpress media. They were then resuspended in this and transferred to the electroporation chamber. This was connected to the ECM1000 and the pre-set programme started (determined based on cells used). AC voltage allows for cells to rearrange in a linear fashion due to cell:cell polarity. DC current allowed for cells in close contact to fuse. Following this process, cells were 'rested' in the electroporation chamber for 15 minutes at room temperature within the laminar flow hood before being transferred to a suitable tissue culture vessel and transferred to an incubator set at 5% CO_2/37c.

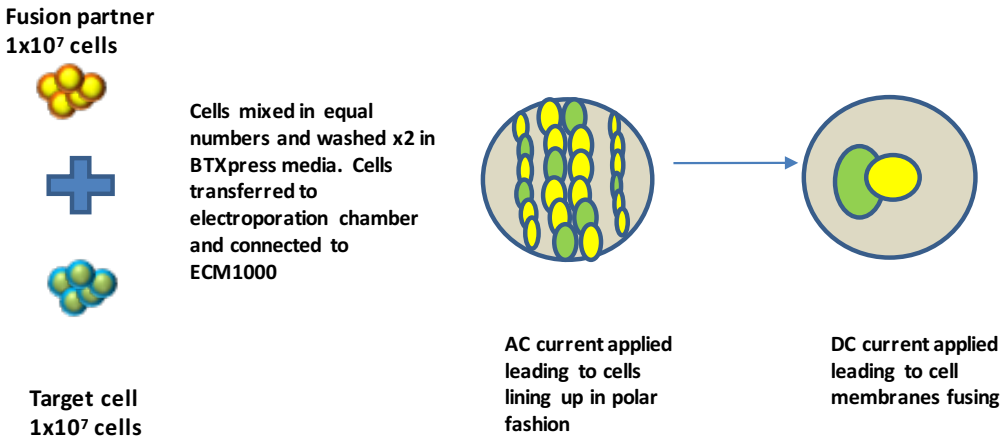

2.16 Lentiviral Transfections

Lenti-X 293T HEK cells (Clontech, CA, USA) were grown on a 24-well plate to 60-80% confluency. DNA of the gene of interest was co-transfected into the cells with gag-pol and VSV-G (1 ml Optimem/ 3 µg gag-pol/ 1 µg VSV-G/ 4 µg DNA GoI/ 8 µl PLUS reagent/ 15 µl LTX reagent), as per manufacturer's instructions (Clontech, CA, USA). After 4 hours incubation, 3 ml D-MEM (Gibco, UK) (10% FBS/ 1% 1x penicillin-streptomycin (Sigma, UK)) was added to the cells. 24 hours post-transfection the medium was replaced with 3 ml of fresh D-MEM (10% FBS/ 1% 1x penicillin-streptomycin). This medium containing virus was then harvested at 48 hours post-transfection, fresh medium added and collected the following day. The virus was then concentrated 10-fold using the Lenti-X concentrator (Clontech, CA, USA), resuspended in phosphate buffered saline (PBS) and stored at -80 ºC.

2.17 Lentiviral Transductions

Cells to be transduced were plated at $5x10^5$ cells per well in 24-well plates in D-MEM (10 % FBS/ 1 % 1x Penicillin-Steptomycin/ 10 mM HEPES - manufacturers as previously described) and grown to 60-80 % confluency. A spinoculation protocol was used to increase contact between the cells and virus as described by Dr Millar by personal communication. The plates were centrifuged at 500 x *g* for 5 minutes, the medium removed and virus containing medium added (1 ml D-MEM (10 % FBS/ 1 % 1x Penicillin-Streptomycin)/ 25 µl virus/ 4 µg/ml polybrene/ 10 mM HEPES). The plates were then centrifuged at 500 x *g* for 90 minutes at room temperature (RT). The medium was then renewed and the cells incubated for 48 hours before selection was initiated. Selection concentrations were determined using standard survival curves for individual cell types (Puromycin (Sigma, UK) at 2 µg/ml, G418 at 500 µg/ml (Fisher, UK) for HT-29 cell lines). The cells were split in two and puromycin ± G418 selection applied to half of the cells. The cells were grown on selection for two weeks, the medium changed weekly and this was stored and tested for protein production.

2.18 HLA typing - HLA PCR (1% agarose gel).

PBMC's were prepared using Sigma-Aldrich GenElute DNA extraction kit (Sigma, UK). Cells were lysed with salt-containing buffer leading to adequate denaturation of macromolecules. Spin columns were used to bind the DNA to the column and the supernatent was discarded. Cells were then subjected to a number of wash steps to remove any cellular debris prior to DNA elution with DNA elution buffer (Sigma, UK). DNA concentration was then established using Nanodrop reader (table 2.2).

Forward primer		Reverse primer		Product size (bp)
A1	GGA CCA GGA GAC ACG GAA TA	A1	AGG TAT CTG CGG AGC CCG	575
A2	TCC TCG TCC CCA GGC TCT	A2	GTG GCC CCT GGT ACC CGT	940
A3	AGC GAC GCC GCG AGC CA	A3	CAC TCC ACG CAC GTG CCA	628
B7	GGA GTA TTG GGA CCG GAA C	B7	TAC CAG CGC GCT CCA GCT	1207
B8	GAC CGG AAC ACA CAG ATC TT	B8	CCG CGC GCT CCA GCG TG	606
B40	CCA CTC CAT GAG GTA TTT CC	B40	TAC CAG CGC GCT CCA GCT	1372
Actin	GCT CCG GCA TGT GCA A	Actin	AGG ATC TTC ATG AGG TAG T	541

Table 2.2 HLA primers for PCR reaction

PCR reactions were set up in 20µl reactions as per manufacturer instructions using Taq polymerase in a read- made mix (Bioline Reagents Ltd, London). Amplification conditions were established on a Gene Amp PCR system 9600 (Perkin-Elmer Corporation, Norwalk, CT, USA) or more recently on an MJ Research PTC 225 machine.

The amplification products were visualised on 1% agarose gel containing 1x SybrSafe (Life Technologies, USA). The gels were run at 150 V for approximately 60 minutes in 1X TBE buffer and visualised using UV illumination. The results were recorded photographically.

2.19 Herpesvirus Saimiri (HVS)

A technique first described in 1992 (Biesinger, Mullerfleckenstein et al. 1992), the use of HVS has been investigated as a means to immortalize T-cells in much the same way that EBV immortalises B-cells. Therefore, stocks of Owl Monkey Kidney (OMK) cells (provided by Dr H De La Pena, University of Birmingham) were used to generate virus for further investigation in this project.

2.19.1 Production of HVS stock

OMK cells were grown in Dulbecco's Modified Eagles Medium (DMEM) (Life Technologies, Paisley, UK) + 10% FCS in T75 flasks. When the density reached ~70% confluence, the flasks were infected with HVS and incubated for 2 weeks at 37°C in 5% CO_2. Clearing of cells will occur after 5-7 days and complete lysis will be seen by 2 weeks. Once the cells had been lysed,

cell supernatant and debris was harvested and spun down at 300 x *g* for 10 minutes, the supernatant collected and stored at -80°C in 1ml aliquots (to avoid repeated freeze-thaw cycles).

2.19.2 Titration of HVS stock

OMK cells were cultured as per standard tissue culture techniques. They were plated in 24 well plates at a density of $1x10^6$ cells/ml on Day 0. On Day 1 Virus was removed from -80°C store and allowed to warm up to room temperature. Serial dilutions were made from neat virus down to a dilution of $1x10^{-14}$ in 15ml tubes by adding 1 ml of virus to 9ml of standard OMK cell media (DMEM (Gibco, UK) + 10% FCS (Sigma, UK)) and 1 ml was added to each respective well. A control well containing media with no virus was also set up. All experiments were done in triplicate. Virus handling was done in a category 2 tissue culture hood with standard precautions in place. The plates were then placed into a designated virus incubator and observed on a daily basis (NB no media change is necessary). A note was made each day as to the degree of confluence. The experiment was terminated at 2 weeks, and the supernatant collected and spun down and frozen at -80°C. This process was repeated at 6 monthly intervals to confirm virus potency and degree of degradation over time (Grassmann, Biesinger et al. 1990, Biesinger, Mullerfleckenstein et al. 1992, Nick, Fickenscher et al. 1993, Klein, Fickenscher et al. 1996, Daubenberger, Nickel et al. 2001, Vella, Zheng et al. 2002). Calculation of TCID50 in appendix 1.

2.19.3 HVS infection of PBMC/T-cells

100µl HVS (previously stored at -80°C) was added per 10^6 T-cells suspended in 1.6ml complete media (RPMI (Gibco, UK) + 10% FCS (Sigma, UK)). Cells had a media change twice per week with fresh RPMI 1640 supplemented with 10% FCS and 100 IU/ml of IL-2

(Sigma, UK). The success of the transformation was measured by using microscopy and Flow Cytometry (FACS) analysis and compared with the growth or death of a control culture.

2.20 Human Induced Pluripotent Stem Cells (hiPS) cells derived from PBMC, T-cell lines and T-cell clones

In depth protocols are available in the appendices of this project. A brief schematic is produced here to describe the outline for the project (fig. 2.9).

Fig 2.9: Schematic describing generation of hIPSc from T-cells, and PBMC's.
PBMC's were isolated and a T cell line generated from them as per standard methods as previously described. Cells were pre-conditioned prior to transduction with sendai virus with a variety of cytokines as per kit guideline (CytoTune 2.0) and following viral transduction, were washed in plain non-supplemented media and resuspended in standard growth media containing appropriate cytokines to encourage iPSc formation. Detailed protocols available in text and appendix 1.

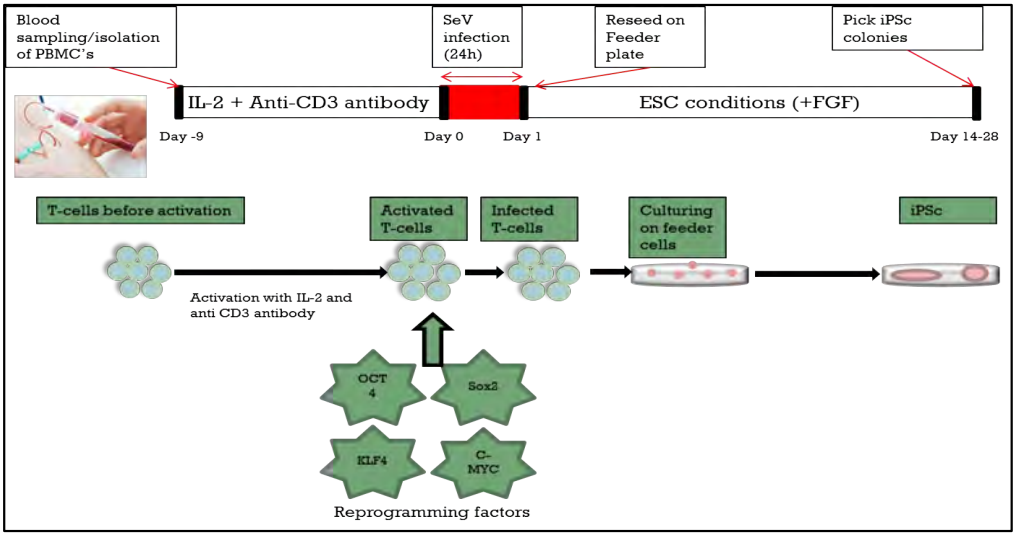

Fresh PBMC's were obtained and cultured in 'PBMC media' comprising StemPro 34, 1% Glutamax, 100ng/ml SCF, 100ng/ml FLT-3, 20ng/ml IL3, 20ng/ml IL6) all obtained from Life Technologies, Paisley, UK. Media was exchanged on alternate days for 9 days starting on day -9. On day 0, cells were transferred to a suitable vessel and washed twice with plain StemPro 34 media (no supplements). A Sendai virus kit (CytoTune iPS 2.0 Sendai Reprogramming Kit, Life Technologies, Paisley, UK) was defrosted on ice and the correct volume (as per manufacturer's guideline) was added to 1ml PBMC media per reaction. Cells were transferred to a 12well plate and centrifuged at 300 x *g* for 90minutes. 1ml further of PBMC media was

added to each well and cells placed in an incubator (5% CO_2, humidified). The following day (day 1) cells were washed at 300 x *g* in StemPro34 media and resuspended in PBMC media and returned to cell culture plate and replaced in incubator. On day 3 cells were washed at 300 x *g* and resuspended in StemPro 34 media + 1% Glutamax (Life Technologies, Paisley, UK), without the addition of any cytokines, and transferred to a prepared MEF (mouse embryonic Feeder cell coated 10cm plate). MEF cells were obtained from AMSBio, UK, strain CF1 (irradiated at source). Media was exchanged on alternate days. On day 7 cells had half the media replaced with 'IPSc media' (DMEM/F12, 10% Knockout-serum replacement, 1% Glutamax, 1% NEAA, 1% Penicillin/streptomycin, 0.1% FGF 0.007% B-mercaptoethanol – Life Technologies, Paisley, UK). Media was replaced daily until colonies emerged which were transferred to new 24w feeder plates (modified protocol (Takahashi and Yamanaka 2013).

**Following production of hIPSC clones, further characterisation was made including ability to differentiate into different germinal layers, staining for alkaline phosphatase, confocal microscopy and qPCR (see appendix for protocols).

2.20.1 Differentiation of mouse embryonic thymocytes into T-cells using OP9 DL1 cells

Mouse embryonic thymocytes were obtained on day 13 gestation. Thymocytes were transferred onto OP9 DL1 cells and grown in standard OP9 media (see section 2.1). OP9 DL1 cells were grown in OP9 media (as standard protocol) and allowed to reach 70% confluence in 6well plate. Media was changed every 3 days. On day 6 the cells were reseeded on fresh OP9DL1 cells and the media supplemented with Flt3-L at 10ng/ml (Sigma, UK). On day 10 cells were harvested by gentle pipetting and transferred to fresh OP9DL1 cells. Media was supplemented with Flt3-L 10ng/ml and IL7 1ng/ml (Sigma, UK). Cells were cultured in the fashion with media changes every 3 days and transferred to fresh OP9DL1 cells weekly. On day 40, cells were aspirated and analysed on Facs Fortessa (BD, UK) – fig. 2.10.

Fig 2.10: Schematic describing co-culture of mouse embryonic thymocytes on OP9DL1 cells.
Embryonic thymocytes were obtained on day 13 post vaginal plug identification (VP) in adult female mouse and resuspended in standard OP9 media. These were then transferred onto a monolayer of pre-prepared OP9DL1 cells which had been cultured in 6 well plates and reached 70% confluency prior to thymocyte addition.
Media was changed every 3 days. On day 6 cells were resuspended in media supplemented with Flt-3 10ng/ml on fresh OP9DL1 cellls. Co-culture continued and on day 10 media was further supplemented with IL-7 1ng/ml. The cells continued to have media changes every 3 days and continued in aMEM supplemented with Flt-3 and IL-7 until day 40,when they were harvested and taken to the flow cytometer for analysis.

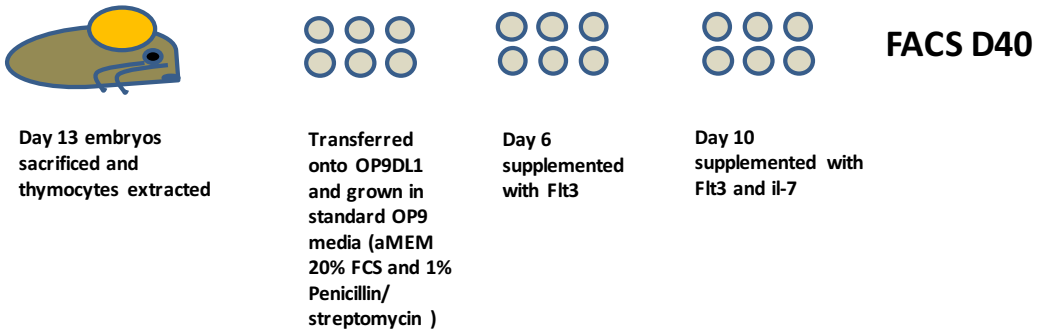

2.20.2 Differentiation of mouse induced pluripotent stem cells into T-cells

Mouse IPSc were grown on standard Black-6 feeder (MEF) cells as per protocol above. OP9 DL1 cells were grown in OP9 media (as standard protocol) and allowed to reach 70% confluence in 6well plate. Mouse IPSc (obtained by Dr C Ward, School of Infection and Immunity, University of Birmingham) were gently removed from MEF cells using 1:1 volumes of collagenase and dispase (Life Technologies, UK) and transferred into pre-prepared 15ml falcon tubes containing plain knockout-DMEM (Gibco, UK). Cells were allowed to fall by gravity and the supernatant removed. Cells were washed in this fashion 3 times using 2ml Knockout-DMEM. Cells were then resuspended in OP9 media and transferred onto the prepared OP9 DL1 feeder cells. Media was changed every 3 days. On day 6 the cells were reseeded on fresh OP9DL1 cells and the media supplemented with Flt3-L at 10ng/ml (Sigma, UK). On day 10 cells were harvested by gentle pipetting and transferred to fresh OP9DL1 cells. Media was supplemented with Flt3-L 10ng/ml and IL7 1ng/ml (Sigma, UK). Cells were cultured in the fashion with media changes every 3 days and transferred to fresh OP9DL1 cells

weekly. On day 40, cells were aspirated and analysed on Facs Fortsessa (BD, UK) (Nagata, Toyoda et al. 2009).

2.21 Statistical analysis

Statistical analysis was performed using Graphpad Prism 6.0 (GraphPad Software Inc, USA). SPSS 22.0 (IBM Analytics, USA) was used for the Fisher's exact test. Unless stated otherwise in the text, error bars on figures represent SEM (standard error of mean).

Chapter 3: THE ROLE OF PHOSPHOPEPTIDE IMMUNITY IN CANCER

3.1 Introduction

Cancer is widely accepted as an immune mediated process; however, the target of this immune response has for some time been the subject of much debate and continues to be a source of much scientific activity and investment. Infusion of cytotoxic T-cells (CTLs) has been used to target PTLD. Viral epitopes have been proposed as the target used by CTLs (Bollard, Savoldo et al. 2003, Chiereghin, Bertuzzi et al. 2016) (Bollard, Dotti et al. 2010, Heslop, Slobod et al. 2010). The question remains if the responses seen by these cytotoxic T-cells are purely towards viral epitopes or whether there is another process driving this?

Phosphorylation is termed a posttranslational modification. It is both reversible and transient in nature. Proteins are phosphorylated by kinases and dephosphorylated by phosphatases. Intracellular phosphorylation can therefore be seen to have a number of important roles. It modifies protein stability, location or formation of complexes. It clearly has a key intracellular role e.g. DNA transcription and is pivotal to intracellular signalling. Moreover, phosphorylation could be considered as a control mechanism, which exerts influence over a number of key functions (Ozlu, Akten et al. 2010). If phosphorylation is so important to cellular control mechanisms, then it stands to reason that a loss of this control could be implicated in cancer. Entire pathways could be altered, many of which could be implicated in tumorigenesis. Immunotherapies are an attractive potential anti-cancer therapy, and have generated much interest scientifically, however until relatively recently; they have been hampered by a lack of specific targets.

MHC class I associated phosphopeptides have previously been identified as a potential new class of tumour-specific target (Zarling, Polefrone et al. 2006, Cobbold, De La Pena et al. 2013, Abelin, Trantham et al. 2015, Penny, Abelin et al. 2012). This is based on the observation that dysregulation of signalling in cancers can lead to dysfunctional phosphorylation. Using an

autologous model of cancer established in healthy individuals (LCLs derived from healthy donor PBMC's), as described by Dr Penny of this group, it was shown that phosphopeptides appear to represent a significant CTL target (Zarling, Polefrone et al. 2006, Cobbold, De La Pena et al. 2013) - fig. 3.1.

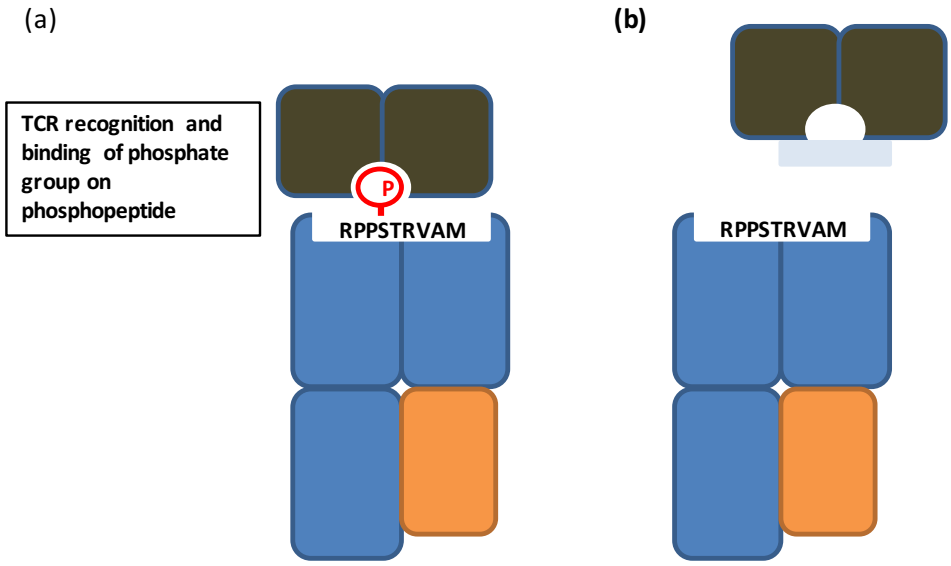

Fig. 3.1: Schematic showing showing recognition and binding of the phosphopeptide - a proposed method of tumour recognition. (a) Recognition of phosphorylated peptide sequence by TCR, leading to binding of the phosphate group. In the absence of the phosphate group (b) The TCR is unable to bind to the tumour. This is the process underlying the hypothesised mechanism of tumour recognition by T-cells recognising phosphopeptide.

MHC class-I and class-II phosphorylated peptides derived from phosphoproteins are abundant on the surface of tumours (Zarling, Polefrone et al. 2006, Cobbold, De La Pena et al. 2013, Abelin, Trantham et al. 2015). These antigens exhibit differential expression between healthy and malignant tissue with aggressive tumours displaying the most phosphopeptides (Zarling, Polefrone et al. 2006, Cobbold, De La Pena et al. 2013). Memory-like $CD8^+$ T-cells against phosphoantigens are present in healthy donors, but are thought to be reduced in patients with cancer. Many phosphorylated peptide antigens have previously been discovered in a multitude of cancers, including melanoma, breast cancer, colorectal tumours as well as haematological malignancies, all of which have been demonstrated in adults. Post-translational

phosphorylation is a modality that a cancer cell uses to proliferate and evade immune control. It is therefore proposed that this is the means by which PTLD can evade immune recognition and destruction. Previous studies by this group and others have shown MHC class –I phosphopeptides are differentially expressed on tumour surfaces compared to healthy tissue and therefore these would seem a logical step to target as a cancer immunotherapy (Syka, Coon et al. 2004, Cobbold, Polefrone et al. 2007, Mohammed, Cobbold et al. 2008, Depontieu, Qian et al. 2009, Li, Depontieu et al. 2010, Penny, Abelin et al. 2012, Cobbold, De La Pena et al. 2013, Abelin, Trantham et al. 2015). The overall contribution of phosphopeptides to T-cell immunity against transformed cells is not fully understood, and therefore it was our aim to investigate this further and assess their contribution to the anti-tumour response. The *in vitro* LCL model will be examined, whereby EBV-naïve individuals will be investigated as they will not possess an EBV viral response and thus any recognition and response from T-cells can be considered an anti-tumour phosphopeptide response.

3.2 $CD8^+$ T-cell responses to LCLs are found in EBV naïve individuals

Healthy donors should be able to recognise transformed B-cells. The question to be answered here is how do they manage this? We hypothesised EBV-naive individuals could recognise LCLs, and that this recognition would be due to malignant epitopes expressed on the transformed B-cell surface. By virtue of their construction, LCLs are generated due to viral infection of B-cells by EBV and subsequent reduction in T-cells using cyclosporin (as described in chapter 2). Therefore, recognition of LCLs by T-cells is quite likely to be due to a viral epitope; however, it is unlikely this is the only form of recognition on the T-cell's repertoire. Therefore, to test this theory an EBV-naïve donor was selected as any response of these T-cells to the LCLs was proposed to be as a result of tumour recognition as opposed to viral epitopes as this donor had not previously been exposed to EBV.

As shown in Fig. 3.2a, PBMCs from an EBV naïve donor were obtained by standard techniques (as described in chapter 2) magnetically selected ($CD8^+$ cells). These cells were then co-cultured with irradiated, autologous donor-derived LCLs for up to 7 days.

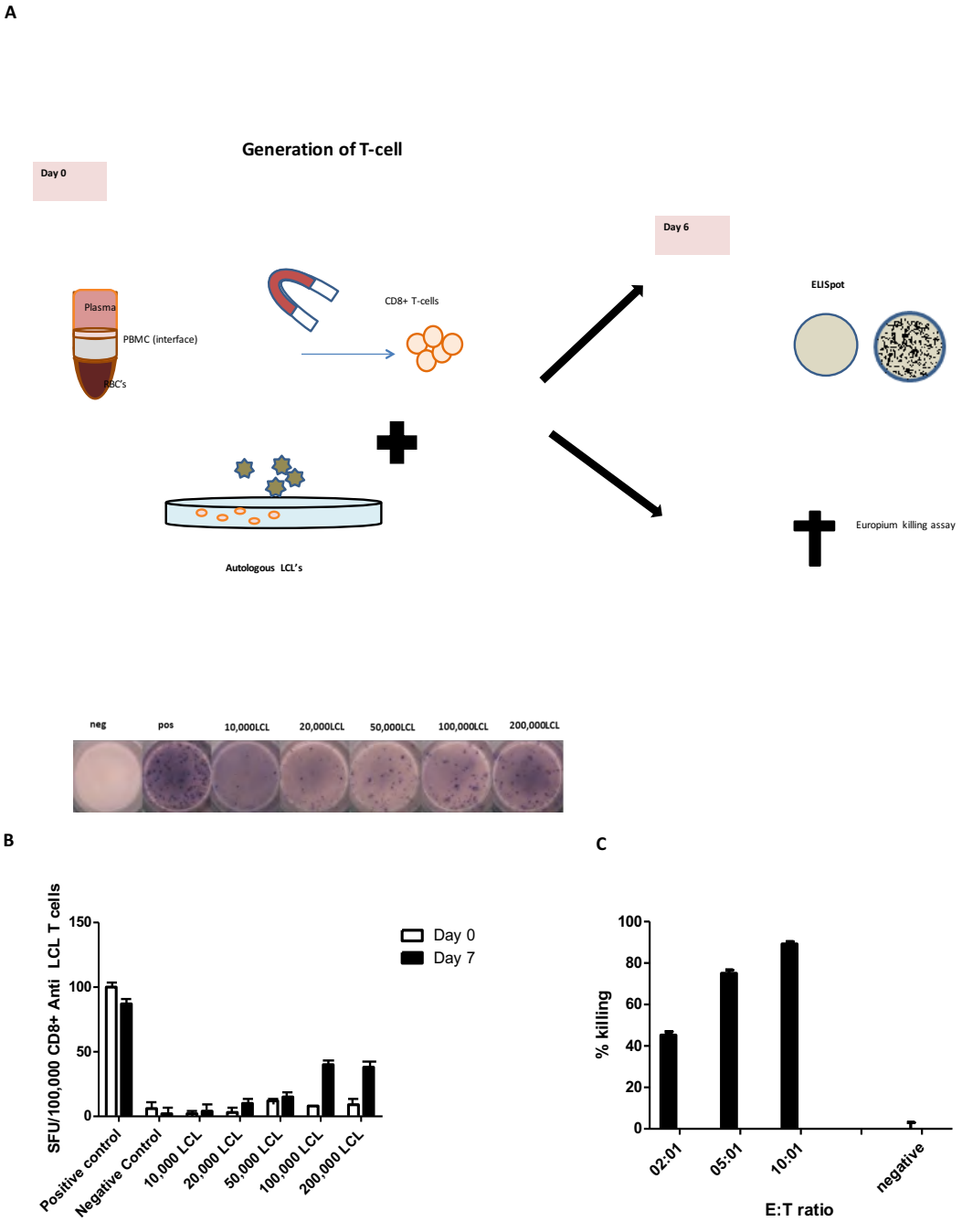

Fig. 3.2 An EBV-naïve healthy donor has T-cells recognising LCL-associated antigens. (A) PBMCs, generated as described previously, from an EBV-naïve donor were mixed with antibody coated magnetic beads and were $CD8^+$ selected and co-cultured with irradiated, autologous EBV-transformed B-cells (LCLs) for 7 days. In order to detect whether these cells recognised and became activated in response to these LCLs (B) an IFNγ ELISpot assay was used to assess immunity of EBV-donor to autologous LCLs and (C) a 3 hour europium release killing assay was used to assess functional killing by these T-cells. These graphs are representative of 3 repetitions of this experiment. Error bars represent SEM.

IFNγ ELISpot was used to determine their relative activation and subsequent cytokine release in response to the autologous LCLs (Fig. 3.2b). (NB, an EBV peptide was used in order to demonstrate that the healthy donor control was EBV-naïve - designated negative-control on the figure). We were able to demonstrate a clear cell-number-dependent response to the LCLs, both immediately *ex vivo* (albeit small on day 1) and a more expanded response after 6 days of culturing with the irradiated, donor autologous-LCLs (Fig. 3.2b), thus demonstrating that these T-cells were recognising a non-viral epitope expressed on the transformed B-cell surface. This response appeared to plateau at 100,000 cells on day 6 which could suggest whatever target is expressed by the LCL has saturated the T-cell recognition and so no further activation is achieved. It has been proposed that phosphopeptides represent the target for T-cells; and therefore if this is the case then this would suggest all T-cell receptors on the T-cells have bound to phosphopeptide. In order to explore this further, we assessed whether increasing the number of T-cells would increase functional killing. We predicted that increasing availability of receptors on the T-cells (effector cells) would lead to increased target recognition and thus increased killing. To test this a europium killing assay was performed whereby the anti-LCL T-cells which have been expanded in culture were used to target LCLs (Fig. 3.2c). This experiment demonstrated efficient killing in a ratio dependent fashion - for instance almost all LCLs had been destroyed by 3 hours when in a 10:1 effector:target ratio. The negative control in this instance was T-cells alone (i.e. without any target cells), thus demonstrating no non-specific cell death.

3.3 T-cell immunity to EBV-transformed cells targets phosphopeptides

It has been demonstrated that there is a CD8 T-cell response towards autologous LCLs in an EBV-naïve healthy donor. The T-cells are not recognising viral epitopes by virtue of the fact that the donor has not previously been infected by EBV and therefore there are no EBV-specific

T-cells within the circulating pool. We wanted to see whether the responses seen in an EBV-naïve donor were replicable in EBV-seropositive donors. We hypothesized that the T-cells in EBV-seropositive donors would recognise LCLs but that this recognition may largely be due to viral epitope recognition. In order to ascertain if there was a phosphopeptide response we phosphatase treated the LCLs. We proposed that phosphatase treatment of LCLs would essentially remove any phosphopeptide response (by removal of phosphorylated peptides from the cell surface) and thus any resultant recognition would be due to other means i.e. viral recognition.

We have established that the T-cells recognising antigens expressed on the LCLs were expandable in a healthy EBV naïve donor control. We therefore considered if this was reproducible in two age and HLA-matched EBV seropositive donors (Fig. 3.3A).

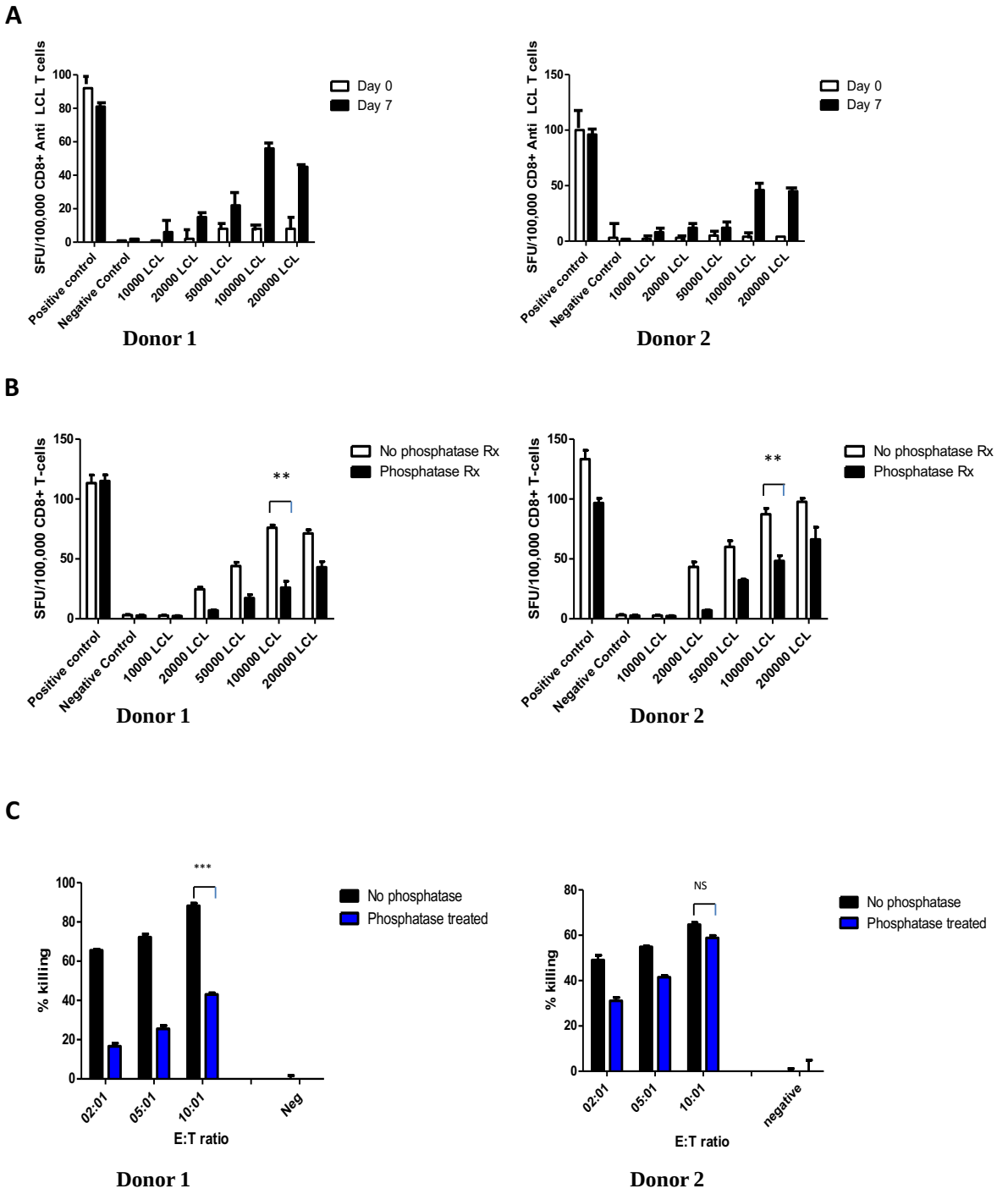

Fig 3.3 T-cells from two EBV-seropositive donors recognise LCL-associated antigens PBMCs from two EBV seropositive healthy donors were co-cultured with irradiated, autologous EBV-transformed B-cells (LCLs) for 7 days. (**A**) After this period of 7 days, an IFNγ ELISpot assay was performed to assess the activation of T-cells in response to LCLs. This represents the viral-derived and phosphoprotein derived immune reaction in both donor 1 and donor 2. (**B**) an IFNγ ELISpot assay to assess immunity of the EBV-seropositive donor 1 and 2 to respective autologous LCLs following phosphatase treatment (labelled Phosphatase Rx) in the same donors demonstrating a significant reduction (**) in IFNγ release as a result of removal of the phosphate group and thus removal of the phosphopeptide response. (**C**) a 3-hour europium release killing assay showing dose-dependent killing. *** P<0.001 Graphs representative of 5 repetitions of these experiments, each done in triplicate. Error bars represent SEM.

We demonstrated that like the EBV-naïve healthy donor there is a dose dependent response of T-cells to LCLs, however again we note that there is a plateauing of this response at 100,000 LCLs, suggesting that there is a ceiling to the effectiveness of T-cell:LCLs – an optimal number after which the recognition sites have become saturated and no further binding is possible. Donor 1's response is more similar to the EBV-naïve donor's responses in terms of SFU/100,000 $CD8^+$ T-cells being a dose dependent concept with a gradual increase in SFU from 2, 8, 17, 27, 57 at 10,000LCL, 20,000LCL, 50,000LCL and 100,000LCL respectively. Donor 2 appears to have relatively poor responses at 7 days (little variation in SFU between 10,000 and 50,000LCLs) until 100,000 LCLs are added at which point the response climbs from 20 SFU/100,000 $CD8^+$ T-cells up to 49 SFU/100,000 $CD8^+$ T-cells (fig. 3.3A).

The T-cell response towards the LCLs may be wholly composed of an anti-EBV viral response. We hypothesised that there would be T-cell responses to other epitopes displayed on the surface of LCLs that could be used to identify a tumour cell. The immune system has a variety of processes for recognition of transformed cells. One characteristic of a transformed cell which the immune system recognises is phosphorylation, a so-called posttranslational modification. Furthermore, we proposed that these tumour epitopes may be phosphorylated peptides which could be an anti-tumour (and not anti-viral) T-cell response towards LCLs. In order to test this hypothesis, lightly fixed and phosphatase treated, or untreated, autologous LCLs were tested by co-culturing with T-cells, using IFNγ ELISpot (fig 3.3b). This revealed a significant difference (by two-way anova) between the response demonstrated in relation to phosphopeptide replete LCLs and phosphopeptide deplete LCLs ($p<0.001$). Removing the phosphorylated peptide epitopes from the LCL cell surface using phosphatases led to a 67% reduction in recognition, activation and thus cytokine release as demonstrated by IFNγ release, suggesting that up to 2/3 of the memory responses to transformed self were against these phosphorylated epitopes i.e. phosphopeptides (B).

Fig. 3.3c demonstrates the effect of phosphatase on the ability of T-cells to kill LCLs using a Europium release killing assay in both EBV-seropositive donors. Phosphatase reduces the effectiveness of T-cell killing showing that killing of target LCLs is at least in part due to non-viral epitopes. Donor 1 showed reduction in killing by phosphatase by between 57-65% when compared to non-phosphatase treated $p<0.005$ by paired t-test. Donor 2 showed a reduction by between 5.9% and 14%, however this is less efficient reduction in killing following phosphatases suggesting that killing in this cell line is largely viral-epitope driven.

We hypothesised phosphatase-treating LCLs should have no effect on the anti-viral- response, only the anti-phosphopeptide response. Previously, it was shown that the T-cells responding to phosphopeptide will not recognise non-phosphorylated epitopes of the same sequence as would be demonstrated by phosphatase treating the LCLs (Cobbold, De La Pena et al. 2013). Therefore, it is the phosphate group that forms part of the TCR recognition and loss of the phosphate will result in loss of anti-phosphopeptide response. In order to test this hypothesis, a peptide-specific T-cell line was grown against the CMV-derived HLA-A2 binding epitope NLVPMVATV and cultured with HLA-matched non-autologous LCLs which had been pulsed with exogenous NLV peptide and phosphatase treated (fig. 3.4a).

There appears to be a direct relationship between number of LCLs and number of SFU's. There is an increase in SFU between 20,000 LCLs and 50,000 LCLs from 21 SFU/100,000 T-cells to 50 SFUs. The results plateau at 100,000 LCLs suggesting this is the point when all possible target binding sites have been exhausted. Positive control was activation of T-cells with PMA/Ionomycin and negative was 1% DMSO (used as peptides were dissolved in this as a solvent)– with readout in terms of SFU being as would be expected for each. There is not a significant reduction in T-cell activation following phosphatase treatment therefore confirming our prediction that the viral response is not significantly dampened by phosphatase treatment (fig. 3.4b).

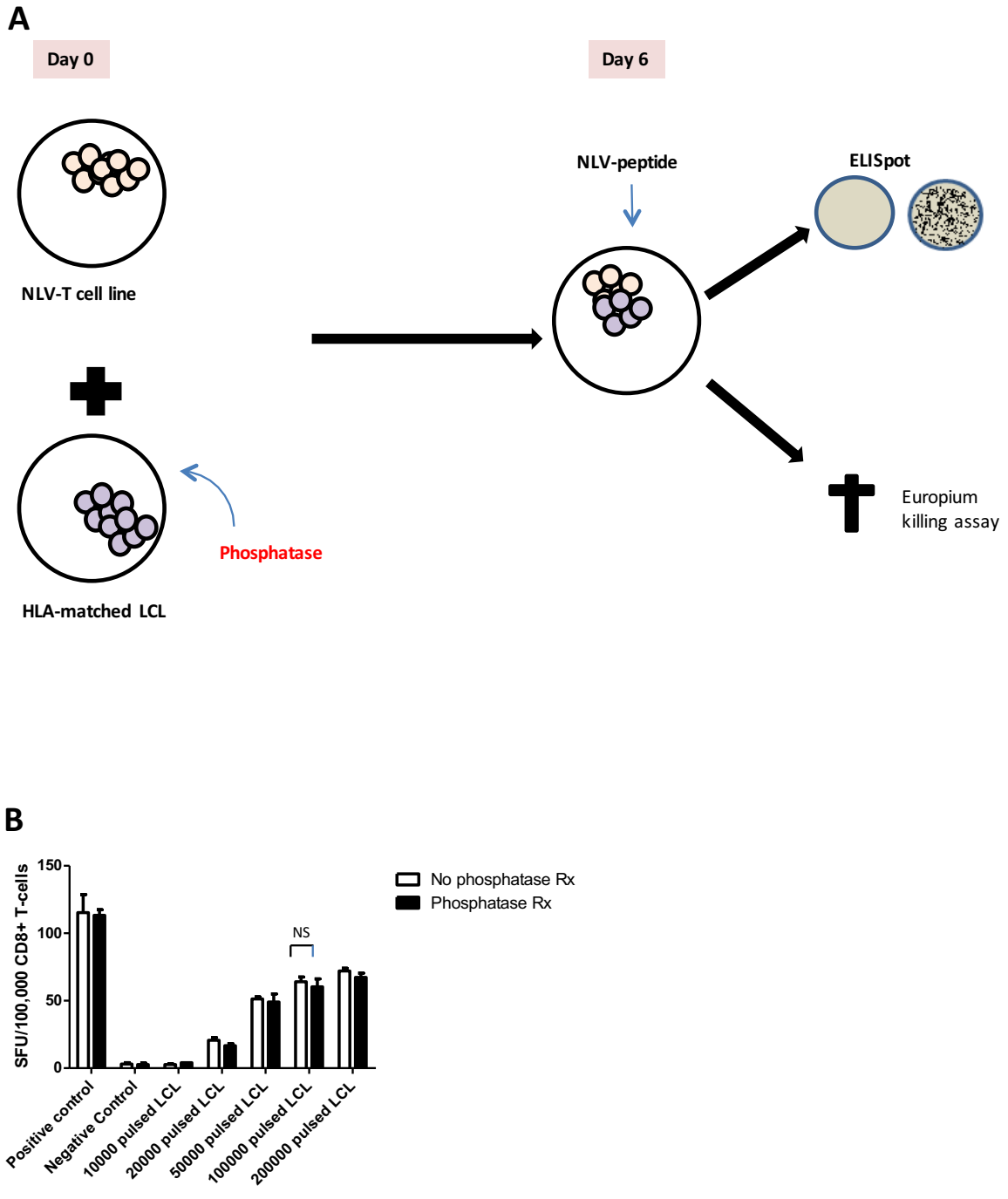

Fig 3.4 NLV-viral peptide specific T-cells can recognise non-autologous LCLs despite phosphatase treatment (**A**) LCLs from a donor with known CMV-viral peptide response were phosphatase treated and added to an NLV-viral peptide specific T-cell line (labelled NLV-T cell line on figure above). (**B**) Cells were co-cultured for 7 days and an IFNγ ELISpot assay was used to assess immunity of the NLV-T-cell line to the NLV-peptide pulsed LCLs following phosphatase treatment (labelled Phosphatase Rx), thus demonstrating no loss of viral-mediated immune response after phosphatase treatment. This graph is representative of 5 experimental repetitions, each done in triplicate. Error bars represent SEM. Positive control are cells stimulated with PMA + ionomycin, negative control were cells treated with 1% DMSO. The remainder of the cells were used for a Europium killing assay to demonstrate efficient killing in response to target cell (data not shown).

EBV naïve healthy donors demonstrated $CD8^+$ T-cell responses to autologous LCLs (suggesting this was not a viral response). As a result, we sought to establish in which compartment these $CD8^+$ T-cell responses lay. Flow-cytometry sorting was used to sort the T-cells into their discrete compartments making the following assumptions: Naïve - $CD27^+CD45RA^+$, central memory (CM - $CD27^+CD45RA^-$), effector memory (EM - $CD27^-CD45RA^-$) and terminal effector memory compartments (TEMRA - $CD27^-CD45RA^+$) - fig 3.5 After sorting (performed in Biosciences, University of Birmingham), using techniques as previously described by Dr Penny of this group (personal communication) these cells were co-cultured with irradiated, autologous LCLs for 6 days, after which they were expanded and used in an IFNγ ELISpot assay in order to determine which T-cell population contained anti-LCL responses (Fig. 3.5b). Responses were observed in all memory compartments in the EBV-seronegative donor, but the responses in the central memory and terminal effector memory compartments were demonstrably higher (5 and 12 SFU respectively versus 2-4 in the other memory compartments).

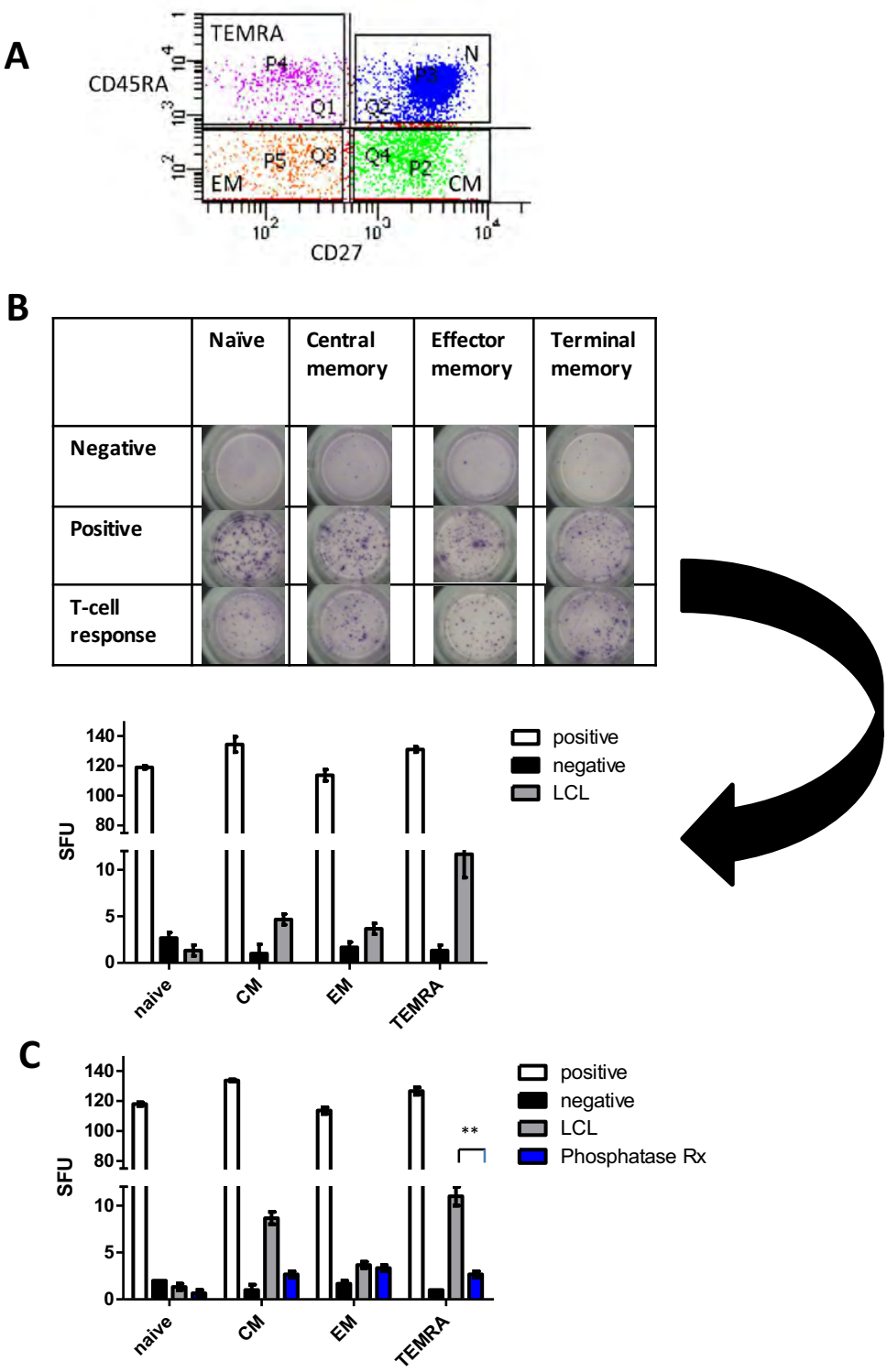

Fig. 3.5 The CD8$^+$ T cell responses against LCLs reside predominantly in the central memory and terminal effector memory compartments (**A**) CD8$^+$ T-cells were FACS-sorted into Naïve - CD27$^+$CD45RA$^+$, central memory (CM - CD27$^+$CD45RA$^-$), effector memory (EM - CD27$^-$CD45RA$^-$) and terminal effector memory compartments (TEMRA - CD27$^-$CD45RA$^+$) phenotypes using antibodies to CD27 and CD45RA. **(B)** 100,000 sorted cells of each phenotype were co-cultured for 6 days with irradiated, autologous LCLs. On day 6, an IFNγ ELISpot was performed to assess each compartment's responses to the LCLs in an EBV-naïve healthy donor. **(C)** Effect of phosphatase on T-cell activation. ** P<0.01, *** P<0.001. These graphs are representative of 3 experimental repetitions, each repetition done in triplicate. Error bars represent SEM. Positive control are cells treated with PMA + Ionomycin, negative control are cells treated with 1% DMSO.

Having established which compartments the T-cell responses lay, we proposed that phosphatase treating the LCLs would lead to a reduction in T-cell activation, however we wanted to establish if this was the same for all compartments equally. Unfortunately, this assay was inconclusive and due to availability of cells, it was not possible to repeat this with this donor (data not shown). This was therefore repeated in an EBV-seropositive donor and the results demonstrated marked reduction in T-cell activation (fig. 3.5c). TEMRA compartment showed the largest reduction in response from 12 SFU to 2SFU, which is a significant reduction when paired T-test is performed ($p<0.002$). These data in part validate the results seen in the EBV-naïve donor as in the EBV-naïve donor we saw the biggest activation in TEMRA and Central memory – which is the same trend seen in the sero-positive donor. The biggest reduction in activation was seen in both TEMRA and CM following phosphatase treatment suggesting the phosphopeptide response is the main contributor to this as compartmentalisation, i.e. viral epitopes have a lesser contribution to T-cell activation in this instance when recognising LCLs.

Finally we considered whether using established anti-LCL T-cell lines in these experiments lead to skewing of the data – as these were lines which had been generated previously in response to autologous LCL i.e. had developed 'memory'. We hypothesised that this could lead to data skewing and therefore in order to overcome this fresh PBMC's were obtained from (one EBV-seronegative donor the two EBV-seropositive donors, donor 1 and 2 (fig. 3,6a, b) and co-cultured with autologous LCLs (already established). LCLs were phosphatase treated.

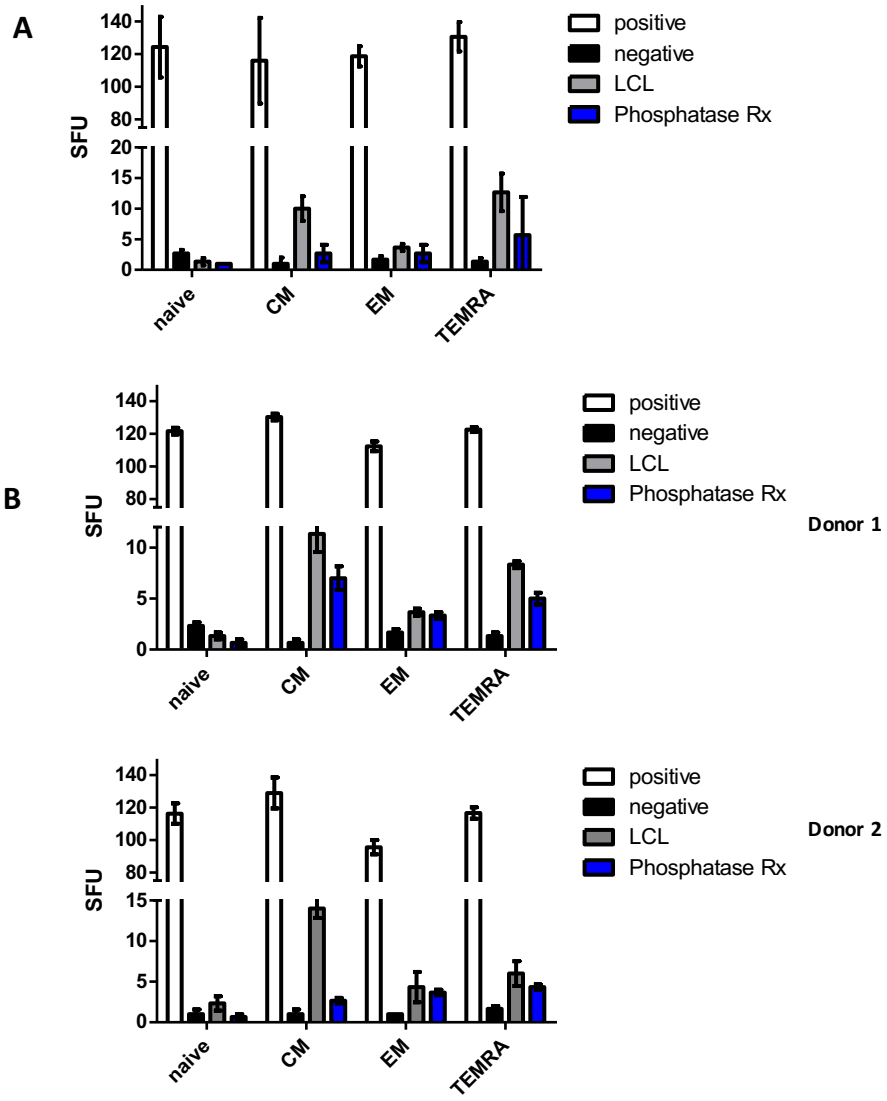

Fig. 3.6 The CD8$^+$ T cell responses against LCLs reside predominantly in the central memory and terminal effector memory compartments
Fresh PBMC's obtained from an (A) EBV-naïve healthy donor and (B) two EBV seropositive donors were FACS sorted into naïve, central memory, effector memory and terminal effector phenotypes using antibodies to CD27 and CD45RA as described previously. 100,000 cells of each type were co-cultured for 6 days with irradiated, autologous LCLs (phosphatase treated). On day 6, an IFNγ ELISpot was performed to assess each compartment's responses to the LCLs. These graphs are representative of 3 experimental repetitions, each repetition performed in triplicate. Error bars represent SEM. Positive control are cells stimulated with PMA + ionomycin. Negative control are cells treated with 1% DMSO.

These data show a similar trend to the previous results seen in anti-LCL T-cells thus validating these previous results. In the EBV-naïve donor (fig. 3.6A) there is the greatest response seen in the CM compartment (10SFU/100,000 CD8 T-cells down to 3SFU/100,000 CD8 T-cells), with TEMRA also demonstrating a large reduction from 12-6SFU/100,000 T-cells. This is similar to that seen in the T-cells with regards to the two compartments implicated being CM

and TEMRA (although in T-cells it is TEMRA which shows the biggest reduction). When assessing the EBV-Seropositive donors we can see a similar reduction in activation when LCLs are phosphatase treated.

Using PBMC's rather than T-cells lead to the biggest reduction in CM in all donors (seen more markedly in sero-positive donor 2) 12-7SFUs and 8-2SFUs respectively. Both TEMRA and CM have been implicated as forming part of the phosphopeptide response; however in the T-cell data (fig 3.5 C) we saw a larger reduction in TEMRA. This may hint that culturing T-cells against autologous LCLs may lead to data bias.

3.4 T cells from an EBV naive donor kill LCLs in a phosphopeptide dependent manner

Having established that EBV naïve T-cells become activated in the presence of transformed B-cells, we sought to test if these cells had the ability to perform targetted killing. It has long been established that CTL's can be used for the treatment of PTLD (the *in vitro* model of which are LCLs) (Haque, McAulay et al. 2011, Ricciardelli, Brewin et al. 2013, Ricciardelli, Blundell et al. 2014, Stubbins, Peters et al. 2015, Chiereghin, Bertuzzi et al. 2016, Dharnidharka, Webster et al. 2016). We predicted that as viral epitopes do not play a role here, that phosphatase treating the LCLs would result in inefficient killing of the LCLs (Fig 3.7a). This was tested by performing a europium killing assay comparing phosphatase treated cells to non-treated cells in an EBV-naïve donor (fig. 3.7b). This would be the case if the target for the effector cells is phosphorylated. Interestingly we can see that there is still killing following phosphatase treatment, up to 40%, but this is markedly reduced compared to non-phosphatase treated cells which has efficiency up to 92% at an E:T ratio of 10:1. This would suggest that the effector T-cells are recognising an alternative target on the cell surface – it is not immediately clear what this may be – but an alternative hypothesis may be that phosphatase does not completely eliminate phosphorylated peptides on the cell surface. What is clear is

there is a significant reduction in target cell recognition by up to 50% (two way anova shows $p<0.001$) confirming our hypothesis phosphatase reduces killing efficiency and therefore demonstrating that phosphopeptides are the likely target epitope here (fig. 3.7b). Put another way ANOVA was used to compare the regression lines (fig. 3.7c) and there was a significant difference demonstrated following phosphatase treatment of LCLs (***) $p=0.0011$.

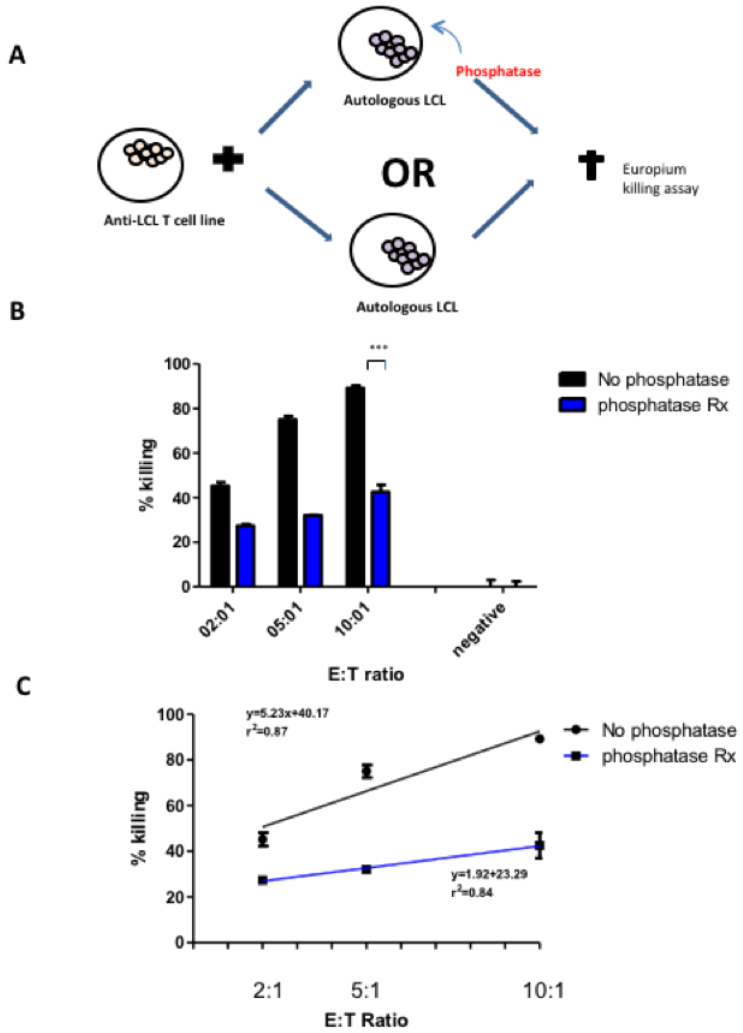

Fig. 3.7 Anti-LCL T-cell lines can efficiently recognise and kill LCLs in a dose dependent manner and this effect is driven by a phosphorylated target. (A) experimental protocol for testing the hypothesis that phosphatase will reduce efficient killing. An anti-LCL T-cell line was used as the effector cells. BATDA loaded autologous LCLs were used as targets. Prior to BATDA loading half the LCLs were treated with phosphatase. (B) Europium killing assay was performed as described previously and demonstrates a significant reduction in target killing when these cells are pre-treated with phosphatase. (C) Linear regression lines of same data demonstrating significant reduction in killing $p<0.005$. Experiments performed in triplicate. Error bars represent SD.

3.5 MHC class I associated phosphopeptides identified on LCLs

Until now we have identified that phosphopeptides are likely HLA-associated, and that recognition of these phosphopeptides is one of the mechanisms by which T-cells can identify and kill transformed cells. Using the commercially available and well established EBV-transformed B-cell line JY, phosphopeptides presented at the surface of this cell line have been identified (table 3.1). This was achieved by *in vitro* expansion, immunopurification using the antibody W6/32 and peptide acid elution. Subsequently purification was achieved using IMAC and characterised further by LC-MS/MS and manual sequence assignment. 154 phosphopeptides were identified as being expressed by JY(Zarling, Polefrone et al. 2006, Cobbold, Polefrone et al. 2007, Mohammed, Cobbold et al. 2008, Cobbold, De La Pena et al. 2013, Abelin, Trantham et al. 2015). As some of this data is historical, absolute amounts of expression are not known as they were not quantified, however it can be seen that of the phosphopeptides which have been quantified, all except two are expressed at higher levels in JY than healthy control B-cells (spleen and tonsil). Many more phosphopeptides were identified on JY compared to healthy B-cells – 154 vs 16 respectively. As demonstrated in the table, a number of key cancer pathways appear to be implicated by these phosphopeptides; with source proteins including RAS, BCL2, LSP1, MAPK-II, Beta-Catenin.

Table 3.1 HLA A2 or B7 associated phosphopeptides identified on the LCL cell line JY compared to healthy control B-cells (healthy spleen and tonsil tissue was obtained from HBRC tissue bank, University of Birmingham). Small 's' or 't' denotes phosphorylation. This was achieved by *in vitro* expansion, immunopurification using the antibody W6/32 and peptide acid elution. Samples were frozen rapidly in liquid nitrogen and subsequently packaged on dry ice and shipped to University of Virginia for further processing. Purification was achieved using IMAC and characterised further by LC-MS/MS and manual sequence assignment. Sequence sets were then returned and source protein analysed.

Phosphopeptide	Source Protein	Predicted HLA binding	JY	Spleen (B cell)	Tonsil (B cell)
RQLsSGVSEI	Heat shock protein beta-1	A2			
ALDsGASLLHL	Receptor-interacting serine/threonine-protein kinase 4	A2			
ALGsRESLATL	RAS protein activator like-3	A2			
ALYsPAQPSL	Sphingomyelin phosphodiesterase 4	A2			
AMAAsPHAV	Heterogeneous nuclear ribonucleoprotein A0	A2			
AMLGSKsPDPYRL	Protein SON	A2			
AVIHQsLGL	Protein CNPPD1	A2			
AVVsPPALHNA	Bromodomain-containing protein 4	A2			
GLLGsPVRA	M-phase inducer phosphatase 2	A2			
GLLsPARLYAI	Leucine-rich PPR motif-containing protein, mitochondrial	A2			
ILDsGIYRI	Hermansky-Pudlak syndrome 5 protein	A2			
ILKsPEIQRA	60S ribosomal protein L4	A2			
IMDRtPEKL	Breast cancer anti-estrogen resistance protein 3	A2			
KIFsGVFVKV	60S ribosomal protein L7-like 1	A2			
KLDsPRVTV	Family with sequence similarity 86, member A, isoform CRA_h	A2			
KLFPDtPLAL	Interleukin enhancer-binding factor 3	A2			
KLFsPSKEAEL	Protein cramped-like	A2			
KLIDIVsSQKV	Serine/threonine-protein kinase Chk1	A2			
KLIDRTEsL	Lymphocyte-specific protein 1	A2			
KLLQFYPsL	Linker for activation of T-cells family member 2	A2			
KLLSSAQRtL	Krueppel-type zinc finger protein	A2			
KLMAPDIsL	BCL2/adenovirus E1B 19 kDa protein-interacting protein 2	A2			
KLMsPKADVKL	Protein hinderin	A2			
KMDsFLDMQL	NEDD4-binding protein 2	A2			
KMYsEIDIKV	116 kDa U5 small nuclear ribonucleoprotein component	A2			
KVAsLLHQV	TNFAIP3-interacting protein 2	A2			
KVLsTEEMEL	Mitotic-spindle organizing protein 2A	A2			
KVQVtSLSV	unknown	A2			
LMFsPVTSL	SET domain-containing protein 5	A2			
mLAEsPSVPRL	unknown	A2			
REAsIELPSM	Lymphocyte-specific protein 1	A2			
RLAsLNAEAL	Bromo adjacent homology domain-containing 1 protein	A2			
RLAsLQSEV	unknown	A2			
RLDsYVRS	Trafficking protein particle complex subunit 1	A2			
RLDsYVRSL	Trafficking protein particle complex subunit 1	A2			
RLLsPLS(+18)SA	unknown	A2			
RLLsPLSSA	Ribonucleoprotein PTB-binding 1	A2			
RLQsTSERL	ATP-dependent zinc metalloprotease YME1L1	A2			
RLSsPLHFV	Protein FAM134A	A2			
RLSsYVRS	Trafficking protein particle complex subunit 1	A2			
RQAsIELPSMAV	Lymphocyte-specific protein 1	A2			
RQAsLSISV	Serine/threonine-protein kinase D2	A2			
RQAsIELPSM	unknown	A2			
RQAsIWLPSAAV	unknown	A3			
RQIsFKAEV	Ubiquitin-conjugating enzyme E2 J1	A2			
RQIsFQAEV	Ubiquitin-conjugating enzyme E2 J1	A2			
RQIsQDVKL	AMP deaminase 2	A2			
RTYsGPMNKV	Protein POF1B	A2			
RVPsPTPAPK	Serine/arginine repetitive matrix protein 2	A2			
SLLTsPPKA	E3 ubiquitin-protein ligase TRIP12	A2			
SMTRsPPRV	Serine/arginine-rich splicing factor 8	A2			
TLAsPSVFKST	Protein aurora borealis	A2			
VLKGsRSSEL	UPF0693 protein C10orf32	A2			
VLLsPVPEL	Anaphase-promoting complex subunit 1	A2			
VLmKsPsPAL	Probable ATP-dependent RNA helicase YTHDC2	A2			
VMFRtPLASV	F-box only protein 5	A2			
YLDsGIHSGA	Catenin beta-1	A2			
YLDSGIHsGA	Catenin beta-1	A2			
YQLsPTKLPSI	Nibrin	A2			

0.05-0.5 copies/cell
0.5-5 copies/cell
5-10 copies/cell
10-50 copies/cell
expressed, not quantified

Phosphopeptide	Source Protein	Predicted HLA binding	JY	Spleen (B cell)	Tonsil (B cell)
GPRSAsLLSL	G-protein-signaling modulator 3	B7			
HPRsPNVLSV	Hypoxia-inducible factor 1-alpha	B7			
HPRsPtPTL	Proline-rich protein 11	B7			
KPRsPPRAL	Retrotransposon-derived protein PEG10	B7			
KPRsPPRALV	Retrotransposon-derived protein PEG10	B7			
KPRsPVVEL	Beta-adrenergic receptor kinase 1	B7			
KPSsLRRVTI	Lymphoid-restricted membrane protein	B7			
LPRGsSPSVL	Homeobox protein TGIF2	B7			
MPRQPsATRL	Mitotic-spindle organizing protein 2B	B7			
RPAKsMDSL	Rho GTPase-activating protein 30	B7			
RPAsAGAML	Myocyte-specific enhancer factor 2D	B7			
RPAsPAAKL	KAT8 regulatory NSL complex subunit 3	B7			
RPAsPQRAQL	unknown	B7			
RPDsRLGKTEL	Histone-lysine N-methyltransferase SETD2	B7			
RPFsPREAL	Leucine zipper protein 1	B7			
RPIsPGLSY	Coiled-coil domain-containing protein 6	B35			
RPKsDIVLL	B-lymphocyte antigen CD20 (N to D conversion)	B7			
RPKtPPVVI	Synapse-associated protein 1	B7			
RPNsPSPTAL	Serine/threonine-protein kinase tousled-like 1	B7			
RPRANsGGVDL	Ras-responsive element-binding protein 1	B7			
RPRARsVDAL	Lipolysis-stimulated lipoprotein receptor	B7			
RPRPHsAPSL	Migration and invasion-inhibitory protein	B7			
RPRPVsPSSL	Serine/threonine-protein kinase SIK1	B7			
RPRsAVLL	A-kinase anchor protein 13	B7			
RPRsPRENSI	Ataxin-2	B7			
RPRsPRQNSI	Ataxin-2	B7			
RPRsPTGPSNSF	Splicing factor 45	B7			
RPRsPTGPSNSFL	Splicing factor 45	B7			
RPVsPFQEL	unknown	B7			
RPVsPGKDI	Transcription factor HIVEP2	B7			
SPAsPKISL	Ataxin-2-like protein	B7			
SPKsPTAAL	Centrosomal protein of 55 kDa	B7			
SPRRsRSISL	Serine/arginine-rich splicing factor 7	B7;C6			
SPRsPGRSL	unknown	B7			
SPR(s)P(s)TTYL	Chromatin assembly factor 1 subunit A	B7			
TPRsPPLGL	Mitogen-activated protein kinase kinase kinase 11	B7			
APRKGsFSAL	Cullin-4A	B7			
APRRYsSSL	Rho GTPase-activating protein 17	B7			
LPAsPAHQL	Histone-lysine N-methyltransferase, H3 lysine-79 specific	B7			
RPKsNIVLL	B-lymphocyte antigen CD20	B7			
YPSsPRKAL	Signal-induced proliferation-associated 1-like protein 1	B7			
APRAPSAsPLAL	MICAL-like protein 1	B7			
GAQPGRHsV	LIM domain-containing protein ajuba	B7			
GPRAPsPTKPL	Sororin	B7			
GPRPGsPSAL	RNA pseudouridylate synthase domain-containing protein 1	B7			
GPRsPKAPP	ARHGAP4 protein	B7			
HPKRSVsL	BCL2/adenovirus E1B 19 kDa protein-interacting protein 3-like	B7			
IPRPLsLIGSTL	Dedicator of cytokinesis protein 10	B7			

	0.05-0.5 copies/cell
	0.5-5 copies/cell
	5-10 copies/cell
	10-50 copies/cell
	expressed, not quantified

Phosphopeptide	Source Protein	Predicted HLA binding	JY	Spleen (B cell)	Tonsil (B cell)
KLRsPKSEL	Tyrosine-protein phosphatase non-receptor type 22	B7			
KPAsPARRL	Microtubule-associated protein 1A	B7			
KPAsPKFIVTL	Zinc finger CCCH domain-containing protein 14	B7			
KPPYRSHsL	Centrosomal protein of 95 kDa	B7			
KPRRFsRsL	Arginine/serine-rich coiled-coil protein 2	B7			
KPRsPPRALVL	Retrotransposon-derived protein PEG10	B7			
KPRsPPRALVLP	Retrotransposon-derived protein PEG10	B7			
KPYsPLASL	Nuclear factor of activated T-cells, cytoplasmic 2	B7			
LPAsPRARL	Histone-lysine N-methyltransferase, H3 lysine-79 specific	B7			
LPIFSRLsI	Zinc finger protein 36, C3H1 type-like 2	B7			
LPKsPPYTAF	Eukaryotic translation initiation factor 4B	B7			
MPREPsATRL	Mitotic-spindle organizing protein 2B	B7			
MPRQPsATRL	Mitotic-spindle organizing protein 2B	B7			
QPRsPGPDYSL	Zinc finger protein Gfi-1	B7			
QPRtPSPLVL	Lymphocyte-specific protein 1	B7			
RARGIsPIVF	YTH domain-containing protein 1	B7			
RPAFFsPSL	Uncharacterized protein KIAA0930	B7			
RPKLSsPAL	Histone acetyltransferase p300	B7			
RPKsNINLL	B-lymphocyte antigen CD20	B7			
RPPsPGPVL	Sterol regulatory element-binding protein cleavage-activating prot	B7			
RPQRATsNVF	Myosin regulatory light polypeptide 9	B7			
RPRIPsPIGF	Eukaryotic translation initiation factor 4E transporter	B7			
RPRsLSSPTVTL	E3 ubiquitin-protein ligase NEDD4-like	B7			
RPRSLsSPTVTL	E3 ubiquitin-protein ligase NEDD4-like	B7			
RPRsPGSNSKV	General transcription factor II-I	B7			
RPRsPPPRAP	Prickle-like protein 3	B7			
RPRsPRQPSI	unknown	B7			
RPSsLPDL	AT-rich interactive domain-containing protein 1B	B7			
RPTsRLNRL	Nuclear receptor coactivator 1	B7			
RPVtPVSDL	Krueppel-like factor 10	B7			
RPWsPAVSA	Ski oncogene	B7			
RPYsPPFFSL	Protein FAM53C	B7			
RQAsIELPSMAV	Lymphocyte-specific protein 1	B7			
RQAsIELPSM	Lymphocyte-specific protein 1	B7			
SPGsPRPAL	DNA replication factor Cdt1	B7			
SPKsPGLKA	CapZ-interacting protein	B7			
SPRAPVsPLKF	Ribosomal protein S6 kinase beta-2	B7			
SPRERsPAL	Thyroid hormone receptor-associated protein 3	B7			
SPRsPGKPM	unknown	B7			
SPRsPSTTYL	Chromatin assembly factor 1 subunit A	B7			
SPRTPVsPVKF	Ribosomal protein S6 kinase beta-1	B7			
SPSTSRSGGsSRL	Arginine/serine-rich protein 1	B7			
TPAQPQRRsL	Targeting protein for Xklp2	B7			
TPRsPPLGLI	Mitogen-activated protein kinase kinase kinase 11	B7			
TSPsYIDKL	Serine/threonine-protein kinase Chk1	B7			
VPREVLRLsL	AT-hook-containing transcription factor	B7			

	0.05-0.5 copies/cell
	0.5-5 copies/cell
	5-10 copies/cell
	10-50 copies/cell
	expressed, not quantified

3.6 Discussion

Treatment of PTLD using CTL's was initially thought to target viral epitopes expressed at the cell surface (Haque, McAulay et al. 2011, Stubbins, Peters et al. 2015, Chiereghin, Bertuzzi et al. 2016). However, a competing hypothesis involves CTLs recognising an alternative target. It is likely that a combination of both viral and non-viral responses contributes to the targeting of PTLD. As we have demonstrated here, EBV-naïve individuals do mount a response to LCLs and in fact removal of the phosphorylation of the peptide targets leads to inefficient killing – suggesting that phosphorylated proteins (phosphopeptides) are at least one of the classes of non-viral epitopes targeted. This stands to reason given phosphorylation is a post-translational transformation seen in cancer cells and termed a 'Hallmark of Cancer' (Hanahan and Weinberg 2011).

In this chapter, we have demonstrated that EBV-naïve individuals do have a targeted response to autologous LCL (fig 3.2) which is probably not due to an anti-viral response given their EBV serostatus. These T-cells demonstrate (i) an ability to expand in the presence of their cognate antigen and (ii) efficient killing of target LCL populations. A similar response has been demonstrated in EBV-seropositive donors (fig. 3.3) however, these donors have previously encountered EBV infection, and thus the activation seen in response to LCLs is likely to include this so called 'viral' response. In order to delineate this, cells were phosphatase treated (thereby removing the phosphate group from any presented phosphopeptides and consequently the phosphopeptide response) with the remaining cell responses considered virally driven. In order to assess this further we considered if viral non-EBV peptide-specific T-cells could recognise non-autologous LCLs following phosphatase treatment (Fig 3.4) therefore demonstrating that the T-cell activation is due to viral epitope not tumour, and also that phosphatase treatment does not affect the non-phosphorylated protein recognition. It was hypothesised that they should be able to, as phosphatase does not affect ability to recognise

non-phosphorylated proteins. To answer this question, CMV peptide-pulsed LCLs from a donor with known CMV-viral peptide response were phosphatase treated. They were added to a CMV-viral peptide specific T-cell line. Following a period of 7 days of co-culturing, we were able to show that these cells were indeed not affected by phosphatase treatment and they continued to possess the ability to recognise and become activated by viral peptides expressed on the LCLs, thus confirming that T-cell activation towards LCLs in a non-autologous cell line was in fact viral driven not cancer epitope driven.

Conventionally it is considered that it is the effector T-cells which are able to respond quickest to antigen stimulation, as demonstrated here by IFNγ release, and the central memory T-cells may also do this but at a slower rate as they will only actively do this when they have started to expand and differentiate. As a result of this observation, we decided to assess this presumption further, by analysing the memory phenotypes of the anti-LCL $CD8^+$ T-cells, as demonstrated in an EBV naïve donor (fig. 3.5). It was found (following FACS sorting) that the majority of responses were in the TEMRA compartment with similar frequencies of responses in both CM and EM cells. Very few naïve $CD8^+$ T cells were demonstrated. All four compartments showed expansion following stimulation with LCLs (Fig. 3.5b) when assessed in the positive control. This is in direct contrast to previous studies which had demonstrated a stronger CM response rather than TEMRA (Bhaduri-McIntosh, Rotenberg et al. 2008). Unsurprisingly phosphatase treatment of the autologous LCLs in the EBV-naïve donor drastically reduced the response to LCLs, with a reduction in TEMRA from 12-2SFUs, which would be expected as these cells should not possess a viral response to the LCLs by virtue of the donor being EBV-naive. Of note however, is that following phosphatase treatment, the central memory response was much less than the TEMRA response – and thus actually does confirm previous observation that CM is most involved in LCL recognition via phosphopeptides in the naïve donor (i.e. Phosphatase treatment has removed the

phosphopeptide response). I wondered whether there was skewing the data obtained (due to using anti-LCL T cells rather than fresh PBMC's), as by the nature of derivation of the anti-LCL T-cell line, they were not truly 'naïve' and thus had the potential to have developed an anti-viral response. To test this theory the same experiment was performed with fresh PBMC's which had been FACS sorted as previously into the different T-cell compartments (Fig 3.6a, b). Phosphatase treatment once again significantly reduced the overall response to target cells in CM from 10SFUs to 3SFUs and TEMRA from 12-6SFU/100,000 T-cells, which confirmed that CM following phosphatase treatment was where the majority of the memory responses lie. Both TEMRA and CM have been implicated as forming part of the phosphopeptide response; however, in the T-cell data (fig 3.5 C) we saw a larger reduction in TEMRA. This may hint that culturing T-cells against autologous LCLs may lead to data bias.

In the EBV-seropositive donors we showed similar responses (Fig 3.6b), but phosphatase treatment allowed demonstration of the viral-targeted contribution. This therefore confirms previous observation that there does appear to be an expandable, functional, cytotoxic T cell response to transformed-self, of a CM phenotype, which contrasts to the observation noted by Dr Penny which showed EM to be the predominant type. The implications of this finding are based on the assumption that these donors have a fully functional cytotoxic T cell response against phophopeptides and therefore they possess this T-cell response to protect them from cancer. We would therefore hypothesise that the loss of this T cell response could result in them acquiring a B cell cancer (or other types of cancer if more than one cell type presents the same phosphopeptide).

Furthermore, it was demonstrated that these anti-LCL $CD8^+$ T cells in EBV naïve individuals (and EBV-seropositive individuals in the presence of phosphatase treatment) were capable of killing (Fig. 3.3c and 3.7b,c).

JY is a long established cell-line which is derived from a patient with PTLD. This was therefore used as a cell line model to study PTLD. Phosphopeptides have been identified on this cell line (Table 3.1) as well as in healthy B-cells (spleen and tonsil). However, it can be seen that there are far more phosphopeptides identified on JY than in healthy tissue, which again fits with the assertion that cancers possess post-translationally modified proteins, and phosphorylation thereof is a hallmark of this. This observation being accepted, it therefore stands to reason that tumour immunotherapy targets would be expressed on tumour and not healthy cells.

Clearly, we have identified a vast number of phosphopeptides many of which could be implicated in cancer tumour pathways. On analysing the source proteins we can see a number have previously been implicated in cancer pathways such as those which code for proteins MAP kinases, LSP1, NFAT and B-catenins. This will be investigated further in chapter 4.

One key question to be answered is: *is it likely that every patient with a tumour possesses at least one phosphopeptide on that tumour, allowing T-cells to target that tumour?* The answer to this is likely to be yes given how many phosphopeptides we have identified on JY compared to healthy untransformed B-cells (10 fold more). The next chapter explores overlap between tumours with regards to phosphopeptide expression, and will aim to come closer to answering this question. Certainly previous studies have shown overlap between tumours but the fact that there are so many more phosphopeptides expressed on transformed cells compared to healthy controls would suggest that these are 'cancer epitopes'. Related to this is the observation that healthy B-cells do possess phosphopeptides as well. This could therefore point to a role for phosphopeptide outside of tumour recognition which is as yet unidentified, or it may purely be a coincidence – as we have seen that those phosphopeptides expressed by normal cells are on the whole expressed at a lesser level than transformed cells suggesting that this could be non-specific 'background' expression. Clearly phosphopeptides expressed on

healthy cells would be unhelpful in a cancer immunotherapy as they would lead to T-cells targetting healthy cells – something clearly immunotherapies are aiming to avoid. One potential explanation is that these phosphopeptides are expressed on healthy tissues, and malignant transformation may lead to increased expression perhaps due to upstream upregulation of protein source.

In conclusion, we have demonstrated that transformed B-cells express phosphopeptides at higher levels than healthy tissues. We have also shown that T-cells derived from healthy donors are able to recognise phosphopeptides and perform effective killing. This has therefore led us to believe that phosphopeptide-recognition could play a role in tumour recognition and destruction, and potentially play a protective role in healthy individuals, Based on this observation we can now go on to investigate whether these cells could form the basis of a cancer immunotherapy.

Chapter 4: IDENTIFICATION OF TUMOUR-SPECIFIC MHC CLASS I-ASSOCIATED PHOSPHOPEPTIDES

4.1. Introduction

In order for immunotherapy to work, tumours must express a specific target which can delineate healthy and tumour tissue. Mutations and epigenetic changes accumulate in tissues, which finally lead to a dysregulation of major signalling pathways that are important for malignant transformation. Therefore, deregulation of signalling pathways with altered intracellular protein phosphorylation is a documented 'hallmark' of cancer. As established by this group, phosphoproteins involved in these signalling cascades can be degraded to phosphopeptides that are then subsequently presented on the cell surface by major histocompatibility complex (MHC) molecules and recognized by T-cells (Zarling, Polefrone et al. 2006, Cobbold, Polefrone et al. 2007, Penny, Abelin et al. 2012, Cobbold, De La Pena et al. 2013).

Previously, it has been established that phosphopeptides could represent a likely target for T-cell responses to malignant transformation. The aim of this study was to see what role these phosphopeptides played in paediatric cancer, and in particular (1) Hepatic tumours (i) hepatoblastoma and (ii) hepatocellular carcinoma and (2) Post-Transplantation Lymphoproliferative Disease (PTLD) as this was a key objective of this Phd, having worked in the liver transplant field, and aspiring to be a paediatric hepatologist.

Clearly, with regards to PTLD, immunity plays a role, as it develops following initiation of immunosuppression in response to viral infection with EBV. As discussed previously, LCLs are a useful *in vitro* equivalent to PTLD and a lot of what has already been established was based on the JY LCL as an *in vitro* model (Penny, Abelin et al. 2012, Cobbold, De La Pena et al. 2013, Abelin, Trantham et al. 2015). A role for the immune response and in particular

phosphopeptide response has also been identified in a number of other tumours including melanoma, leukaemia and colorectal tumours (Penny, Abelin et al. 2012, Cobbold, De La Pena et al. 2013).

In hepatocellular carcinoma (a predominantly adult tumour) a role for recognition of tumour-associated antigens is also evident (Stenner-Liewen, Luo et al. 2000, Thorgeirsson and Grisham 2002, Chen, Fu et al. 2008, Mizukoshi, Nakamoto et al. 2011, Liang, Ding et al. 2013); however until recently very few of these antigens have been identified. In hepatoblastoma, there has been an implication that FAS/FAS ligand plays a role in apoptosis (Ozdemirli, ElKhatib et al. 1996, Scaffidi, Fulda et al. 1998, Yoshikawa, Toyohara et al. 1998, Allan, Parikh et al. 2013, Hsiao, Kao et al. 2013). Wnt-signalling, B-catenins and NF-Kappa B also appear to play a pivotal role in development of tumour, and are targets for chemotherapy (Pritchard, Brown et al. 2000, Hartmann, Kuechler et al. 2009, Armengol, Cairo et al. 2011, Mokkapati, Niopek et al. 2014). FAS Ligand plays a key role in T-cell expansion during immune responses and it is also involved in cell responsiveness to chemotherapy as originally described in leukaemias. However, more recently it has been implicated in chemosensitive tumours such as hepatoblastoma, neuroblastoma and some brain tumours (Micheau, Solary et al. 1997, Muller, Strand et al. 1997, Fulda, Los et al. 1998, Scaffidi, Fulda et al. 1998).

Many tumours are recognised by antigen specific MHC Class-I specific cytotoxic T-cells, the most extensively investigated being melanoma, with peptides identified as the targets for these CTL's (Romero 1996, Wang, Gulden et al. 1997). This has even prompted a number of Phase I trials looking at cancer vaccines based around these peptides (Jager, Ringhoffer et al. 1996, Jager, Ringhoffer et al. 1996, Nestle, Alijagic et al. 1998, Rosenberg, Yang et al. 1998, Marchand, van Baren et al. 1999). Therefore, there may be a role for phophopeptides in other tumour types including hepatoblastoma and PTLD, but as yet this has not been considered.

Immunotherapy is predicted to improve outcome in high risk hepatoblastoma patients who are more prone to developing chemoresistance. The use of monoclonal antibodies to direct immunity towards tumour cells has recently been studied using humanised antibodies which recognised EpCAM or CD326 which is known to be overexpressed in hepatic tumour cells, with the data obtained suggesting improved targeting of cells and potentially better long term outcome (Armeanu-Ebinger, Hoh et al. 2013). We therefore propose that recognition of phosphopeptide in conjunction with cancer vaccines or monoclonal antibodies, or indeed a combination thereof, may be a key cancer immunotherapy to be considered in the future.

4.2 Characterisation of MHC Class-I phosphopeptides

Leading on from these initial observations, we hypothesised that phosphopeptides are presented by MHC molecules in increasing amounts on the surface of altered hepatocytes. We further proposed that the immune system monitors the liver for malignant transformed hepatocytes and clears those cells with the help of phosphopeptide-specific cytotoxic T-cells. In order to test both of these hypotheses, MHC class I-associated phosphopeptides were isolated from tumour using techniques described previously (and adjacent normal tissue where available) and characterised in hepatoblastoma cell lines, primary liver tumours, PTLD cell lines and blood from a patient with PTLD, in order to identify tumour-associated phosphopeptides.

4.2.1 Hepatoblastoma-associated phosphopeptides identified

HepG2 is a well established cell line, which is known to be HLA-A2. This cell line was grown to a density of $1x10^6$ cells/ml, and the MHC class I complexes purified and the peptides eluted as per standard protocols (see materials and methods section 2.10). Using IMAC technology, phosphopeptides were purified from this mixture, which were further characterised by LC-

MS/MS and manual sequence assignment by the Hunt laboratory in Virginia using their standard protocols (fig. 4.1).

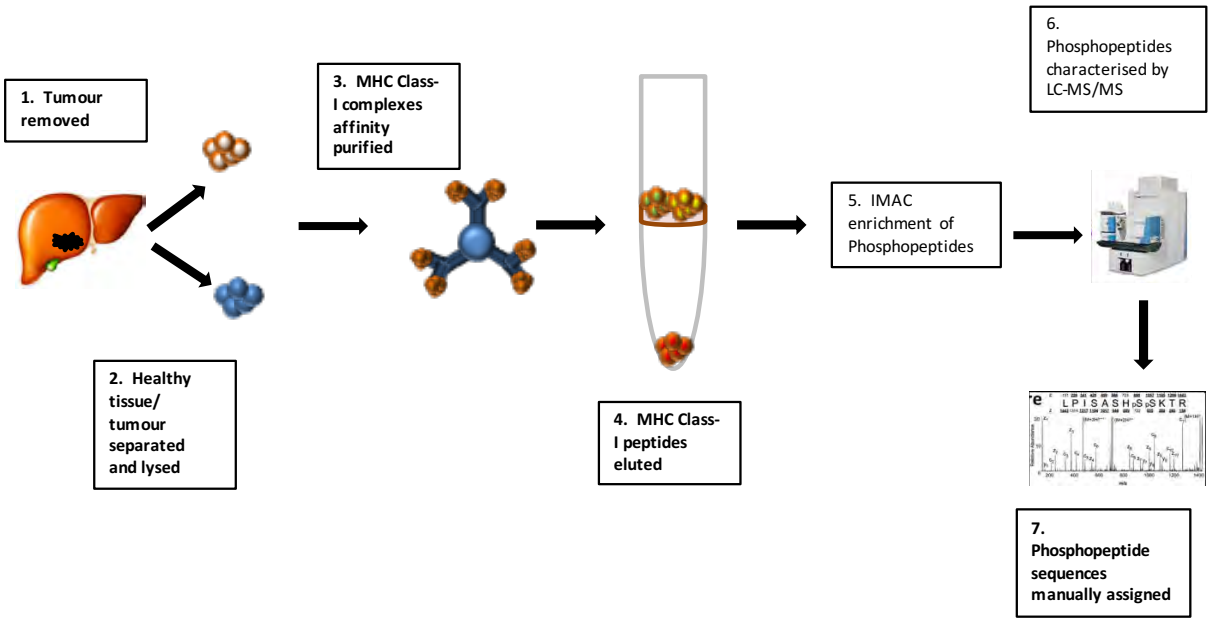

Fig. 4.1 Schematic describing work-flow for tumour-specific, MHC class I-associated phosphopeptide discovery from patient samples. Tumour and normal tissue were taken from the same patient at tumour resection/explant. These were each lysed and the MHC class I complexes affinity purified using pan class-I antibody, W6/32. The MHC class I-associated peptides were eluted in acid and phosphopeptides enriched using IMAC. These phosphopeptides were characterised using CAD and ETD LC-MS/MS and the sequences manually assigned.

Additionally, four primary HB tumour samples, each with adjacent matched 'normal' healthy tissue were similarly processed and analysed. The HLA types of these samples, as obtained from records held by Birmingham Children's Hospital Liver Transplant Unit, are detailed in Table 4.1. Key HLA types investigated here were A2 and B7 as these were more commonly identified in the tumour tissues available to the project. As already identified in chapter 3, phosphopeptides appear to be only expressed within a specific HLA type i.e. 'HLA specific', and therefore this influenced the subsequent healthy donor's identified for this stage of the project.

	Class I HLA Allele		
Sample	**A locus**	**B locus**	**C locus**
HB 02	A*02	B*07	C*06
	A*29	B*27	
HB 05	A*02	B*07	C*07
	A*24	B*35	
HB 06	A*02	B*07	C*06
	A*29	B*57	
HB 07	A*01	B*07	C*06
	A*03	B*15	
HepG2 line	A*02	B*15	C*06
	A*24	B*35	

Table 4.1: HLA type of tumour samples and HepG2 the hepatoblastoma cell line. HLA was assigned using standard PCR methods. Full HLA type not available.

As per accepted 'in house' definitions, phosphopeptides were considered 'tumour-associated' if the levels detected in the tumour tissue were at least twice those levels detected on the normal tissue (corrected for weight of sample available). Only 11% of tumour-associated phosphopeptides were found at any detectable level in the healthy tissues. By using UniProt software (www.uniprot.org) the protein source for the phosphopeptide was assigned. Using the "MHC-I binding predictions" program from IEDB (tools.immuneepitope.org), along with the information available about the HLA type of the cell line/patient, peptide-HLA binding was predicted. All patients undergoing liver transplantation had a HLA tissue typing conducted as part of their transplant preparation protocol. This information was gathered by Ms Julie Taylor and shared as per our transfer agreement. The phosphopeptides identified, the protein which they originate from, their predicted HLA binding and their relative levels in each of the samples is described in tables 4.2 (HLA-A), 4.3 (HLA-B) and 4.4 (Unknown HLA). These were described in this way in order to make a further comparison to data available in other tumours as studied by other members of the laboratory including Dr Penny (colorectal, gastro-

oesophageal) and Dr Buttner (HCC tumours in adult samples) thus facilitating a direct comparison. Small 's' or 't' denotes phosphorylation.

Table 4.2: Phosphopeptides identified from Hepatoblastoma samples predicted to bind HLA-A

Phosphopeptide	Source Protein	Predicted HLA binding	Primaries								Cell line
			HP02		HP05		HP06		HP07		HepG2
			Healthy	Tumour	Healthy	Tumour	Healthy	Tumour	Healthy	Tumour	
YPLsPTKISQY	Homeodomain-interacting protein kinase 1	A1									
YPLsPAKVNQY	Homeodomain-interacting protein kinase 2	A1									
STDsETLRY	Synaptotagmin-like protein 2	A1									
KTMsGTFLL	Signal transducer and activator of transcription 2	A2									
RQLsSGVSEI	Heat shock protein beta-1 (HSPB1)	A2									
RQAsIELPSM	Lymphocyte-specific protein 1	A2									
RTFsPTYGL	Synemin	A2									
KLAsPELERL	Transcription factor AP-1	A2									
ALDsGASLLHL	Receptor-interacting serine/threonine-protein kinase 4	A2									
RQDsTPGKVFL	Nuclear receptor subfamily 2 group C member 1	A2									
KLMsPKADVKL	Uncharacterized protein KIAA1328	A2									
KLMsDVEDV	Bromodomain and WD repeat-containing protein 1	A2									
RQIsQDVKL	AMP deaminase 2	A2									
KAFsPVRSV	DNA-binding protein inhibitor ID-2	A2									
SLFsGDEENA	Programmed cell death protein 4	A2									
RQLsALHRA	60S ribosomal protein L15	A2									
RLAsLQSEV	?	A2									
SLFGGsVKL	Programmed cell death 6-interacting protein	A2									
VLLsPVPEL	Anaphase-promoting complex subunit 1	A2									
KLIDIVsSQKV	Serine/threonine-protein kinase Chk1	A2									
ELFSsPPAV	Nuclear factor of activated T-cells 5	A2									
KLFPDtPLAL	Interleukin enhancer-binding factor 3	A2									
RSLsQELVGV	Zinc finger protein 318	A2									

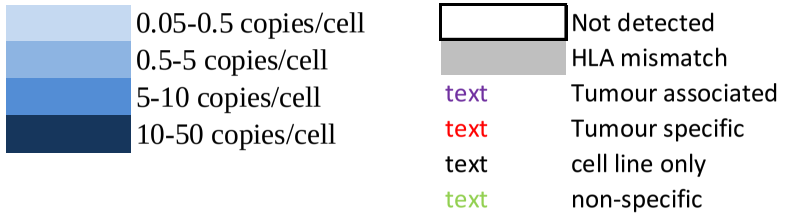

Table 4.2: Phosphopeptides identified from Hepatoblastoma samples predicted to bind HLA-A continued

Phosphopeptide	Source Protein	Predicted HLA binding
RLSsPLHFV	Protein FAM134A	A2
RLLsTDAEAV	Transcription initiation factor TFIID subunit 7	A2
AVVsPPALHNA	Bromodomain-containing protein 4	A2
ALDsGASLLHL	Receptor-interacting serine/threonine-protein kinase 4 (RIPK4)	A2
RLAsYLDKV	Keratin, type I cytoskeletal 19	A2
FLDtPIAKV	Protein naked cuticle homolog 1	A2
KVAsLLHQV	TNFAIP3-interacting protein 2	A2
VMIGsPKKV	Tensin 3 (TNS3)	A2
SMTRsPPRV	Serine/arginine-rich splicing factor 8	A2
KLDsPRVTV	Family with sequence similarity 86, member A, isoform CRA_h	A2
STAPPVHNV	Mucin 1, cell surface associated (MUC1)	A2
ALSNLEVTL	Fermitin family homolog 1 (c20orf42)	A2
ILAPVILYI	NADPH oxidase 1 (Nox-1)	A2
ILDQKINEV	Ornithine decarboxylase (ODC)	A2
KLMDLDVEQL	Proliferating Cell Nuclear Antigen (PCNA)	A2
ALFVRLLALA	Transforming growth factor beta 1 (TGFB1)	A2
TMAsPGKDNY	karyopherin subunit alpha 6	A3
RyQTQPVTL	Supervillin	A24
VYTyIQSRF	Dual specificity tyrosine-phosphorylation-regulated kinase 4	A24
KSLsPSLLGY	Nuclear factor of activated T-cells, cytoplasmic2	A29
RPIsVIGGVSLY	Spermatogenesis-associated protein 13	A29

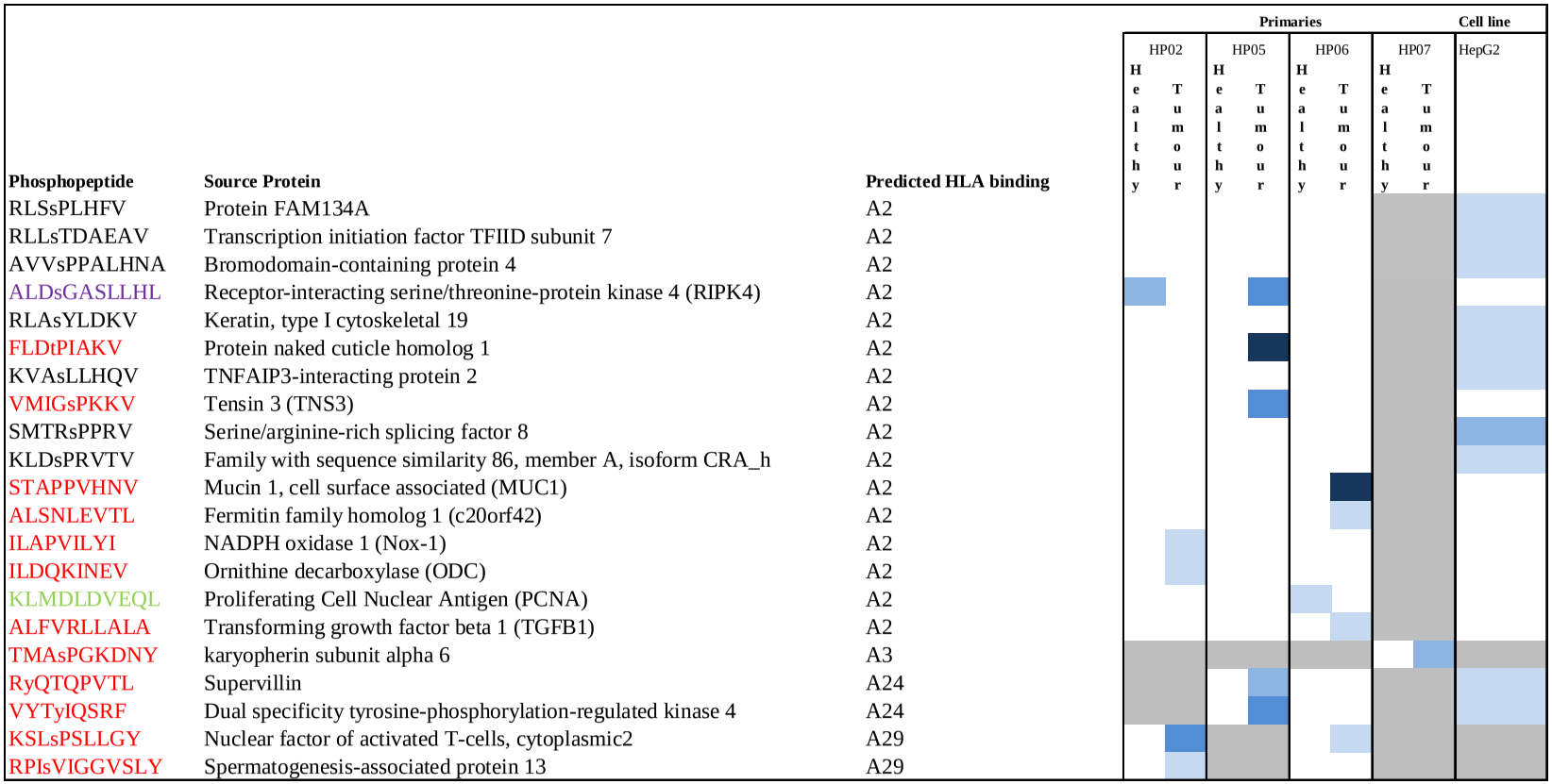

Table 4.3: Phosphopeptides identified from Hepatoblastoma samples predicted to bind HLA-B

Phosphopeptide	Source Protein	Predicted HLA binding	Primaries								Cell line
			HP02		HP05		HP06		HP07		HepG2
			Healthy	Tumour	Healthy	Tumour	Healthy	Tumour	Healthy	Tumour	
KPFKLSGLsF	MARCKS-related protein	B7									
KPAsPKFIVTL	Zinc finger CCCH domain-containing protein 14	B7									
KPRsPVVEL	Beta-adrenergic receptor kinase 1	B7									
TPRsPPLGL	Mitogen-activated protein kinase kinase kinase 11	B7									
RPFHGISTVsL	DENN domain-containing protein 4C	B7									
RPFsPREAL	Leucine zipper protein 1	B7									
RPVsPFQEL	unknown	B7									
RPWsPAVSA	Ski oncogene	B7									
RPYsPPFFSL	Protein FAM53C	B7									
RPLsPILHI	Protein transport protein Sec24B	B7									
SPFKRQLsL	Numb Homolog (Drosophila)-Like	B7									
SPFKRQLsL	cDNA FLJ53174, highly similar to Numb-like protein	B7									
RPAFFsPSL	Uncharacterized protein KIAA0930	B7									
TPRsPPLGL	Mitogen-activated protein kinase kinase kinase 11	B7									
RPKPsSSPVIF	Poly(rC)-binding protein 2	B7									
TPRsPPLGLI	Mitogen-activated protein kinase kinase kinase 11	B7									

0.05-0.5 copies/cell
0.5-5 copies/cell
5-10 copies/cell
10-50 copies/cell

Not detected
HLA mismatch
text Tumour associated
text Tumour specific
text cell line only
text non-specific

Table 4.3: Phosphopeptides identified from Hepatoblastoma samples predicted to bind HLA-B continued

Phosphopeptide	Source Protein	Predicted HLA binding	Primaries				Cell line
			HP02	HP05	HP06	HP07	HepG2
			Healthy / Tumour	Healthy / Tumour	Healthy / Tumour	Healthy / Tumour	
RPTKIGRRsL	adenosylhomocysteinase like 2	B7					
RPDsAHKML	Palladin, Cytoskeletal Associated Protein	B7					
RAHsEPLAL	DDB1- and CUL4-associated factor 15	B15					
RAHSsPASL	YAP1 (yes-associated protein 1)	B15					
RSHsSPASL	WW Domain Containing Transcription Regulator 1	B15					
RSRsPLEL	DNA damage-binding protein 2	B27					
KRYsGNMEY	Large Tumor Suppressor Kinase 1	B27					
RRGsFEVTL	Selenoprotein H	B27					
RRPsLLSEF	Nuclear receptor corepressor 1	B27					
RRsSFLQVF	Protein transport protein Sec23A	B27					
RPIsPGLSY	Coiled-coil domain-containing protein 6	B35					
RPIsPPHTY	Roundabout homolog 1	B35					
RPmsESPHm	ZFP36 Ring Finger Protein-Like 1	B35					
LPKsPPYTAF	Eukaryotic translation initiation factor 4B	B35					
KAFsPVRSV	DNA-binding protein inhibitor ID-2	B57					
KSGELLAtW	salt inducible kinase 2	B57					

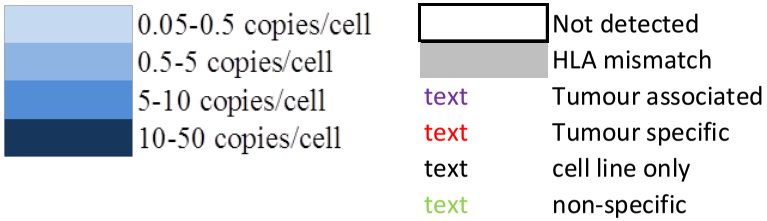

Table 4.4: Phosphopeptides identified from hepatopblastoma cells with unknown HLA binding

Phosphopeptide	Source Protein	Predicted HLA binding	Primaries					Cell line
			HP02		HP05		HP06	HP07		HepG2
			Healthy	Tumour	Healthy	Tumour	Healthy	Tumour	Healthy	Tumour	
RTHsLLLLL	Ribonuclease 4	U									
RKSsIIIRM	Plasminogen-like protein B	U									
QPRsPGPDYSL	Growth Factor Independent 1 Transcription Repressor	U									
ITQGtPLKY	Nuclear Receptor Corepressor 2	U									
KPAsPKFIVTL	zinc finger CCCH-type containing 14	U									
RRPsLLSEF	Nuclear Receptor Corepressor 1	U									
RFKtQPVTF	Anterior gradient protein 2 homolog	U									
RTHsLLLLL	ribonuclease A family member 4	U									
KRLsVERIY	Topoisomerase (DNA) II Alpha	U									
TRKtPESFL	Epsin 1	U									
RRIsDPEVF	Filamin A Interacting Protein 1-Like	U									
SFDsGSVRL	Interferon regulatory factor 6	U									
RKPsIVTKY	ATP-dependent helicase ATRX	U									
RRPsLLSEF	Nuclear receptor corepressor 1	C6									
RRLsFLVSY	Glutamine--tRNA ligase	C6									
RRsSFLQVF	Protein transport protein Sec23A	C6									
KAFsPVR	DNA-binding protein inhibitor ID-2	C6									
KAFsPVRSV	DNA-binding protein inhibitor ID-2	C6									
RSAsFSRKV	Nephrocystin-4	C6									
LSSsVIREL	Neuroguidin	C6									

0.05-0.5 copies/cell
0.5-5 copies/cell
5-10 copies/cell
10-50 copies/cell

Not detected
HLA mismatch
text Tumour associated
text Tumour specific
text cell line only
text non-specific

Initial observation of these tables suggests that the greatest number of phosphopeptides identified were on HepG2, the hepatoblastoma cell line. This could be due to it being an established line generated a number of years ago and subsequent mutation of the line, although this can only be surmised. Information was not available in relation to passage number of these cells. It is likely this does represent a heterogeneous cell line however. Hepatoblastoma tumour sample HP02 demonstrated a larger number of phosphopeptides (35) compared to sample HP05 (24), HP06 (19) and HP07 (13). All tumour samples were normalised for tumour sample size. The reason for this variation could be related to where the sample was obtained from (i.e. position within the tumour – central versus periphery) or how the sample was processed by surgical centre (i.e. different surgical teams, different histopathologist, time of day specimen was obtained – as many were obtained at liver explant during transplantation surgery and as a result samples may degrade as a result of short term storage if surgery occurred overnight/bank holiday/at the weekend. Samples were to be processed 'fresh' (i.e. not fixed in formalin/wax or liquid nitrogen) and therefore any delay even small could result in tissue degradation. To further emphasise this point, sample HB07 for instance was a sample which was taken during transplant surgery over a weekend period and therefore the sample was stored in a refrigerator for 36 hours prior to transfer to the Tissue BioBank (HBRC, University Hospitals Birmingham) prior to sample release, and this would therefore appear to have influenced the sample outcome. However, in view of small numbers of clinical samples being available the decision was made to include this sample anyway.

Overviewing the data there are a number of phosphopeptides expressed across a number of samples/HepG2. In particular, the phosphopeptide RPWsPAVSA coding for the Ski oncogene is expressed in 3 of the hepatoblastoma tumour samples (HP02, HP05 and HP06). This is therefore strongly suggestive of this being a potential T-cell target on hepatoblastoma and therefore was considered a phosphopeptide of interest which was identified as one to

investigate further. The phosphopeptide RTHsLLLL which codes for the protein ribonuclease 4 is expressed in all samples both tumour and healthy tissue as well as the HepG2 cell line. This phosphopeptide is therefore discounted as a possible target phosphopeptide for this tumour group, as it is unlikely a tumour target would also be expressed at such high levels in normal healthy tissue.

There were an increased number of phosphopeptides identified in the tumour samples compared with the healthy tissue, on average, 68 vs. 25 (fig. 4.2A). This suggests that the level of phosphopeptide expressed on the cell surface would be higher in tumour tissue than healthy tissue ($\chi 2$ test $p<0.01$). Where phosphopeptides were found on both normal and tumour tissues, they were expressed at higher levels on tumour tissue suggesting they were 'tumour associated'. Fig 4.2b is a Euler diagram showing the overlap of phosphopeptide presentation on hepatoblastoma tumours, healthy tissues and hepatoblastoma (HepG2) cell line. This shows that 41 phosphopeptides have been found unique to hepatoblastoma and not on healthy tissue or previously in the HepG2 cell line. There is an overlap of 16 phosphopeptides found on both tumour and cell line (HepG2). If phosphopeptides are the target for immune cells to recognise tumour, we propose these targets will be in the tumour or tumour/cell line crossover. We discounted those phosphopeptides found exclusively in the cell line, as these have not been seen in any other samples and hence validity as a target is in doubt, as we could not support or refute the suggestion that this is a tumour target as we have not demonstrated it on a tumour sample.

Fig 4.2c demonstrated phosphopeptides found to be present in the healthy liver tissues were found at significantly different levels in the tumour tissue, $p<0.001$ Wilcoxons t-test, but weren't significantly different to expression in the HepG2 cell line i.e. there were significantly more phosphopeptides found on tumours and the HepG2 cell line, and the numbers of copies per cell of phosphopeptide overall in the tumours and the cell line were significantly higher

than levels found in healthy tissues. When considering the phosphopeptides identified in normal tissues (fig. 4.2D) we demonstrated that those found were not significantly higher in tumour than normal tissue, which further bolstered the idea that these phosphopeptides are unlikely to be an immune target as there is not a sufficient difference when comparing healthy and abnormal tissues (Wilcoxon signed rank p=0.802 (fig.4.2 D).

Fig. 4.2e demonstrates the number of hepatoblastoma associated phosphopeptides identified on the hepatoblastoma tumour samples. HLA-A2 and B7 were identified as being commonest amongst the samples obtained (three and four samples respectively) which is perhaps not surprising given the population sampled and hence selected to be explored further following this observation.

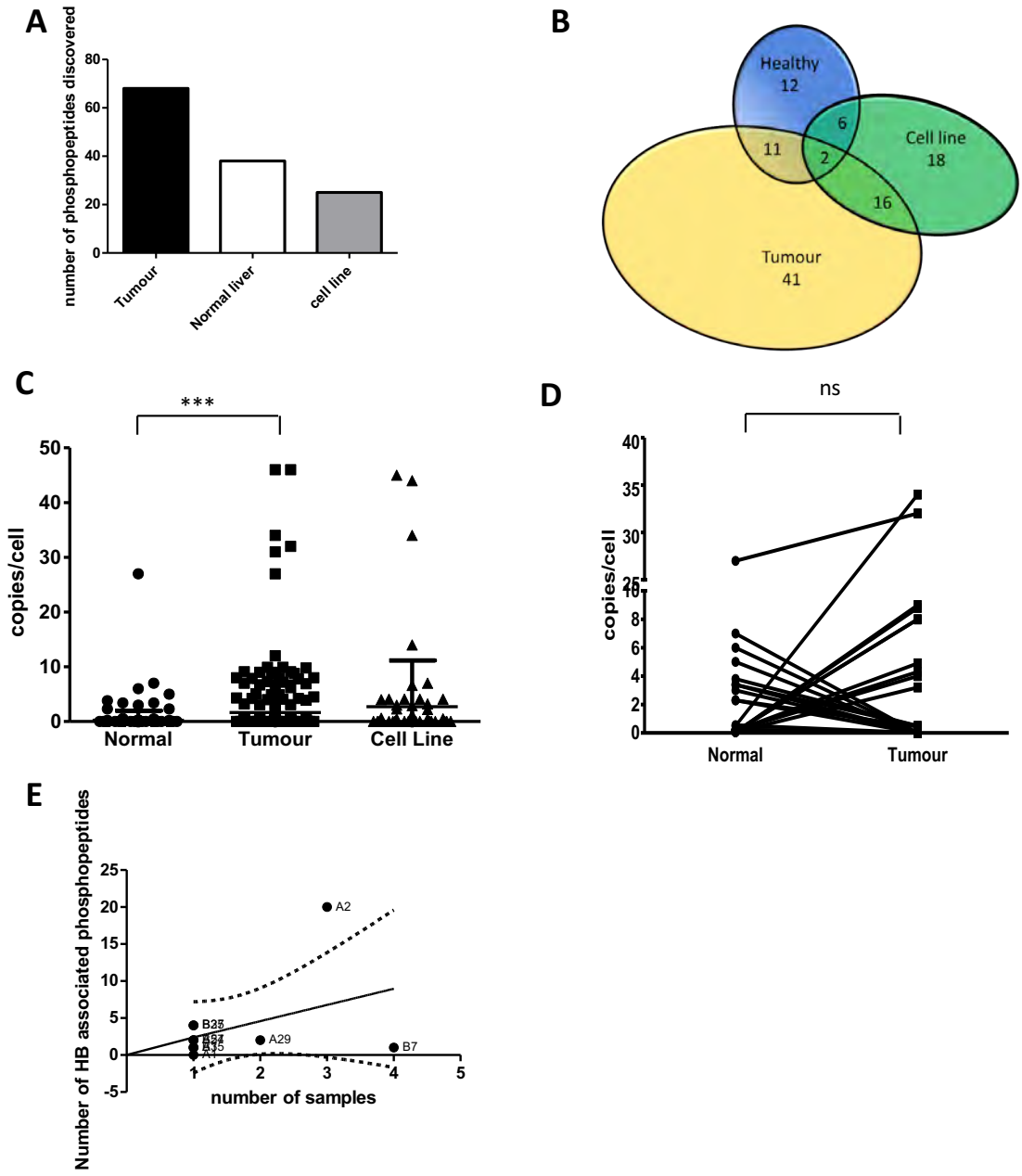

Fig. 4.2 Comparison of phosphopeptide levels in healthy and Hepatoblastoma tumour tissue samples The number of phosphopeptides identified by our collaborators at University of Virginia using techniques previously described was compared in hepatoblastoma tumour primaries and adjacent healthy tissue obtained at time of surgery from the same patient. (A) More phosphopeptides were seen in tumour than normal liver tissue $\chi 2$ $p<0.001$. Phosphopeptides not identified were said to be at a level below detection (0.1 fmol/gram). Significantly more phosphopeptide was present in tumour tissue than healthy liver tissue, Wilcoxon signed rank $p<0.001$. (B) Euler diagram showing the overlap of phosphopeptide presentation on hepatoblastoma tumours, healthy tissues and hepatoblastoma (HepG2) cell line. (C) The phosphopeptides present in healthy liver tissue were found at significantly different levels in the tumour tissue, $p<0.0001$ Wilcoxons t-test(***). (D) Phosphopeptides identified on normal tissue were not found at significantly different levels in tumour tissue by Wilcoxon signed rank $p=0.802$ (ns). (E) Correlation between the number of phosphopeptides identified and the number of samples for each HLA type.

4.2.2 Characterisation of PTLD tumour-specific MHC class I-associated phosphopeptides

MHC class I-associated phosphopeptides were isolated and characterised from three LCL cell lines (an *in vitro* equivalent to PTLD), and blood obtained from a patient with PTLD. The patient was initially diagnosed with short gut secondary to antenatally diagnosed gastroschisis and subsequent multiple surgical resections necessitating combined small bowel and liver transplant for Intestinal Failure associated Liver Disease (IFALD) at the age of 3y 9 months. PTLD developed 7 months subsequent to this and was determined to be EBV-mediated.

The cell line JY, as already discussed in chapter 3, which is natively HLA-A2 was grown to $1x10^6$ cells/ml and the MHC class I complexes purified as per standard protocols and the resultant peptides eluted. Using IMAC, phosphopeptides were purified and further characterised by LC-MS/MS and manual sequence assignment by the Hunt Laboratory in Virginia, USA. Additionally, two LCL cell lines were generated from healthy donors (designated donor 1 and donor 2), by methods described in chapter 2 which were similarly processed and analysed. All three cell lines and the patient sample were HLA typed (table 4.5). NB only one patient sample was obtained, HLA was already known as the patient had recently undergone solid organ transplantation 7 months prior to development of PTLD.

Table. 4.5 HLA type of LCL/PTLD samples

	Class I HLA Allele		
Sample	**A locus**	**B locus**	**C locus**
JY	A*02	B*07	-
	-	-	
Donor 1 LCL	A*01	B*07	C*06
	A*02	B*27	
Donor 2 LCL	A*02	B*07	C*06
	A*02	B*13	
PTLD 01	A*02	B*07	C*06
	A*03	B*27	

Table 4.6 overleaf describes phosphopeptides isolated by our collaborators at the University of Virginia. Again, as per our agreed accepted 'in house' definition, phosphopeptides were considered 'tumour-associated' if the levels in the tumour were at least twice that of the normal tissue. The majority of tumour-associated phosphopeptides detected on the LCLs were not found at any level in the healthy B-cells (only 10% were found to be present). UniProt was used to identify the representative protein source of the phosphopeptide (www.uniprot.org). Prediction software was used to predict peptide binding to HLA - “MHC-I binding predictions” programme from IEDB (tools.immuneepitope.org), along with the information about the HLA type of the patient or healthy donors. The phosphopeptides identified, their protein, their predicted HLA-binding and relative levels in each of the samples is described in tables 4.6 (HLA-A), 4.7 (HLA-B) and 4.8 (Unknown HLA). These were described in this way in order to make a further comparison to data available in other tumours as studied by other members of the laboratory including Dr Penny (colorectal, gastro-oesophageal) and Dr Buttner (HCC tumours in adult samples) thus facilitating a direct comparison. Small 's' or 'p' denotes phosphorylation.

Table 4.6: Phosphopeptides identified from PTLD/LCL cells with predicted HLA-A+ binding

Phosphopeptide	Source Protein	Predicted HLA binding	HB	Donor 1	Donor 2	PTLD (A)	Spleen (B cell)	Tonsil (B cell)
ITQGtPLKY	Nuclear receptor corepressor 2	A1						
NTDsPLRY	40S ribosomal protein SA	A1						
SLDsPsYVLY	Protein farnesyltransferase type-1 subunit alpha	A1						
KAFsPVRSV	DNA-binding protein inhibitor ID-2	A2;C6						
RQLsSGVSEI	Heat shock protein beta-1	A2						
RLLsPRPSL	Nuclear receptor corepressor 2	A2						
ALDsGASLLHL	Receptor-interacting serine/threonine-protein kinase 4	A2						
ALGsRESLATL	Ras GTPase-activating protein	A2						
ALYsPAQPSL	Sphingomyelin phosphodiesterase 4	A2						
AMAAsPHAV	Heterogeneous nuclear ribonucleoprotein A0	A2						
AMLGSKsPDPYRL	Negative regulatory element-binding protein	A2						
AVIHQsLGL	CNPPD1 family	A2						
AVVsPPALHNA	bromodomain containing 4	A2						
GLLGsPVRA	cell division cycle 25B	A2						
GLLsPARLYAI	Leucine-rich PPR motif-containing protein	A2						
ILDsGIYRI	alpha integrin binding protein 63	A2						
ILKsPEIQRA	60S ribosomal protein L1	A2						
IMDRtPEKL	breast cancer anti-estrogen resistance 3	A2						
KIFsGVFVKV	60S ribosomal protein L7-like 1	A2						
KLDsPRVTV	FAM86A	A2						
KLFPDtPLAL	NFAT90	A2						
KLFsPSKEAEL	Hematological and neurological expressed 1-like protein	A2						
KLIDIVsSQKV	unknown	A2						
KLIDRTEsL	leukocyte-specific protein 1	A2						
KLLQFYPsL	linker for activation of B cells	A2						
KLLSSAQRtL	Zinc finger protein 169	A2						
KLMAPDIsL	BCL2/adenovirus E1B 19kDa interacting protein 2	A2						
KLMsPKADVKL	hinderin	A2						
KMDsFLDMQL	BCL-3 binding protein	A2						
KMYsEIDIKV	EFTUD2	A2						

Phosphopeptide	Source Protein	Predicted HLA binding	Donor 1	Donor 2	JY	PTLD (A)	Spleen (B cell)	Tonsil (B cell)
KLDsPRVTV	FAM86A	A2						
KLFPDtPLAL	NFAT90	A2						
KLFsPSKEAEL	Hematological and neurological expressed 1-like protein	A2						
KLIDlVsSQKV	unknown	A2						
KLIDRTEsL	leukocyte-specific protein 1	A2						
KLLQFYPsL	linker for activation of B cells	A2						
KLLSSAQRtL	Zinc finger protein 169	A2						
KLMAPDIsL	BCL2/adenovirus E1B 19kDa interacting protein 2	A2						
KLMsPKADVKL	hinderin	A2						
KMDsFLDMQL	BCL-3 binding protein	A2						
KMYsEIDIKV	EFTUD2	A2						
KVAsLLHQV	Fetal liver LKB1-interacting protein	A2						
KVLsTEEMEL	family with sequence similarity 128	A2						
KVQVtSLSV	unknown	A2						
LMFsPVTSL	SET domain-containing protein 5	A2						
mLAEsPSVPRL	unknown	A2						
REAsIELPSM	unknown	A2						
RLAsLNAEAL	BAH domain-containing protein 1	A2						
RLAsLQSEV	unknown	A2						
RLDsYVRS	BET5 homolog	A2						
RLDsYVRSL	BET5 homolog	A2						
RLLsPLS(+18)SA	Ribonucleoprotein PTB-binding 1	A2						
RLLsPLSSA	Ribonucleoprotein PTB-binding 1	A2						
RLQsTSERL	ATP-dependent metalloprotease FtsH1	A2						
RLSsPLHFV	Protein FAM134A	A2						
RQAsIELPSMAV	leukocyte-specific protein 1	A2						
RQAsLSISV	protein kinase D2	A2						
RQIsFKAEV	Ubiquitin-conjugating enzyme E2 J1	A2						
RQIsFQAEV	unknown	A2						
RQIsQDVKL	adenosine monophosphate deaminase 2	A2						
RTYsGPMNKV	POF1B	A2						

Phosphopeptide	Source Protein	Predicted HLA binding	Donor 1	Donor 2	JY	PTLD (A)	Spleen (B cell)	Tonsil (B cell)
RVPsPTPAPK	Serine/arginine repetitive matrix protein 2	A2						
SLLTsPPKA	Thyroid receptor-interacting protein 12	A2						
SMTRsPPRV	Pre-mRNA-splicing factor SRP46	A2						
TLAsPSVFKST	aurora borealis	A2						
VLKGsRSSEL	BLOC-1 related complex subunit 7	A2						
VLLsPVPEL	anaphase promoting complex subunit 1	A2						
VLMKsPsPAL	YTH domain containing 2	A2						
VMFRtPLASV	Early mitotic inhibitor 1	A2						
YLDsGIHSGA	Beta-catenin	A2						
YLDSGIHsGA	Beta-catenin	A2						
VQLsPTKTPSL	Cell cycle regulatory protein p95	A2						
ROAtSIEPLPSM	unknown	A2						
RQApSIWLPSAAV	unknown	A2						
KVLtPIKEK	Centrosomal protein of 120 kDa	A3						
RTAsPPPPPK	Serine/arginine repetitive matrix protein 1	A3						
RTMsEAALVRK	Ras association domain-containing protein 6	A3						
RTRsLSSLREK	Protein furry homolog-like	A3						
RVKtPTSQSYR	Zinc finger protein 281	A3						
RVYsPYNHR	E3 ubiquitin-protein ligase Topors	A3						
KVKsSPLIEKL	CapZ-interacting protein	A3						
SVRRsVLMK	Phosducin-like protein 3	A3						
GIMsPLAKK	AT-rich interactive domain-containing protein 5A	A3						

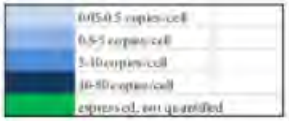

Table 4.7: Phosphopeptides identified from PTLD/LCL cells with predicted HLA-B+ binding

Phosphopeptide	Source Protein	Predicted HLA binding	Donor 1	Donor 2	JY	PTLD (A)	Spleen (B cell)	Tonsil (B cell)
FPRRHsVTL	Zinc finger protein 36, C3H1 type-like 1	B7						
GPRSAsLLSL	G-protein-signaling modulator 3	B7						
HPRsPNVL	Hypoxia-inducible factor 1-alpha	B7						
HPRsPNVLSV	Hypoxia-inducible factor 1-alpha	B7						
HPRsPtPTL	Proline-rich protein 11	B7						
HRYsTPHAF	RAF proto-oncogene serine/threonine-protein kinase	B7						
KPRsPPRAL	Retrotransposon-derived protein PEG10	B7						
KPRsPPRALV	Retrotransposon-derived protein PEG10	B7						
KPRsPVVEL	Beta-adrenergic receptor kinase 1	B7						
KPSsLRRVTI	Lymphoid-restricted membrane protein	B7						
LPRGsSPSVL	Homeobox protein TGIF2	B7						
MPRQPsATRL	Mitotic-spindle organizing protein 2B	B7						
RPAKsMDSL	Rho GTPase-activating protein 30	B7						
RPAsAGAML	Myocyte-specific enhancer factor 2D	B7						
RPAsPAAKL	KAT8 regulatory NSL complex subunit 3	B7						
RPAsPQRAQL	Unknown	B7						
RPDsRLGKTEL	Histone-lysine N-methyltransferase SETD2	B7						
RPFsPREAL	Leucine zipper protein 1	B7						
RPKsDIVLL	B-lymphocyte antigen CD20 (N to D conversion)	B7						
RPKtPPVVI	Synapse-associated protein 1	B7						
RPNsPSPTAL	Serine/threonine-protein kinase tousled-like 1	B7						
RPQRAtsNVF	Myosin regulatory light polypeptide 9	B7						
RPRANsGGVDL	Ras-responsive element-binding protein 1	B7						
RPRARsVDAL	Lipolysis-stimulated lipoprotein receptor	B7						
RPRPHsAPSL	Migration and invasion-inhibitory protein	B7						

Phosphopeptide	Source Protein	Predicted HLA binding	Donor 1	Donor 2	JY	PTLD (A)	Spleen (B cell)	Tonsil (B cell)
RPRPVsPSSL	Serine/threonine-protein kinase SIK1	B7						
RPRPVsPSSLL	Serine/threonine-protein kinase SIK1	B7						
RPRsAVLL	A-kinase anchor protein 13	B7						
RPRsPRENSI	Ataxin-2	B7						
RPRsPRQNSI	Ataxin-2	B7						
RPRsPTGPSNSF	Splicing factor 45	B7						
RPRsPTGPSNSFL	Splicing factor 45	B7						
RPRTNtPKQL	Nuclear receptor coactivator 3	B7						
RPVsPFQEL	Unknown	B7						
RPVsPGKDI	Transcription factor HIVEP2	B7						
RVRKLPsTTL	Ribosomal protein S6 kinase alpha-1	B7						
SPAsPKISL	Ataxin-2-like protein	B7						
SPKsPTAAL	Centrosomal protein of 55 kDa	B7						
SPRRsRSISL	Serine/arginine-rich splicing factor 7	B7;C6						
SPRsPGRSI	Unknown	B7						
SORsPsTTYL	Chromatin assembly factor 1 subunit A	B7						
SPSsPSVRRQL	Ankyrin repeat domain-containing protein 17	B7						
SPVsPMKEL	Uncharacterized protein C1orf106	B7						
TPRsPPLGL	Mitogen-activated protein kinase kinase kinase 11	B7						
APRKGsFSAL	Cullin-4A	B7						
APRRYsSSL	Rho GTPase-activating protein 17	B7						
LPAsPAHQL	Histone-lysine N-methyltransferase, H3 lysine-79 spe	B7						
RPKsNIVLL	B-lymphocyte antigen CD20	B7						
SPFKRQLsL	cDNA FLJ53174, highly similar to Numb-like protei	B7						
YPSsPRKAL	Signal-induced proliferation-associated 1-like protein	B7						

Phosphopeptide	Source Protein	Predicted HLA binding	Donor 1	Donor 2	JY	PTLD (A)	Spleen (B cell)	Tonsil (B cell)
APRAPSAsPLAL	MICAL-like protein 1	B7						
GAQPGRHsV	Protein ajuba	B7						
GGSFGGRSSGsP	Heterogeneous nuclear ribonucleoprotein A3	B7						
GPRAPsPTKPL	cell division cycle associated 5	B7						
GPRPGsPSAL	ribosomal large subunit pseudouridine synthase C like	B7						
GPRsPKAPP	Rho-GAP hematopoietic protein C1	B7						
HPKRSVsL	BCL2/adenovirus E1B 19 kDa protein-interacting pr	B7						
IPRPLsLIGSTL	dedicator of cytokinesis 10	B7						
KLRsPKSEL	Hematopoietic cell protein-tyrosine phosphatase 70Z	B7						
KPAsPARRL	MAP1 light chain LC2	B7						
KPAsPKFIVTL	Zinc finger CCCH domain-containing protein 14	B7						
KPPYRSHsL	coiled-coil domain containing 45	B7						
KPRRFsRsL	arginine/serine-rich coiled-coil 2	B7						
KPRsPPRALVL	embryonal carcinoma differentiation regulated	B7						
KPRsPPRALVLP	embryonal carcinoma differentiation regulated	B7						
KPYsPLASL	NFAT pre-existing subunit	B7						
LPAsPRARL	arginine/proline rich coiled-coil 1	B7						
LPIFSRLsI	Butyrate response factor 1	B7						
LPKsPPYTAF	Eukaryotic translation initiation factor 4B	B7						
MPREPsATRL	unknown	B7						
MPRQPsATRL	MOZART2	B7						
QPRsPGPDYSL	growth factor independence-1	B7						
QPRtPSPLVL	leukocyte-specific protein 1	B7						

Phosphopeptide	Source Protein	Predicted HLA binding	Donor 1	Donor 2	JY	PTLD (A)	Spleen (B cell)	Tonsil (B cell)
RARGIsPIVF	Putative splicing factor YT521	B7						
RLSsYVRS	unknown	B7						
RPAFFsPSL	chromosome 22 open reading frame 9	B7						
RPKLSsPAL	E1A binding protein p300	B7						
RPKsNINLL	unknown	B7						
RPPsPGPVL	SCAP	B7						
RPQRATsNVF	myosin regulatory light chain 1	B7						
RPRIPsPIGF	eIF4E transporter	B7						
RPRsLSSPTVTL	E3 ubiquitin-protein ligase NEDD4-like	B7						
RPRSLsSPTVTL	E3 ubiquitin-protein ligase NEDD4-like	B7						
RPRsPGSNSKV	BTK-associated protein 135	B7						
RPRsPPPRAP	prickle homolog 3	B7						
RPRsPRQPSI	unknown	B7						
RPSsLPDL	androgen receptor signaling pathway	B7						
RPTsRLNRL	Hin-2 protein	B7						
RPViPVSDL	EGR-alpha	B7						
RPWsPAVSA	Ski oncogene	B7						
RPVsPPEESI	FAM53C	B7						
RQAsIELPSMA	unknown	B7						
RQAsIELPSM	unknown	B7						
SPGsPRPAL	DNA replication factor Cdt1	B7						
SPKsPGLKA	CapZ-interacting protein	B7						
SPRAPVsPLKF	polypeptide 2	B7						
SPRERsPAL	TRAP150	B7						
SPRsPGKPM	unknown	B7						

Phosphopeptide	Source Protein	Predicted HLA binding	Donor 1	Donor 2	JY	PTLD (A)	Spleen (B cell)	Tonsil (B cell)
SPRsPSTTYL	CAF-1 subunit A	B7						
SPRTPVsPVKF	polypeptide 1	B7						
SPSTSRSGGsSRL	Arginine/serine-rich protein 1	B7						
TPAQPQRRsL	microtubule-associated protein homolog	B7						
TPRsPPLGLI	MAP3K11	B7						
TSPsYIDKL	CHK1 checkpoint homolog	B7						
VPREVLRLsL	AKNA transcript F2	B7						
FSIsPSSRM	unknown	B7						
KPPMsSPLVL	unknown	B7						
RAPsSPSSRM	unknown	B7						
KPPtPGASF	unknown	B7						
RSLsPDKVL	unknown	B7						
RPPsSPSPTAL	unknown	B7						
KPRsSPDHVL	unknown	B7						
RPTKIGRRsL	adenosylhomocysteinase 3	B7						
RPDsAHKML	Palladin	B7						
RRFsPPRRM	RNA-binding protein with serine-rich domain 1	B27;C6						
RRNsAPVSV	Rho GTPase-activating protein 31	B27;C6						
RRFsGTAVY	Zinc finger protein 518A	B27;C6						
FRRsPTKSSL	RNA-binding protein 14	B27;C6						
FRRsPTKSSLDY	RNA-binding protein 14	B27						
KRYsGNMEY	Serine/threonine-protein kinase LATS1	B27;C6						
RPIsPGLSY	Coiled-coil domain-containing protein 6	B35						
RPMsESPHM	Zinc finger protein 36, C3H1 type-like 1	B35						

0.05-0.5 copies/cell
0.5-5 copies/cell
5-10 copies/cell
10-50 copies/cell
expressed, not quantified

Table 4.8: Phosphopeptides identified from PTLD/LCL cells with predicted HLA-C+/unknown binding

Phosphopeptide	Source Protein	Predicted HLA binding	Donor 1	Donor 2	JY	PTLD (A)	Spleen (B cell)	Tonsil (B cell)
RKPsIVTKY	Transcriptional regulator ATRX	C6						
RRRsAPPEL	Rho-related GTP-binding protein RhoV	C6						
TRKtPESFL	Epsin-1	C6						
RPHsPEKA	unknown	U						
RSRsPRPAL	unknown	U						
HTAsPTGMMK	Protein transport protein Sec24D	U						
HVYtPSTTK	Ankyrin repeat family A protein 2	U						

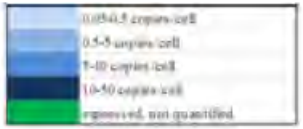

Only twenty one phosphopeptides were identified on normal tissue (Spleen and tonsil) obtained from patients with a non-malignant pathology (tonsillar hypertrophy, patients with chronic Idiopathic thrombocytopenic purpura) compared to 152 on JY, 119 on healthy donor derived LCL lines and 75 on the patient tumour sample (fig. 4.3 A, B). Thus, there was significantly more phosphopeptide on tumour tissue than normal (Wilcoxon's t-test $p<0.001$) (Fig. 4.3c). There were no significant differences in phosphopeptide expression demonstrated between (i) tumour (PTLD) and JY, (ii) tumour and healthy donor derived LCLs or (iii) JY and healthy donor derived LCLs (two-tailed Mann-Witney) – fig. 4.3C. Using unpaired T-test to compare phosphopeptides expressed in normal cells versus PTLD there is no significant difference between both data sets, suggesting phosphopeptides expressed in normal healthy tissues bare no significance to tumour development as expression levels are comparable in both healthy and malignant tissues supporting the idea that these phosphopeptides are not solely responsible for tumour development (Fig 4.3D).

Fig. 4.3 Comparison of phosphopeptide levels in healthy B cells and PTLD cell lines and a PTLD patient sample
The number of phosphopeptides identified was compared in a patient blood sample (newly diagnosed with PTLD) and the commercially available PTLD cell line JY, as well as two LCL lines generated from healthy donors following infection with EBV as per standard protocols. (A). More phosphopeptides were seen in tumour/tumour lines than healthy B cells $\chi 2$ $p<0.001$. Phosphopeptides not identified were said to be at a level below detection (0.1 fmol/gram). Significantly more phosphopeptide was present in tumour tissue than healthy B cells, Wilcoxon signed rank $p<0.001$ (*). (B) Euler diagram showing the overlap of phosphopeptide presentation on PTLD tumour derived line, JY, Healthy donor derived LCL lines and healthy B cells. (C) The phosphopeptides present in healthy liver tissue were found at significantly different levels in the tumour tissue, $p<0.001$ Wilcoxons t-test (**). (D) Phosphopeptides identified on normal tissue were not found at significantly different levels in tumour tissue by unpaired t-test $p=0.508$.

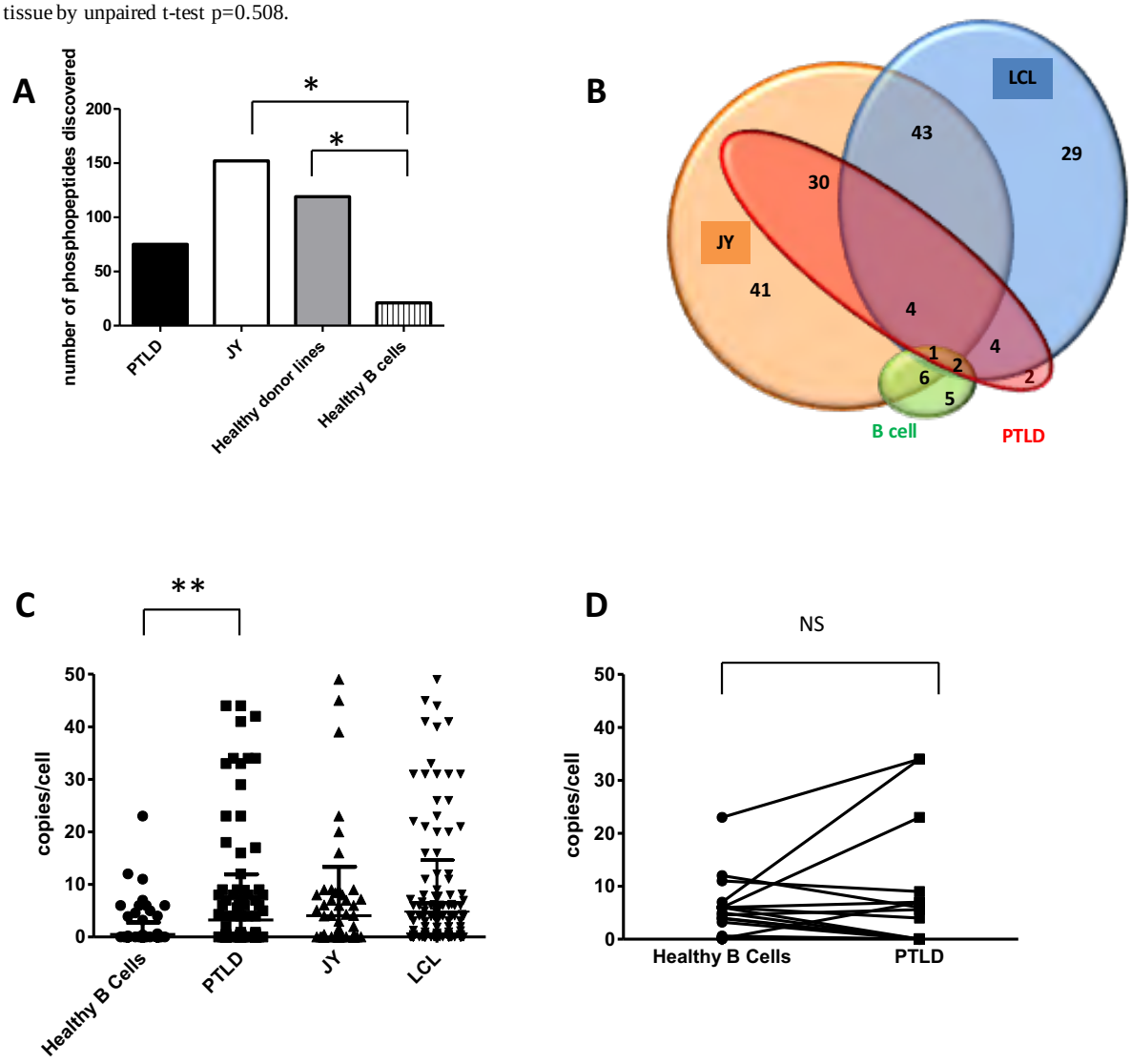

4.2.3 Comparisons and analysis

Identifying phosphopeptides on each tumour type was informative, and could represent a target for tumour immunotherapy, but as we found phosphopeptides on tumour and healthy tissues, perhaps more important are identifying those specific phosphopeptides that may represent

potential markers of an oncogenic process i.e. identification of a cancer phenotype – phosphopeptides that are integral to a cancer's existence, and are found on any tumour cell regardless of the organ type i.e. a marker of malignancy. On analysis of the phosphopeptides obtained from HB tissue, we noted that a number of these phosphopeptides had been identified on other tumours (fig. 4.4).

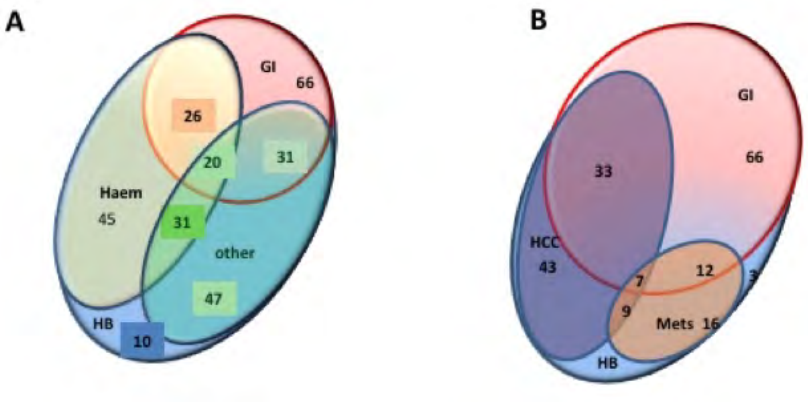

Fig. 4.4 Phosphopeptides expressed on different tumour types which are also expressed on hepatoblastoma On analysis of phosphopeptide expression in hepatoblastoma tissue samples. Aa number of phosphopeptides were previously found to have been expressed on other tumour types. (A) Here we use a Euler plot to demonstrate crossover between different tumour types, where GI refers to oesophageal and colorectal adenocarcinomas (as studied by Dr Penny, Haem refers to all haematological malignancies (as studied by Dr Cobbold and Dr De La Pena), other includes other solid tumours e.g. breast, melanoma and ovarian (data available from our collaborators in University of Virginia). (B) We also observed crossover between different liver tumours, both primary (hepatoblastoma and hepatocellular carcinoma) as well as liver metastases detected on patient samples collected from patients with GI malignancy.

In order to identify what crossover there was, euler-venn diagrams were created. Fig 4.4A shows a comparison of hepatoblastoma (HB) with gastrointestinal tumours (Colorectal and oesophageal adenocarcinoma), haematological malignancies (AML, ALL, T and B cell lymphomas) and other solid tumour primaries (including melanoma, breast carcinoma and ovarian carcinoma, termed 'other'). The colorectal adenocarcinomas, as studied by Dr Sarah Penny also had a subset of patients with liver metastases, and on assessing phosphopeptides seen on these secondary malignancies a number were also identified on HB tumour samples, suggesting that these phosphopeptides may be involved in a hepatological development and tissue differentiation pathways. They could play an important role in hepatic tissue dysplasia for instance (B). It is also noted that there are a number of phosphopeptides identified on adult

hepatocellular carcinoma samples (as studied by Dr Nico Büttner of this group), again bolstering this view of a role in hepatic dysplasia (Table 4.9).

In order to understand their role in hepatic tumours a few of the key signalling pathways were further examined and proteins involved identified (fig 4.5) – signalling pathways of interest highlighted in red. Interestingly these pathways have all been implicated in malignant transformation of cells, which would suggest that these are reasonable targets to investigate further.

Table 4.9: Phosphopeptides identified on primary and secondary liver tumours
Following identification of phosphopeptides on hepatoblastoma tumour samples, correlation was made with previous hepatic tissues studied by this group. Key pathways were identified including MAPKinase, JAK/STAT cascade, NFKappa-B, T-cell receptor signalling, TGF-B and Wnt/Catenin B pathways (information collected using UniProt software).

Phosphopeptide Sequence	Protein	Pathway	Mechanism of action proposed
KTMsGTFLL	Signal transducer and activator of transcription 2	JAK/STAT cascade	regulation of transcription from RNA polymerase II promoter
RQLsSGVSEI	Heat shock protein beta-1 (HSPB1)	MAPKAP kinase 2	Cell motility; negative regulation of apoptosis and protein kinase activity; positive regulation of angiogenesis, blood vessel endothelial cell migration, interleukin-1 beta production, tumour necrosis factor biosynthetic process, I-kappaB kinase/NF-kappaB cascade, mRNA stability, translational initiation and the vascular endothelial growth factor receptor signalling pathway
RQAsIELPSM	Lymphocyte-specific protein 1	MAPKAP kinase 2	Phosphorylated by casein kinase II, protein kinase C and MAPKAPK2. PKC induced phosphorylation leads to translocation from membrane to cytoplasm. Phosphorylation by MAPKAPK2 is thought to regulate neutrophil chemotaxis.
RTFsPTYGL	Synemin		intermediate filament cytoskeleton organization and biogenesis
RQDsTPGKVFL	Nuclear receptor subfamily 2 group C member 1		Binds the IR7 element in the promoter of its own gene in an autoregulatory negative feedback mechanism. Together with NR2C2, forms the core of the DRED (direct repeat erythroid-definitive) complex that represses embryonic and foetal globin transcription. Also found to be an activator of OCT4 gene expression. As a result, it maybe involved in stem cell proliferation and differentiation. Belongs to the nuclear hormone receptor family. NR2 subfamily.
KAFsPVRSV	DNA-binding protein inhibitor ID-2		Implicated in the negative regulation of DNA-dependent transcription, neuron fate commitment and the regulation of lipid metabolism
ELFSsPPAV	Nuclear factor of activated T-cells 5	T-cell receptor signalling pathway	Regulates hypertonicity-induced cellular accumulation of osmolytes. Homodimer when bound to DNA, completely encircles its DNA target. Does not bind with Fos and Jun transcription factors. Highest levels in skeletal muscle, brain, heart and peripheral blood leukocytes. Also expressed in placenta, lung, **liver**, kidney, pancreas, spleen, thymus, prostate, testis, ovary, small intestine and colon.
KLFPDtPLAL	Interleukin enhancer-binding factor 3	T-cell receptor signalling pathway	a double-stranded RNA (dsRNA)-binding protein implicated in the regulation of gene expression. Phosphorylated in a double-stranded RNA-dependent manner possibly by PKR.
RLSsPLHFV	Protein FAM134A		Belongs to the FAM134 family. Membrane protein, multi-pass; Membrane protein, integral
AVVsPPALHNA	Bromodomain-containing protein 4	G1/S-specific transcription in mitotic cell cycle; positive regulation of I-kappaB kinase/NF-kappaB cascade; positive regulation of RNA elongation from RNA	an atypical protein kinase of the Brd family. Contains a double bromodomain. Binds to chromatin and regulates cell cycle progression at multiple stages. Associates with chromosomes during mitosis. The cognate gene is the chromosome 19 target of translocation t(15;19)(q13;p13.1), resulting in the BRD4-NUT oncogene identified in a lethal carcinoma of young people. Binds to papillomavirus E2 protein and is required for its transforming ability. Two alternatively spliced isoforms have been described.

		polymerase II promoter; positive regulation of transcription from RNA polymerase II promoter; regulation of inflammatory response	
ALDsGASLLHL	Receptor-interacting serine/threonine-protein kinase 4 (RIPK4)	activation of NF-kappaB transcription factor; morphogenesis of an epithelium	Appears to activate NFkappaB in both a kinase-dependent as well as a kinase-independent manner.
FLDtPIAKV	Protein naked cuticle homolog 1	Wnt-B-Catenin signalling	Cell autonomous antagonist of the canonical Wnt signalling pathway. May activate a second Wnt signalling pathway that controls cell polarity. Expression is induced by activation of the Wnt signalling pathway. Expressed in colon, heart, kidney, leukocyte, **liver**, lung, ovary, pancreas, placenta, prostate, skeletal muscle, small intestine and spleen.
KVAsLLHQV	TNFAIP3-interacting protein 2	positive regulation of B cell activation; positive regulation of I-kappaB kinase/NF-kappaB cascade; positive regulation of macrophage activation; positive regulation of transcription from RNA polymerase II promoter; protein stabilization; stress-activated MAPK cascade; toll-like receptor 2 signalling pathway; toll-like	Inhibits NF-kappa-B activation by blocking the interaction of RIPK1 with its downstream effector NEMO/IKBKG. Involved in activation of the MEK/ERK signalling pathway during innate immune response.. Implicated in the regulation of apoptosis of endothelial cells. May act as transcriptional coactivator when translocated to the nucleus.

		receptor 3 signalling pathway; toll-like receptor 9 signalling pathway	
SMTRsPPRV	Serine/arginine-rich splicing factor 8		Involved in pre-mRNA alternative splicing. Belongs to the splicing factor SR family.
RPFHGISTVsL	DENN domain-containing protein 4C		Role in malignancy unclear
RPFsPREAL	Leucine zipper protein 1		This is a protein that contains a leucine zipper motif. Role in malignancy unclear
RPWsPAVSA	Ski oncogene	Functions as a repressor of TGF-beta signalling	Negative regulation of activin receptor signalling pathway, BMP signalling pathway, cell proliferation, transcription from RNA polymerase II promoter and transforming growth factor beta receptor signalling pathway. Positive regulation of DNA binding, transcription from RNA polymerase II promoter and apoptosis.
SPFKRQLsL	cDNA FLJ53174, highly similar to Numb-like protein	NOTCH1 signalling	Plays a role in the process of neurogenesis.
TPRsPPLGL	Mitogen-activated protein kinase kinase kinase 11	activation of JNK activity; activation of MAPK activity; cell proliferation; JNK cascade; microtubule-based process; positive regulation of JNK activity; positive regulation of JNK cascade; protein amino acid autophosphorylation; protein amino acid phosphorylation	a TKL kinase of the MLK family. Has an amino-terminal SH3 domain followed by the kinase domain, two leucine zipper domains, a cdc42/Rac1 binding (CRIB) domain and several other domains/motifs at the carboxy-terminal region. Phosphorylates IkappaB and activates SEK1 and MKK7.
TPRsPPLGLI	Mitogen-activated protein kinase kinase kinase 11	activation of JNK activity; activation of MAPK activity;	a TKL kinase of the MLK family. Has an amino-terminal SH3 domain followed by the kinase domain, two leucine zipper domains, a cdc42/Rac1 binding (CRIB) domain and several other domains/motifs at the carboxy-terminal region. Phosphorylates IkappaB and activates SEK1 and MKK7.

		cell proliferation; JNK cascade; microtubule-based process; positive regulation of JNK activity; positive regulation of JNK cascade; protein amino acid autophosphorylation; protein amino acid phosphorylation	
RPDsAHKML	Palladin, Cytoskeletal Associated Protein	muscle alpha-actinin binding; protein binding	Cytoskeletal; Motility/polarity/chemotaxis
KRYsGNMEY	Large Tumour Suppressor Kinase 1	Hippo Signalling	A likely tumour suppressor which plays a critical role in maintenance of ploidy through its actions in both mitotic progression and the G1 tetraploidy checkpoint. Negatively regulates G2/M transition by down-regulating CDC2 kinase activity, causing G2 arrest. Involved in the control of p53 expression. LATS1-associated CDC2 has no mitotic cyclin partner and no apparent kinase activity. Binds phosphorylated zyxin, locating this protein to the mitotic spindle and suggesting a role for actin regulatory proteins during mitosis. Knockout mice are susceptible to soft-tissue sarcomas and sensitive to chemical carcinogenesis. Human soft tissue sarcomas have downregulated, mutated, and/or hypermethylated LATS1.
RRsSFLQVF	Protein transport protein Sec23A	antigen processing and presentation of exogenous peptide antigen via MHC class II; antigen processing and presentation of peptide antigen via MHC class I; COPII coating of Golgi vesicle; ER to Golgi vesicle-mediated transport; vesicle-mediated transport	role in malignancy unclear

RTHsLLLLL	Ribonuclease 4		endonuclease activity; ribonuclease activity
KPAsPKFIVTL	zinc finger CCCH-type containing 14		Binds the polyadenosine RNA oligonucleotides.
RFKtQPVTF	Anterior gradient protein 2 homolog	Unknown function	Unknown function
RRIsDPQVF	Filamin A Interacting Protein 1-Like	Unknown function	Acts as a regulator of the antiangiogenic activity on endothelial cells. When overexpressed in endothelial cells, leads to inhibition of cell proliferation and migration and an increase in apoptosis.
KPRsPVVEL	Beta-adrenergic receptor kinase 1	Unknown	Unknown
RPYsPPFFSL	Protein FAM53C	P53	P53
RPAFFsPSL	Uncharacterized protein KIAA0930	Unknown	unknown
RRGsFEVTL	Selenoprotein H	Unknown	May be involved in a redox-related process
RRPsLLSEF	Nuclear receptor corepressor 1	JNK	Negative regulation of JNK cascade; negative regulation of transcription from RNA polymerase II promoter; spindle assembly; transcription from RNA polymerase II promoter
RPIsPPHTY	Coiled-coil domain-containing protein 6	Rho protein signal transduction	Caspase activation; cell adhesion; cell migration during sprouting angiogenesis; negative regulation of cell migration; positive regulation of axonogenesis; positive regulation of Rho protein signal transduction
RPmsESPHm	ZFP36 Ring Finger Protein-Like 1	Akt	regulation of mRNA stability
RPVsPFQEL	unknown	Unknown	unknown
RKSsIIIRM	Plasminogen-like protein B	apolipoprotein binding; protein domain specific binding; receptor binding; serine-type endopeptidase activity; serine-type peptidase activity	Involved in the process of blood coagulation e.g.platelet degranulation; positive regulation of fibrinolysis

ITQGtPLKY	Nuclear Receptor Corepressor 2	Component of the N-Cor repressor complex	Negative regulation of transcription from RNA polymerase II promoter
TRKtPESFL	Epsin 1	EGFR	Negative regulation of epidermal growth factor receptor signalling pathway
SFDsGSVRL	Interferon regulatory factor 6	May regulate WDR65 transcription	cell cycle arrest; negative regulation of cell proliferation; positive regulation of transcription, DNA-dependent
RKPsIVTKY	ATP-dependent helicase ATRX	Unknown	Involved in chromatin remodeling; DNA damage response, signal transduction by p53 class mediator; DNA methylation; DNA recombination; DNA replication-independent nucleosome assembly; nucleosome assembly; positive regulation of telomere maintenance; positive regulation of transcription from RNA polymerase II promoter; regulation of transcription, DNA-dependent; replication fork processing. Acquired mutations in ATRX have been observed in pre-leukemic conditions.
RRLsFLVSY	Glutamine--tRNA ligase	catalyzes the formation of L-glutaminyl-tRNA	brain development; glutaminyl-tRNA aminoacylation; tRNA aminoacylation for protein translation
RSAsFSRKV	Nephrocystin-4	Unknown	Unknown
LPAsPVARR	SH2 domain-containing protein 3C	JNK cascade	an adaptor protein linking integrin and tyrosine kinase receptors to the c-Jun N-terminal kinase/stress-activated protein kinase signalling pathway Positively regulates T cell receptor-mediated interleukin-2 production by Jurkat cells.
HVSLItPTKR	AN1-type zinc finger protein 3	Unknown	Unknown
SRSSSVLsL	Pleckstrin homology domain-containing family G member 3	Unknown	Unknown
SImsPEIQL	Protein capicua homolog	ERB	negative regulation of transcription from RNA polymerase II promoter

Fig. 4.5 Potential pathways involved in hepatic malignancy
(A) Schematic showing T cell receptor signalling pathway (B) MAP Kinase signalling pathway (C) TGF-Beta signalling pathway (D) JNK/SAP signalling (E) Wnt/B-Catenin signalling – source Cell Signaling Technology http://www.cellsignal.com/contents/science/cst-pathways/science-pathways

A

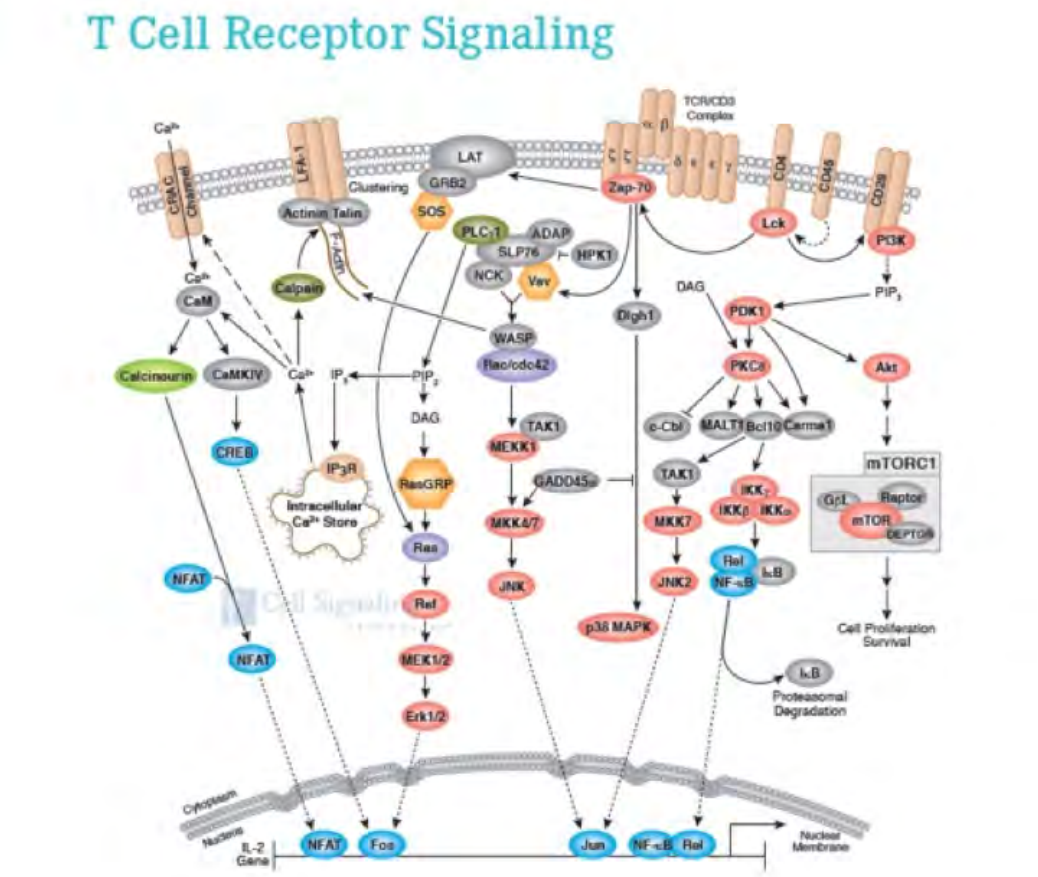

Fig. 4.5 Potential pathways involved in hepatic malignancy
(A) Schematic showing T cell receptor signalling pathway (B) MAP Kinase signalling pathway (C) TGF-Beta signalling pathway (D) JNK/SAP signalling (E) Wnt/B-Catenin signalling – source Cell Signaling Technology http://www.cellsignal.com/contents/science/cst-pathways/science-pathways

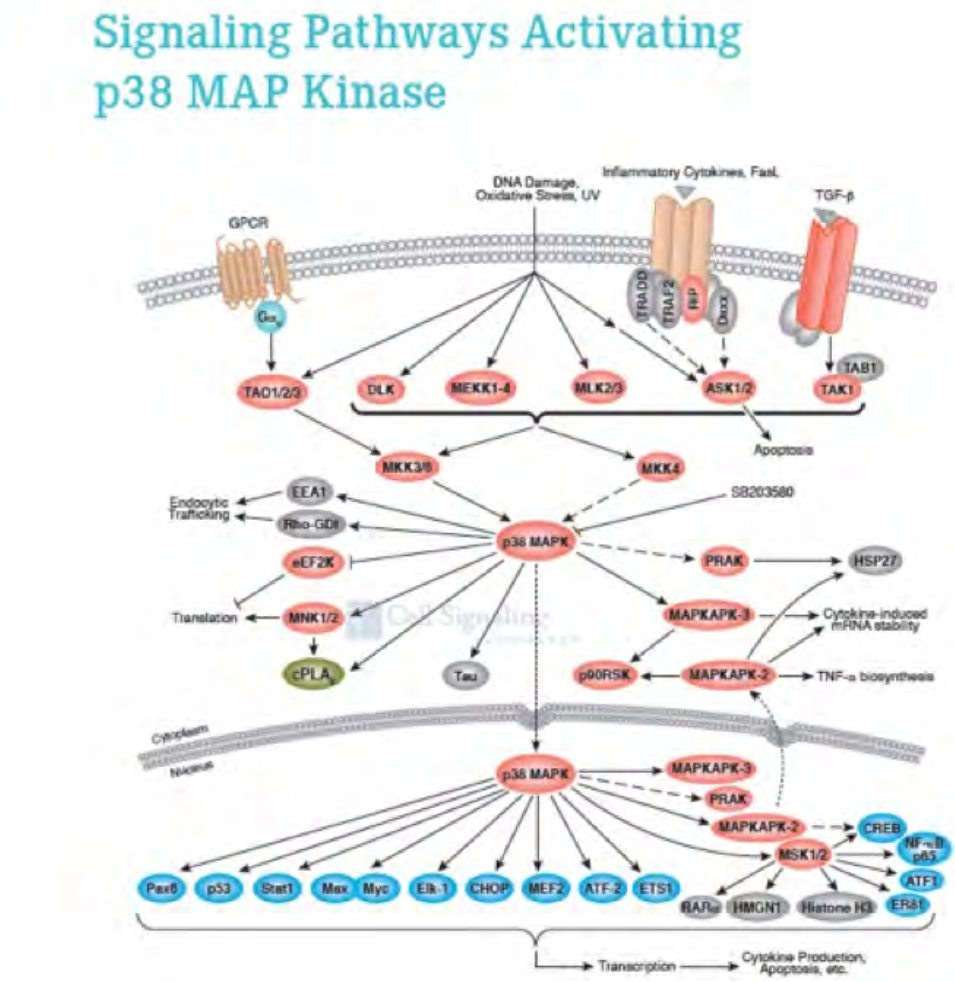

Fig. 4.5 Potential pathways involved in hepatic malignancy
(A) Schematic showing T cell receptor signalling pathway (B) MAP Kinase signalling pathway (C) TGF-Beta signalling pathway (D) JNK/SAP signalling (E) Wnt/B-Catenin signalling – source Cell Signaling Technology http://www.cellsignal.com/contents/science/cst-pathways/science-pathways

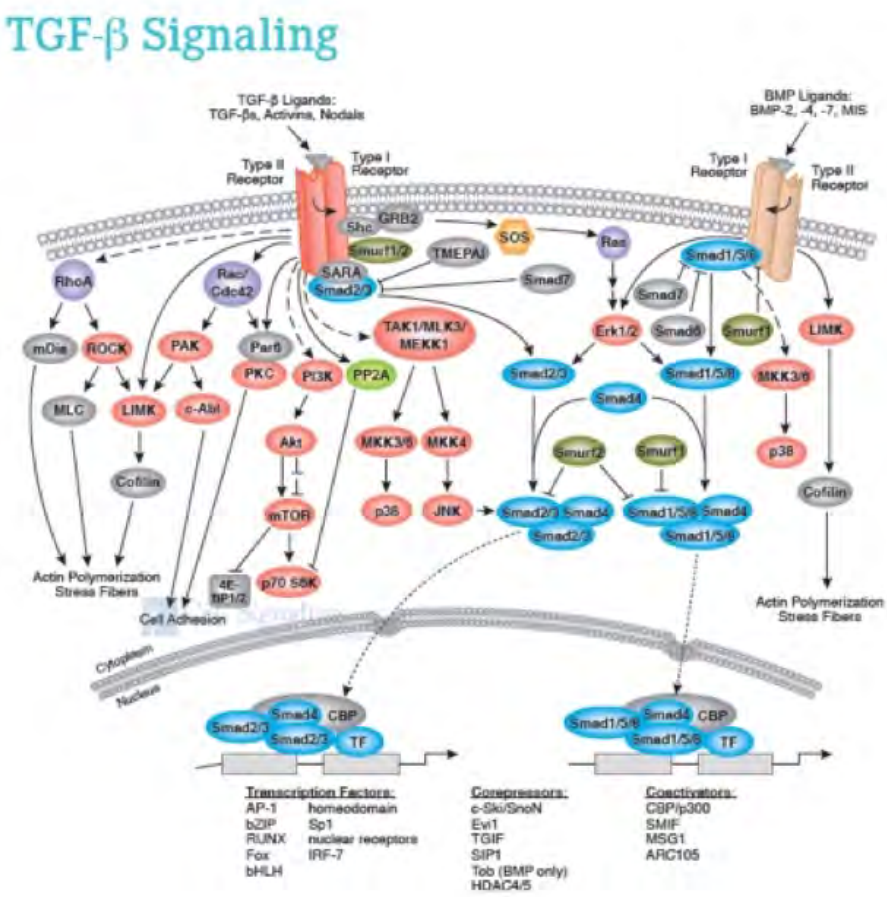

Fig. 4.5 Potential pathways involved in hepatic malignancy
(A) Schematic showing T cell receptor signalling pathway (B) MAP Kinase signalling pathway (C) TGF-Beta signalling pathway (D) JNK/SAP signalling (E) Wnt/B-Catenin signalling – source Cell Signaling Technology http://www.cellsignal.com/contents/science/cst-pathways/science-pathways

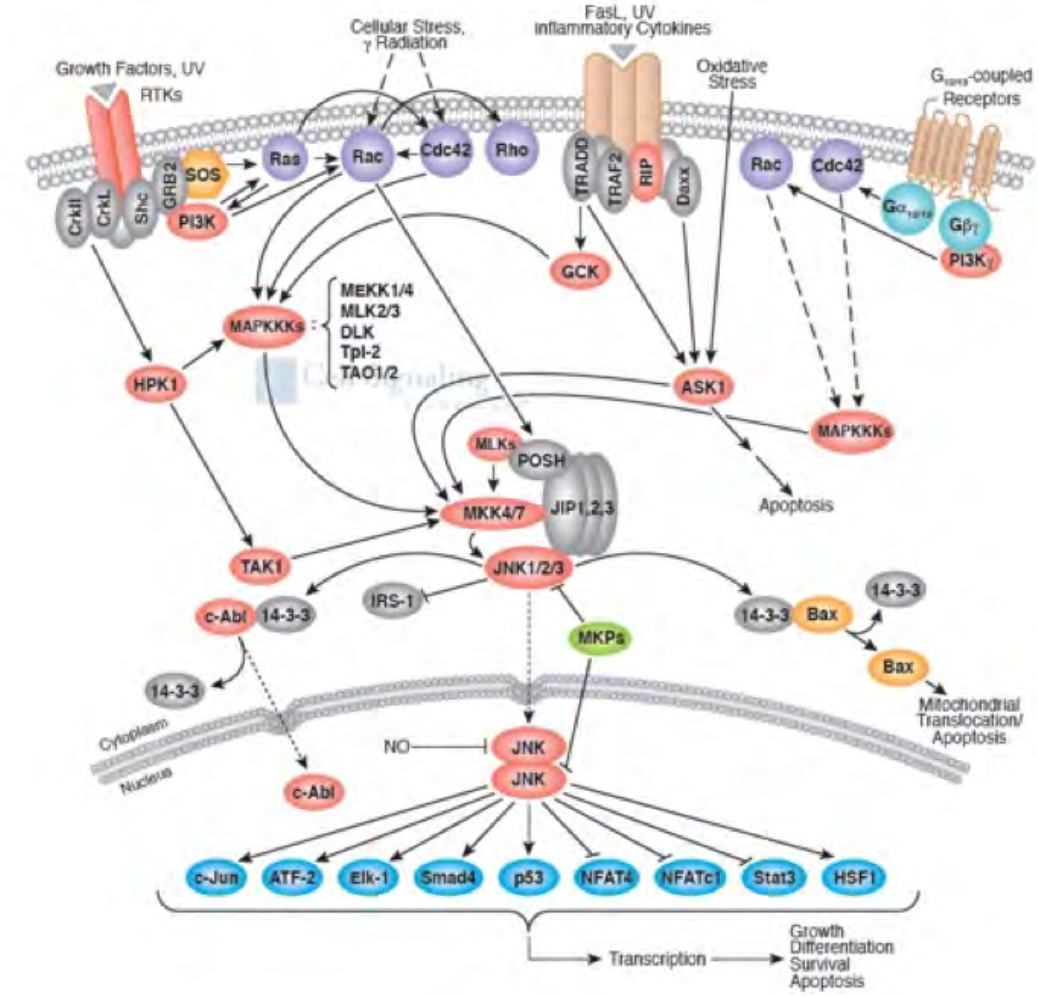

Fig. 4.5 Potential pathways involved in hepatic malignancy
(A) Schematic showing T cell receptor signalling pathway (B) MAP Kinase signalling pathway (C) TGF-Beta signalling pathway (D) JNK/SAP signalling (E) Wnt/B-Catenin signalling – source Cell Signaling Technology http://www.cellsignal.com/contents/science/cst-pathways/science-pathways

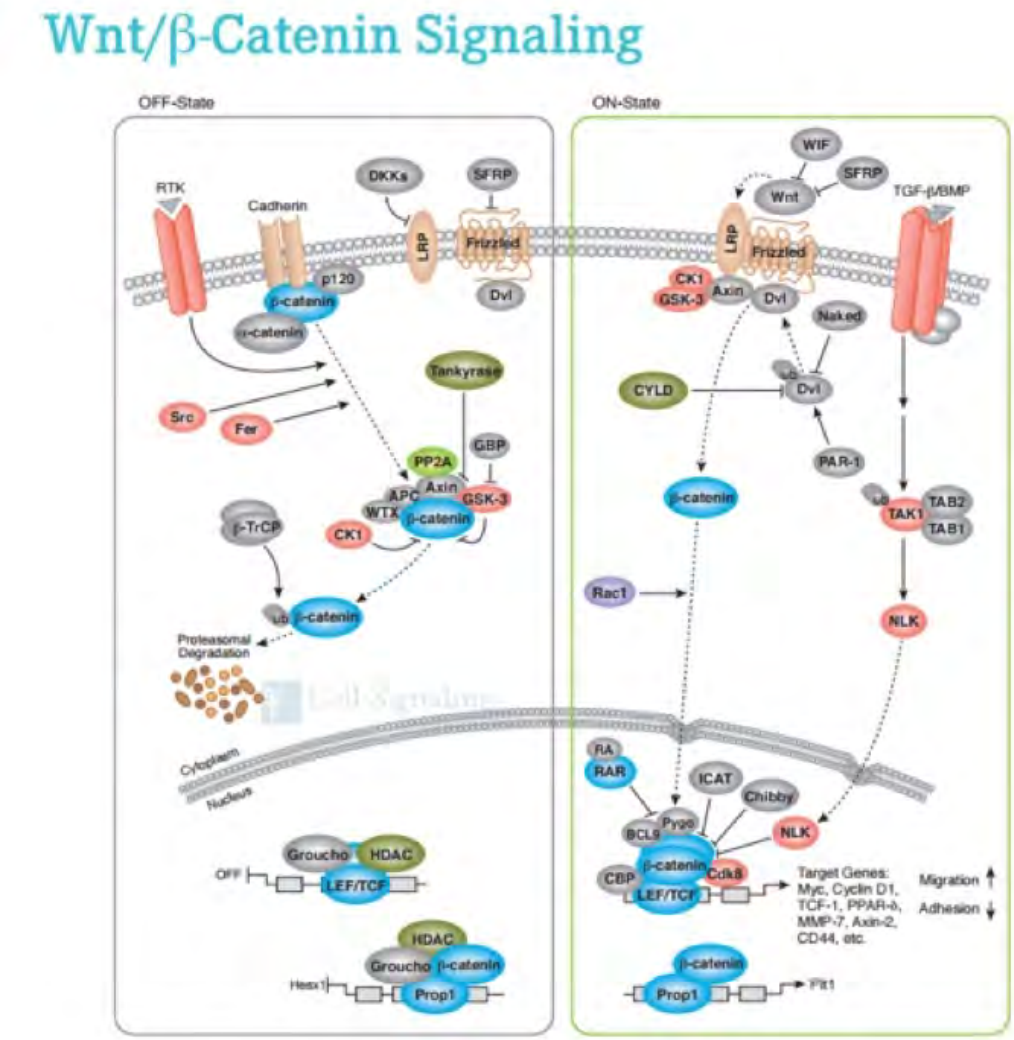

Of the 46 phosphopeptides that are shared between different hepatic malignancies in this list, 23 (50%) were from established cancer pathways. It is therefore possible that these proteins are cancer specific, be it coded for by tumour suppressor genes, or oncogenes. Their end result appears to be hepatic dysplasia and malignancy.

4.3 T-cell responses to tumour specific peptides

There is a clear need for immunotherapeutic targets in paediatric hepatoblastoma and PTLD, and prognosis following a diagnosis of malignancy is variable but typically morbidity is high with side effects of tumour therapies. The aim therefore of this project is to identify a tumour specific target. Memory $CD8^+$ T cell infiltration has been well described as being a key prognostic indicator in a number of tumours including colorectal adenocarcinoma and melanoma. In a number of these tumours tumour infiltrating lymphocytes (TILs) have been implicated as targeting and destroying malignant-transformed cells, although how they achieve this has not been fully established (Pages, Galon et al. 2010, Emens, Silverstein et al. 2012, Galon, Pages et al. 2012). Phosphopeptides have been proposed as a possible epitope used to facilitate this tumour cell identification, based on the dysregulation of signalling in cancers which is known to lead to aberrant protein phosphorylation.

As has already been described earlier in this chapter, we have identified 84 HB-associated MHC class I phosphopeptides on HB primary tumours and the HepG2 cell line. We found 4.4 times as many different phosphopeptides on tumour-transformed cells than healthy tissues, at far higher levels (7.6-fold higher). A number of these phosphopeptides were found to be from proteins which are identified as pivotal in a number of already well-established and described cancer pathways, leading these to be considered as a marker of malignant potential.

Based on the initial observations of phosphopeptide expression we proposed that a significant part of the immune response to transformed cells is the targeting of phosphopeptides. We considered if this may be related to eventual clinical outcome. Dr Cobbold, of this laboratory has previously described, in haematological malignancy, responses to phosphopeptides in both patients and healthy donors (Cobbold et al., 2013). He also noted that loss of phosphopeptide response which had previously been present was also a poor prognostic indicator.

Healthy individuals possess mechanisms for recognising and eliminating tumour and we predict that phosphopeptides are one of the potential tumour recognition targets. We hypothesised that healthy donor T-cells could recognise tumour derived phosphopeptide. We wondered if this may aid us in establishing whether phosphopeptide-specific memory T-cells could have a pivotal role in the functional immune response observed in malignant transformation. In order to test this hypothesis a number of phosphopeptides presented by HLA-A2 and B7 on tumour samples (both hepatoblastoma and PTLD/LCL) were selected for further analysis. These phosphopeptides were pulsed onto appropriate target cells and cultured with HLA-matched healthy donor T-cells to establish if the T-cells could recognise these tumour-specific phosphopeptides (fig 4.6). A number of the phosphopeptides chosen are considered 'liver' in phenotype – being consistently present on hepatoblastoma/HepG2/Hepatocellular carcinoma or liver secondary tumours. I also selected a number of phosphopeptides which were identified on the PTLD tumour samples also – keeping the same HLA group as the liver tumours in order to set up a panel of phosphopeptides to test on healthy donors.

Fig 4.6: Schematic describing the work-flow for testing of healthy donor T-cell responses to tumour-specific, MHC class I-associated phosphopeptides discovered in patient samples
Tumour and normal tissue were taken from the same patient at surgical resection. These were each enzymatically lysed (as per protocol previously described in chapter 2) and the MHC class I complexes affinity purified using the pan class-I antibody, W6/32 (produced in house). The MHC class I-associated peptides were eluted in acid and phosphopeptides enriched using IMAC by our collaborators at University of Virginia. These phosphopeptides were characterised using LC-MS/MS and the sequences manually assigned. The phosphopeptides were then synthesised and the assignment verified.
Once phosphopeptides were identified, healthy donor PBMC's were obtained from HLA-matched donors. These cells were pulsed with these phosphopeptides *in vitro* on day 0 and day 6, and analysed by intracellular staining protocols (ICS) for evidence of phosphopeptide recognition and T-cell activation. Cells found to recognise Phosphopeptide were expanded and T-cell lines generated.
TILs were taken from the patient tumours at resection and expanded, using high-dose IL-2 (6000 IU/ml). TIL responses to the phosphopeptides were then tested. TILs were stimulated with phosphopeptide and cultured for 5 days before being re-stimulated in an intracellular cytokine staining assay assessing production of TNFα, IFNγ and IL-2.

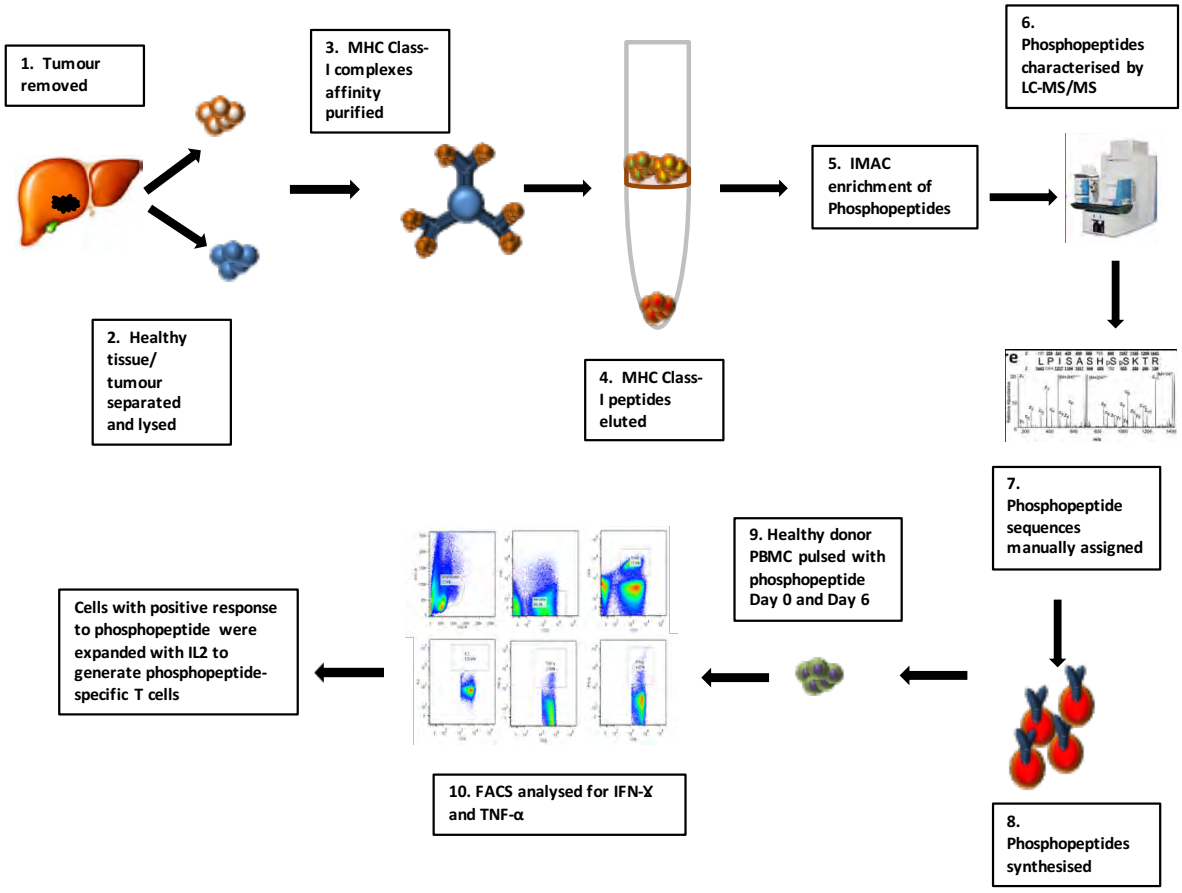

Intracelllular staining techniques were employed to assess activation and response of healthy donor cells to tumour phosphopeptides on day 1 and day 7, demonstrated in representative plots fig. 4.7a,b and 4.8a,b (further plots for other donors are available in the appendix 1 fig. S2-S7, the data from which is used to compile fig 4.7c and 4.8b). Combination gates were

then used to assess the individual expression of interleukin 2 (IL-2), interferon gamma (IFNγ) and tumour necrosis factor alpha (TNFα) – all considered markers of T-cell activation (fig 4.7c, Fig 4.8b). These plots demonstrated limited response on day 1across the range of donors in both the A2 and B7 responses, which were more marked by day 7. We assessed the T-cell responses to the phosphopeptides using a 12 hour intracellular cytokine staining (ICS) assay to test production of cytokines (TNFα, IFNγ and IL-2). The responses at this time point were considered low (for three out of four of the B7 donors for instance, initial responses to phosphopeptide were all <2% at day 1) and therefore a further assay was performed at 7 days, with restimulation of cells with phosphopeptide at 6 days.

We assessed the individual T-cell line's cytokine repertoires. We noted a degree of background staining seen in the TNFα and IFNγ staining in this assay in the negative controls for each line, which was considered low (e.g. in donor H when considering B7 responses at day 7, this donor had 0.844% $IFN\gamma^+$ cells, 0.540% $TNF\alpha^+$ cells and 0.017% $IL\text{-}2^+$ cells – combined total of 1.401%) – but this was taken into account when assessing the phosphopeptide responses. In contrast positive controls (stimulation of cells with PMA/ionomycin as per methods chapter) resulted in an increase in positive cells to 18.1% $IFN\gamma^+$, 27.3% $TNF\alpha^+$ and 0.120% $IL\text{-}2^+$ cells respectively with a combined total of 45.52%). T-cell response to viral peptide was also tested and where demonstrated included as a further positive control. The same donor (H) also had good responses to the phosphopeptides tested at 7 days with totals ranging from 19.2% to 42.6% polyfunctional responses to the peptides investigated. In contrast donor C demonstrated only low responses to the phosphopeptides tested (ranging from 6.2% to 14.2%) on day 7, but with comparable positive and negative controls (fig. 4.7c).

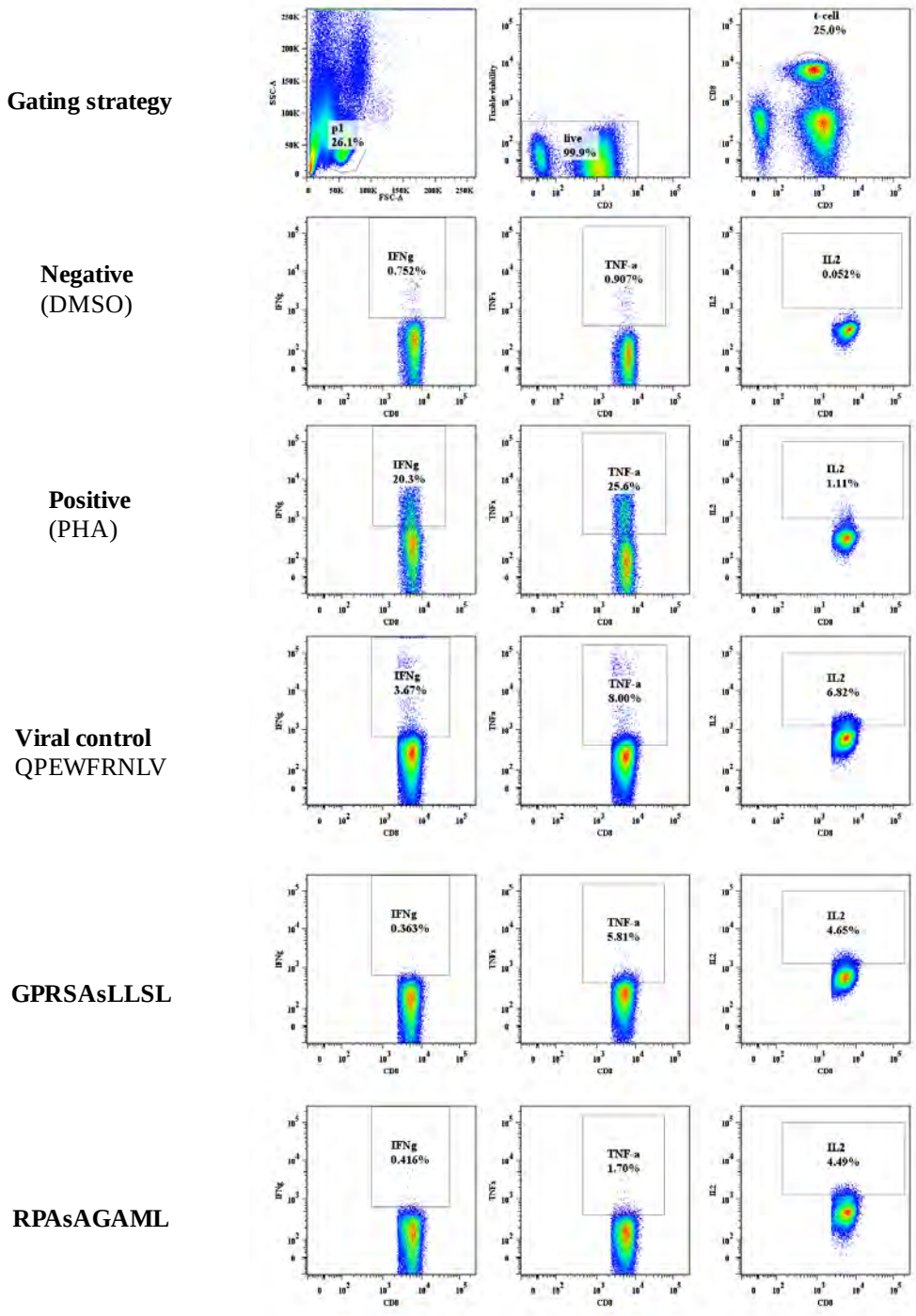

Fig. 4.7a:Phosphopeptide responses in Healthy Donor H (day 0)
PBMC's were generated from healthy donors as previously described and responses of these cells to tumour-associated phosphopeptides were then assessed using an intracellular staining (ICS) assay. The FACS plots depicted show the gating strategy employed and representative IFNγ ,TNFα, and IL-2 responses (from left to right). NB notation on figures, IFNg = IFNγ , TNFa = TNFα. These are representative plots of cells obtained from donor H. Experiment performed in triplicate.

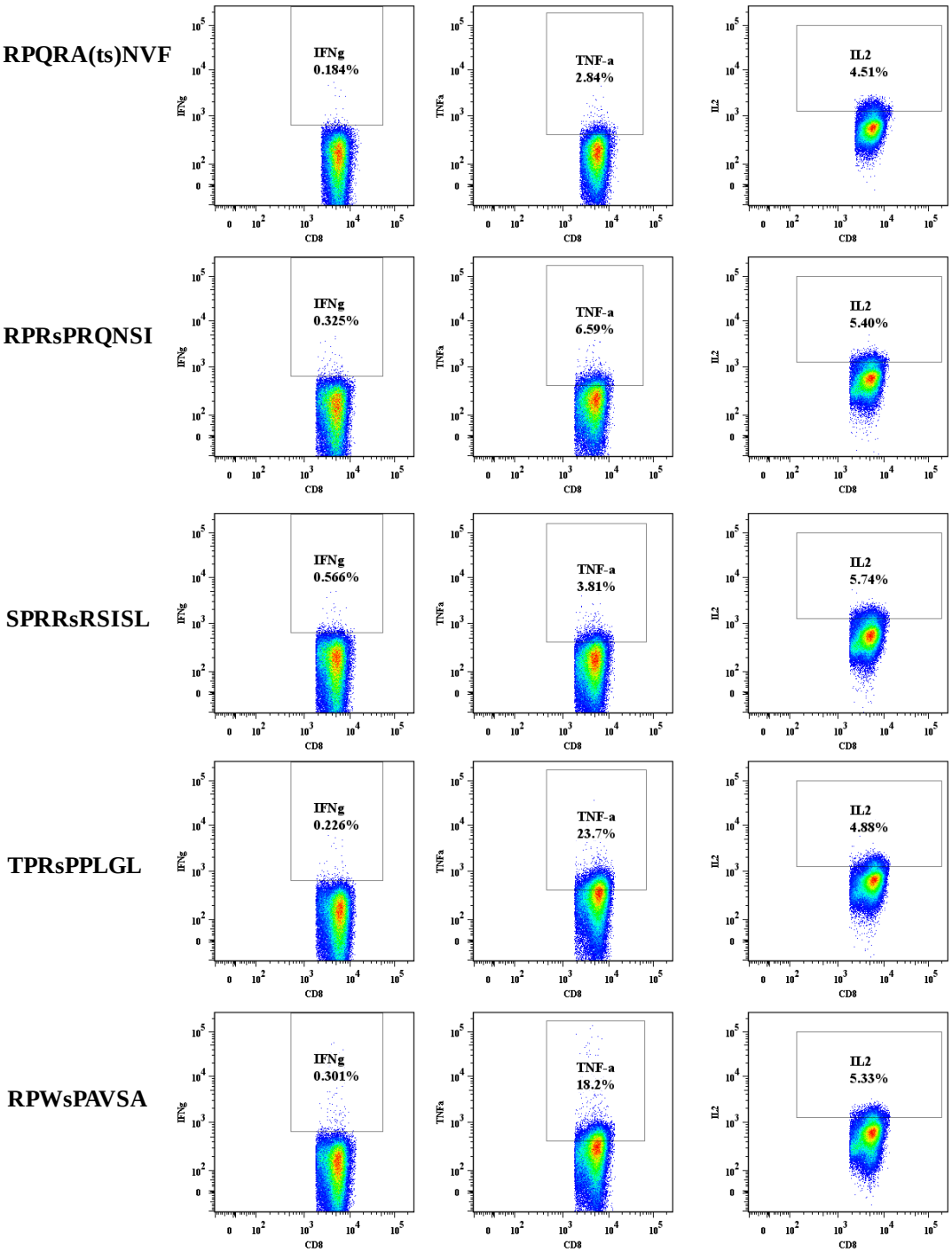

Fig. 4.7a:Phosphopeptide responses in Healthy Donor H(day 0) cont..
PBMC's were generated from healthy donors and responses of these to tumour-associated phosphopeptides were then assessed using an ICS assay. The FACS plots depicted show the gating strategy employed and representative IFNγ ,TNFα, and IL-2 responses (from left to right). NB notation on figures, IFNg = IFNγ , TNFa = TNFα. These are representative plots of cells obtained from donor H. Experiment performed in triplicate.

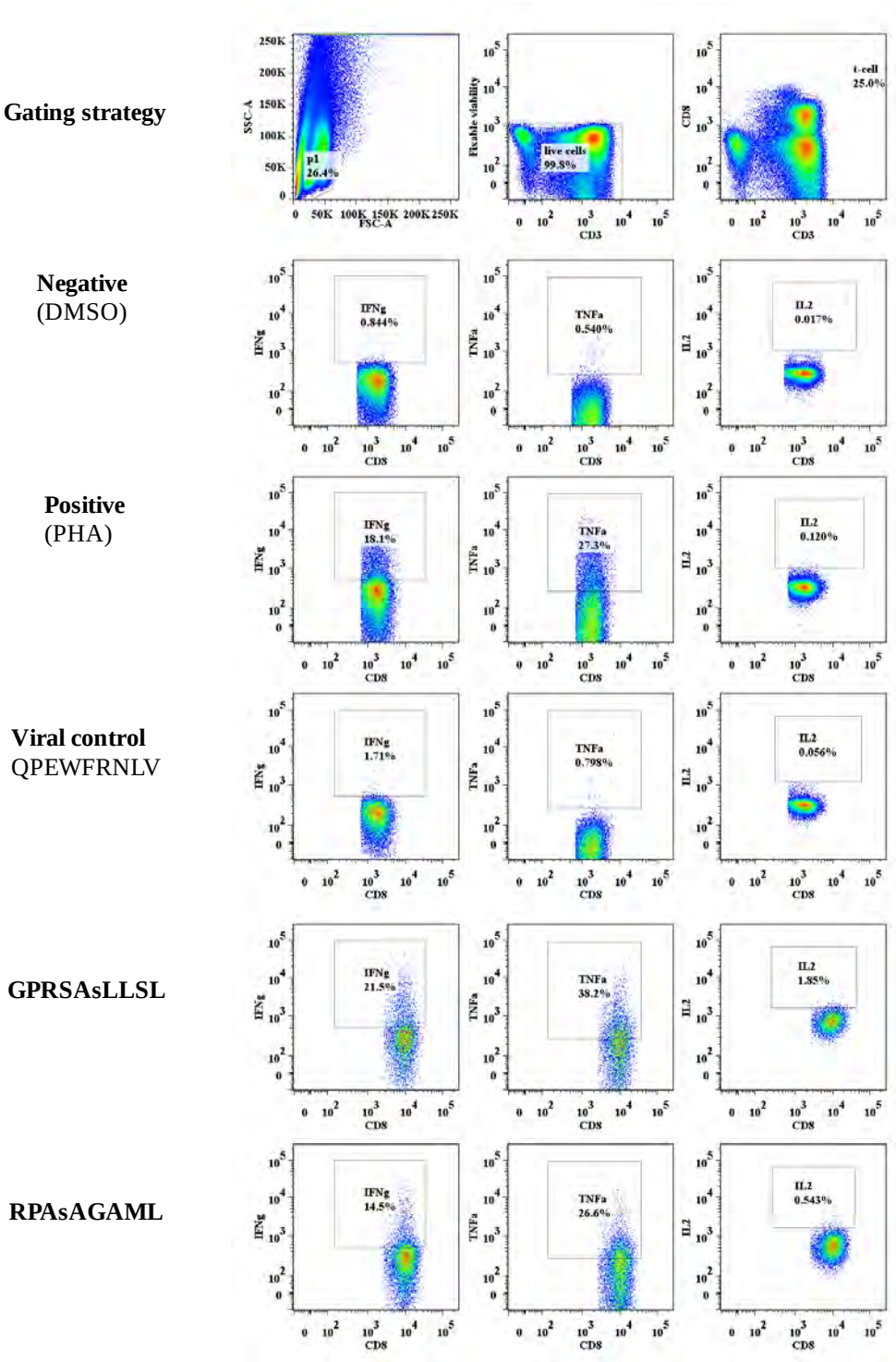

Fig. 4.7b:Phosphopeptide responses in Healthy Donor H (day 7)
PBMC's were generated from healthy donors and responses of these to tumour-associated phosphopeptides were then assessed using an ICS assay. The FACS plots depicted show the gating strategy employed and representative IFNγ ,TNFα, and IL-2 responses (from left to right). NB notation on figures, IFNg = IFNγ , TNFa = TNFα. These are representative plots of cells obtained from donor H. Experiment performed in triplicate.

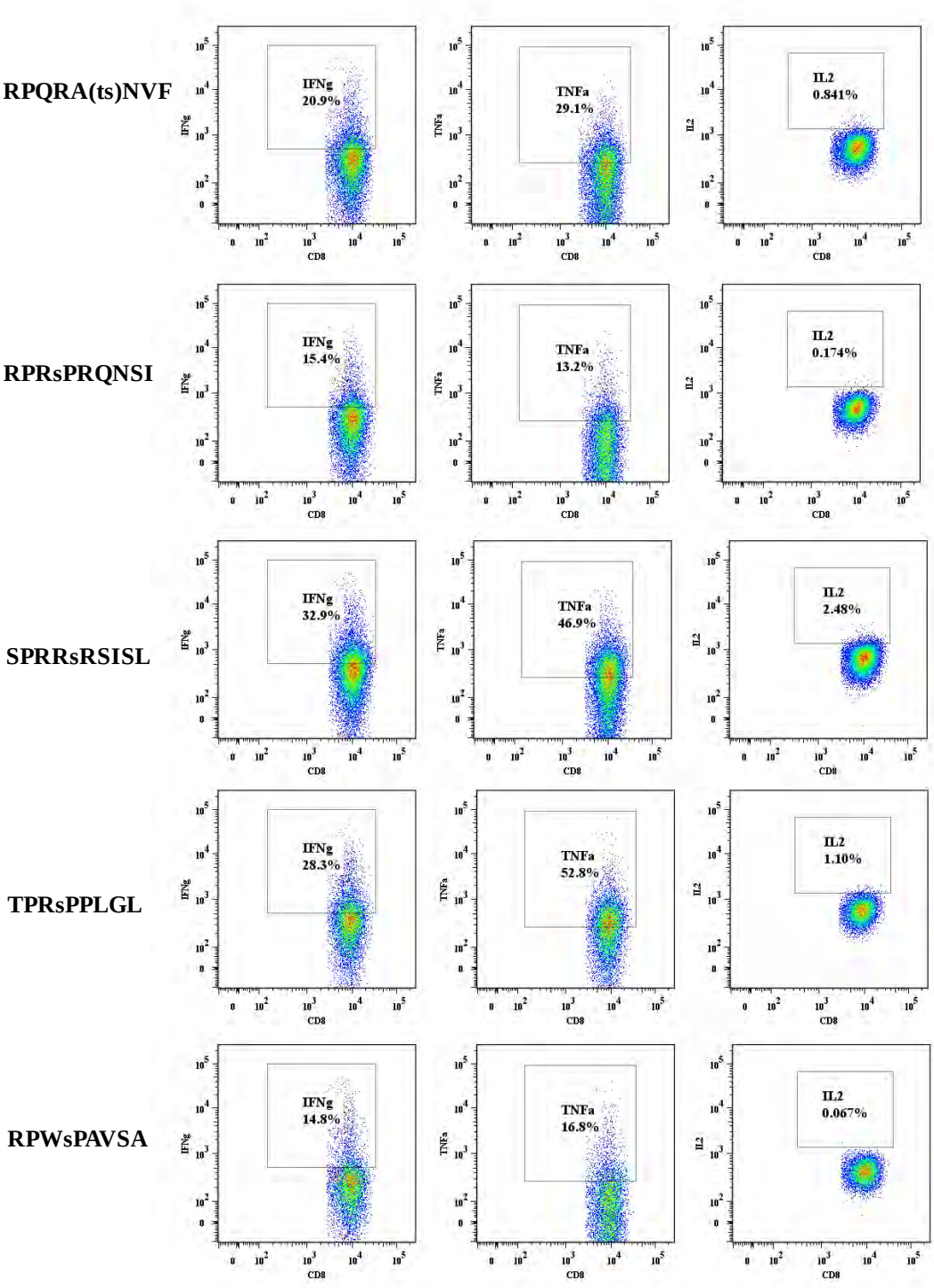

Fig. 4.7b:Phosphopeptide responses in Healthy Donor H(day 7) cont..
PBMC's were generated from healthy donors and responses of these to tumour-associated phosphopeptides were then assessed using an ICS assay. The FACS plots depicted show the gating strategy employed and representative IFNγ ,TNFα, and IL-2 responses (from left to right) (See also fig s2-4). NB notation on figures, IFNg = IFNγ , TNFa = TNFα. These are representative plots of cells obtained from donor H. Experiment performed in triplicate.

Donor P

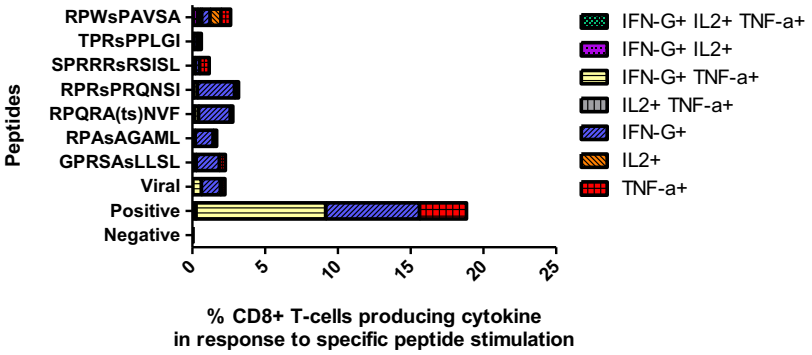

Day 1

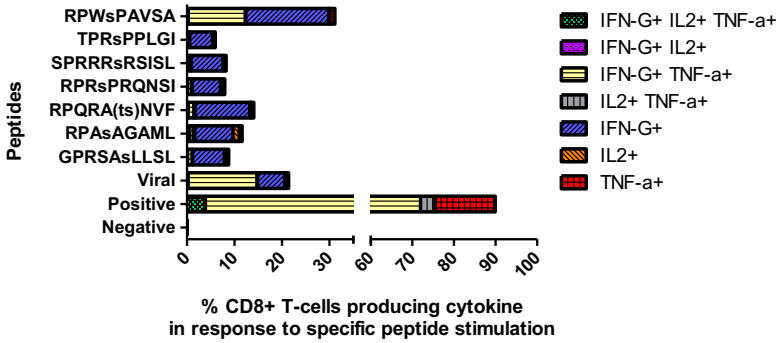

Day 7

Donor H

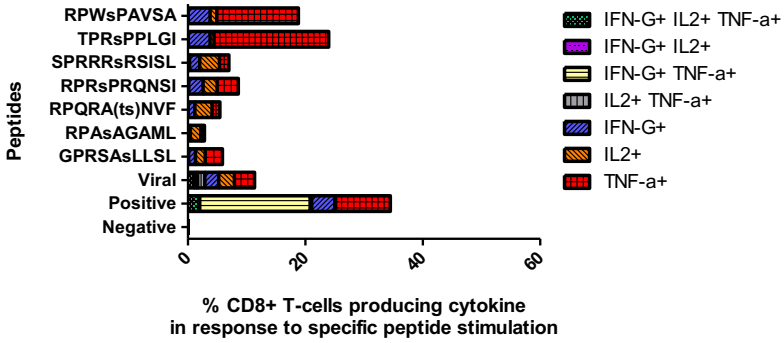

Day 1

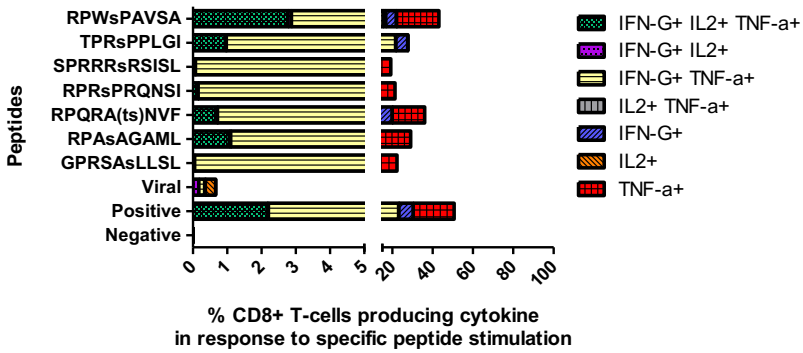

Day 7

Donor C – day 7

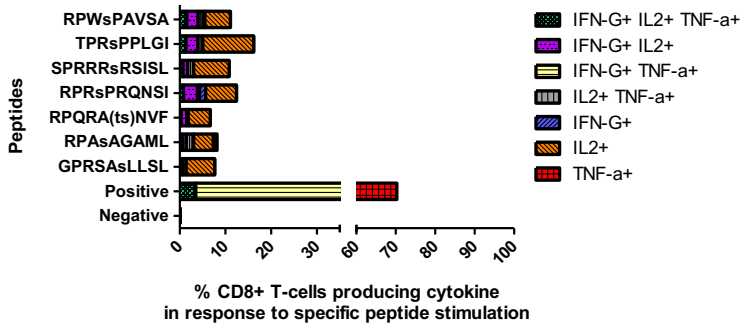

Donor O – day 7

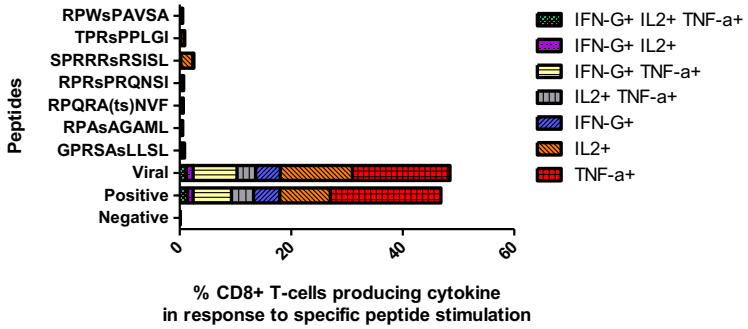

Fig. 4.7c: B7 Phosphopeptide responses in healthy donors
PBMC's were generated from healthy donors as per methods previously described, and responses of these cells to tumour-associated phosphopeptides were then assessed using an intracellular staining (ICS) assay. These were further analysed using combination gates to assess the expression of IFNγ ,TNFα, and IL-2 (denoted IFNg, TNFa and IL2 on the plot)– see fig s2-4 also for additional donor plots.

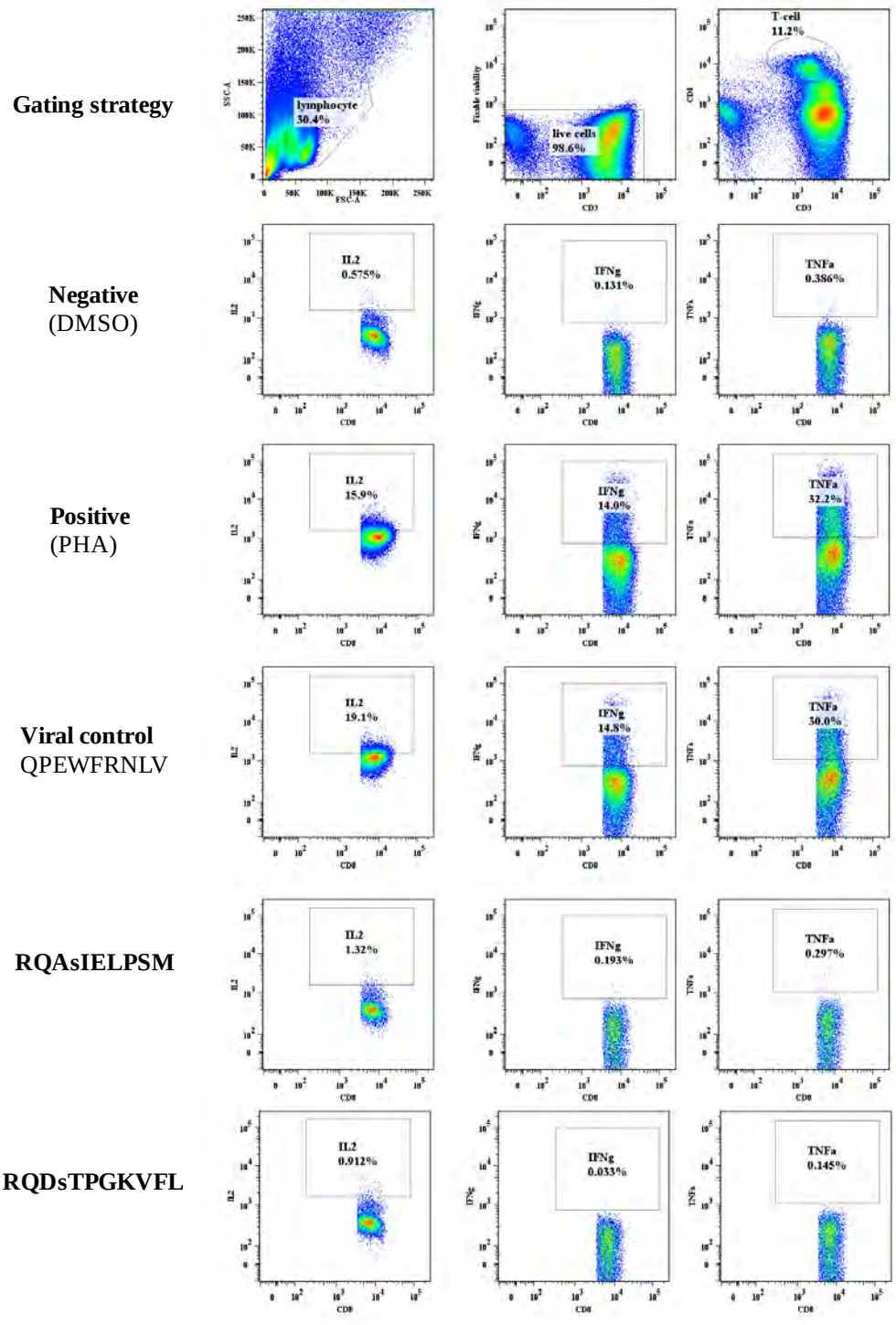

Fig. 4.8a:Phosphopeptide A2 responses in Healthy Donor O (day 7)
PBMC's were generated from healthy donors and responses of these to tumour-associated phosphopeptides were then assessed using an ICS assay. The FACS plots depicted show the gating strategy employed and representative IFNγ ,TNFα, and IL-2 responses (from left to right) – denoted IFNg, TNFa and IL2 on the plots. See fig S5-7 for additional donor plots.

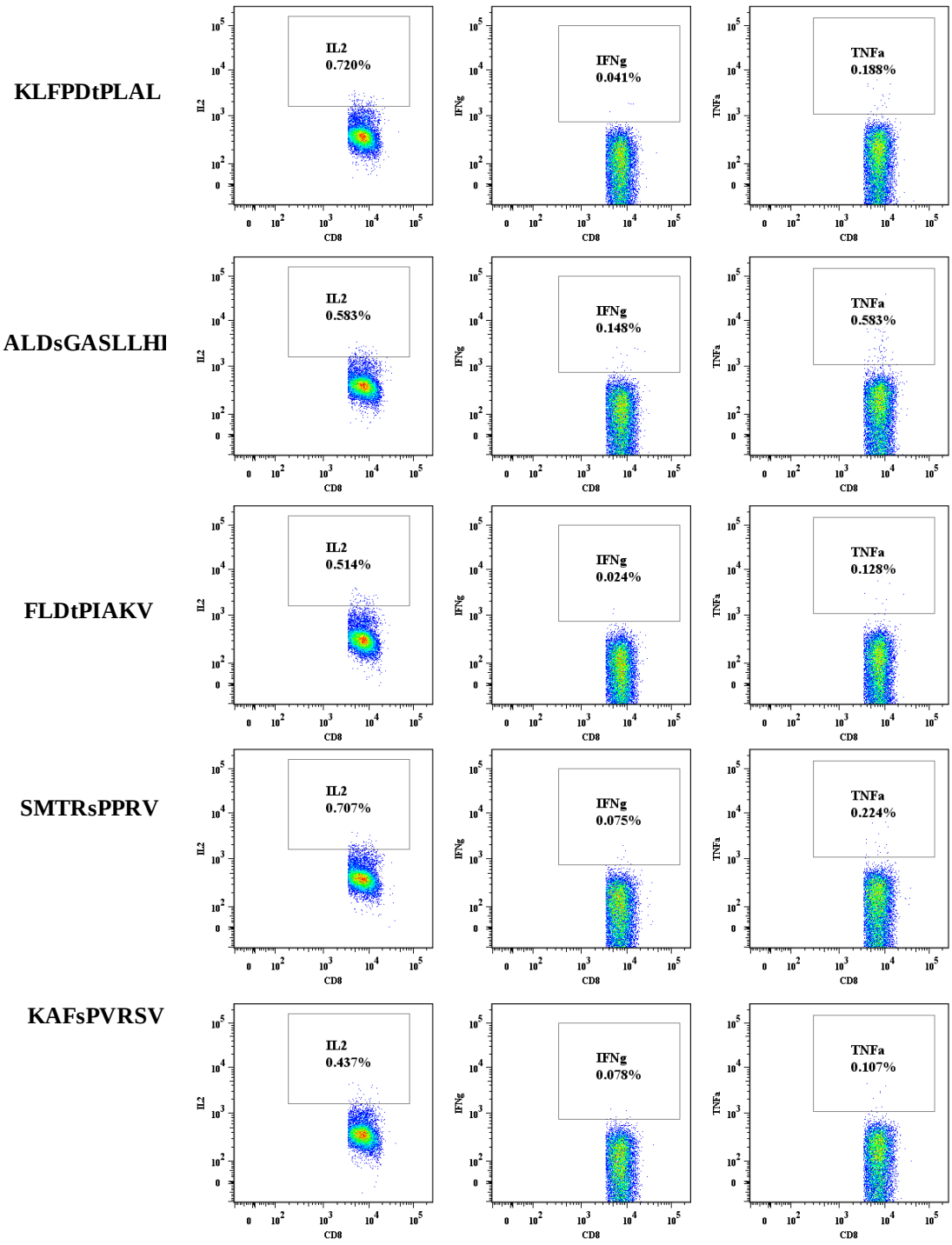

Fig. 4.8a:Phosphopeptide responses in Healthy Donor O (day 7) cont..
PBMC's were generated from healthy donors and responses of these to tumour-associated phosphopeptides were then assessed using an ICS assay. The FACS plots depicted show the gating strategy employed and representative IFNγ ,TNFα, and IL-2 responses (from left to right) – denoted IFNg, TNFa and IL2 on the plots. See fig S5-7 for additional donor plots.

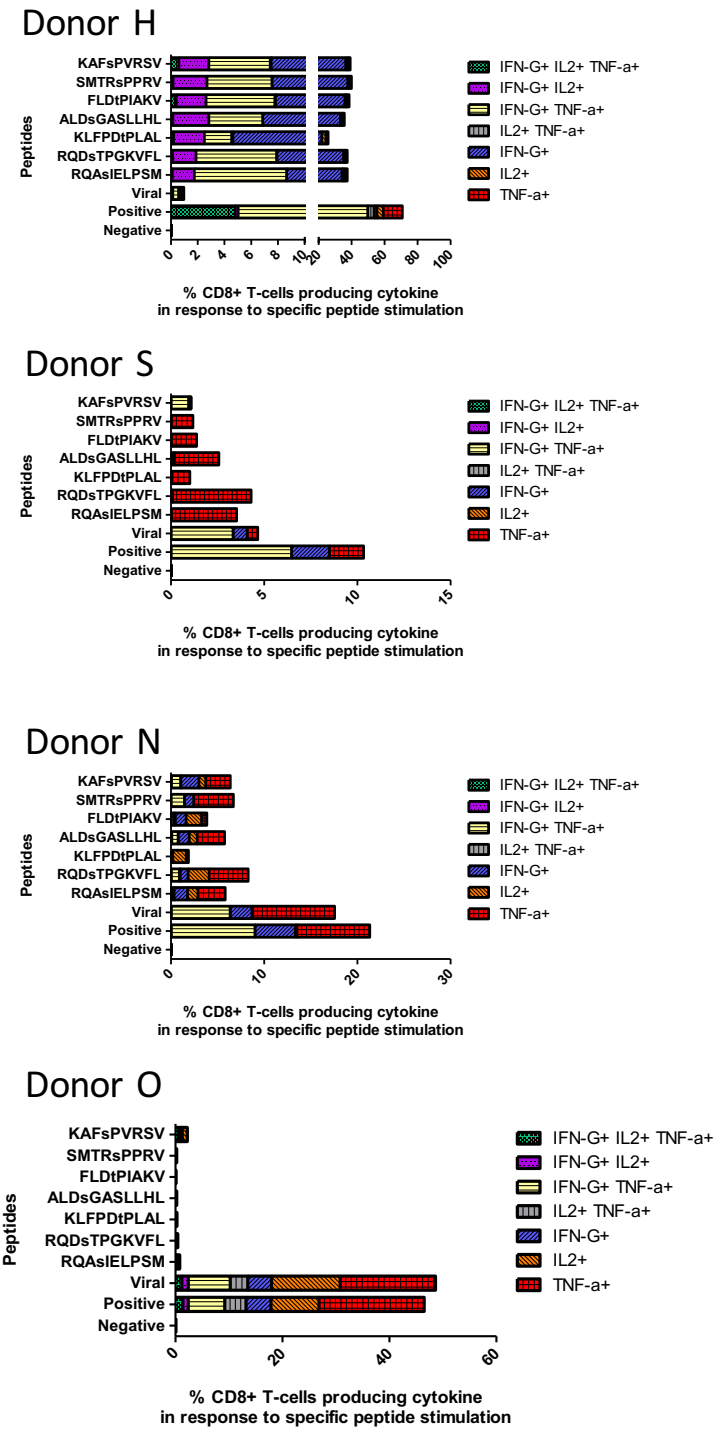

Fig. 4.8b: A2 Phosphopeptide responses in healthy donors at 7 days
PBMC's were generated from healthy donors and responses of these to tumour-associated phosphopeptides were then assessed using an ICS assay. These were further analysed using combination gates to assess the expression of IFNγ ,TNFα, and IL-2 , and combinations thereof (denoted IFN-G, TNF-a and Il2 on the plots). See fig S5-7 for additional donor plots.

RPWPAVSA and TPRsPPLGL emerged as potential targets of these healthy B7 donor T-cells, whilst in the A2 donor T-cells RQDsTPGKVFL appeared to be a possible target. Across the healthy donors, a T-cell response was demonstrated to a number of phosphopeptides, but this

response was noted to vary between donors, for example RPWsPAVSA produced a strong T-cell response in the two older donors (P and H) 30.2% and 42.1% respectively, but minimal response in the younger donors (O and C). H was the oldest donor at 61y of age and C the youngest donor at 34 years of age. Recognition of phosphopeptide was therefore proposed to be age related with a direct correlation between number of responses and amplitude of that response to phosphopeptide (fig. 4.9). However this is an assumption based on limited numbers (one donor in each of the 60y+ group and the 50-60y group, and two donors in the 40-50y group - fig 4.9), and further experimental analysis would be necessary to confirm this. It does however correlate with observations seen by previous members of the group (by private communication). Wilcoxon paired t-test showed on comparison of the youngest donor with the oldest donor there was a significant difference (**) in recognition and stimulation of T-cells in response to phosphopeptide p=0.031.

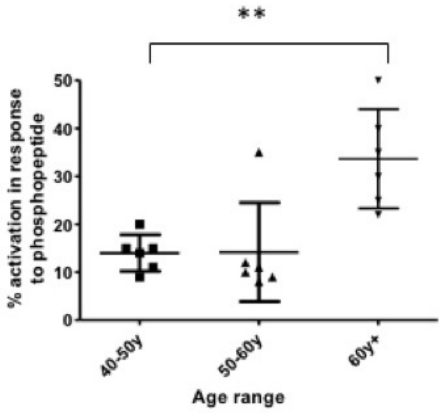

Fig. 4.9: Phosphopeptide B7 responses in Healthy Donor at 7 days
Comparison was made of total cytokine expression (denoted activation on the figure above) of each healthy donor in response to individual HLA-B7 phosphopeptides as determined by the FACS analysis presented previously. A significant difference was noted between the youngest and the oldest donor p=0.013 – Wilcoxon paired t-test (**).
NB there was no significant difference between positive control response exhibited by either group when analysisng FACS data previously, therefore it was considered valid to compare each of the donors in this fashion. Overall numbers of healthy donors was small, with only one donor was in the 60y+ group and two donors in the 40-50y group.

Likewise, on comparison of HLA-A2^{+} donors (fig. 4.10), it can be seen that there is a significant difference (**) based on age of donor, however as n=4 further analysis of this data is unlikely to be beneficial at this stage (i.e. one donor was in group 60y+, 2 donors were 30-40y and one was 20-30y). It can be seen that the mean number of responses to phosphopeptide is much higher in the 60+ age group (31.8%) compared to the younger age groups (14.2% in 40-50y age group) in the B7 responses at 7 days. This trend was repeated in the A2 phosphopeptide responses noted in healthy donors with the highest number of responses seen in the oldest age group (39.2%) versus 3.8% responses in the youngest age group (20-30y).

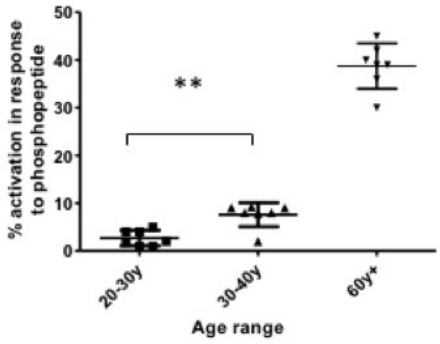

Fig. 4.10: Phosphopeptide A2 responses in Healthy Donor at 7 days
Comparison was made of total cytokine expression of each donor in response to individual phosphopeptides. A significant difference was noted between the youngest and the oldest donor p=0.025– Wilcoxon paired t-test (**). NB the donor in age range 60y+ was included with caution in this analysis. This is because the cytokine response to positive control was very different in this donor compared to any other donor (i.e. upto 75% CD8^{+} T-cells producing cytokine versus 10-40% in the other donors). One donor was age 20-30y, two donors were 30-40y and one donor was 60y+).

4.3.1 Can phosphopeptide-specific T-cells recognise HLA matched tumour

Having identified healthy donor T-cells that recognised tumour associated phosphopeptides, it was hypothesised that these cells could recognise HLA matched tumour samples. When liver tumour samples were first obtained, in addition to IMAC/MHC-I phosphopeptide extraction,

samples were also used to generate TiLs (using methods as previously described) and additional solid tumour sample and an aliquot of TiLs line were frozen.

Healthy donor derived T-cells which recognised phosphopeptide were expanded *in vitro* with media which was initially not supplemented until the 10^{th} day after phosphopeptide addition, when it was supplemented with IL-2 to maintain cell growth. These included hepatoblastoma-specific phosphopeptides: RPWsPAVSA, TPRsPPLGL, RQDsTPGKVFL and ALDsGASLLHL. The PTLD/LCL specific phosphopeptides assessed were: RPQRAtsNVF, RPQsAGAML and RPRsTRQNSI. We also looked at a number of phosphopeptides identified on both tumour types: KAFsPVRSV, KLFPDtPLAL and SMTRsPPRV. Once sufficient numbers had been grown an assay was set up to establish whether T-cells recognised tumour when pulsed with the relevant phosphopeptide and whether this response was the same as for TiLs lines already established in the case of hepatoblastoma. We proposed that the TiLs response would be less than the phosphopeptide specific T-cell response as the TiLs line is a heterogenous line and so overall phosphopeptide specific cell number would likely be less as it was cultured with IL-2 alone which is a non-specific agent causing expansion of all T-cells, not just the T-cells which recognise the peptide of interest. The healthy donor-derived line should have more phosphopeptide-specific T cells in it as it was cultured with the peptide of interest initially and only supplemented with IL-2 following a 10-day period without so in theory the cells of interest should only be those stimulated by peptide.

We wanted to establish that the tumour recognition wasn't just a random response and so healthy donor B-cells were obtained from fresh PBMC's using magnetic Beads (Miltenyi Biotec, UK). We considered if the phosphopeptide specific T-cells were able to recognise these B-cells as well as assessing response to non phosphopeptide pulsed cells (i.e. neither the healthy B-cells or the non-phosphopeptide pulsed cells should generate any significant T-cell activation if the T-cell response is specific to malignant target which we proposed was

phosphopeptide). Samples of supernatent were taken at varying timepoints, and ELISA was performed to assess individual response to tumour (fig. 4.11a and b). For the LCL/PTLD-phosphopeptides no TiLs were available, however in order to assess tumour response versus viral response we tested LCL response of healthy donor cells – obviously this could potentially encompass a viral response and therefore to negate this we had an additional control of phosphatase-treated cells – as this would then represent the viral response of donor T-cells.

Fig. 4.11a demonstrates the T-cell activation responses (release of IFNγ) as a response to different stimuli. We considered whether the phosphopeptide-specific T-cell lines which had been generated previously were able to recognise HLA-matched tumour samples. We hypothesised that pulsing the tumour samples with phosphopeptide would lead to T-cell activation, if the T-cells were using that phosphopeptide to target tumour. In order to test this theory, we selected a number of phosphopeptide lines, and looked at response to hepatoblastoma and PTLD (LCL) lines. When the hepatoblastoma tumour specimens became available, TiLs lines were also generated in conjunction with this and a sample of solid tumour frozen in liquid nitrogen. We therefore considered if the phosphopeptide-specific T-cell lines were able to recognise the solid tumour samples and mount a response. To do this, solid tumour samples were defrosted, cut into small pieces and digested enzymatically (collagenase). Cells were counted and equal numbers of tumour to T-cell line were added to the respective wells. A number of controls were included:

1) Phosphopeptide specific T-cell line alone (designated by the first 3 letters of the peptide sequence on fig. 4.11)

2) Phosphopeptide-specific T-cell line with healthy B-cells (negative control)

3) Phosphopeptide-specific T-cell line with LCL (positive control as cells will likely have a viral and phosphopeptide response)

4) Phosphopeptide-specific T-cell line with LCL (phosphatase treated therefore removing the phosphopeptide response resulting in any response being viral only

5) Phosphopeptide-specific T-cell line with tumour (in the absence of phosphopeptide stimulation, cells should not be able to recognise tumour)

6) Phosphopeptide-specific T-cell line with tumour and phosphopeptide

These were compared to TiLs responses to the same tumours using the same conditions. We also considered the responses of phosphopeptide-specific T-cells to LCL lines (B) but have no TiLs lines in this case. Finally, we considered phosphopeptide-specific T-cell lines which had been identified as being expressed on LCLs and hepatoblastomas looking at the same conditions as listed above (C). Cells were cultured as described and the supernatant sampled for ELISA analysis looking for IFNγ release (fig. 4.11a) and TNFα release (fig. 4.11b). Supernatent was sampled at 3 timepoints (day 1, day 7 and day 14).

Fig. 4.11a: ELISA data demonstrating IFNγ release from phosphopeptide specific T-cell lines compared to a TiLs obtained from HLA matched tumour. Phosphopeptide-specific T-cell lines were generated as per protocols described previously. The cell lines were then compared to TiLs which were generated at the time of tumour harvest and snap frozen at -80c. (A) Comparison was made of cytokine release of each phosphopeptide-specific cell line, designated by the first 3 letters of the phosphopeptide sequence (shown in bold) (**TPR**sPPLGL, **RQD**sTPGKVFL, **RPW**sPAVSA and **ALD**sGASLLHL found in hepatoblastoma tumours compared to TiLs derived from HLA matched tumour using an ELISA assay and standard protocol. Phosphopeptide-specific cell line alone was considered background cytokine release. The cell line was then tested with healthy B-cells (negative control), LCL lines (positive control), phosphatase treated LCLs (removing phosphopeptide response and thus demonstrating viral response), tumour (snap frozen at time of tumour harvest) and finally tumour with phosphopeptide (designated +PP on graph x-axis). Cells were samples on days 1, 7 and 14. (B) comparison made in PTLD-derived phosphopeptide-specific T-cell lines **RPA**sAGAML, **RPQ**RAtsNVF and **RPR**sPRQNSI and (C) Derived from hepatoblastoma and PTLD lines **KLF**PDtPLAL, **KAF**sPVRSV and **SMTR**sPPRV These graphs represent 2 repetitions of each experiment, performed in duplicate. Error bars represent SEM.

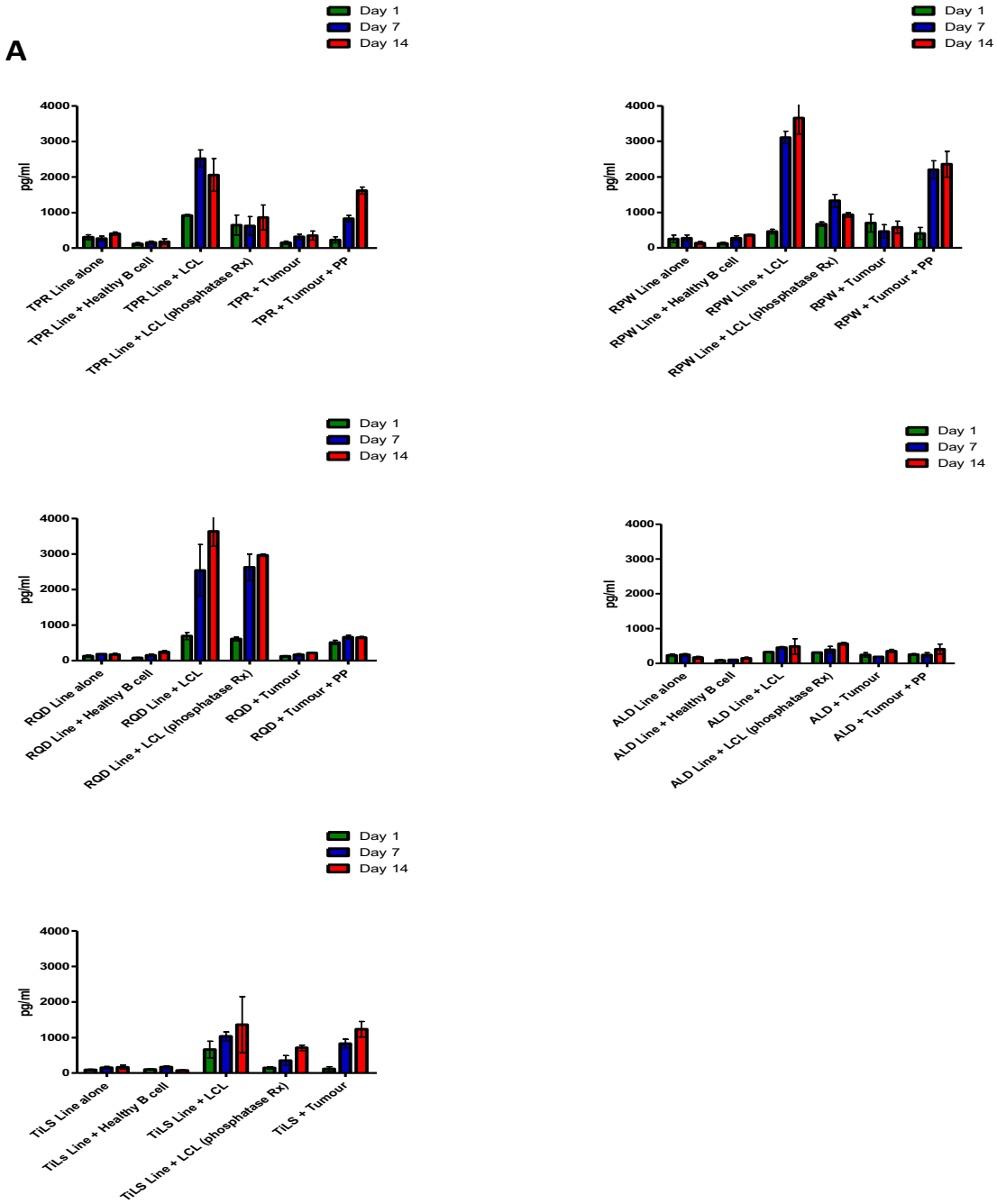

B

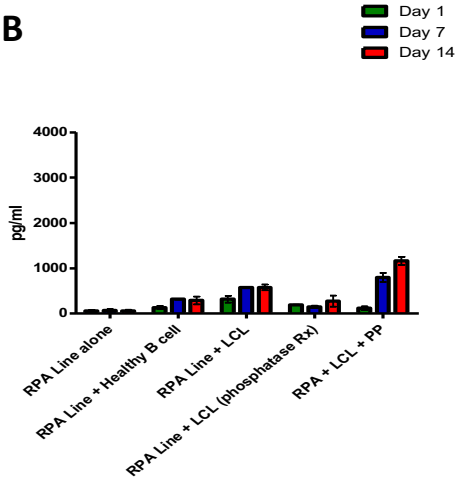
Day 1
Day 7
Day 14
pg/ml
4000
3000
2000
1000
0
RPA Line alone
RPA Line + Healthy B cell
RPA Line + LCL
RPA Line + LCL (phosphatase Rx)
RPA + LCL + PP

C

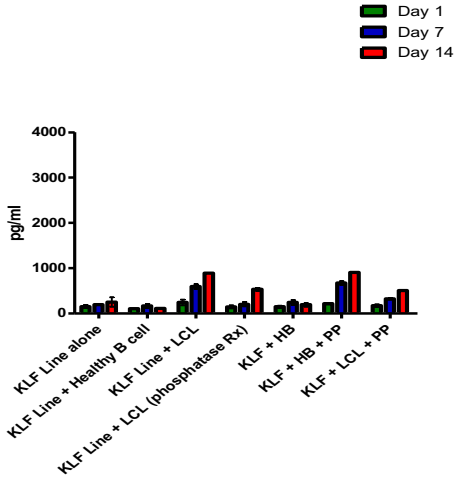
Day 1
Day 7
Day 14
pg/ml
4000
3000
2000
1000
0
KLF Line alone
KLF Line + Healthy B cell
KLF Line + LCL
KLF Line + LCL (phosphatase Rx)
KLF + HB
KLF + HB + PP
KLF + LCL + PP

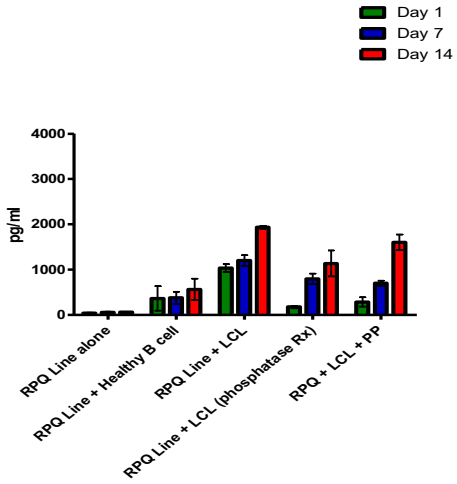
Day 1
Day 7
Day 14
pg/ml
4000
3000
2000
1000
0
RPQ Line alone
RPQ Line + Healthy B cell
RPQ Line + LCL
RPQ Line + LCL (phosphatase Rx)
RPQ + LCL + PP

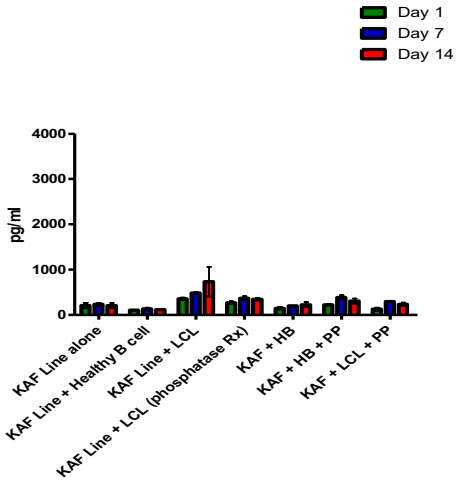
Day 1
Day 7
Day 14
pg/ml
4000
3000
2000
1000
0
KAF Line alone
KAF Line + Healthy B cell
KAF Line + LCL
KAF Line + LCL (phosphatase Rx)
KAF + HB
KAF + HB + PP
KAF + LCL + PP

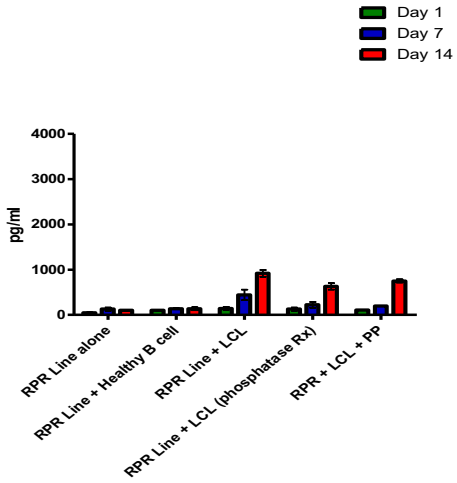
Day 1
Day 7
Day 14
pg/ml
4000
3000
2000
1000
0
RPR Line alone
RPR Line + Healthy B cell
RPR Line + LCL
RPR Line + LCL (phosphatase Rx)
RPR + LCL + PP

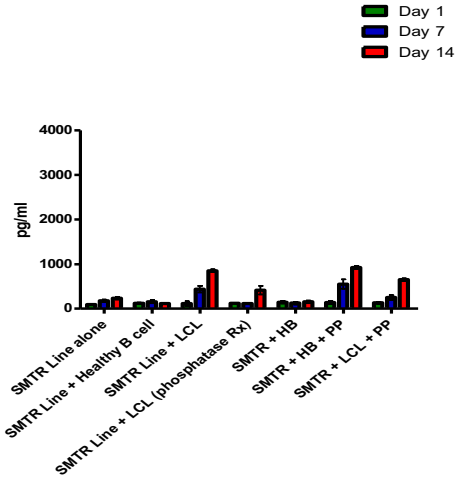
Day 1
Day 7
Day 14
pg/ml
4000
3000
2000
1000
0
SMTR Line alone
SMTR Line + Healthy B cell
SMTR Line + LCL
SMTR Line + LCL (phosphatase Rx)
SMTR + HB
SMTR + HB + PP
SMTR + LCL + PP

Fig. 4.11b: ELISA data to show TNFα- release from phosphopeptide specific T-cell lines compared to a TiLs obtained from HLA matched tumour. Phosphopeptide-specific T-cell lines were generated as per protocols described previously. The cell lines were then compared to TiLs which were generated at the time of tumour harvest and frozen at -80c. (A) Comparison was made of cytokine release of each phosphopeptide-specific cell line, designated by the first 3 letters of the phosphopeptide sequence (shown in bold) (**TPR**sPPLGL, **RQD**sTPGKVFL, **RPW**sPAVSA and **ALD**sGASLLHL found in hepatoblastoma tumours compared to TiLs derived from HLA matched tumour. We assessed the phosphopeptide-specific cell line alone as considered background cytokine release. The cell line was then tested with healthy B-cells (negative control), LCL lines (positive control), phosphatase treated LCLs (removing phosphopeptide response and thus demonstrating viral response), tumour (snap frozen at time of tumour surgery) and finally tumour with phosphopeptide (designated +PP on graph x-axis) (B) comparison made in PTLD-derived phosphopeptide-specific T-cell lines **RPA**sAGAML, **RPQ**RAtsNVF and **RPR**sPRQNSI and (C) Derived from hepatoblastoma and PTLD lines **KLF**PDtPLAL, **KAF**sPVRSV and **SMTR**sPPRV. These graphs represent 2 repetitions of each experiment, performed in duplicate.

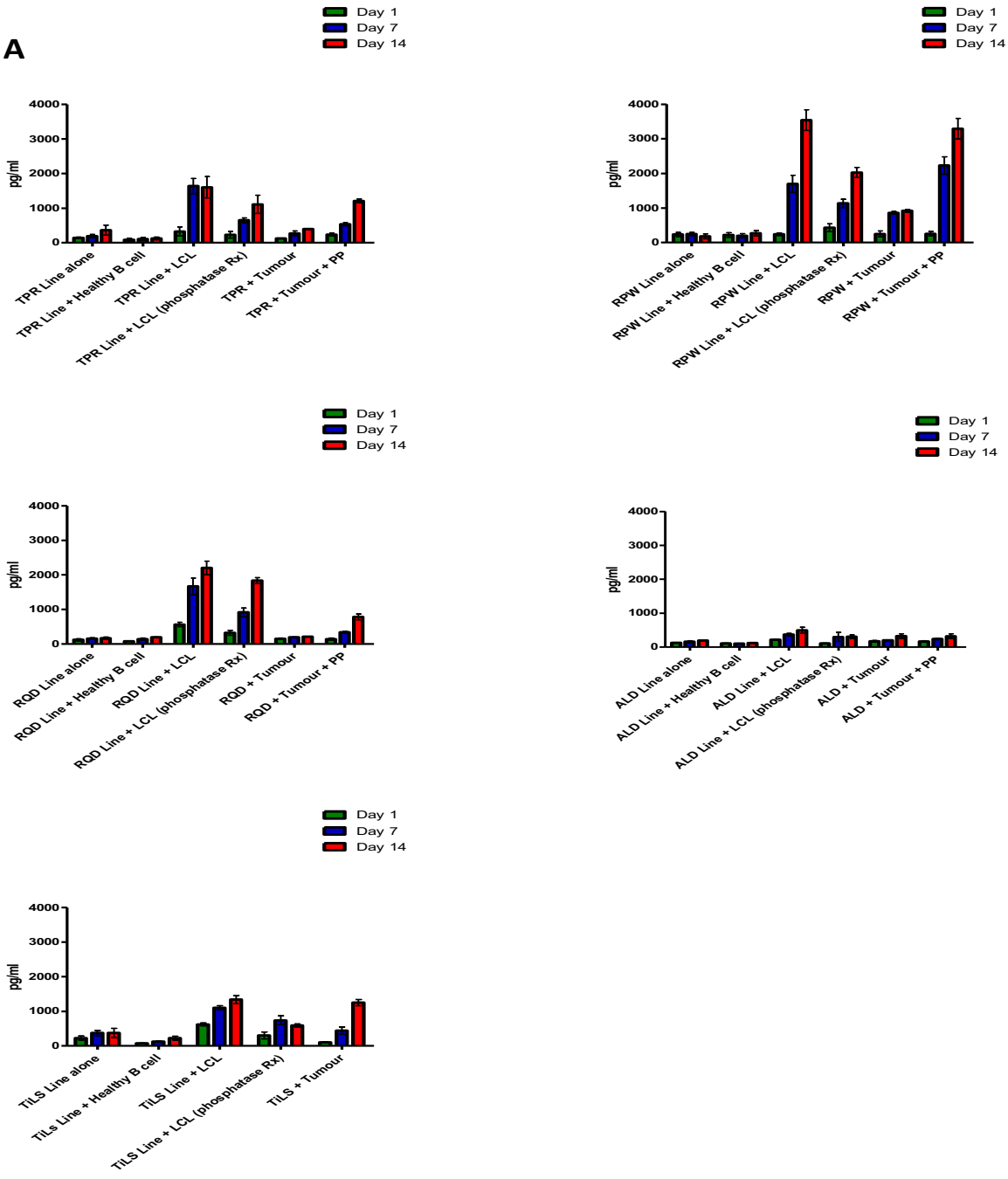

B

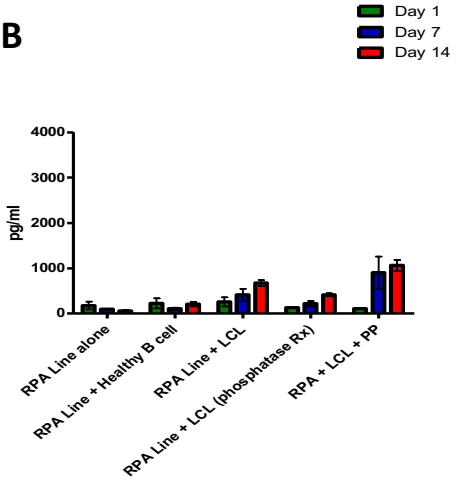
Day 1
Day 7
Day 14
pg/ml
4000
3000
2000
1000
0
RPA Line alone
RPA Line + Healthy B cell
RPA Line + LCL
RPA Line + LCL (phosphatase Rx)
RPA + LCL + PP

C

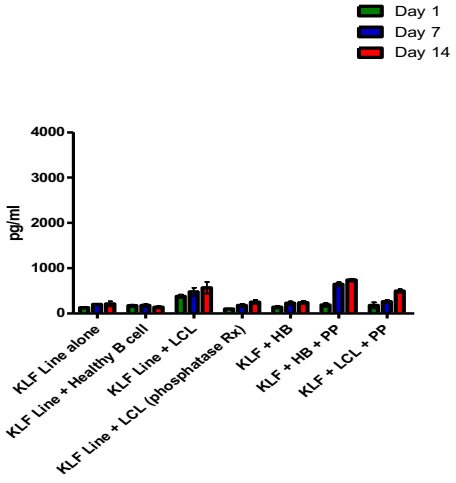
Day 1
Day 7
Day 14
pg/ml
4000
3000
2000
1000
0
KLF Line alone
KLF Line + Healthy B cell
KLF Line + LCL
KLF Line + LCL (phosphatase Rx)
KLF + HB
KLF + HB + PP
KLF + LCL + PP

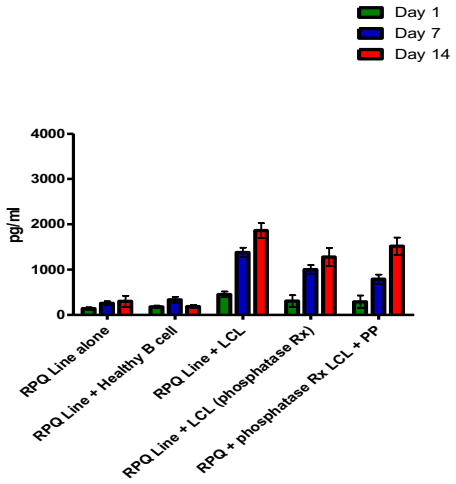
Day 1
Day 7
Day 14
pg/ml
4000
3000
2000
1000
0
RPQ Line alone
RPQ Line + Healthy B cell
RPQ Line + LCL
RPQ Line + LCL (phosphatase Rx)
RPQ + phosphatase Rx LCL + PP

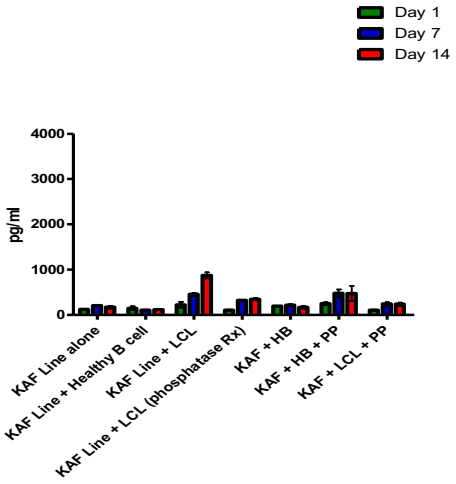
Day 1
Day 7
Day 14
pg/ml
4000
3000
2000
1000
0
KAF Line alone
KAF Line + Healthy B cell
KAF Line + LCL
KAF Line + LCL (phosphatase Rx)
KAF + HB
KAF + HB + PP
KAF + LCL + PP

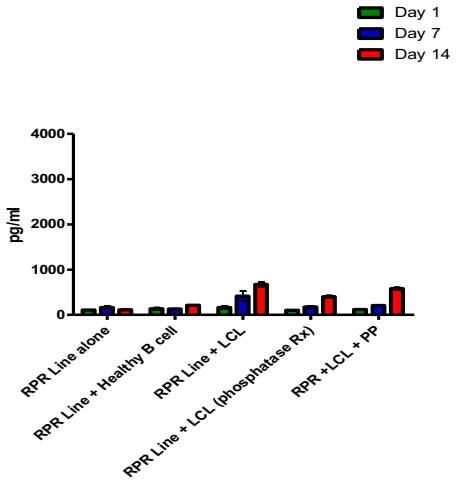
Day 1
Day 7
Day 14
pg/ml
4000
3000
2000
1000
0
RPR Line alone
RPR Line + Healthy B cell
RPR Line + LCL
RPR Line + LCL (phosphatase Rx)
RPR +LCL + PP

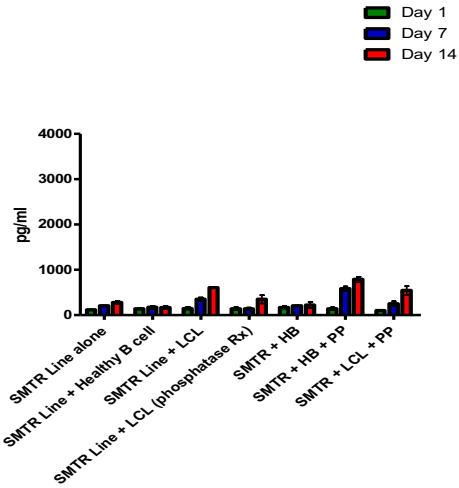
Day 1
Day 7
Day 14
pg/ml
4000
3000
2000
1000
0
SMTR Line alone
SMTR Line + Healthy B cell
SMTR Line + LCL
SMTR Line + LCL (phosphatase Rx)
SMTR + HB
SMTR + HB + PP
SMTR + LCL + PP

Phosphopeptide specific T-cells can recognise HLA matched tumour samples, seen most noticeably at 14 days. RPWsPAVSA, TPRsPPLGL, RPAsAGAML, SMTRsPPRV and KLFPDtPLAL specific T-cells all had demonstrable responses with IFNγ release of 2200ng/ml, 1960ng/ml, 1135ng/ml, 990ng/ml and 960ng/ml respectively to tumour plus phosphopeptide in the case of hepatoblastoma or LCL plus phosphopeptide in the case of PTLD/LCL (an effective response in the LCL experiment showing that recognition was largely phosphopeptide-specific not viral specific as following phosphatase treatment there was a negligible response of the phosphopeptide specific T-cells). T-cell responses to LCL were considered 'false positive' in RPQRA(ts)NVF, RQDsTPGKVFL, ALDsGASLLHL and KAFsPVRSV. This is because although the phosphopeptide-specific T-cells are activated in the presence of LCLs, following addition of phosphatase, there is still T-cell activation seen, thus demonstrating viral recognition as phosphopeptide driven response would be removed by phosphatase treatment, yet levels of IFNγ and TNFα release is not significantly reduced following treatment with phosphatase.

TiLs can recognise hepatoblastoma tumour, but this response is less than that seen in the phosphopeptide specific T-cells for reasons already stated, that the healthy donor derived lines should have more phosphopeptide-specific T-cells as it was cultured with the peptide of interest. The TiL line will have less as it was cultured with a non-specific agent (IL-2) that will cause all T-cells to expand and not just the T-cells that recognise the peptide of interest. Due to availability of tumour tissue this was not possible to be repeated but provides reasonable proof of principle that these cells are able to recognise tumour.

4.3.2 Can phosphopeptide-specific T-cells effectively kill tumour cells?

After demonstrating phosphopeptide specific T-cells can recognise tumour pulsed with phosphopeptide, I proposed that these cells could also demonstrate effective killing, if as

predicted these cells use phosphopeptide as a target for killing. Although this is an artificial *in vitro* model system, using T-cells derived from healthy HLA-matched donors, the initial data would suggest that T-cells may use phosphopetide as a tumour target and this may induce these T-cells to kill target (tumour) cells.

In order to test this theory two of the cell lines tested previously and shown to recognise tumour were used in a Europium release killing assay (RPWsPAVSA and TPRsPPLGL) alongside TiLs derived from hepatoblastoma tumour. Tumour cells were pulsed with phosphopeptide prior to the assay (fig. 4.12). Fig 4.12a directly compares the two phosphopeptide-specific T-cell lines with TiLs and assesses response to HLA-matched tumour. Two different E:T ratios were investigated as it was proposed that more Phosphopeptide-specific T-cell would lead to a greater killing response, but we considered if there was a ceiling effect to this. The phosphopeptide specific T-cell lines were able to recognise and kill tumour cells, but this was far more efficient when pulsed with phosphopeptide. RPWsPAVSA showed a greatest killing response (25.5%) when in a 3:1 E:T ratio with tumour pulsed with phosphopeptide, compared to 13.2% at a 1:1 ratio. T-cells exposed to non-pulsed tumour showed no increase in killing response (3.1% vs 3.2% 1:1 and 3:1 respectively). TiLs do demonstrate dose dependent killing of tumour cells, but this is only in the region of 9.7% and 12.2% respectively at 1:1 and 3:1 ratios. This shows that although the TiLs are a heterogeneous line, there are T-cells contained within this line that appear to be able to target the tumour. The data obtained shows that addition of the phosphopeptide RPWsPAVSA to the tumour prior to addition of phosphopeptide specific T-cells did significantly increase effective killing from 3.2% to 25.5% (paired t-test p=0.0012)– which further suggests that T-cells target the tumour by means of phosphopeptide recognition (fig. 4,12b). Interestingly, T cells against the RPW peptide aren't able to target the tumour without the addition of exogenous peptide. RPW peptide was found in three of the tumour samples by mass spectroscopy, therefore it would be expected that the

phosphopeptide-specific T-cells should recognise tumour cells without the addition of exogenous peptide. We propose that potentially this phosphopeptide was degraded during storage of the solid tumour sample, or that the process of generating a tumour cell line (by enzymatic digestion as described previously) led to loss of endogenous peptide, therefore necessitating the addition of exogenous peptide. Linear regression shows a significant difference in tumour killing when phosphopeptide is added ($p=0.0026$). There was also a significant increase in response to addition of exogenous TPRsPPLGL ($p=0.0296$) although not as marked as was seen for RPWsPAVSA.

Fig. 4.12: Europium Release Killing Assay demonstrating a dose dependent response of T-cells to phosphopeptide pulsed HLA matched tumour

This experiment employed the Europium Release killing assay as described previously in chapter 2 to attempt to demonstrate recognition and killing of tumour cells by the effector cells. (A) Two phosphopeptide specific T-cell lines (RPWsPAVSA and TPRsPPLGL) derived from a healthy donor 'P' were tested in this assay (designated by the first 3 letters of the phosphopeptide sequence on the x-axis) using HLA matched hepatoblastoma-derived tumour cells (designated +tumour on x-axis) pulsed with phosphopeptide (designated +PP on the x-axis). TiLs derived from hepatoblastoma tumour were tested alongside these phosphopeptide specific T-cell lines. E:T ratio of 1:1 denotes equal numbers of phosphopeptide specific T-cells to tumour-derived cells. E:T 3:1 denotes 3x as many phosphopeptide-specific T-cells to target tumour-derived cells. The effect of phosphopeptide pulsing on each individual cell line (B) RPWsPAVSA and (C) TPRsPPLGL are shown in these linear regression lines. The addition of phosphopeptide (blue line) increases the killing efficiency significantly. These graphs represent 2 repetitions of each experiment, performed in duplicate. Error bars represent SD.

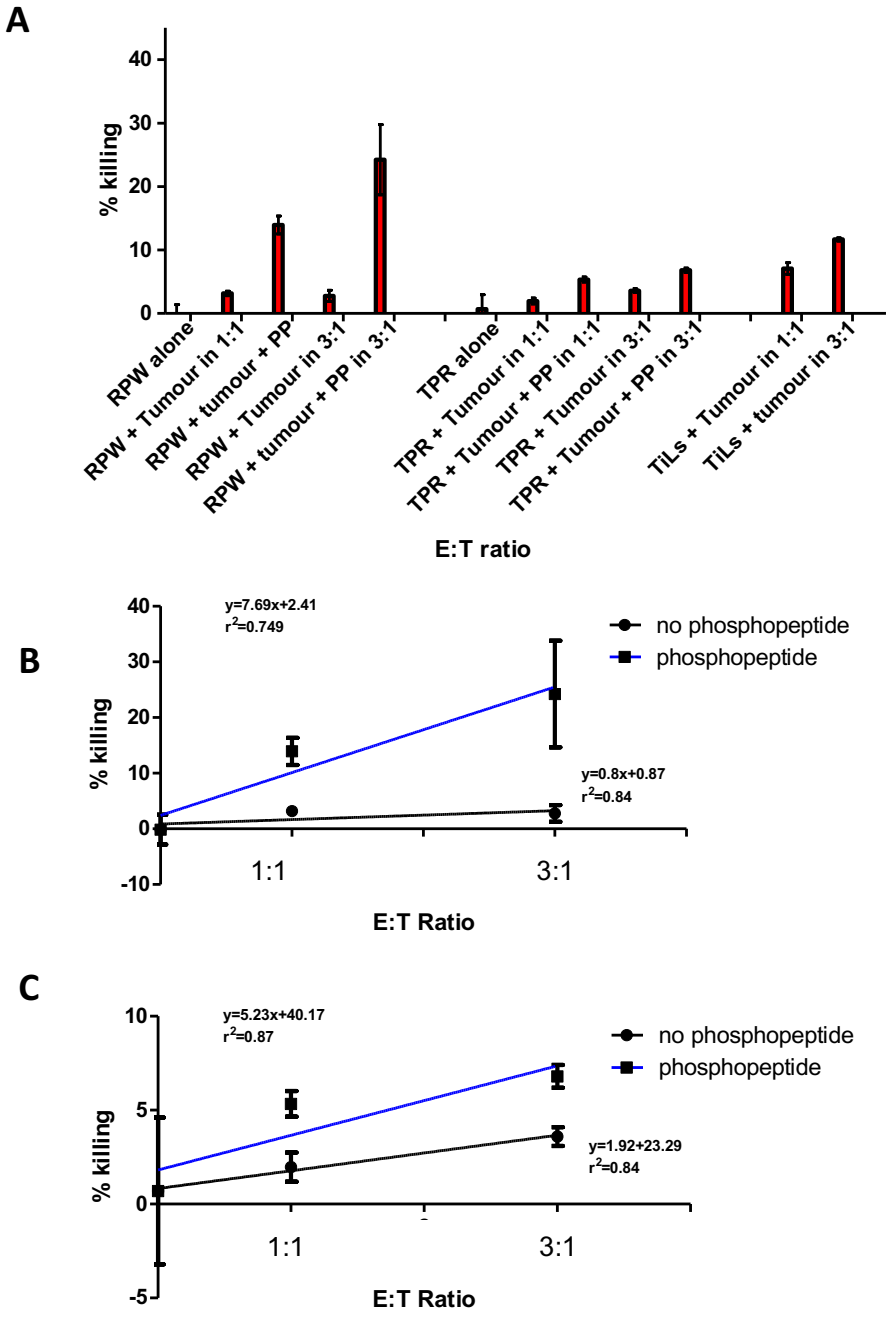

4.4 Summary

Previously we have identified phosphopeptides as potential HLA-specific targets and this chapter sought to identify specific MHC class 1 phosphopeptides on hepatoblastoma tumour samples as well as HepG2 (a hepatoblastoma cell line) and also a small number found on healthy tissue. It has been shown that there are an increased number of phosphopeptides seen on tumour samples compared to healthy liver tissue, and their expression level is also increased compared to healthy tissue. This would suggest that as part of the tumour process proteins become phosphorylated resulting in more phosphopeptides being expressed. It appears that it is these that may be targeted by CD8 T-cells. Therefore, it is a possibility that one of the reasons that the majority of people do not develop cancer is because these phosphopeptides allow tumours to be recognised and eradicated by the immune system. Although none of the phosphopeptides identified on hepatoblastoma samples analysed here were unique, i.e. they had all been found on other tumour types including melanoma, colorectal adenocarcinoma and others (fig.4.4) and only 2 were unique on the PTLD sample, it is considered that their presence is indicative of malignant transformation and therefore a potential target for T-cell responses. Of course this is a broad statement to make and therefore this chapter sought to analyse responses of T-cells to tumour associated phosphopeptide further.

A number of key cancer pathways were identified as being intimately associated with proteins the phosphopeptides were derived from, providing yet more evidence that these could be tumour associated. 12 phosphopeptides were identified as being implicated in a number of hepatic malignancies (hepatoblastoma, hepatocellular carcinoma, hepatic metastases/secondary tumours), and therefore these were chosen to be investigated further. HLA-matched healthy donors were identified, and T-cells magnetically selected. These T-cells were stimulated with phosphopeptide which had previously been identified on tumour samples and then these cells were cultured to see if over time they mounted a response to this

peptide stimulus and became activated. This was to establish if healthy individuals had the ability to recognise tumour-associated phosphopeptide. We predicted that they would, as this is the basis for the proposed hypothesis that T-cells have a tumour-specific target, and by nature of the fact that a healthy individual does not have that specific malignancy it would suggest that they are able to recognise that target and eradicate it.

Responses to HLA-specific hepatoblastoma-associated phosphopeptides were tested in three HLA-matched healthy donors. Many of these phosphopeptides were identified on cell lines and were shared across other malignancies. RPWsPAVSA was seen on most HLA-$B7^+$ cancer samples and not on healthy tissue; and healthy donor responses to this were seen in all three healthy donors to varying degrees. It was noted however that in older healthy donors, there appeared to be stronger and more plentiful responses to phosphopeptides in general – suggesting that possession of phosphopeptide responses is age dependent. Three HLA-$A2^+$ donors were also identified and their responses to tumour associated phosphopeptides assessed. Again age appeared to play a role in recognition; however, RQDsTPGKVFL consistently induced a response in these donors. Due to limits on the amount of tumour tissue available these weren't tested in more individuals, but in order to strengthen this observation it would be ideal to test this in more healthy donors.

Unfortunately, we were only able to obtain one PTLD tumour sample as when diagnosing this disease process the majority of the biopsy specimen is used for histological analysis – and therefore the PTLD patient sample was derived from a blood sample obtained at time of diagnosis. As a proxy for PTLD, healthy donor PBMC's were transformed into LCL lines by methods previously described and then these were used to identify phosphopeptides expressed. These were combined with data available from the commercially available cell line JY (190 phosphopeptides identified on tumour tissue versus 23 on healthy tissue). This provided further evidence that phosphopeptide expression was vastly different on tumour samples

compared to healthy tissue and could therefore be a potential target for tumour recognition. Phosphopeptides identified on LCL lines were used to test responses of healthy donor T-cells and we were able to demonstrate that a number of these phosphopeptides did lead to healthy T-cells becoming activated.

4.5 Discussion

This chapter sought to build on the knowledge gained in chapter 3 relating to phosphopeptides, and identify suitable targets on liver tumours and PTLD. The questions to be answered included: (i) what is the target on tumours for T-cells; (ii) what role do these play in cancer; (iii) can healthy donors also respond to these phosphopeptides; (iv) can we generate a phosphopeptide-specific T-cell line and (v) can this phosphopeptide-specific T-cell line successfully target and kill HLA-matched tumour?

82 tumour-associated phosphopeptides were identified on hepatoblastoma samples and 75 tumour associated on the PTLD sample (152 on JY line and 119 on healthy donor derived LCL lines). This compares favourably with normal healthy tissues with far fewer phosphopeptides identified. This could therefore suggest that phosphopeptides result from tumour formation and this then could result in T cell responses towards them.

Previous work done by this group and our collaborators has identified phosphopeptides found on a number of other tumour groups including melanoma, breast cancer, leukaemia, colorectal tumours and others (Meadows, Wang et al. 1997, Wang, Gulden et al. 1997, Zarling, Ficarro et al. 2000, Syka, Coon et al. 2004, Zarling, Polefrone et al. 2006, Cobbold, Polefrone et al. 2007, Mohammed, Cobbold et al. 2008, Penny, Abelin et al. 2012, Cobbold, De La Pena et al. 2013, Abelin, Trantham et al. 2015)

There are cytotoxic T-cells present in tumours (TiLs). We considered if these T-cells were able to target the tumour-associated phosphopeptides identified during our initial experiments

and hence actually be a novel target for immunotherapy in paediatric liver tumours and PTLD? To test this hypothesis, 13 phosphopeptides from liver tumour samples (including those identified on cell lines, and those found previously on other hepatic tumours e.g. hepatocellular carcinomas and hepatic metastases) and PTLD/LCLs were generated and their immune responses were investigated in HLA-matched healthy donors of varying age groups (7 HLA-$B7^+$ and 6 HLA-$A2^+$ phosphopeptides were selected). It was not possible to test age-matched controls due to issues around consent. The phosphopeptides tested had varying functions implicated in cancer including mRNA splicing, mRNA processing, DNA binding and protein binding.

Initially, we considered the healthy donor T-cells responses to the target phosphopeptides. On day 0 (at 6 hours post-stimulation), responses to two of the target phosphopeptides identified were significantly higher than background (and at similar levels to viral control response) – RPWsPAVSA, from SKI oncogene, key in the TGF-beta signalling pathway, and TPRsPPLGL a MAP kinase involved in JNK signalling (Fig. 4.5, 4.7). We identified that RPWsPAVSA was the only peptide that generated a multifunctional response encompassing all three of the cytokines tested by ELISpot and FACS – IL-2, IFNγ and TNFα. The other peptides only elicited low/no responses compared to background.

After a further 6 days of expansion, we identified more responses to the phosphopeptides in all 6 healthy donors at varying levels (Figs. 4.7, 4.8). We also determined that some of these responses were multifunctional (with release of a combination of cytokines), which may represent cytotoxic potential, although this was not formally tested in this instance. In particular donor H had multifunctional responses to all HLA-B7 peptides tested (this donor was also the oldest donor tested). Of particular note were the responses to RPWsPAVSA and TPRsPPLGL. Both of these HLA-B7 phosphopeptides were identified as potentially being implicated in hepatic malignancy, and interestingly every donor tested for these had a response

to them. However, RPWsPAVSA had good expansion when looking at day 0 and day 7 responses, whereas TPRsPPLGL did not expand as well with similar levels seen to day 0. It is slightly harder to identify a pattern in the HLA-A2 phosphopeptides assessed as the only donor with consistently high responses was donor H. Donor H was the oldest healthy donor assessed hence leading to the hypothesis that possession of phosphopeptide responses may be directly proportional to age. On further investigation it can indeed be seen that older healthy donors possessed a significantly higher number of responses than younger donors (fig. 4.9, 4.10).

We compared the cytokine responses seen before and after phospopeptide-induced expansion. This revealed a number of key differences in the various donors. An example of this is seen in the response to RPAsAGAML in donor H could not be seen at all pre-expansion, but expanded well over time, whereas the response to TPRsPPLGL in the same donor did not expand well – having been seen at baseline but not increasing over time. This could partly be explained by the fact that the protocol used different concentrations of phosphopeptide at different time points e.g. on day 0, 50 µg/ml was used, whereas on day 7, only 10 µg/ml was used (as per well established laboratory group protocols based on the assumption that higher concentrations may lead to overstimulation and death). T-cells with a high functional avidity only require a small amount of antigen to grow. We predict that by using a higher concentration of peptide, the T-cells with a lower functional avidity may demonstrate a better growth potential. Higher functional avidity is likely to be beneficial in cancer treatment, therefore we considered that the day 7 results are likely to be more meaningful (Zeh, Perry-Lalley et al. 1999, Xue, Gao et al. 2013, Zhong, Malecek et al. 2013, Rashin and Jernigan 2016). Whilst we were unable to demonstrate expansion of the responses to TPRsPPLGL, there were still multifunctional responses demonstrated by day 7, however, overall the responses seen were at a similar level to those seen on day 0 (Fig. 4.7c). This leads us to question whether it is the degree of individual

response or the quality (i.e. multifunctional versus not) that is most important. It has previously been proposed that multifunctional T-cells could be pivotal in controlling infection for instance (Betts, Nason et al. 2006). A further illustration of this point is seen on day 7 where a similar total amount of responses were seen to GPRSAsLLSL; however, we were unable to demonstrate any of these T-cells producing IL-2, IFNγ and TNFα (i.e. no multifunctional response), on day 0, only very limited responses were seen.

Based on the phosphopeptide responses seen, can these T-cells recognise HLA matched tumour; and if they can, are they able to mount a response to it and perform effective killing? In order to answer this question, phosphopeptide-specific T-cell lines were generated from those donor T-cells which showed a good response to phosphopeptide stimulation, by rapid expansion with IL-2. Cells were then applied to hepatoblastoma tumour to identify if phosphopeptide pulsing can induce T-cell activation and cytokine release as a surrogate marker of this (we also tested response to LCL, but were mindful of the fact that the responses here may well be due to viral epitope recognition). A number cell lines were generated including: **TPR**sPPLGL, **RQD**sTPGKVFL, **RPW**sPAVSA and **ALD**sGASLLHL found in hepatoblastoma tumours; PTLD-derived phosphopeptide-specific T-cell lines **RPA**sAGAML, **RPQ**RA(ts)NVF and **RPR**sPRQNSI and finally **KLF**PDtPLAL, **KAF**sPVRSV and **SMTR**sPPRV which were found on both hepatoblastoma and PTLD. In addition, TiLs were rapidly expanded in the presence of IL-2 and their response compared to the phosphopeptide-specific T-cell lines (fig. 4.12).

Cells were assayed at day 1, 7 and 14 looking at IFNγ and TNFα release, and in the case of those phosphopeptides expressed on hepatoblastomas, compared with TiLs derived from these tumours. Unsurprisingly TiLs recognised tumour, however their activation was limited with relatively low levels of IFNγ and TNFα release. This is likely due to the line being rather heterogeneous and so a mixed population of cells targeting multiple different tumour surface

antigens. When assessing the phosphopeptide-specific responses, it is possible that cells do recognise target tumour, albeit at low levels, and pulsing with phosphopeptide does appear to enhance tumour recognition and T-cell activation. In particular, RPWsPAVSA had a good response at day 7 which was reproduced on day 14. The other phosphopeptide-specific cell lines also appear to recognise pulsed tumour, but the level of activation appears lower in comparison, with levels of cytokine release similar to that seen with the TiLs.

When assessing phosphopeptide responses in the PTLD-associated lines it was necessary to assess if recognition of LCL is tumour related or viral related. In order to do this, the T-cell line recognition of phosphatase treated LCLs was also assessed as the addition of phosphatase should remove the phosphopeptide response. Therefore, any cytokine release in response to the phosphatase-treated cells would be due to a viral response present in the T-cell line. We therefore identified RPAsAGAML, RPQRA(ts)NVF and SMTRsPPRV as being phosphopeptide-specific T-cell lines which were able to recognise tumour and a demonstrable reduction in cytokine release following treatment with phosphatase suggesting this was partly phosphopeptide driven.

In relation to functional avidity, it has previously been proposed that this could be intimately related to TCR affinity and its respective co-receptor interactions and thus there is a real risk of autoimmunity as it may be impossible to target epitopes present on healthy tissue,due to the presence of high affinity T-cells (Zhong, Malecek et al. 2013). Our primary endpoint is an appropriate immune response with resultant killing of target cells. The ideal T-cell would be one which can produce cytokine in response to target phosphopeptide of interest and perform effective killing. Therefore, to answer this question, a Europium release killing assay was set up, using two of the phosphopeptide-specific T-cell lines used previously: RPWsPAVSA (due to its high cytokine release and multifunctional response) and TPRsPPLGL (lower cytokine release and non-multifunctional response). Again these were compared to TiLs (fig. 4.12).

What is immediately obvious is addition of phosphopeptide unsurprisingly does induce better tumour recognition. The response seen in terms of killing is higher in RPWsPAVSA than TPRsPPLGL – which may add to the argument that high avidity cell lines are preferential in tumour killing.

This remains a preliminary study of small size, with data only available on 6 healthy donors assayed for responses to phosphopeptide epitopes identified on both paediatric liver tumours and LCLs. The results would be greatly strengthened by increasing subject numbers in both healthy donors and their relative response to phosphopeptide as well as greater numbers of tumours to be analysed. The overall aim of increasing subject numbers would be to allow for identification of any possible association between the immune responses to these phosphopeptides and patient survival. This may also allow for confirmation of the role played by phosphopeptide immunity in patients.

Chapter 5: T-CELL MANIPULATION – THE QUEST FOR IMMORTALITY

5.1. Introduction

Immunotherapies targeting tumour-specific antigens requires a ready supply of cells, and the study of *in vitro* cultured and manipulated T-cells are an exciting addition to the expanding field of cancer treatment. However, they are dogged by the issue that *ex vivo* culturing reduces the functionality of isolated T-cells (Nino, Kwan et al. 2016). Cryopreservation has been attempted but there have been concerns about possible effects on functionality (Coulie, Van den Eynde et al. 2014) and a lack of studies directly aimed at looking at this.

It has been observed that T-cells grown in culture long term (>6 weeks) gradually appear to lose specificity and functionality. In mixed T-cell cultures, CD4 T-cells begin to outgrow the peptide-specific CD8 T-cells over a period of weeks which ultimately results in loss of cell line specificity. T-cell lines that aren't able to produce cytokines towards peptide-pulsed target cells over time lose functionality. Anti-viral T-cells are the easiest to grow and can be cultured for few months as a cell line or longer as a clone but this can be very labour intensive with a lot of work required to achieve this. Compare this with generating and maintaining a B-cell line (LCL), which requires cell-splitting once or twice a week and a very basic media – which is clearly less labour intensive and cost effective, which is therefore the aim with T-cells.

Generating an immortal T-cell to allow further *in vitro* study would be of benefit to a number of therapies, but it would be desirable for it to have the ability to alter its makeup, such as transducing specific proteins into it therefore manipulating it to possess for instance an anti-tumour response. This becomes particularly important when considering the concept of T-cell exhaustion. This chapter therefore covers techniques designed to overcome the challenges posed by culturing T-cells long term and thus provide experimental models for the study of patterns of antigen recognition *in vitro*.

With this in mind, this chapter has sought to explore some of these experimental techniques in order to generate a limitless supply of T-cell derived reagents with which we can pursue the study of phosphoantigen expression. We selected 3 main technologies to explore further (i) **T-cell hybridomas** (ii) **Herpesvirus Saimiri T-cell transduction** and finally (iii) **Induced Pluripotent Stem cell (iPSc)** technology for differentiating T-cells into stem cells for *in vitro* expansion. Clearly these technologies vary in their complexity. There are also biological and ethical considerations which need to be taken into account also. Each will be explored in more detail in subsequent sections.

HVS viral transduction and T-cell hybridomas would generate a theoretical T-cell model which can be manipulated *in vitro* with the aim of exploring antigen expression. iPSc on the other hand have recently made their way into the clinical setting, and thus could be a potential clinical therapy (Kamao, Mandai et al. 2014).

5.1.1 Generation of hybridomas

Fusing cells to form a hybridoma was first conceived as an idea in the early 1970's. The initial method described by Kohler and Milstein in 1975 incorporated fusing B-cells secreting antibody of one specificity with a continuously growing immortal plasmacytoma – the product being a hybridoma which expresses immunoglobulin genes from both the normal antibody forming B-cell as well as the plasmacytoma (Kohler G and Milstein C, 1975). It inherits the potential for immortality and continuous growth from the plasmacytoma, and the antibody-secreting potential from the B-cell. 3 years later the same technique was used to form T-cell hybridomas by Taniguchi and Miller by fusing antigen specific T-cells to a T-cell tumour line (Miller J and Taniguchi M, 1978). This technique allows for the production of immortal T-cells with desired characteristics, to be studied *in vitro*, whilst using the fusion partner (often a tumour cell line) to maintain immortality. Previously, questions have been raised relating to

their genomic stability and potential loss of TCR complexes as well as IL-2 dependence and cytotoxic ability. Due to the low yield and potential sporadic incorporation of cells, this technology has fallen slightly out of favour however if this could be improved then it poses a viable option for immortalising T-cells.

The basis for the production of hybridomas gained Milstein the Nobel Prize for Physiology or Medicine in 1975. They described how B-cells were fused with myeloma cells by electrofusion. The myeloma cells were pre-selected so that they lacked the hypoxanthine-guanine phosphoribosyltransferase (HGPRT) gene, making them sensitive to the HAT (hypoxanthine-aminopterin-thymidine) medium. Fused cells were incubated in HAT medium for up to 2 weeks. Aminopterin is the key to this mechanism working as a form of selection as it blocks nucleotide synthesis. Therefore, unfused myeloma cells die, because they lack HGPRT. Likewise, unfused B-cells die as they naturally have a short life span in culture unless they are fused with the immortal cancer cell line. In this way, only the B-cell-myeloma hybrids survive, since they will possess a functional HGPRT gene from the B cells. These cells produce antibodies (courtesy of the B-cells) and are immortal (a property of tumour cells). This therefore poses the basis for the development of T-cell hybridomas, formed in a similar fashion, but to be investigated in this project, we plan to irradiate the fusion partners (immortal cancer cell lines), select them with 6-thioguanine, and then reselect with HAT medium. Of course no-one is actually going to insert a hybridoma in a clinical setting – this would never be ethically acceptable however it does form the basis of a hypothetical model which could at least demonstrate the effectiveness of T-cells in retaining desirable features and allow for further investigation of these cells in the experimental setting as well as potentially provide a limitless source of reagents with which we can pursue the study of phosphoantigen expression.

5.1.2 Viral transduction of human cells with Herpesvirus saimiri (HVS)

HVS is a gammaherpes virus which naturally infects the Squirrel Monkey. It is non-pathogenic in this natural host (virtually all Squirrel Monkeys are carriers) but has the ability to produce T-cell lymphomas in other New World Monkeys. It is distantly related to Epstein Barr virus which has also been shown to immortalise B-cell lines in a similar fashion. It was Biesinger et al in 1992 that first described the potential utility of HVS to transform human T-cells into stable culture lines. The virus persists as non-integrating episomes in human T-cells under restricted viral gene expression and without production of virus particles. The resultant transformed human T-cells are 'not permissive' to the virus, and reactivation of the virus has not so far been possible despite the efforts of a number of groups Worldwide. The T-cells which are immortalized in culture have the same phenotype as mature activated T-cells with normal CD4/CD8 expression. Also of benefit is that these cells will retain the parental cell's antigen specificity therefore leading to a potential use in immunotherapy due to this preservation of specificity. This model therefore again promises to be a useful basis for the study of antigen presentation and manipulation of cells in the experimental setting.

5.1.3 The use of stem cells

Stem cells are a generic precursor with the ability to become any tissue of the human body given the right growth conditions. It is this ability that makes them attractive as a potential mediator for the generation of a target cell *in vitro* which can be used to make a desired cellular model for research. Embryonic Stem cells have been traditionally used; however their use has met with poor press due to their origin. Nevertheless they have been used in spinal cord injury and diabetes with mixed success (Thomson 1998). Therefore there has been a lot of recent research into the generation of Induced Pluripotent Stem Cells or iPSc's. These are a stem cell

source created from adult somatic cells and their potential use is varied. The use of iPScs allows redifferentiation into effector cells that would then be infused.

The availability of highly-effective "off-the shelf" T-cells with specificity against a portfolio of targets would be a step-change for the field. The recent demonstration that induced pluripotent stem cells (iPScs) can be generated from human antigen-specific T-cell populations offers a new therapeutic strategy for the expansion and delivery of such cells (Vizcardo et al 2013, Nishimura et al 2013). Such an approach affords a potentially limitless supply of antigen-specific T-cells to target a range of diseases that could be delivered in a scalable manner to reach all patients in need. Recently, Masayo Takahashi at the RIKEN Centre for Developmental Biology, Japan has brought iPSc-derived cell therapies to the clinic, the results from which will hopefully validate the safety of using iPSc-derived cells in the clinical setting (Kumaro et al 2014) a potentially limitless supply of cells which have been shown to be both safe and stable *in vivo*. They can be patient specific and therefore could negate the need for immunosuppression for instance in the right setting.

These ''rejuvenated'' cells possessed antigen-specific killing activity and exhibited T-cell receptor gene-rearrangement patterns identical to those of the original patient T-cells. These studies therefore demonstrate an approach to cloning and expanding functional antigen-specific $CD8^+$ T-cells that might be applicable to cell-based therapy of cancer.

In order to understand why this is so important it is necessary to go back 8 years and see the first development of 'Induced Pluripotent Stem Cells' by Shinya Yamanaka and colleagues in Japan (Takahashi K and Yamanaka S, 2006). In the first few days after conception, an embryo consists of pluripotent cells which can develop into all cell types in the body. In 2006, Shinya Yamanaka found a new way to 'reprogramme' defined adult, specialized cells to turn them back into stem cells. He was able to do this following the observation of a number of different transcription factors which have been found in embryonic stem cells which were felt to

contribute to this cell's pluriotency (Nichols J et al 1998, Niwa H et al 2000, Avilion A et al 2003, Chambers I et al 2003, Cartwright P et al 2005). These factors comprised what we now refer to as the Yamanaka factors of Oct4, KLF4, C-Myc and Sox-2. These cells are described as being pluripotent – i.e. they have the ability to produce any type of cell *in vivo* - and are referred to as 'induced' as this isn't a natural process, but they have been exposed to specific factors in order to undergo this change. Only embryonic stem cells are naturally pluripotent but their origin and general availability makes their use untangible. Yamanaka's discovery meant that virtually any dividing cell of the body i.e. skin, blood, neurones can be turned into a pluripotent stem cell, and it went on to win him the Nobel Prize for Science and Technology in 2012.

In order for this to be a possibility they must retain no genomic footprint from the virus used to generate them. Initially retroviruses and subsequently lentiviruses were used in order to generate iPSc but these still retained a small genomic footprint (Takahashi and Yamanaka 2006, Takahashi, Tanabe et al. 2007, Nagata, Toyoda et al. 2009, Takahashi and Yamanaka 2013). The introduction of sendai virus as a vector to insert the Yamanaka factors into the target cell has provided a means by which cells can be differentiated without any genomic footprint being retained, fig 5.1. This is important when considering a system for clinical utility (Cao, Loh et al. 2012, Rao and Malik 2012, Malik and Rao 2013).

Virus	Pros	Cons
Retrovirus	Efficient Validated in multiple cell types	Even with excisable vector there is still a small footprint left behind
Lentivirus	Efficient Validated in multiple cell types	Even with excisable vector there is still a small footprint left behind
Sendai	Zero footprint Good efficiency Validated in multiple cell types Commercial kits available	Commercial kits are expensive If researcher generated then patent issues should be considered and is technically challenging

Fig. 5.1: Comparison of different viral technologies for generating iPSc, abridged from Malik and Rao, 2013.

Use of hIPSc technology to immortalise T-cells was described recently by two groups, in order to overcome T-cell exhaustion (Nishimura, Kaneko et al. 2013, Vizcardo, Masuda et al. 2013).

The observations made by both groups led to our hypothesis that hIPSc may be used to imortalise phosphopeptide-specific T-cells.

5.1.4 T-cell exhaustion As a result of chronic infection or malignancy, a state of so called 'T-cell exhaustion' may occur. This is characterised by T-cell dysfunction, loss of effector function and the expression of inhibitory factors. This inevitably leads to a reduction in efficient control of infection or malignancy. EJ Wherry and subsequently his group proposed a model of hierarchical T-cell exhaustion (fig. 5.2), showing the gradual shift from highly polyfunctional $CD8^+$ T-cells with little apoptosis, to a complete loss of function and increased apoptosis (Wherry 2011, Wherry and Kurachi 2015). Although this is described in virus infection, the same could be applied to how T-cells lose functional recognition of tumours. Therefore, introducing a technique for propagating T-cells without loss of function *in vitro* would be beneficial.

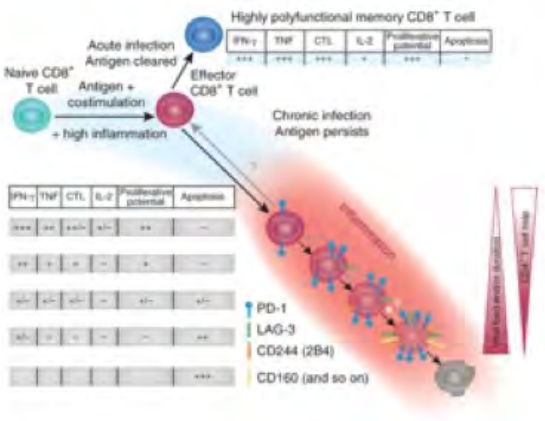

Fig. 5.2: The effect of chronic infection of T-cell functionality – a model for T-cell exhaustion. Here it is demonstrated that during initial infection, naive T cells are primed by antigen, costimulation and inflammation resulting in differentiation into effector T cells. Clearance of infection and antigen results in a subset of these T cells to further differentiate into highly polyfunctional memory T cells. During chronic infection, infection persists after the effector phase. Cells progress through stages of dysfunction, losing effector functions and other properties in a hierarchical manner. There is an increase in the amount and diversity of inhibitory receptors expressed. Ultimately, if the severity and/or duration of the infection is high and/or prolonged, virus-specific T cells can be completely eliminated, leading to loss of virus-specific T cell responses. This model can also be applied to how T-cells recognise tumour (Wherry 2011).

This chapter therefore explores a number of techniques from early biotechnologies such as T-cell hybridomas and viral transduction with herpesvirus saimiri to the use of more novel technologies such as generation of hIPSc using sendai virus. All are predicted and have been shown previously to have the same desired end point and could all potentially be used to generate a stable T-cell line (Kohler and Milstein 1975, Taniguchi and Miller 1978, Grassmann, Biesinger et al. 1990, Biesinger, Mullerfleckenstein et al. 1992, Nick, Fickenscher et al. 1993, Meinl, Hohlfeld et al. 1995, Rao and Malik 2012, Vizcardo, Masuda et al. 2013, Nishimura, Kato et al. 2014). Each of these techniques will be described in subsequent sections in more detail.

5.2 T-cell hybridomas

3 years after B-cell hybridoma technology was first described a similar technique was used to form T-cell hybridomas by Taniguchi and Miller by fusing antigen-specific T-cells to a T-cell tumour line (Taniguchi and Miller 1978). Based around the same technology a fusion partner cell (immortal tumour line) is fused with a T-cell of choice to generate an immortal T-cell which possess characteristics of interest, which is as was seen in B-cell hybridomas, fully selectable.

This in turn does raise important considerations, such as genomic instability and potential loss of TCR complexes as well as IL-2 dependence and cytotoxic ability due to issues similar to those encountered with B-cell hybridomas relating to chromosome loss and mutations (Castillo, Mullen et al. 1994).

The theory behind B-cell hybridomas is similar to that seen in T-cell hybridomas. Cells are engineered to possess characteristics of interest which are selectable by adding selection agents to growth media, with the resultant pure culture of hybridoma cells. The pathway involved in this technology relates to the gene hypoxanthine phosphoribosyltransferase 1 (HGPRT or

HPRT1), which codes for a transferase enzyme that catalyzes conversion of hypoxanthine to inosine monophosphate (IMP) and guanine to guanosine monophosphate (GMP), with resultant transfer of 5-phosphoribosyl group from 5-phosphoribosyl 1-pyrophosphate (PRPP) onto the purine. HGPRT plays a central role in the purine salvage pathway. HGPRTase salvages purines from degraded DNA, reintroducing them into purine synthetic pathways. Hybridomas are immortal, $HGPRT^+$ cells resulting from fusion of mortal, $HGPRT^+$ plasma cells and immortal, $HGPRT^-$ myeloma cells. They are created to produce monoclonal antibodies in biotechnology. Hypoxanthine-aminopterin-thymidine (HAT) medium inhibits *de novo* synthesis of nucleic acids, leading to death of myeloma cells that cannot switch over to the salvage pathway, due to lack of HRPT1. The plasma cells in the culture eventually die as a result of cellular senesence, leaving a pure growth of hybridoma cells. HAT relies on the combination of aminopterin, (folate metabolism inhibitor), with hypoxanthine (a purine derivative) and thymidine (a deoxynucleoside) both of which are intermediates in DNA synthesis. The role of Aminopterin is to block DNA *de novo* synthesis, and therefore prevent cell division. Hypoxanthine and thymidine work by providing the cells with a 'rescue' pathway, producing the necessary building blocks for bypassing the block placed by aminopterin and is hence termed the 'salvage pathway'. This is only possible if the correct enzymes are present which in turn is only possible if the gene or genes coding for them is in a functional state (fig. 5.3).

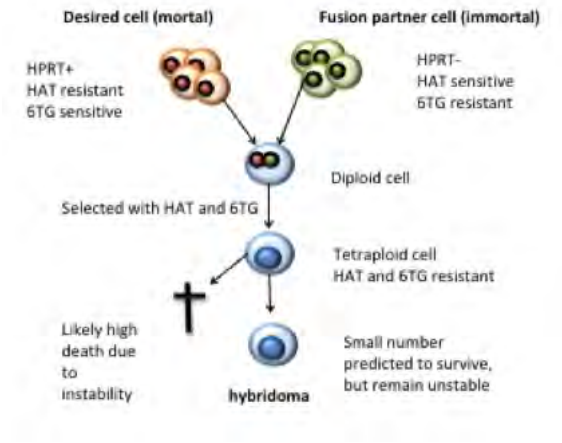

Fig. 5.3: Generation of T-cell hybridoma by fusion of immortal fusion partner line with desired target T-cell. Selection with HAT-supplemented media and 6TG (6-thioguanine - used to remove any unfused T-cells as well as any fusion partner cells which do not possess the HPRT1 gene rearrangement) will remove all unfused cells, resulting in a pure culture of tetraploid cells with desired characteristics. The resultant tetraploid cell is unstable however leading to high rates of cell death with very few cells reaching the hybridoma stage and even fewer that remain stable, with large numbers undergoing apoptosis as a result of genomic instability.

One example of this is the enzyme dihydrofolate reductase, who's main role is the reduction of dihydrofolate to tetrahydrofolate (THF). It is this enzyme which aminopterin blocks.

This has a knock on effect on further downstream enzymes. For example in the absence of THF, deoxyuridine monophosphate (dUMP) cannot be converted to thymidine monophosphate (TMP) via the precursor Thymidylate synthase. One function of dUMP is to be converted to thymidine triphosphate (TTP), and thus be used to make a nucleotide precursor and hence is a DNA building block. However if dUMP is not converted then DNA synthesis is effectively blocked. The only way of overcoming this is if an alternative TMP source is available. One such source is found in HAT medium, as thymidine present can be effectively used, and is readily absorbed, and can be easily converted to TMP by thymidine kinase.

Another role for THF is in the synthesis of IMP. When this is blocked as described above and alternative route of production is by accessing hypoxanthine-guanine phosphoribosyltransferase (HGPRT). Hypoxanthine is absorbed from the medium with PRPP. This leads to production of pyrophosphate, which via the salvage pathways is able to produce IMP (fig.5.4a). This therefore demonstrates the use of HAT medium for cell culture as a form

of artificial selection in cells containing functional forms of the enzymes TK and HGPRT. Addition of selection agents allows death of cells possessing the genes of interest (i.e. the unfused cells) and results in a pure culture of cells with desired characteristics - the tetraploid cells and development of hybridomas.

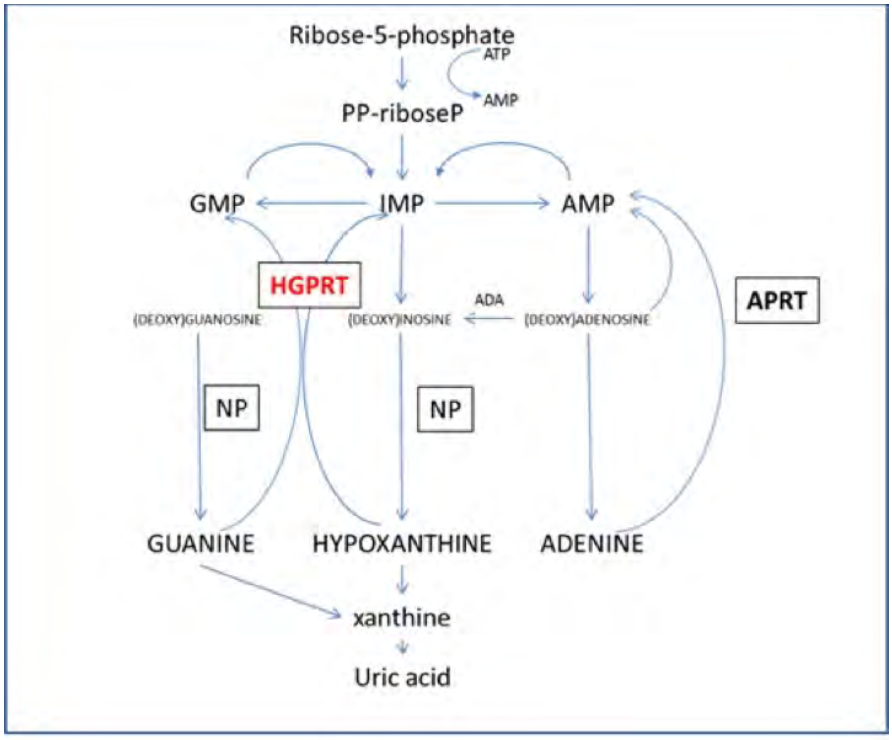

Fig. 5.4a: HGPRT biochemical pathway. HGPRT is a transferase encoded by HPRT1 gene converting hypoxanthine to inosine-monophosphate and guanine to guanosine monophosphate. This transfers the 5-phosphoribosyl group from 5-phosphoribosyl 1-pyrophosphate (PRPP) to the purine. It plays a central role in purine salvage pathway.

In order to generate hybridomas, fused cells are incubated in HAT medium. Aminopterin, as described above leads to blocking of the *de novo* pathway. As a result of this action, any unfused fusion partner cells will succumb due to inability to produce nucleotides needed for DNA synthesis via either the de novo or salvage pathways – fig. 5.4b. Any unfused T-cells of choice will likewise be lost as a result of cellular senescence. As a result, only hybridoma cells (i.e. those that contain characteristics of both the fusion partner and T-cell of choice will survive selection with HAT media as it is only these cells which possess the appropriate

'machinery' to continue to survive in these conditions. This forms the basis of production of a T-cell hybridoma.

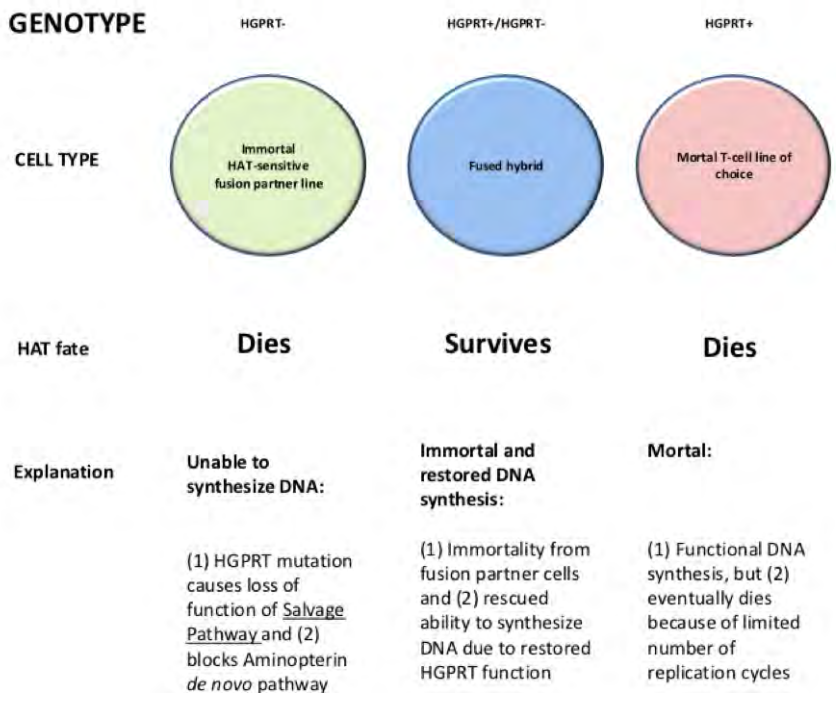

Fig. 5.4b: Demonstration of effect of HAT selection on hybridoma cells. By exploiting the salvage and *de novo* pathways, the only cells to survive possess intact HGPRT (from target cell of interest) and immortality from tumour cell.

Due to low yield and potential sporadic incorporation of cells, this technology has largely fallen out of favour. However, if this could be improved then it poses a viable option for immortalising T-cells for use as an experimental model to assess patterns of antigen expression and probe their expression on both normal tissues and transformed cell types.

5.2.1 Results: Basic fusion protocol

A number of T-cell tumour lines were selected as potential fusion partners including Jurkat (2 lines were available, named 'JKA-NLV' obtained from Dr G Bendle, Cancer Sciences, University of Birmingham – a retrovirus-transfected jurkat line with insertion of a T-cell receptor which recognises the viral peptide sequence for the CMV peptide NLV and 'JKA-GFP' obtained from Dr D Millar, School of Infection and Immunity, University of Birmingham – a lentiviral transfected line with addition of GFP expression and puromycin resistance), HPB-ALL (DSMZ, Germany), SKW-3 (DSMZ, Germany), MOTN-1 (DSMZ, Germany) and CEM

(ATCC, USA). Cells were irradiated and selected as described in chapter 2. Irradiation serves to induce a mutation in the HPRT gene, leading to resistance to 6-thioguanine (6TG), allowing the immortal fusion partner cells to be selectable with 3 cell lines emerging as viable fusion partners (JKA-GFP, JKA-NLV and CEM) – fig. 5.5 shows the selection of JKA-NLV.

Fig. 5.5: Demonstration of 6TG resistance in cell line 'JKA-NLV'. (A) Cells were treated with 6TG and photographed on day 7, showing death of cells following administration of 6TG at 10µM or 20µM. (B) These cells were incubated for a further week showing that despite death on day 7 they had recovered by day 14). (C) Representative flow cytometry plot which revealed similar results with large numbers of cells dying at higher concentrations of 6TG at day 7, with recovery by D14 - dead Jurkats denoted as JKA-D and alive jurkats denoted JKA-A. This is represented graphically in (D).

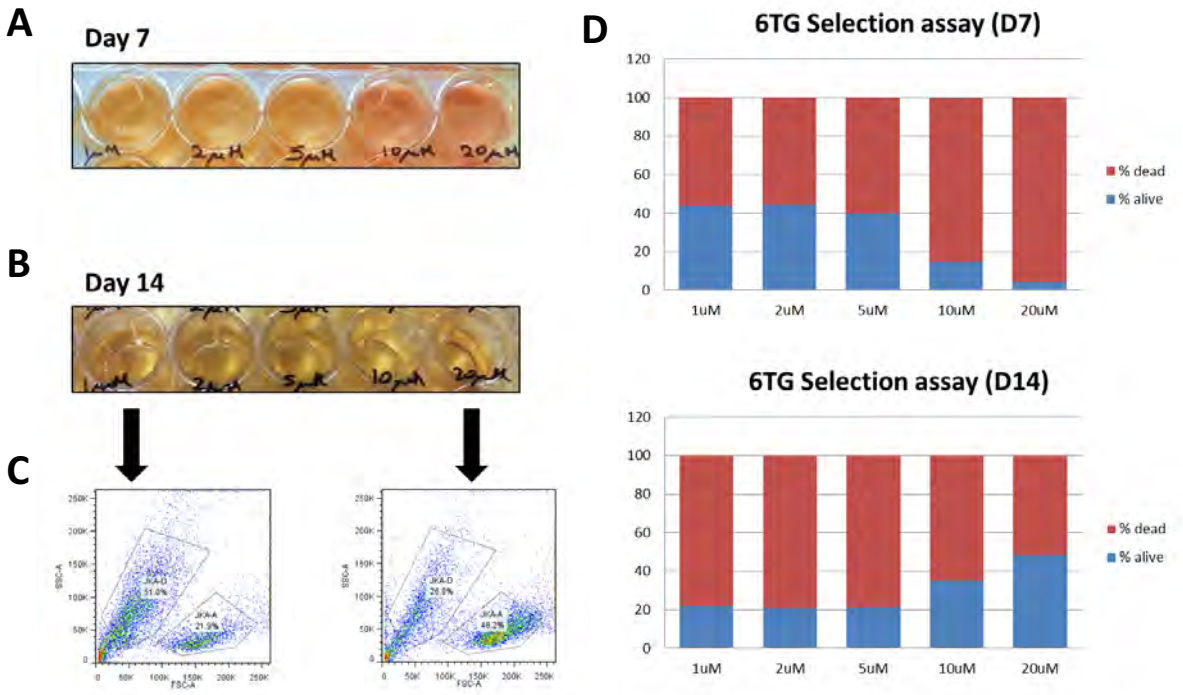

Initially there was death observed amongst cells treated with higher concentrations of 6TG but these cells were maintained in culture, and resistant cells emerged and were allowed to expand and form a stable resistant cell line, whereas cells treated with lower doses of 6TG initially had high viability but as time progressed cells died – suggesting lower doses of 6TG were sub optimal for selecting a pure line – and thus a dose of 20µM 6TG was selected as the optimum dose for selecting suitable fusion partners. It was observed that the lines HPB-ALL and SKW-

3 did not survive after irradiation, and it has therefore been proposed that these tumours are radiosensitive (Fig. 5.6). They were therefore discounted from further input at this stage.

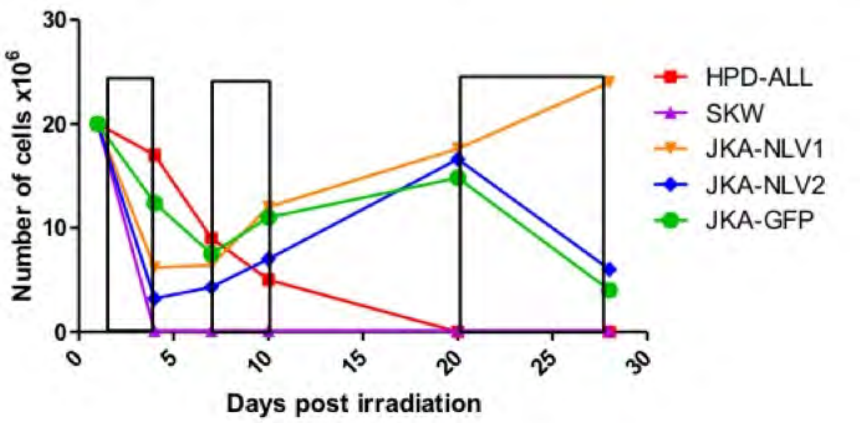

Fig. 5.6: Growth kinetics following selection. T-cell leukaemia lines were irradiated using standard protocols (described in chapter 2). Following this they were pulsed with 20μM 6TG in order to obtain a pure growth of cells resistant to 6TG which can be used as a fusion partner for hybridoma formation. Black rectangles represent times when cells were placed on selection (with 6TG). Cell lines are all T-cell leukaemias. 'JKA-NLV1' and 'JKA-NLV2' are two Jurkat lines which were retrovirally transfected by Dr G Bendle to include the TCR for the CMV-peptide (NLV). 'JKA-GFP' was transfected by Dr D Millar to have a GFP tag. In this example SKW died shortly after irradiation suggesting it is radiosensitive. HPD-ALL also appears to be radiosensitive with a gradual decline in cell numbers. JKA-NLV2 and JKA-GFP both initially appear to expand following 6TG selection, however numbers fell again at day 20. In this experiment the only line which is 6TG resistant is JKA-NLV1.

5.2.2 Efficiency evaluation

In order to evaluate hybridoma formation efficiency, it was necessary to test standard protocols as originally proposed by Taniguchi and Miller. Initial results were not promising and therefore the basic technique was modified as described in chapter 2. A Jurkat fusion partner line which had been previously modified by Dr Millar to contain a GFP tag (generated as described in chapter 2) was mixed with a viral-specific NLV-T cell line which was NLV-tetramer stained. Cells were FACS analysed on day 3 (fig. 5.7). Controls included each cell line (target cell line and partner cell line) on its own, and a mixture of both lines without the addition of polyethylene glycol (PEG). The hybridoma was formed by mixing $1x10^7$ Jurkat (GFP) with an equal number of NLV-peptide specific T-cells, and PEG was used as the fusogen (as described previously in chapter 2). FACS analysis of the cells was performed on day 3 and

demonstrated 98.9% GFP positivity of the Jurkat and 94.7% NLV-tetramer positivity of the T-cells (Fig. 5.7A, B). Both these controls had negligible double positive cells. The hybridoma however showed 54.2% double positivity (shown by red circle) which represents the population of interest and potential hybridomas. Jurkats are also known to be $CD8^-$, and the T-cell line is 94.4% $CD8^+$. The resultant hybridomas would be expected to be $CD8^+$ and GFP^+ (fig. 5.7C). Although hybridomas and T-cells would both be $CD8^+$ and NLV-$tetramer^+$, we can see a clear difference between the two when seen on FACS with a population of cells which may well represent true hybridomas (blue circle) and a separate mixed population of cells spanning $tetramer^{+/-}$ and $CD8^{+/-}$ but not both and therefore these cells are most likely the separate cell groups which are unfused – and therefore should be lost following selection. Of note the NLV-T cells were a cell line i.e. heterogeneous and not clone derived – hence some cells are $tetramer^+$ but $CD8^-$. These cells were stained for GFP/CD8 also to see if a hybridoma population could be identified which were GFP^+CD8^+.

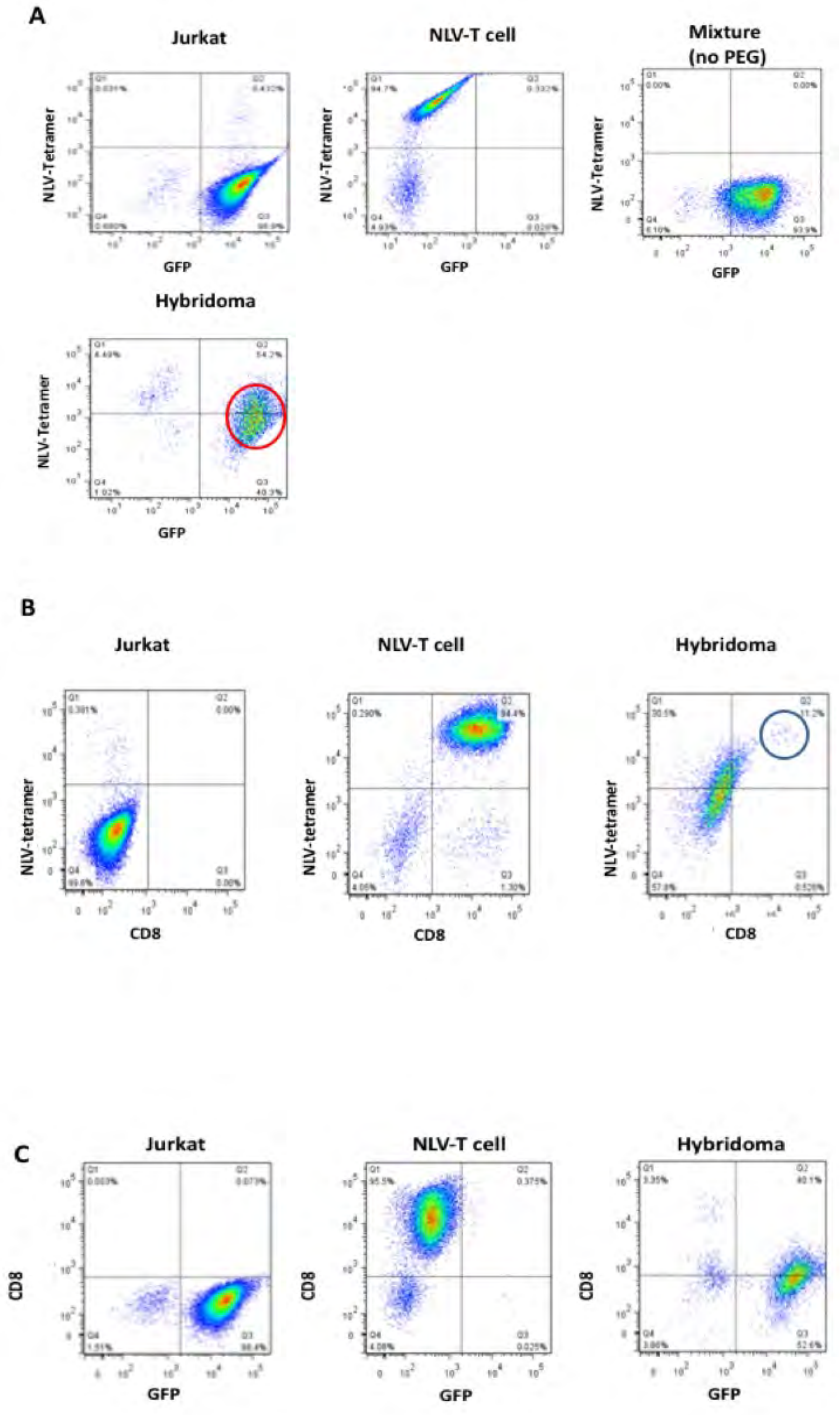

Fig. 5.7: Hybridoma formation using PEG. NLV-peptide specific T-cells (denoted NLV-T cell) were fused with GFP-tagged Jurkat cells using standard protocols as described in chapter 2. Following this on Day 3 cells were analysed using FACS. (A) represents unselected Jurkats, T-cells, mix of cells (no PEG) and 'hybridomas' looking at NLV-tetramer positivity (trait of T-cell) and GFP positivity (trait of Jurkat). There is clearly a shift in population size (red circle) which may represent hybridoma formation. (B) shows FACS staining for tetramer positivity (from T-cell) and CD8 positivity (from T-cell). There is a discreet population of DP cells (blue circle) which may represent hybridoma cells. (C) Shows staining of the same cells for CD8 and GFP demonstrating a shift in the population of cells upwards which may be representative of DP and hybridoma formation as there appears to be CD8/GFP + cells. Selection will help to delineate this further as this should remove any non-fused cells.

Fig 5.7c demonstrates clear differences between the control cell lines and the 'hybridomas'. However it is not clear if these cells truly are hybridomas. They would appear to be GFP positive and at least some of this population may be $CD8^{+}$. But this is by no means clear cut. The only way to actually identify what cells may be included in this population is to put them onto selection with HAT and 6TG.

Although initially following selection with HAT there was a population of cells alive in the 'hybridoma' plate, these cells were considered unstable, failed to expand and eventually after 12 weeks of culture died (fig. 5.8). It should be noted that cells were pulsed on day 3 and then every two weeks for 3 days with HAT in order to remove any unfused Jurkats. Unfused T-cells naturally died without selection, proposed to be due to senescence.

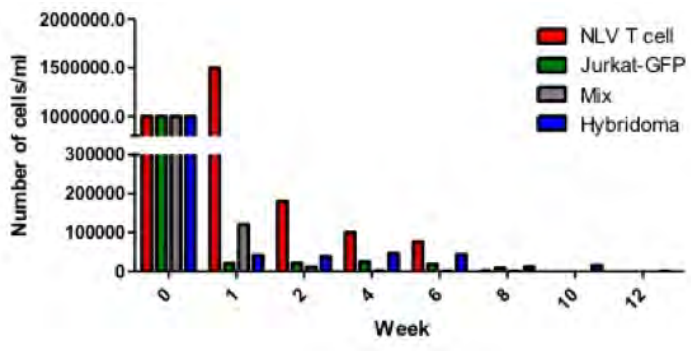

Fig. 5.8: Absolute cell numbers following selection with HAT. Following standard fusion protocols, cells were counted weekly using glass coulter counter and microscope. Week 0 is the day the cells were initially set up at $1x10^{6}$/ml. Cells were placed on HAT selection (20μM) on day 3 and counted initially after 1 week then at 2 weekly intervals. The jurkat line used 'Jurkat-GFP' is HAT sensitive and therefore in control showed a rapid decrease in viability at week 1 which never really recovered. The T-cell line 'NLV T-cell' alone being HAT-resistant survived in culture for 6 weeks (however gradually declined in number from week 2 due to natural cell death. The cell mixture 'mix' (which comprised the jurkat line and T-cell line being mixed in equal numbers) likewise rapidly decreased in number, but when compared to FACS plot in fig 5.7c, it appears these cells were largely Jurkat in origin, so therefore following HAT selection unsurprisingly these cells succumbed. 'Hybridoma' cells appeared to survive until week 10 but cells did not expand in cell number.

We wondered whether lack of cell expansion was due to chromosome instability by virtue of the hybridoma formation process. Clearly a cell line which cannot expand has no potential for

clinical utility. We therefore sought to improve the technique to make it both more efficient and scalable.

5.2.3 Improving fusion efficiency

Following the observation that a number of authors used dimethyl sulfoxide (DMSO) in addition to PEG we hypothesised this may improve fusion efficiency. Although toxic, DMSO at low concentrations has been shown to be fusogenic over prolonged periods of time (Destgroth and Scheidegger 1980, Klebe and Mancuso 1981, Klebe and Mancuso 1982, Hundhausen, Laus et al. 1992). In order to test this hypothesis we chose to fuse PBMC's which had been stained using CellTrace violet (CTV), with a Jurkat line which had GFP tag 'Jurkat-GFP'. We made a direct comparison between PEG and PEG/DMSO in order to see if fusion potential was improved (fig. 5.9).

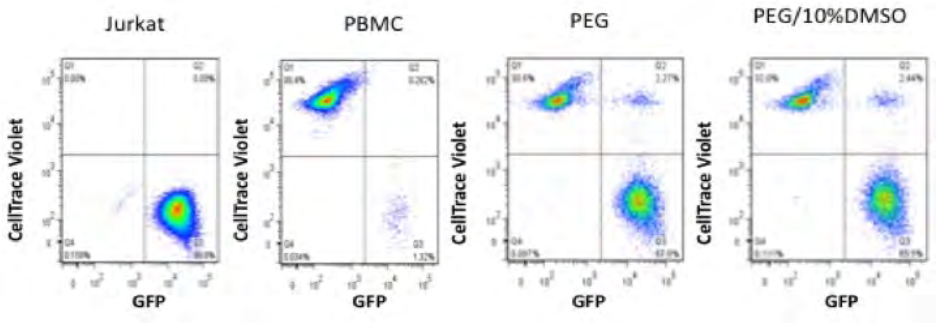

Fig. 5.9: Comparison of PEG vs PEG + 10% DMSO as fusogen in creation of hybridomas. Equal numbers of PBMCs (stained with CellTrace-violet were mixed with Jurkat-GFP using standard protocols as described in chapter 2. PEG alone was directly compared with the combination of PEG/DMSO. 2.27% cells were DP when receiving PEG alone vs 2.44% of cells when receiving PEG/DMSO (NS). Of note there is a small population of PBMCs that were naturally GFP positive (1.32%). These FACS plots were representative of 3 repetitions of this experiment, done in duplicate on each occasion.

These experiments (pre-selection) showed no difference between both fusogen combinations. This was repeated with more cells (data not shown) however the overall fusion equivalents remained the same, therefore we concluded there was no difference between using PEG alone versus PEG combined with DMSO. We wondered if there was any significant effect on these

cells following selection. In order to test this; cells were set up in duplicate directly comparing those hybrids fused using PEG versus those fused using PEG/DMSO. Each week cells were counted using Coulter counter and absolute cell numbers of live cells were recorded. In this case we have demonstrated a similar effect on cell number compared to the initial experiment assessing overall efficacy of fusing cells (fig. 5.8), thus validating these initial data. Using a two-tailed paired-t test to compare PEG with DMSO fused hybrids; there is no significant difference between both groups. We did note an initial drop off in cell number at 1 week following fusion and this may be as a result of DMSO toxicity (fig. 5.10). We therefore concluded there was no advantage to using DMSO + PEG over PEG alone.

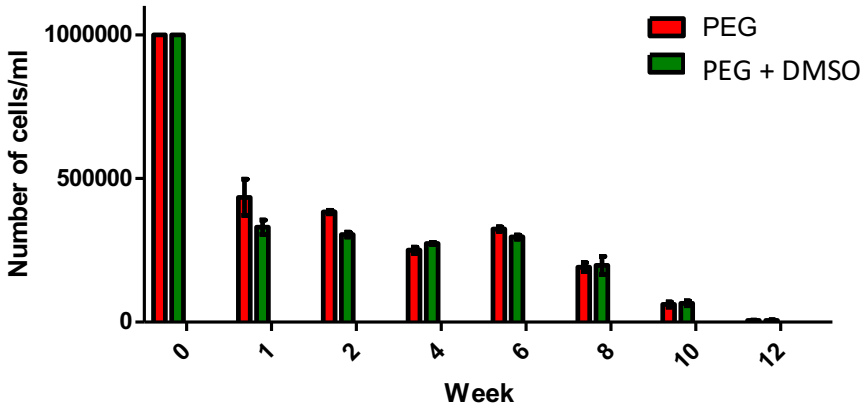

Fig. 5.10: Absolute cell numbers following fusion of PBMC's and Jurkats using DMSO + PEG or PEG alone and subsequent selection with HAT. Following standard fusion protocols, cells were counted weekly using glass coulter counter and microscope. Week 0 is the day the cells were initially set up at $1x10^6$/ml. Cells were placed on HAT selection (20µM) on day 3 and counted initially after 1 week then at 2 weekly intervals. Jurkat-GFP line is a HAT-sensitive Jurkat line therefore unfused cells would be lost following selection. PBMC's which are unfused would naturally decline in the absence of IL2.

5.2.4 Lentiviral transduction of the fusion partner cell lines was not feasible

Having established that the basic fusion protocol is largely inefficient, and that fused cells are unstable, we proposed inserting an anti-apoptotic gene (BCL2) into the fusion partner cell lines. We wondered if this would increase longevity of the resultant hybridoma cell line and prevent premature cell death thus improving the long term culture of hybridoma cells (fig. 5.11).

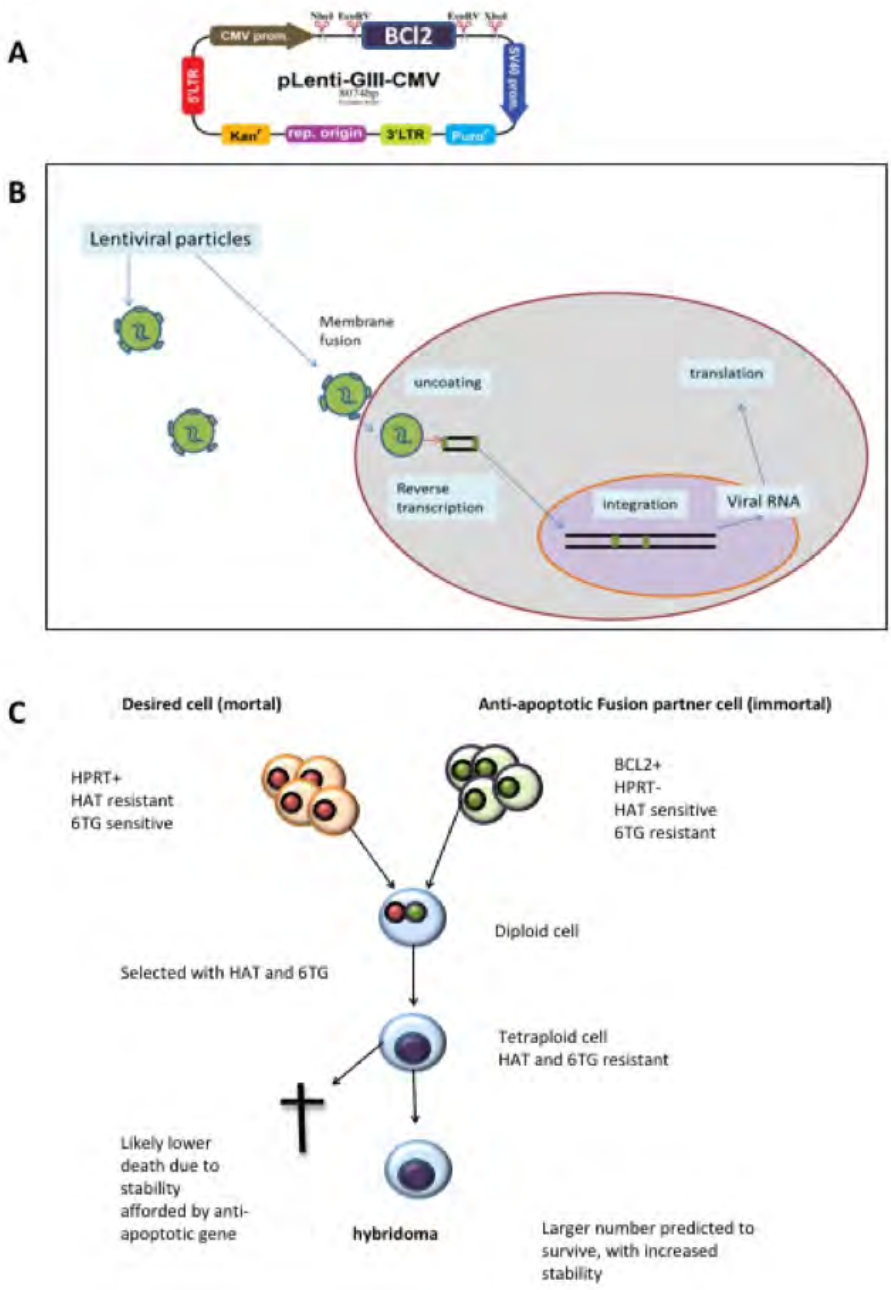

Fig. 5.11: Proposed improvement in hybridoma formation following insertion of anti-apoptotic gene BCl2 (A) viral cassette containing BCL2 gene and puromycin resistance (B) using a lentivirus to incorporate the BCL2 gene leads to incorporation of this DNA into fusion partner line, with (C) resultant proposal of reduced cell death. Insertion of this cassette will also result in puromycin resistance of the fusion partner which would be useful for selection purposes.

The cell lines transduced with BCL2 gene were the fusion partner lines: Jurkat-NLV (derived from the Jurkat line obtained from Dr Bendle which had already been transfected to contain a TCR specific for the CMV peptide NLV) and 'CEM' (derived from the commercially sourced

CEM line, ATCC, USA). Unfortunately, 'Jurkat-GFP' could not be transduced as these cells were already puromycin resistant by virtue of their generation. Standard techniques were used to package the virus ready for transduction and cells were transduced with virus in the presence of polybrene. Puromycin selection was used to isolate cells which had been transduced (a puromycin kill-curve was initially generated for each cell line). Following this cells were pulsed with 6TG to obtain a pure line of 6TG resistant, puromycin resistant (and therefore $BCL2^{+}$) cells. Unfortunately these cells did not remain viable despite multiple attempts (data not shown). We proposed that this may be due to a number of reasons. 1) 'Jurkat-NLV' cells had already been genetically modified to include the TCR for the CMV-peptide NLV and therefore further modification makes the cell too unstable. 2) Irradiation of the cells in order to generate a line which is 6TG resistant is in itself mutagenic and therefore for the same reason these cells were non-viable. In order to test these theories we transduced standard, non-irradiated (and therefore non 6TG resistant) Jurkat cells and CEM cells. These were selected with puromycin and a stable cell line was achieved. However following irradiation neither cell line survived – suggesting that cell viability is dramatically reduced the more 'genetic insults' they receive. We concluded that lentiviral transduction of the fusion partner cell lines was not feasible and therefore did not pursue this avenue further.

5.2.5 Addition of mitogens to growth media was not advantageous

Caspases are involved in apoptosis and cell death and therefore were a target to be investigated further with regards to preventing cell death in hybridoma cells and indeed T-cells in general. Previous work done in this lab (by Ms Lora Steadman) demonstrated there are a number of mitogens capable of supporting cell growth and increasing cell expansion when compared to standard media (RPMI + 10% FCS) – Fig. 5.12a, b.

This preliminary work suggested that addition of ZVAD, Calcitriol and Betulinic acid all appear to improve cell expansion and viability compared to control medias when tested in

A

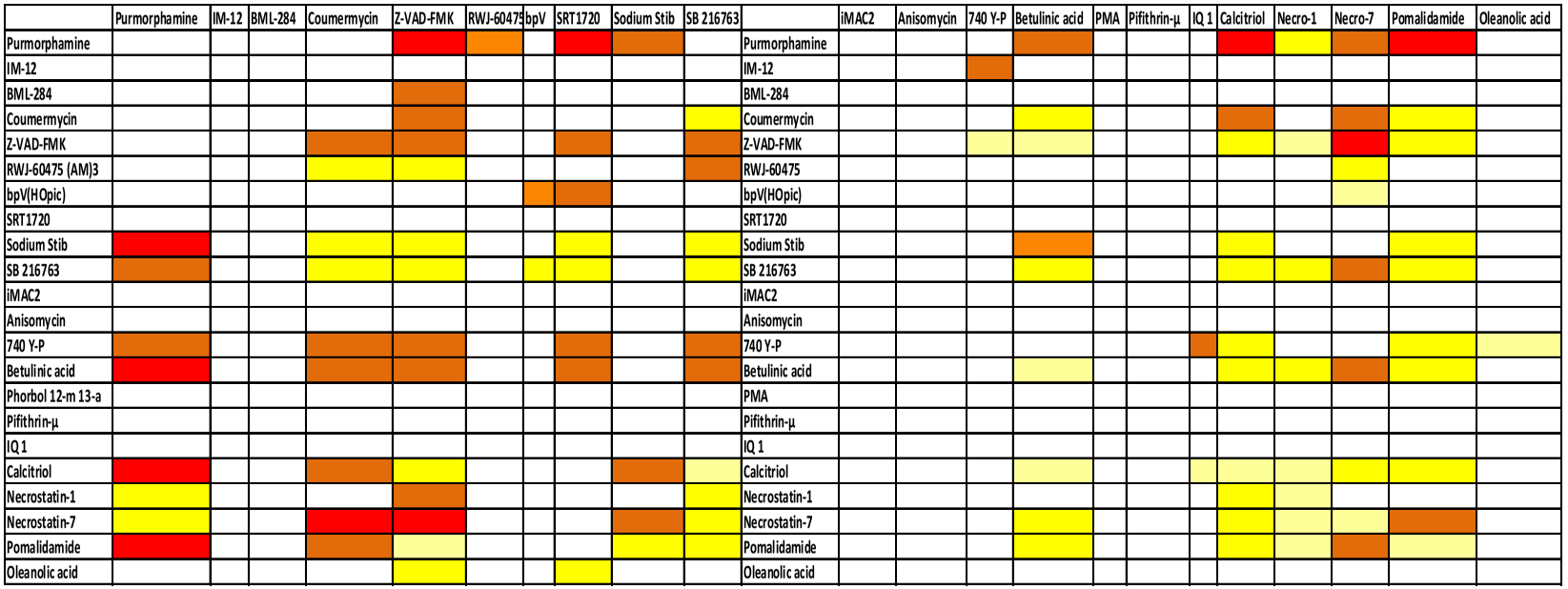

B

Compound	Pathway	Experimental Combinatorial "Hits"
Z-VAD-FMK (Active Alone)	Apoptosis	12
740 Y-P	PI 3-kinase	7
Betulinic acid (Active alone)	NF-kB	8
Calcitriol	VDR	5
Sodium Stibogluconate	SHP-1 Inhibitor	5
SB 216763	GSK-3β inhibitor	6
SRT1720	Apoptosis	5
Puromorphamine		14

Fig. 5.12: 22 mitogens were selected as potential effectors of improved cell growth and expansion when compared to control (RPMI 10% FCS). (A) Jurkat cells were selected as a target line and cells were set up in a 96-well plate with mitogens added at standard concentrations – see appendix). Single mitogens and combinations thereof were assessed. Cells were grown for 2 weeks, after which wells were scored based on the size of the cell pellet – Red being biggest, orange medium sized, yellow being the same as control. Smaller pellets or dead cells are shown as white. (B) The top mitogen performers were further assessed with regards to pathway they're involved in and how many times they performed better than control in (A).

Jurkat cells and therefore we proposed that this may help to expand hybridomas long term also (as these are a fusion of T-cells and Jurkat cells). In order to assess whether mitogens can improve cell growth Jurkat-GFP were fused with an NLV-T cell line. We predicted that the addition of mitogens would afford greater stability to the hybridomas based on the data seen in the Jurkat experiments. We chose to assess the same concentrations as used previously in the Jurkat experiment (fig. 5.12) and also a 2x concentration, to see if doubling the concentration of mitogen could improve cell viability. Cells were stained for NLV-tetramer (tet), CD8 and GFP (fig. 5.13). 'Hybridoma' cells – i.e. $tet^{+}GFP^{+}$ were greater in the RPMI/10% FCS control media across all wells. The prevailing cell line in each is also Jurkat-GFP. We concluded from this that the mitogens were preferentially supporting Jurkat growth but may not be supporting hybridoma growth. We also observed that betulinic acid appears to be toxic to all cells. It is not immediately clear why this should be the case when initial experiments did not show this, however we wondered if this may be as a result of mutation afforded by transduction of these Jurkat cells to be GFP^{+}.

Fig. 5.13: Comparison of media supplemented with mitogens. A Jurkat fusion partner 'Jurkat-GFP' so called as it has been modified to have a GFP tag, was fused with a T-cell line known to be NLV-tetramer positive i.e. CMV-peptide containing, termed 'NLV-T cell' using standard protocols as described in chapter 2 using PEG. Immediately following fusion cells were resuspended in either control media (RPMI/10% FCS) or RPMI/10% FCS media supplemented with mitogen. Cells were allowed to rest for 3 days in incubator 5% CO_2 at 37c and then analysed using flow cytometry following staining for NLV-tetramer and CD8. (A) P1 is the % target population. These cells are considered alive. (B) Shows staining for tetramer and GFP. Hybridoma cells are considered to be the DP population in quadrant 2.

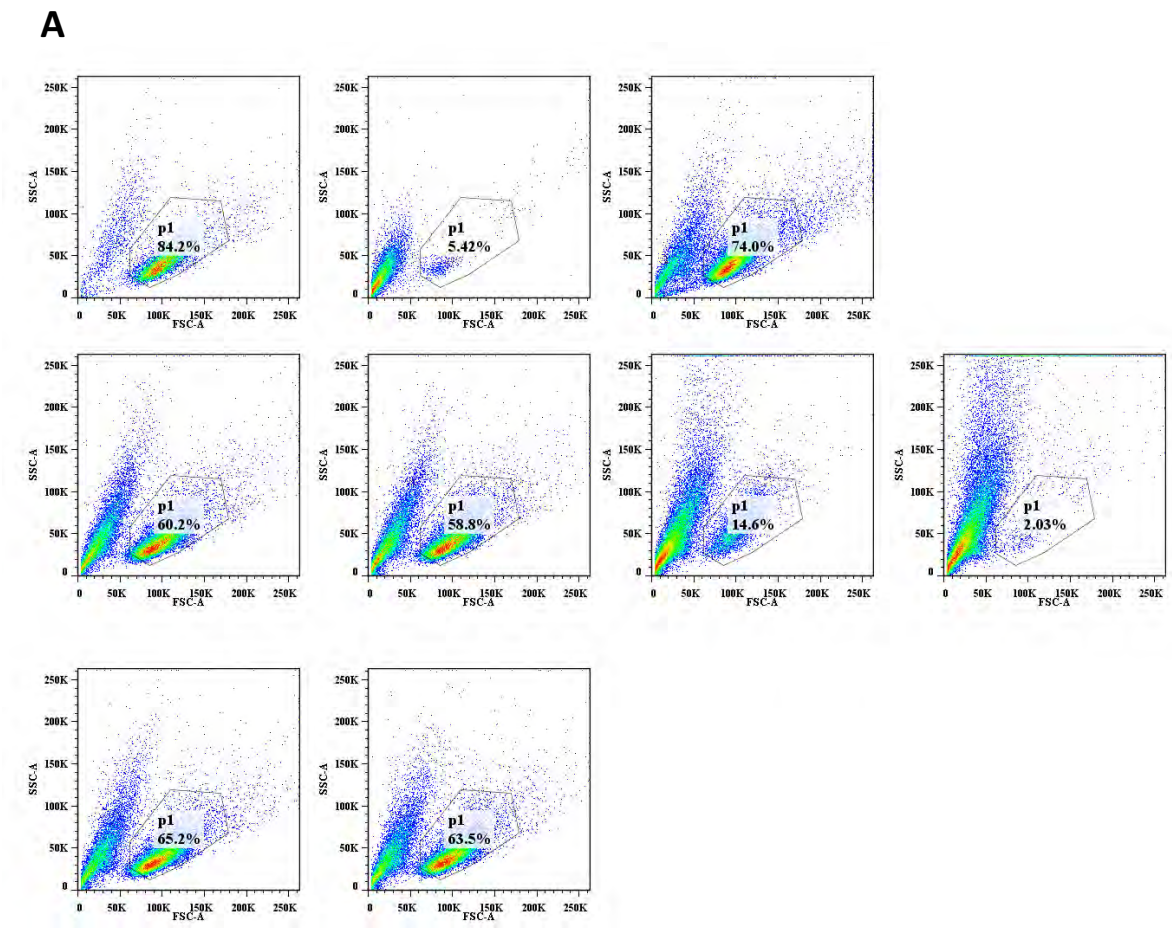

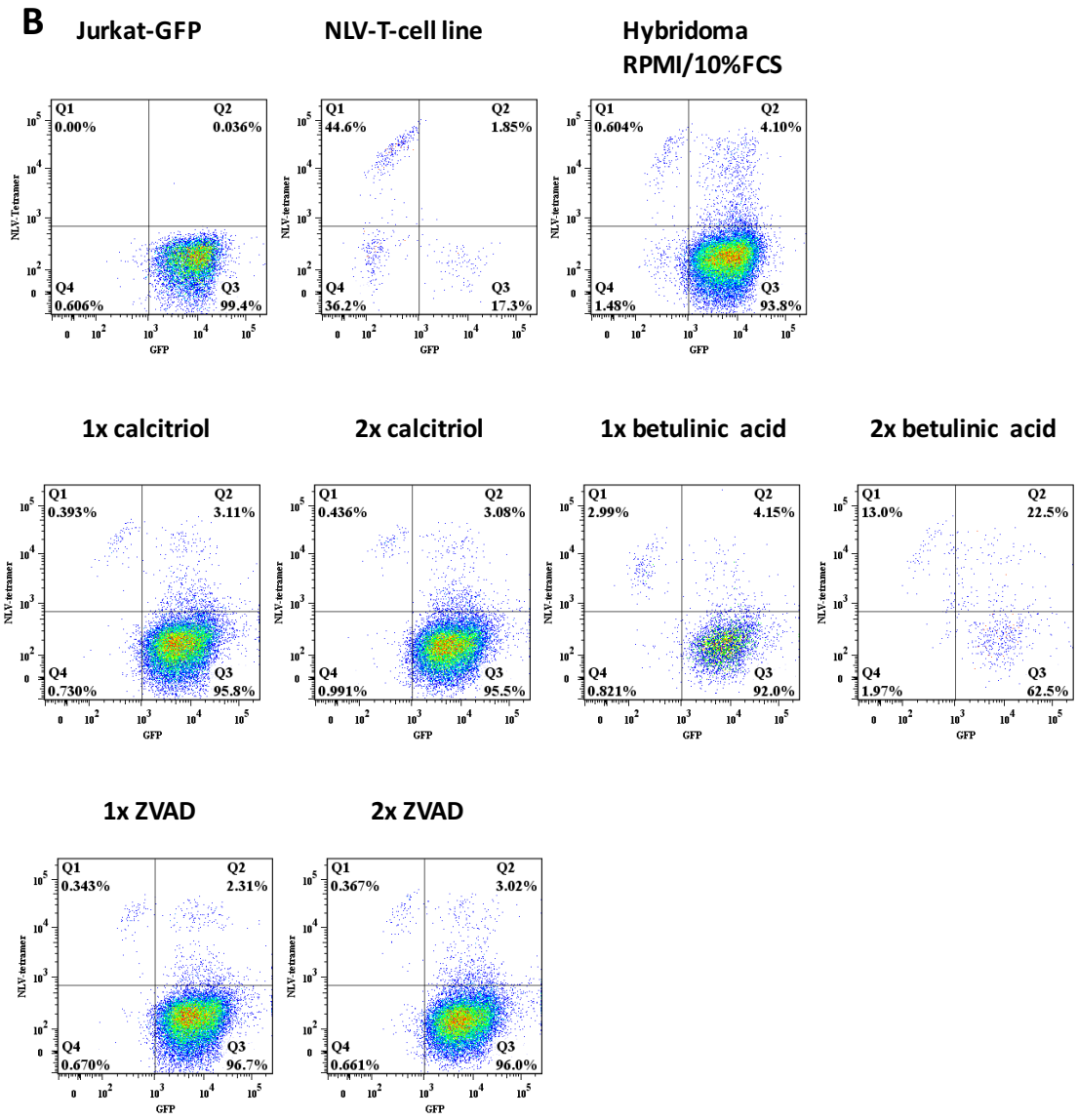

We wondered if longer term hybridoma cell growth would be better supported (i.e. after cells had recovered from initial fusion insult). In order to test this theory we put cells onto HAT selection on day 3 (immediately after the first FACS analysis). Cells were then incubated for a week and repeat FACS analysis performed to see if there had been any recovery of hybridoma cells (Fig. 5.14).

Fig. 5.14: Comparison of media supplemented with mitogens post HAT selection. The same cell lines as described in fig. 5.13 were used for this experiment. 'Jurkat-GFP' were fused with 'NLV-T cells' using standard protocols as described in chapter 2 using PEG. Immediately following fusion cells were resuspended in either control media (RPMI/10% FCS) or media supplemented with mitogen. Cells were allowed to rest for 3 days in incubator 5% CO_2, 37c and then put on HAT selection for a week. (A) shows % target population i.e live cells potentially containing hybridomas. (B) Shows staining for tetramer and GFP. Hybridoma cells are considered to be the DP population in quadrant 2. (C) Shows staining for CD8/GFP, with hybridoma cells considered $GFP^{+}CD8^{+}$. 1x and 2x refers to the concentration of mitogen used, as first described by Ms Steadman.

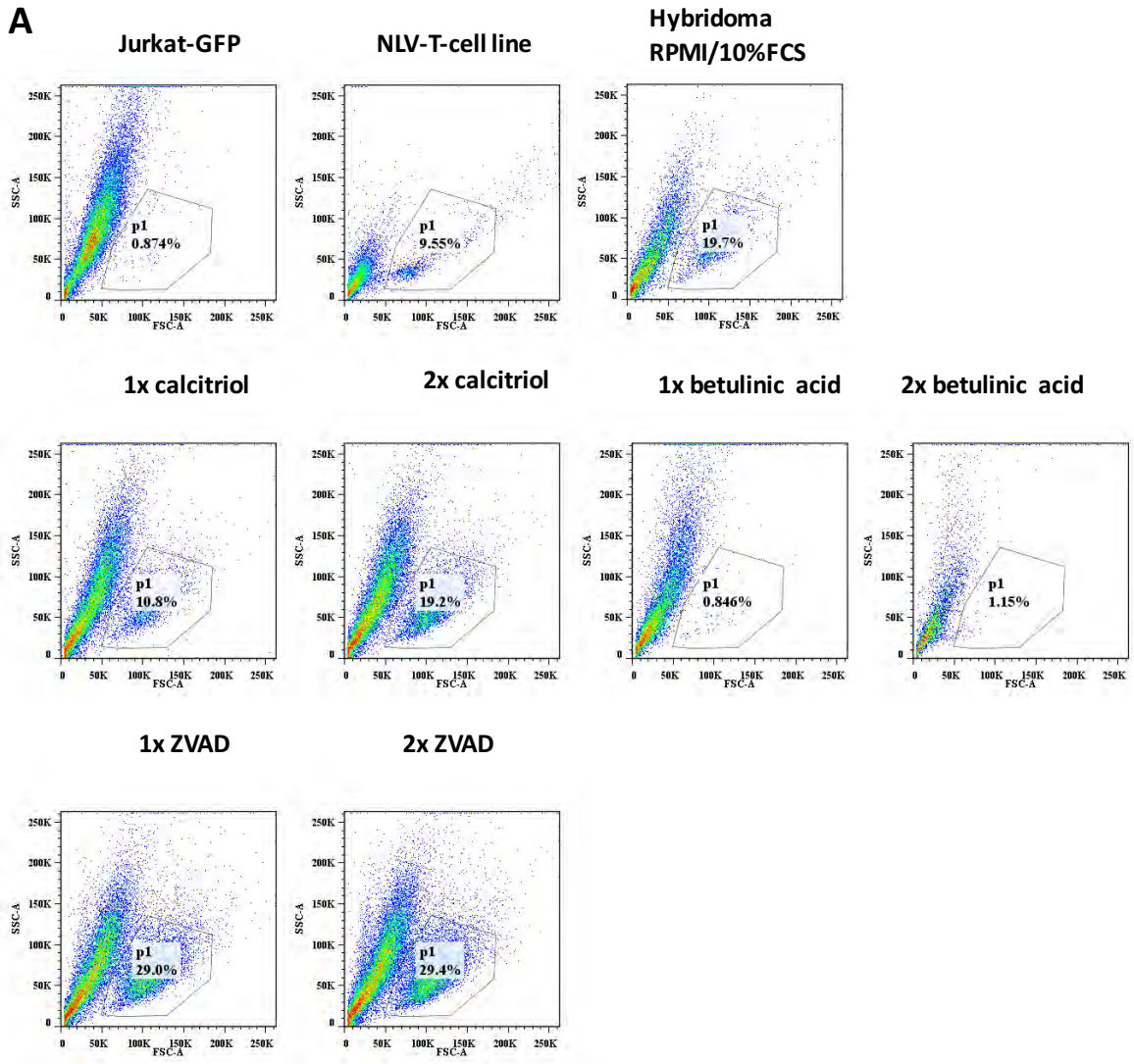

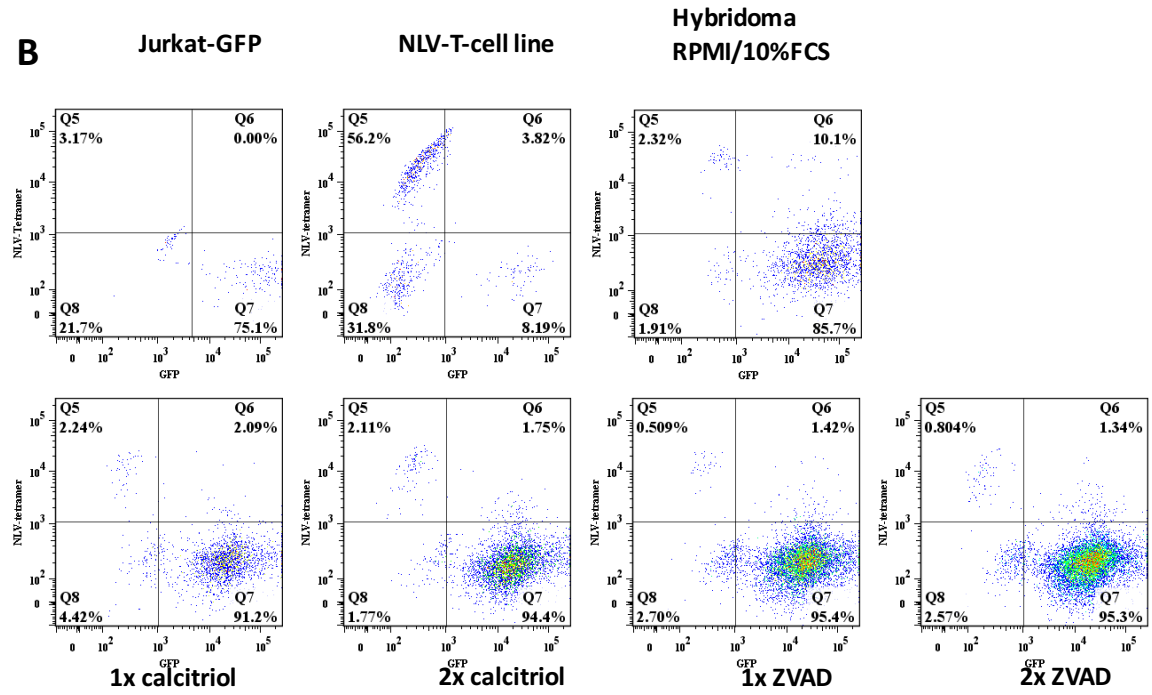

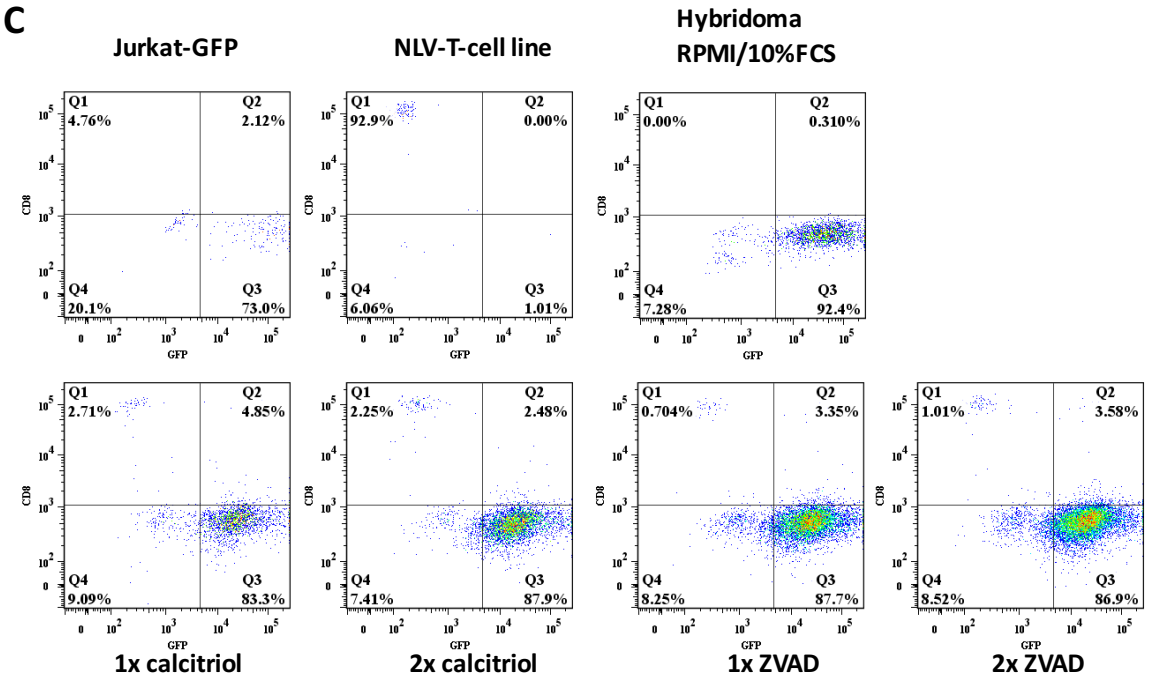

Unsurprisingly the majority of Jurkats (which are HAT sensitive) have died following selection with HAT. The NLV-tetramer^{+} T-cells are HAT-resistant and therefore survive. Although on initial inspection of fig 5.14A it would appear there is a reasonable population of target

population cells (19.7%) in the control well containing RPMI+ 10% FCS. When analysed further, assessing tetramer and CD8 positivity it can be seen that these cells are largely tetramer and CD8 negative. There is a population of cells which are $GFP^{+}CD8^{-}$ which are presumed to be Jurkats (and further suggests that the fusion cell population is possibly mixed with not all possessing the HPRT1 mutation conferring HAT sensitivity and 6TG resistance. The alternative hypothesis is that these could be hybridomas fused with non-$CD8^{+}$ T-cells as this is a heterogeneous cell line not a clone – however this is unlikely given these cells are also NLV-$tetramer^{-}$). It is not immediately clear why HAT was so efficient at killing the Jurkat control, if this is also a heterogeneous line.

One conclusion which may be drawn from looking at the other mitogens is that there is an increase in target population which is directly proportional to the amount of calcitriol 10.8% vs 19.2% respectively (although not better than control RPMI/10% FCS which was 19.1%) – Fig 5.14A. ZVAD also confers an increase in target population (which does not increase significantly when the amount of ZVAD is doubled – 29% vs 29.4% respectively). However when observing tetramer positivity (B) it is clear that very few cells are GFP^{+}NLV-$tetramer^{+}$, and in fact the control well has a population of 10.1% cells which are double positive, which is far more than any of the mitogen wells. It was noted that the GFP^{+}NLV-tetramer- population in quadrant 7 (considered to represent Jurkat cells) increased in the presence of mitogens – which would suggest possibly mitogens confer some resistance to HAT (fig 5.14.B). When analysing $CD8^{+}$ there are very few cells which are $CD8^{+}GFP^{+}$. There does appear to be a very small population in the ZVAD wells (red circle), but again the overriding cell line present appears to be Jurkat in origin.

These data appear to suggest that mitogens support the growth of Jurkats but don't appear to confer much of an advantage to hybridomas. We therefore concluded that addition of mitogens

to growth media was not advantageous to the culture of hybridoma cells and enhancing their stability.

5.2.6 Nucleofection of the pre-mixed cells (PBMC + Jurkat) with VSV-G DNA is more efficient at generating hybridomas than standard protocols

V-fusion has been proposed as a potential improvement to cell fusion technology as it reduces potential for toxicity, optimises efficiency and introduces flexibility (Gottesman, Milazzo et al. 2010). We therefore hypothesised that use of VSV-G DNA could have the potential to enhance the hybridoma formation. Vesicular Stomatitis Virus G (VSV-G) can enhance DNA lipofection efficiency by interacting with liposomes to form fusogenic, serum-stable liposomes with enhanced transfection properties, which is reversible (Okimoto, Friedmann et al. 2001). We therefore predicted that the presence of VSV-G on fusion partners may allow for enhanced fusion with target cells. In order to test this hypothesis, VSV-G DNA was used in combination with Lonza nucleofector 2d, nucleofection kit V (Amaxa, Germany). Jurkat-GFP fusion partner cells were pre-treated with 6TG to obtain a near pure population of 6TG resistant cells and a sample aliquot of these cells was taken to test for HAT sensitivity with 99.2% death following this. VSV-G DNA was added to populations of PBMC, Jurkat or a mixture of both and the cells nucleofected to introduce the DNA into the cell(s) of choice. Addition of the second population of cells (i.e. Jurkats to the nucleofectd PBMCs or PBMCs to the nucleofected jurkats) was delayed for 2 hours to allow the nucleofected cells to express the VSV-G protein. It was noted that pre-nucleofection of PBMC's and then addition of Jurkats resulted in very few double positive cells (0.59%) - fig. 5.15. When this is reversed and Jurkats are pre-nucleofected we saw a higher percentage of double positive cells (2.82%) which is better than the standard hybridoma protocol with PEG as fusogen which saw only 1.61% DP cells. Nucleofection (i.e. application of a current as per pre-selected programme) resulted in very few DP cells which would be as expected as in general application of a charge would

result in cell death and in the absence of a fusogen is likely to be detrimental to the cell population. When VSV-G was added to a premixed population of equal numbers of CellTrace violet-stained PBMC and Jurkat-GFP this produced the highest percentage of double positive cells (7.23% red circle Fig. 5.15). We therefore concluded that nucleofection of the premixed cells (PBMC + Jurkat) with VSV-G DNA is more efficient at generating hybridomas than standard protocols.

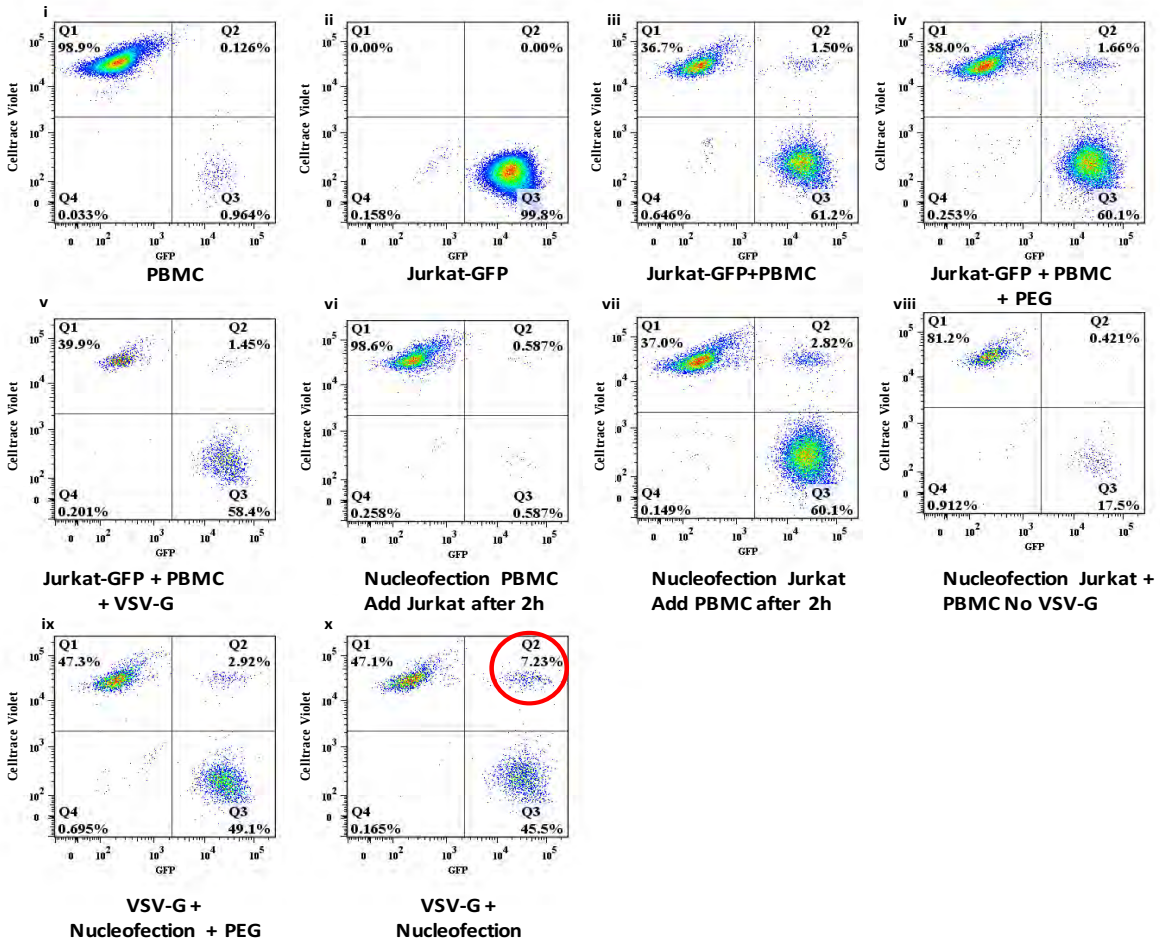

Fig. 5.15: Assessment of the effect of nucleofection of cells with VSV-G. (i) Control PBMC cells were stained with CellTrace-violet. (ii) The control Jurkat fusion partner cell line was GFP^+. We compared (iii) a plain mixture of cells which were not nucleofected with (iv) the standard fusion protocol using PEG and also with nucleofection (v-x). We considered nucleofection of PBMC with subsequent addition of Jurkats (vi) but the resultant population was largely comprised of PBMC alone (Q1). We also considered nucleofection of Jurkats prior to addition of PBMC (vii) which resulted in a mixed population of single positive cells (Q1 and Q3) and also a DP population (Q2) which were considered possible hybridomas (2.82% cells). We predicted nucleofection in the absence of a fusogen or VSV-G would result in high cell death (viii). Finally we considered mixing the PBMC with equal numbers of Jurkats and nucleofecting this mixture with VSV-G both with PEG (ix) and in the absence of PEG (x). This experimental protocol was peformed in triplicate on 3 separate occasions. Similar results were obtained with each.

5.2.7 Concentration of VSV-G DNA does affect fusion efficiency

It was proposed that using higher concentrations of VSV-G may lead to higher fusion rates. The original protocol used 2µg of VSV-G DNA. We therefore sought to identify the optimum concentration of DNA to lead to hybridoma formation with longevity in culture following selection. We also set out to identify if the resultant DP cells were indeed hybridomas. In order to test this theory, PBMCs were again stained with CellTrace Violet, and nucleofection protocol followed as previously with increasing concentrations of VSV-G DNA (0µg, 1µg, 2µg, 3µg, 5µg). Hybridomas were considered to be DP cells (i.e. GFP^+CellTrace $Violet^+$) following initial nucleofection (fig. 5.16a).

However over time when cells proliferate they lose the violet colouration, therefore this could not be relied upon to identify the potential hybridomas after culturing for any prolonged period. Therefore the target population would be green (due to GFP^+ from Jurkat) and HAT resistant (from the PBMC population). Unfused PBMC's die in the absence of IL-2 naturally (however a kill curve was used to establish puromycin toxicity for this line, and this was used to select out unfused PBMC's) and unfused Jurkats die as a result of HAT sensitivity. Cells were therefore pulsed with puromycin and HAT on D3 and D10 (post-nucleofection) and analysed using flow cytometry on day 3, 7, 14 and 21. Hybridomas were considered living GFP^+ cells following selection (Fig. 5.16b). Using paired t-test analysis we considered there was a significant difference (** on figure) between 2µg and 3µg VSV-G DNA ($p<0.05$). 3µg DNA was identified as the optimum concentration for demonstrating expansion of cells following selection.

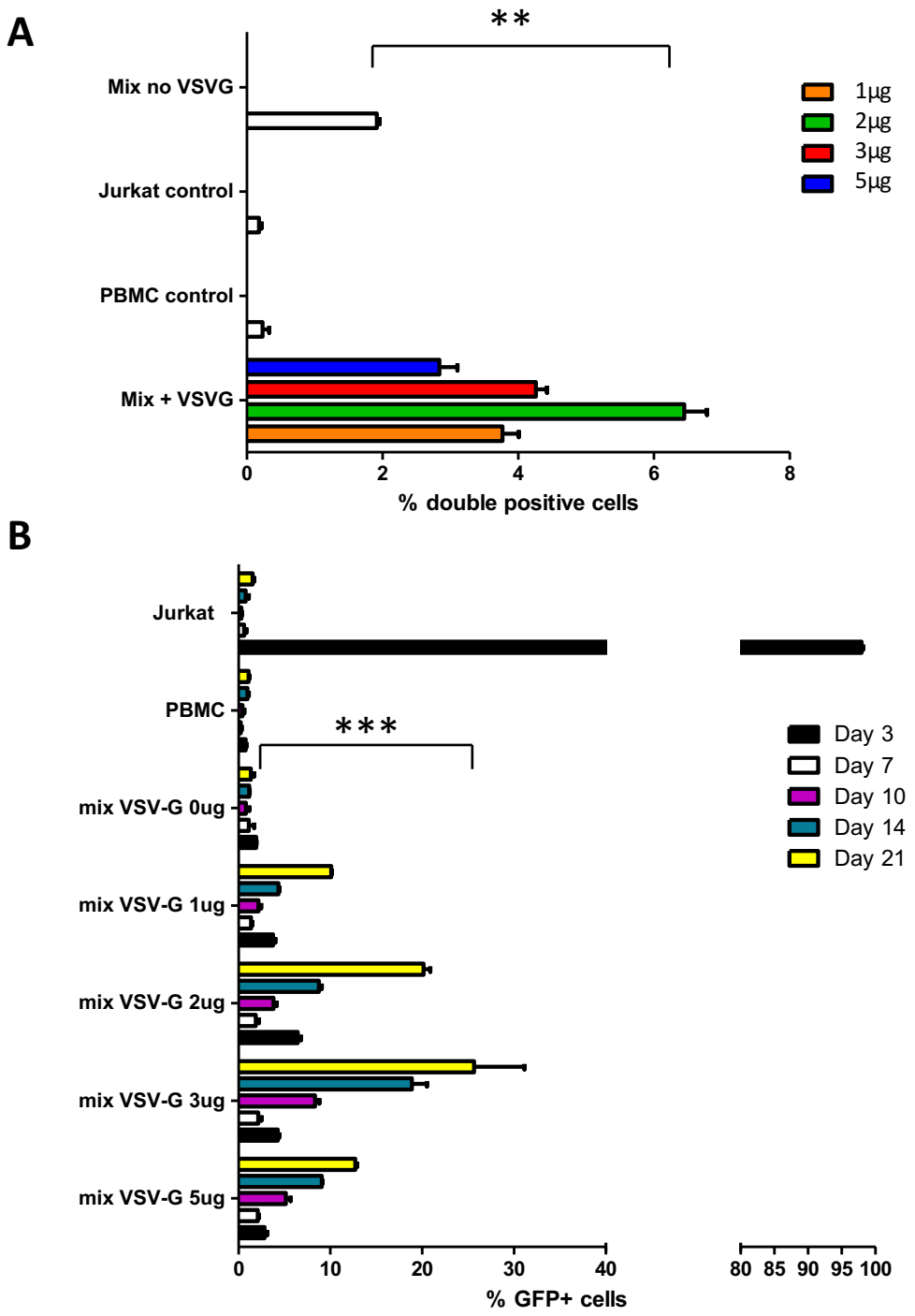

Fig. 5.16: Effect of different concentrations of VSV-G DNA on formation of hybridomas following nucleofection. Equal numbers of PBMC (stained with CellTrace-violet) and 'Jurkat-GFP' (Jurkats previously transduced with a GFP-tag) were mixed together. They were resuspended in appropriate nucleofection solution and VSV-G DNA was added at 1µg, 2µg, 3µg, or 5µg. Lonza 2D nucleofector was used with appropriate programme X-001. Cells were washed and resuspended in RPMI/10% FCS and analysed using flow cytometry on day 3 post nucleofection. (A) Hybridoma cells were considered to be those cells which were GFP^+CellTrace-$violet^+$ i.e. double positive. Significnt differences can be seen in presence of addition of VSV-g DNA (**) (B) shows the same cells following selection with HAT and puromycin on day 3 and day 10. Hybridoma cells were considered to be viable cells which were GFP^+ following selection, as unfused Jurkats are HAT sensitive, and unfused PBMCs puromycin sensitive at established concentrations. At day 21, cells nucleofected with VSV-G DNA were significantly higher in number compared to those not (***)

5.2.8 Polycations and plant lectins do not improve fusion efficiency

Previously it has been proposed that efficiency of fusion can be improved using polycations and lectins (Matsuya and Yamane 1985, Matsuya and Yamane 1985). It has been reported that the use of PEG at high concentrations (>50%) is most effective, however this comes at the cost of viability and cytotoxicity. Therefore the focus of this section is to try to identify a process which achieves effecicient fusion without loss of viability. The mechanism of action of lectins on PEG-mediated cell fusion is not known. One hypothesis proposed is that cell agglutination by lectins creates conditions of close cell-to-cell contact, thereby enhancing the possibility of any subsequent fusion, but the question still remains whether the lectins may induce a structural change in the cell membranes (Reeve, Hewlett et al. 1974, Mercer and Schlegel 1979, Schneiderman, Farber et al. 1979).

Therefore we attempted to assess this protocol modification. As we identified nucleofection of VSV-G as a fairly efficient process we used this as our standard comparator. Polyvinyl pyrrolidone (PVP) was also considered cytoprotective by Matsuya and therefore we also tested this as a possible additional modification to the protocol (see methods) - (Yoshii and Kaetsu 1982, Matsuya and Yamane 1985, Matsuya and Yamane 1985).

PVP has long since been used to block Southern blots, and is a known component of Denhardt's buffer. It has also been demonstrated to absorb polyphenols during the purification of DNA. Polyphenols are commonplace in a number of plant cells, and they have the ability to deactivate a number of proteins/enzymes if not adequately removed. As a result they may influence further molecular analyses such as PCR. They are therefore an important consideration in molecuar biology. They have, as part of their make up, the ability to bind polar molecules, however the mechanism of cytoprotection in this instance is not clearly defined.

We compared (i) standard fusion with PEG, (ii) nucleofection with VSV-G and (iii) various plant lectins and polycations with and without PVP to assess if any were able to further enhance this protocol. Mixing the cells in the absence of any fusogen was taken as the background (false positive) and had a level of 2% DP cells (represented by black bar on graph). Therefore, any DP cells above this threshold were considered to potentially represent hybridomas (fig. 5.17). There is limited effect of using the polycations, although this was slightly improved by the addition of PVP but this was still only in the region of 2-3% (i.e. limited improvement on just mixing the cells). Plant lectins did not enhance the protocol and performed worse than mix alone. When compared with VSV-G nucleofection we demonstrated 6.45% DP cells, which remains the most efficient process for formation of hybridoma cells and remains significantly more efficient than standard PEG hybridoma protocols (paired t-test p,0.005). We therefore concluded that plant lectins and polycations do not improve on the established nucleofection protocol.

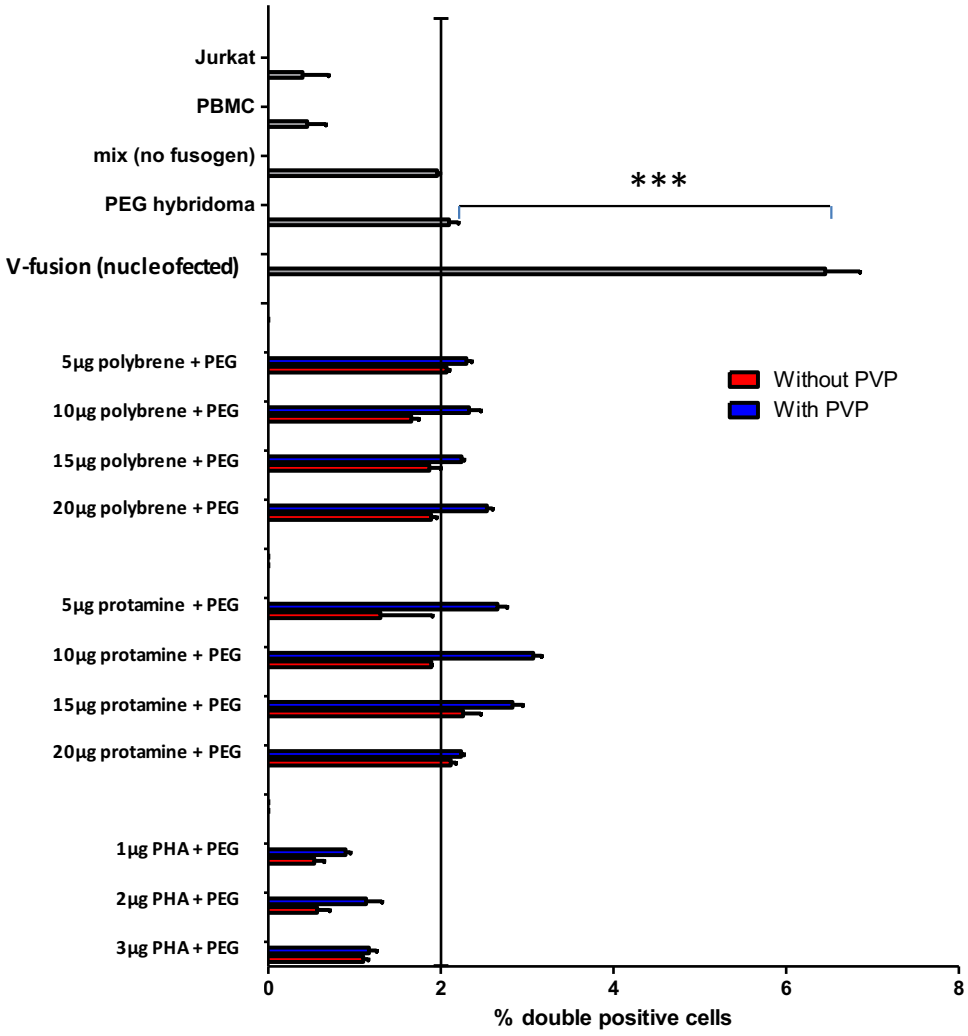

Fig. 5.17: Effect of polycations, plant lectins and PVP on efficency of hybridoma formation. Control cells (grey) received no lectin/polycation or PVP. Background DP was taken as 2% - the threshold of double positivity noted when cells were purely mixed together in the absence of any fusogen (represented by vertical black line). V-fusion is the standard nucleofection protocol with Amaza 2d nucleofector, programme X001, 3µg VSV-G DNA. There is a significant difference between number of double positive cells formed as a result of standard fusion protocols using PEG when compared to nucleofection with VSV-G DNA (***). There is limited effect of polycations, plant lectins or PVP on hybridoma formation above the background double positivity (NS).

5.2.9 Hybridomas technology could potentially capture rare events

Cancer cells are transformed cells which are considered rare in the heterogeneous mixture of cells of the human body. Now we have established a technology which is more efficient than standard PEG fusion, and replicated this, we wanted to ascertain if this could be used to capture these infrequent target events – could this technology be used to immortalise T-cells capable of recognising these transformed cells? We hypothesised that potentially only a small

proportion of T-cells had the ability of recognising these tumours. We have shown by our 'proof of principle' experiments that nucleofection with VSV-G can potentially lead to cell fusion, resultant fusion cells can be selected and the resulting population expanded in culture. This protocol was therefore used on an HLA-$A2^+$ PBMC population, from a donor with a known NLV-tetramer positive response of ~1% i.e. a rare event. We proposed that hybridomas would be able to capture these rare cells and could be used as a technology to expand these in culture. To test this hypothesis, we mixed $1x10^6$ PBMC to equal numbers of fusion partner Jurkat cells which were GFP positive. We would expect only low numbers of DP cells following fusion as background NLV-tetramer positivity in the PBMC population was 1% (Fig 5.18A – red circle). 'Mix without VSV-G' referred to mixing target and fusion cells in equal numbers without the addition of VSV-G DNA or nucleofection, and was included as a control. Cells were selected on D3 and D10 with HAT and puromycin to remove any unfused cells. By D10 the nucleofected cells were proliferating, having expanded from a baseline of 0.834% NLV^+ to 3.12%. By Day 14 these cells had expanded further to 3.89% NLV^+ which suggests viability following selection – and potentially these cells are fused hybridomas which demonstrate proliferation (fig. 5.18B). Unfortunately all cells were dead at the end of this 3 week period; however these results demonstrate the potential of hybridoma technology to increase the tetramer positive cells (i.e. target cells) in a population i.e. can capture a rare event. They did not however lead to a stable cell line, despite 2 further experimental repeats, and therefore we concluded that hybridomas may not be the most efficient way of capturing rare events using the techniques investigated. This lead us to look at further experimental modifications to try to achieve this.

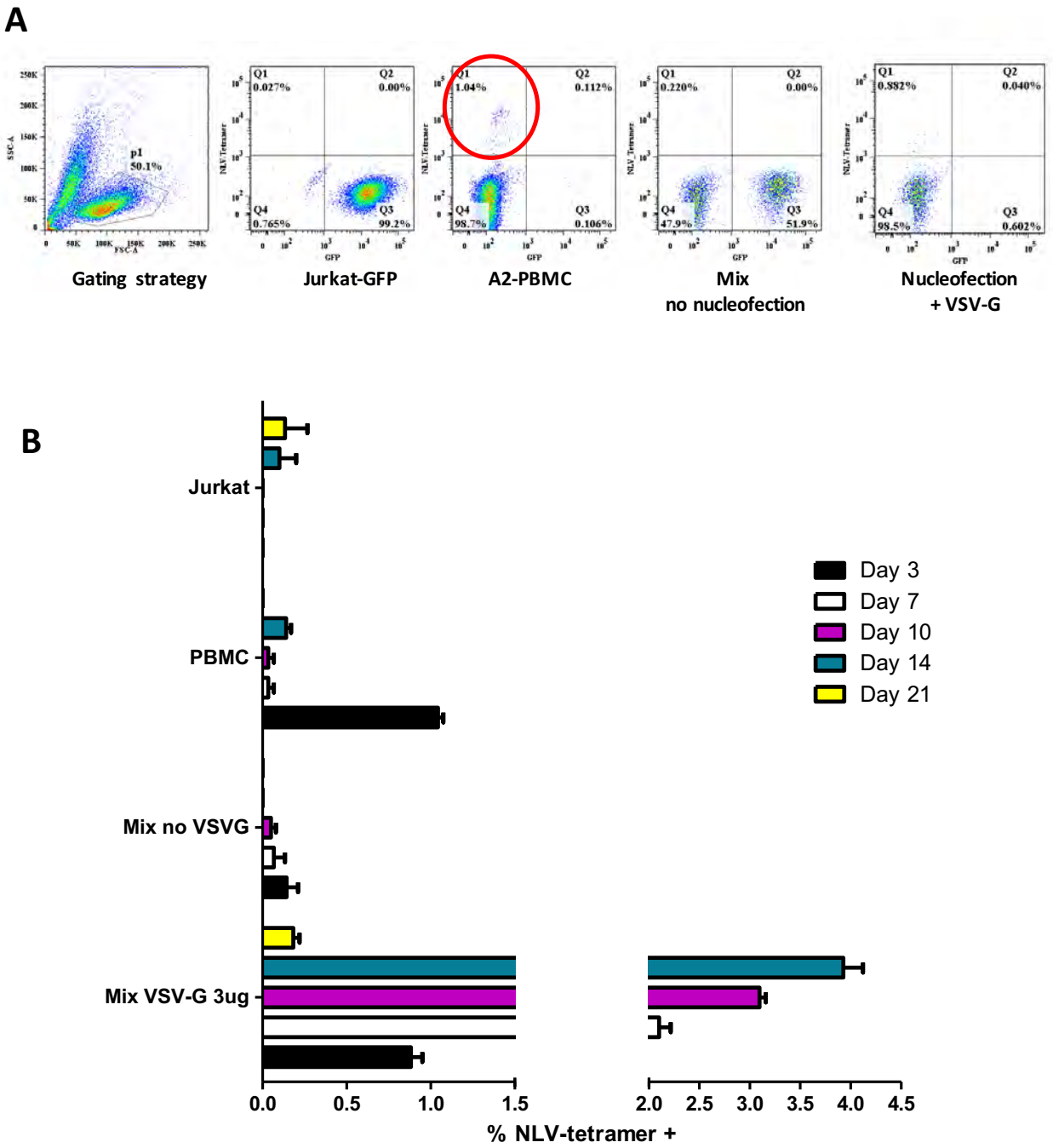

Fig. 5.18: Can hybridoma technology be used to capture rare events? (A) Equal numbers of fusion partner cells 'Jurkat-GFP' a jurkat already modified previously to contain a GFP tag were mixed with HLA-A2 PBMC (targets) with known NLV-tetramer positivity ~1% (red circle). (B) Following nucleofection with Lonza 2d nucleofector and standard protocol as previously described, cells were selected with HAT and puromycin on D3 and Day 10 respectively. These figures represent 3 experimental repetitions, each peformed in triplicate, Error bar represents SD.

5.2.10 Cross-linking CD52 on the cell surface of lymphocytes with fusion partners pre-treated with anti-CD52 does appear to facilitate hybridoma formation

Clearly fusion of cells to form a hybridoma is reliant on a mechanism to bring cells together as cell-to-cell interaction is key to this process being successful. We proposed one such way of doing this would be to coat one of the cells (either fusion partner or target cell) with anti-CD52, which is an antibody toward the CD52 peptide of 12 amino acids, anchored to glycosylphosphatidylinositol (GPI). Since lymphocytes naturally express CD52 we predicted the antibody should recognise and bind the CD52 expressed on the lymphocyte cell surface and result in bringing these cells into close contact prior to application of the nucleofection pulse. A large excess of anti-CD52 antibody is needed to try to prevent both arms of the antibody from binding to CD52 on the same cell (i.e. one arm of the CD52 antibody binding to one cell and the other arm to the second cell forming a bridge). In order to test this hypothesis, the Jurkat fusion partner cells were first 6TG selected to remove any $HGPRT^{+}$ cells, then pre-treated with anti-CD52 30 minutes prior to fusion and washed three times with PBS. Following this they were resususpended in appropriate nucleofection solution as per manufacturer guidance (Fig. 5.19a). PBMC were stained with CellTrace violet to allow visualisation on the flow cytometer. Cells were then nucleofected using standard protocols and resuspended in RPMI/10% FCS. On Day 3 and day 10 cells were put on HAT and puromycin selection to remove any unfused cells (Fig. 5.19b). From this initial pre-selection data, antibody concentrations of 500ng and 1μg α-CD52 appeared to be optimal to allow possible fusion.

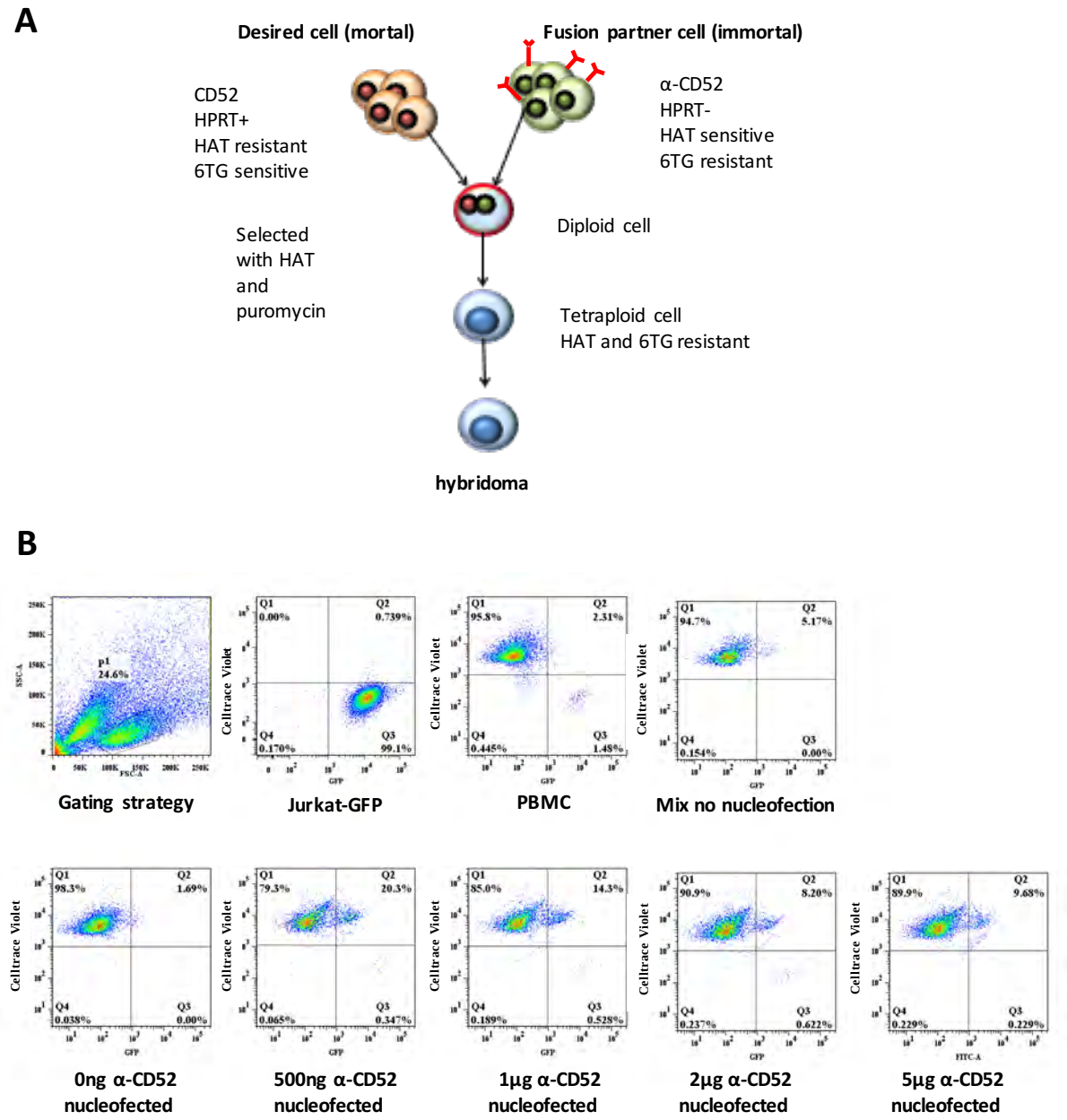

Fig. 5.19: Does crosslinking cells prior to nucleofection lead to hybridoma formation? (A) Schematic overview of protocol for pre-treating fusion partner cells with anti-CD52 and predicted outcome. (B) FACS analysis performed on Day 3 prior to selection with HAT or puromycin. Top row represent control wells. Background double positivity is relatively high in this instance at 5.17% (Mix no nucleofection which represents control well where equal numbers of fusion partner and target cell are mixed together in the absece of antibody or nucleofection). Therefore following nucleofection the DP cells must be greater than this value. Nucleofection in the absence of CD52 antibody was low at 1.69% reflecting cell death as a result of electrical pulse delivered. Higher % DP cells were seen in 500ng and 1µg α-CD52 (20.3% and 14.3% respecitively). Higher concentrations of antibody were less efficient at generating a stable 'hybridoma'.

Cells were selected using HAT and puromycin on Day 3, 10, 21 and FACS analysis was performed. As seen previously the CellTrace Violet is lost over time due to cell proliferation and therefore hybridoma cells were considered to be those alive following selection and GFP^{+}.

In order to assess stability of cells, absolute cell number was calculated using microscope and manually counting an aliquot of cells at weekly intervals (fig 5.20) counting specifically live cells as determined using trypan blue staining. Cells were also analysed by FACS looking at live cells, GFP^+ and $CD8^+$ (as Jurkats are GFP^+CD8^-, T-cells GFP^- $CD8^+$, and hybridomas considered GFP^+CD8^+). Fig. 5.20 demonstrates cells following selection with HAT and puromycin on day 3.

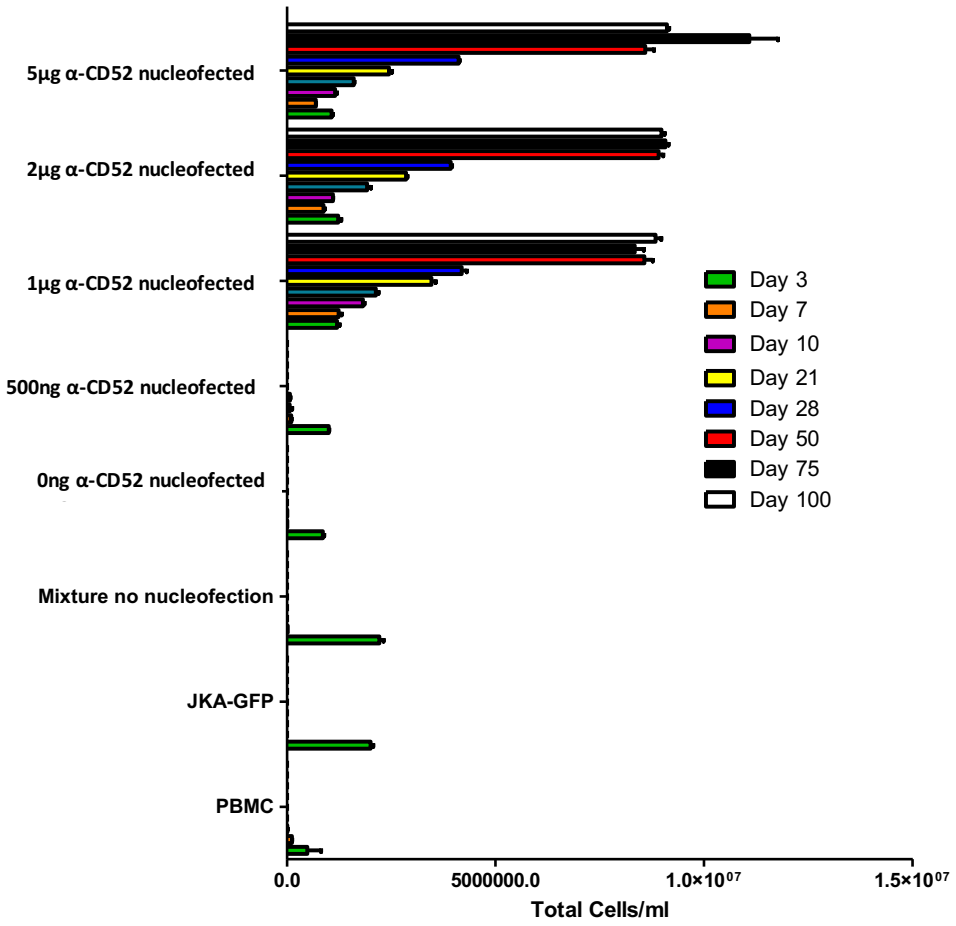

Fig. 5.20: Does crosslinking cells prior to nucleofection lead to hybridoma formation which is sustainable long term? As described previously, target cells were stained with CellTrace violet. Fusion partner cells (Jurkat-GFP) were pre-mixed with cd52-antibody at various concetrations (1-5 µg). These jurkat cells were then washed x2 with PBS and resuspended in culture media as previously described. Equal numbers of target cells and fusion partner cells were mixed and subsequently nucelofected. HAT and Puromycin selection pressures were applied on Day 3, Day 10 and Day 25. Cells were anaysed using FACS machine as well as manually counted using Coulter Counter and trypan blue staining in order to identify live and dead cell populations. Cells were sampled sequentially over a period of 100 days.

It was noted that HAT leads to quick decline of sensitive cells, but puromycin appears to take longer to act – an observation seen previously. Jurkat cells were all dead following HAT selection (plot not shown) at this time point. The trend which becomes clear is that cells initially expand well following hybridoma formation; however, they appear to slow down between days 50-75. In 5µg cd52-antibody wells there is an expansion at Day 75 but this is felt to be a spurious result as at day 100 the number of cells has fallen back to similar levels at day 50. Therefore, due to lack of expansion and stable cell numbers we proposed that these cells were senescent.

We considered if media supplementation with cytokines may start the proliferation process again. We therefore selected a number of cytokines to test based on their properties intracellularly. Initially we tested these cytokines on PBMCs obtained from healthy donors in order to look at their effect *in vitro* before attempting to use them on hybridomas (this was done because the hybridoma cell numbers were small and therefore we did not wish to lose any cells by testing out the different supplements (fig. 5.21).

Fig. 5.21: Day 21 Assessment of different growth medias on growth/viability of PBMC's. (A) Fresh PBMC were obtained from healthy donors and were grown in RPMI/10% FCS with different cytokines added to enhance cell growth as indicated. FACS was used to assess viability and visualise cell populations. Any combination with >40% live cells is shown in the FACS plots below. The top two rows depict controls – either single cytokines or all cytokines in combination. The bottom two rows depict the best performers in terms of viability/live cells. (B) Any combination with >40% live cells is shown in the chart overleaf, with coloured squares representing cells which are more than 40% viable at different time points. Cells with >40% viable on Day 3 are shaded yellow. By day 7 red, day 15 blue and day 21 green. (C) Shows individual effect on cell populations as assessed using flow cytometry. (NB. TiLS Exp Media is the standard T-cell media used for a expansion of TiLs as used in the phosphopeptide section of this thesis. We chose to test this media as well for potential to expand these often difficult to expand cells. This media comprises: AIM-V, Human serum, IL2, Anti-CD3). (D) Breakdown of individual cell numbers by FACS analysis. Plots representative of 3 experimental repetitions. NB due to small cell numbers graph (C) was the result of a single sample from each well. The student accepts this is difficult to draw conclusions from, however the results obtained on subequent repetitions of this experimental protocol were replicated. This graph is a fair representation of the results obtained from this part of the experiemntal analysis.

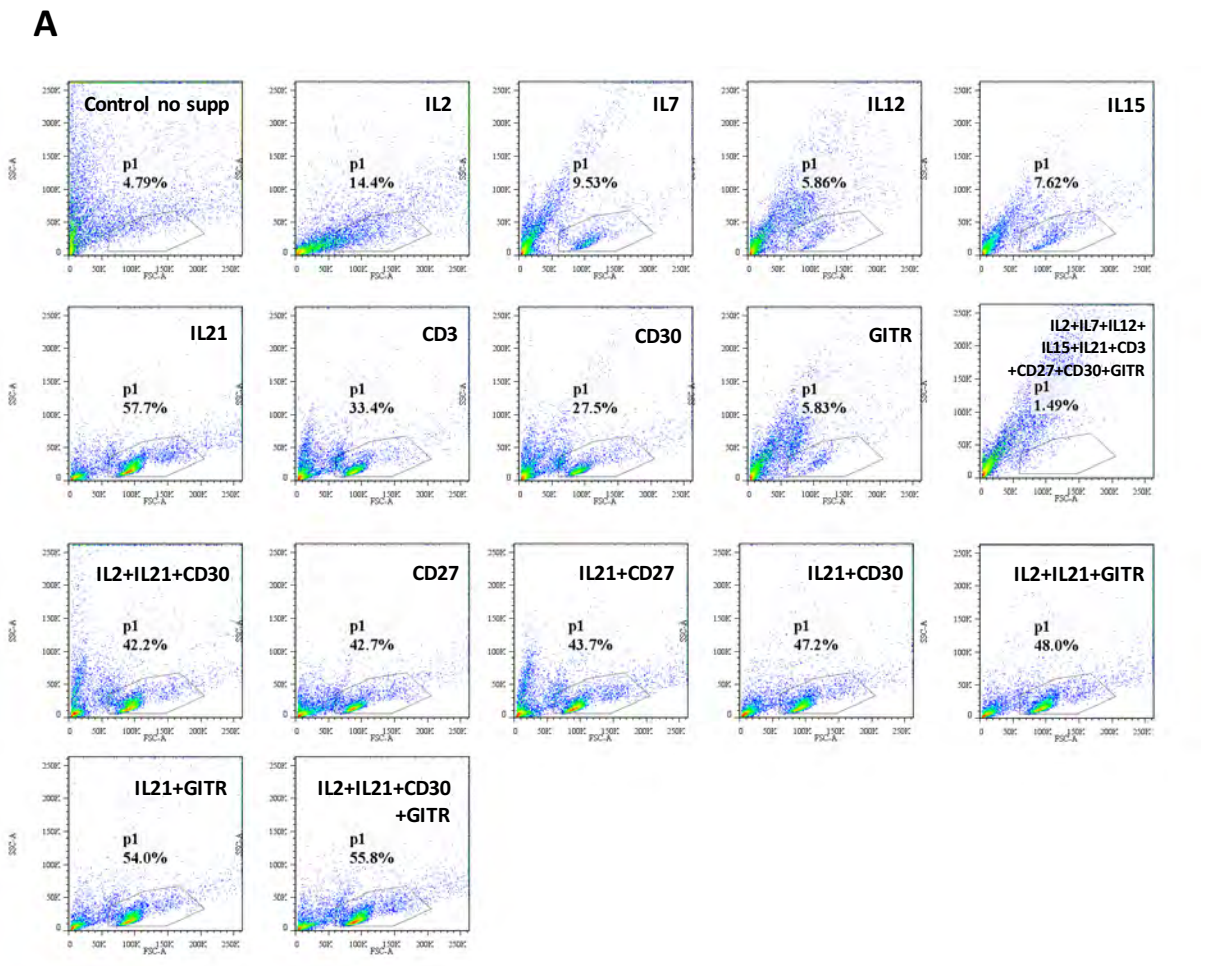

B

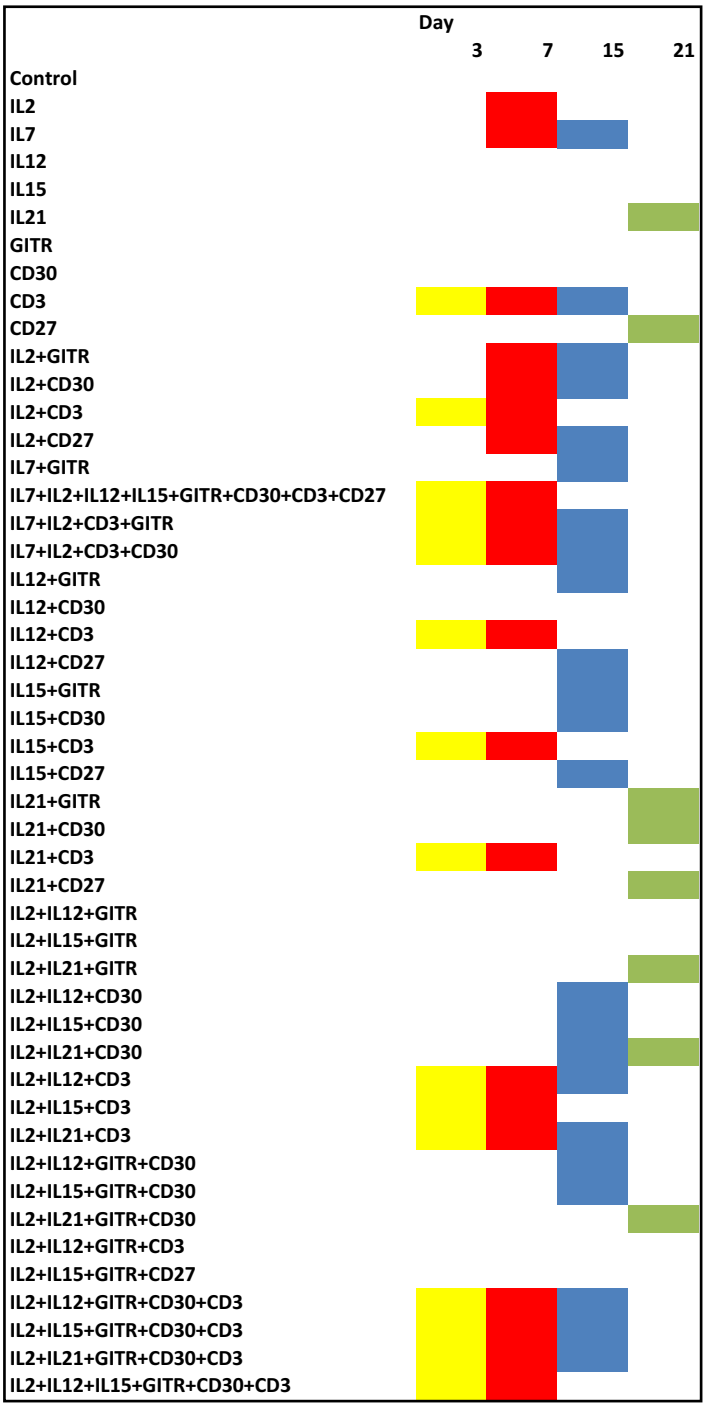
Day
3
7
15
21
Control
IL2
IL7
IL12
IL15
IL21
GITR
CD30
CD3
CD27
IL2+GITR
IL2+CD30
IL2+CD3
IL2+CD27
IL7+GITR
IL7+IL2+IL12+IL15+GITR+CD30+CD3+CD27
IL7+IL2+CD3+GITR
IL7+IL2+CD3+CD30
IL12+GITR
IL12+CD30
IL12+CD3
IL12+CD27
IL15+GITR
IL15+CD30
IL15+CD3
IL15+CD27
IL21+GITR
IL21+CD30
IL21+CD3
IL21+CD27
IL2+IL12+GITR
IL2+IL15+GITR
IL2+IL21+GITR
IL2+IL12+CD30
IL2+IL15+CD30
IL2+IL21+CD30
IL2+IL12+CD3
IL2+IL15+CD3
IL2+IL21+CD3
IL2+IL12+GITR+CD30
IL2+IL15+GITR+CD30
IL2+IL21+GITR+CD30
IL2+IL12+GITR+CD3
IL2+IL15+GITR+CD27
IL2+IL12+GITR+CD30+CD3
IL2+IL15+GITR+CD30+CD3
IL2+IL21+GITR+CD30+CD3
IL2+IL12+IL15+GITR+CD30+CD3

C

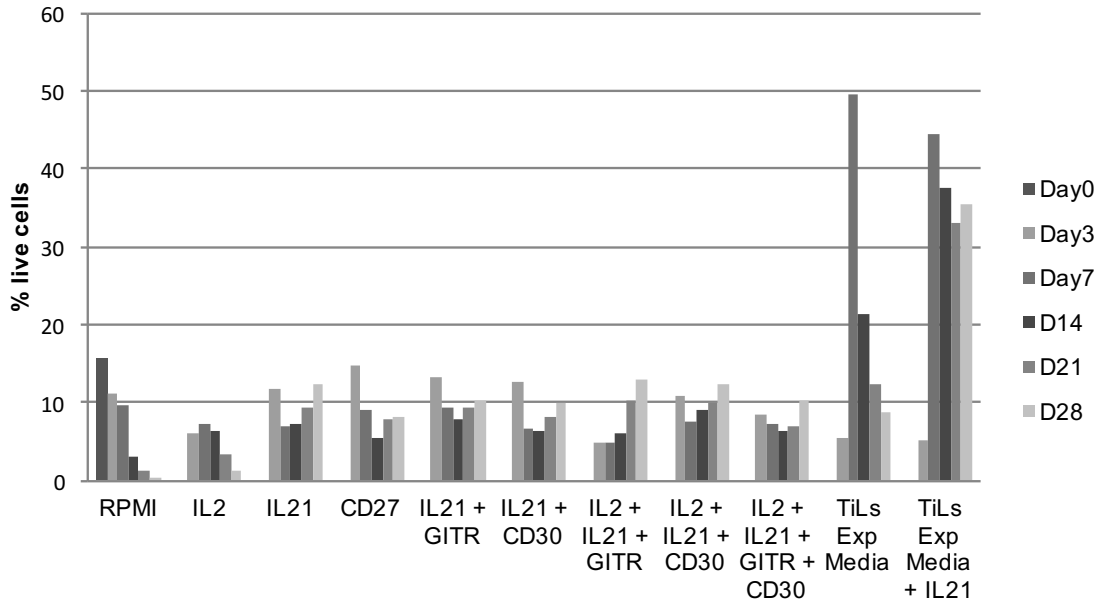

D

Media	Day 0			Day 3			Day 7			Day 14			Day 21			Day 28		
	%CD8	%CD4	%B cell	%CD8	%CD4	%B cell	%CD8	%CD4	%B cell	%CD8	%CD4	%Bcell	%CD8	%CD4	%Bcell	%CD8	%CD4	%Bcell
RPMI	23	47.3	16.6	23.1	47.7	16.9	30.7	54.5	1.78	14.4	51.9	0	12	22.1	0	10	12.45	0
IL2				25.8	41.5	19.6	34.7	51.4	2.14	25.7	43.9	0.7	22.3	40.7	0.2	20.1	37.6	0.1
IL21				24.1	46.5	18.2	28.6	58.6	2.92	20.4	58.6	2.21	18.7	52.6	2.2	24.7	48.99	1.9
CD27				24.1	46.2	16.5	31.3	53.9	2.55	26.5	60.1	1.63	25.4	53.7	1.54	28.2	54.1	1.45
IL21 + GITR				22.7	47.4	18.6	31.7	54.2	3.26	29.1	48.6	2.08	33.2	46.2	1.98	34.6	47.9	1.87
IL21 + CD30				23.8	50.1	16.4	29.6	52.6	3.45	27.8	49.8	2.49	29.3	53.1	3.01	31.2	54.3	3.11
IL2 + IL21 + GITR				23.8	43.4	19.5	20.7	20.2	2.23	27.5	44.7	4.58	28.2	45.3	4.11	29.7	44.9	2.88
IL2 + IL21 + CD30				21.2	46.6	17.9	20.7	46.2	2.96	15.3	49.5	4.15	20.3	45.99	2.22	22.8	47.3	2.01
IL2 + IL21 + GITR + CD30				20.1	41.8	23.5	24.1	55.8	2.34	14	39.3	1.87	18.2	39.2	2.01	19.6	40.01	2.01
TiLs Exp Media				4.82	6.42	18.6	33.3	43.6	2.68	29	59.5	0.09	27.2	45.7	0	22.3	44.7	0
TiLs Media + IL21				4.66	5.92	20.6	30.6	39.9	3.22	28.7	57.33	2.22	28.1	44.9	1.22	33.6	53.6	1.05

Fig. 5.21A demonstrates the effect of the different cytokine combinations on cell viability/live cells on day 21. Following the observation that IL-21 in particular was beneficial to cells grown long term (with >40% cells alive in all wells treated with IL-21 either on its own or in combination - fig. 5.21B) we decided to explore this cytokine further. All test cytokine combinations were continued in culture for up to 4 weeks in order to identify which combinations supported growth and viability (fig. 5.21C) at set weekly timepoints. As can be seen in fig. 5.21C - IL-21 only plays a role after 2 weeks of culturing, and prior to that other cytokines e.g. IL-2 were better at supporting cell viability. This suggested that both IL-2 and

IL-21 may play a synergistic role in aiding cell growth. Interestingly, combinations of cytokines with IL-21 appear to support T-cell growth long term at the expense of B-cell growth, however it is $CD4^+$ cells which appear to predominate over $CD8^+$ cells (fig. 5.21D). We predicted that addition of IL-21 to standard growth media (RPMI/10% FCS) would support growth and potentially lead to better cell expansion long term, but may need further modification to achieve high CD8 T-cell numbers. We also proposed addition of extra IL-2 and changing the amount of FCS as viable options for restarting cell expansion from the senescent state they appear to be in. We screened a number of combinations, including some of the mitogens previously seen to be beneficial in Jurkat growth support (ZVAD) looking at effect on PBMC, Jurkat and hybridoma cells (fig. 5.22).

Initially we proposed doubling the amount of FCS would improve cell growth (fig. 5.22A). PBMC's were set up in triplicate and wells compared at different time points up to 28 days. It was demonstrated that addition of IL-2 is certainly beneficial to growth of PBMC's at a concentration of 100units/ml. There is a significant increase in cell expansion/number when cells are exposed to IL-2 regardless of FCS concentration ($p<0.02$). We compared 10% versus 20% FCS and were unable to demonstrate any significant benefit to increasing the amount of FCS supplementation to 20%.

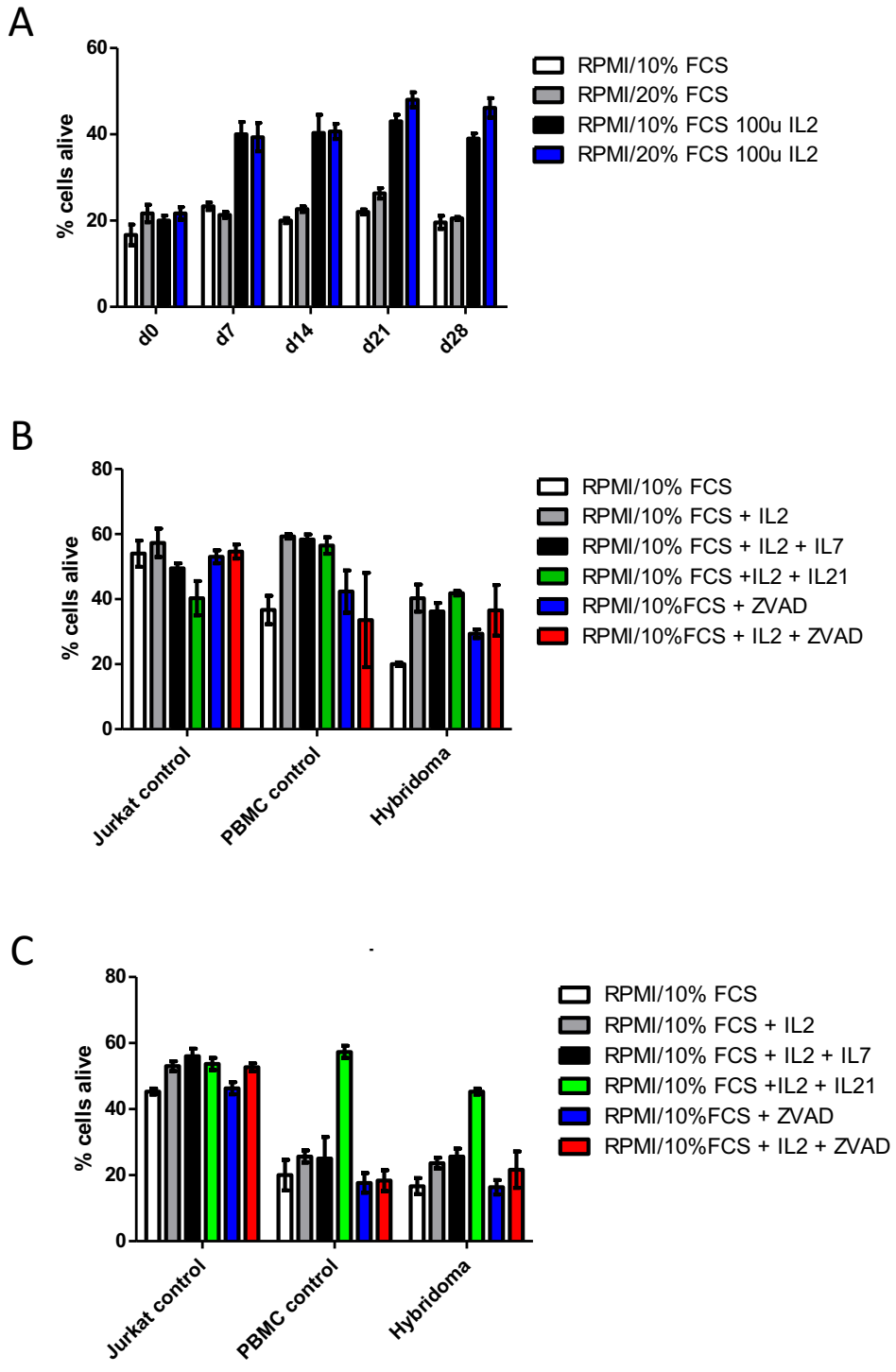

Fig 5.22: Effect of media supplementation on growth potential of cells. (A) Initially we compared simply doubling the available FCS from 10% to 20% on standard PBMC's. Paired t-test demonstrated no significant difference between addition of 20% FCS compared to standard 10% FCS. (B) Then we compared the addition of cytokines IL7 and IL21 to standard media as well as the mitogen ZVAD previously demonstrated to confer some benefit to cells in culture directly comparing PBMC to Jurkats and the cultured (senescent) hybridomas at 7days. (C) Finally we looked at a comparison of cells and medias at 28 days to see if there is any longer term benefit to any particular media combination.

We sought to assess the impact of addition of IL-21, IL-7 and ZVAD to the standard media to see if this may be of benefit. We predicted that IL-21 in addition to IL-2 would be beneficial as both cytokines have been shown to support cell growth and expansion. We also chose to investigate ZVAD further as we had previously shown it was of benefit for hybridoma growth (fig.5.14) and therefore proposed that ZVAD in combination with cytokines would support hybridoma growth and expansion. We directly compared PBMC's with Jurkats and hybridomas, and assessed their growth at 7 days and 28 days (fig 5.22 B, C). At day 7 it was noted that RPMI/10% FCS unsurprisingly did not support expansion of cells with 50% less hybridoma cells being alive compared to standard RPMI/10% FCS + IL-2. We noted ZVAD was of limited benefit (38% live cells versus 20% in unsupplemented media) and ZVAD in addition to RPMI/10% FCS + IL-2 versus RPMI/10% FCS + IL-2 alone conferred no benefit. RPMI/10% FCS supplemented with IL-2 and IL-21 was not significantly better than supplementation with IL-2 alone. Jurkats and PBMC's were included as control cells. By day 28, the only media which appeared to be beneficial to hybridomas was RPMI/10% FCS + IL-2 + IL-21 demonstrating a significant increase in live cells compared to any of the other medias tested (paired T-test comparing RPMI/10%FCS + IL-2 + IL-21 versus RPMI/10% FCS + IL-2 + IL-7 which was the next best media performer showed significant improvement in cell viability $p=0.0023$). We concluded from these experiments that IL-21 supplementation does appear to be beneficial to hybridoma growth and may lead to improved cell survival.

Following these observations we wanted to know if the cells were senescent. Cells had been grown in culture for 4 months, with little evidence of cell expansion with regard to cell number. Cells were however alive – therefore we wondered if they were in a resting state or if rate of death was equal to the rate of division. We sought to answer this question with a simple assay – staining the cells with with CellTrace violet – then sampling them weekly. We predicted that

if cells were proliferating we would see a loss of staining (fig. 5.23). Hybridoma cells were supplemented with IL-2 and IL-21 as demonstrated to be optimal for cell growth (fig 5.22).

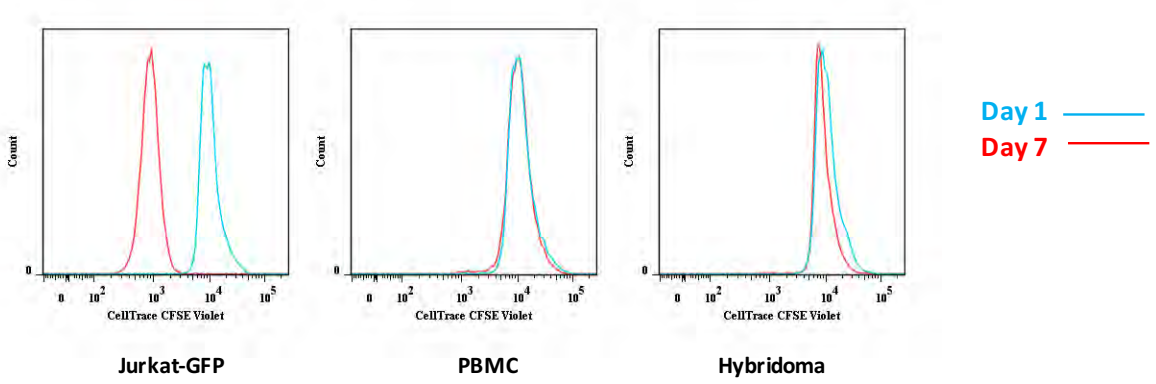

Fig. 5.23: Are hybridoma's actively proliferating? Cells were loaded on day 0 with CellTrace CFSE violet and assessed using Flow Cytometry on Day 1 (blue line) and Day 7 (red line). Cells were grown in standard cell culture media supplemented with IL2 (also with IL21 in the case of hybridomas). Proliferation should lead to loss of CellTrace violet staining and a shift of the curve to the left, as demonstrated in the jurkat plot.

Here we have demonstrated that hybridoma cells are not in an actively dividing state, as there is no reduction in CellTrace violet staining and therefore no cell division this is in contrast to the jurkat cells (control for actively dividing cells) which during the same time period have lost the CellTrace Violet staining which is considered to represent proliferation of cells. PBMC were used as control of non-dividing cells. We therefore concluded that the hybridoma cells appeared to be senescent. We have demonstrated that hybridoma cells are unstable and we therefore propose that senescence has resulted from loss of DNA during the formation of hybridomas and their subsequent instability.

We questioned if these cells were able to mount a functional response towards standard T-cell stimuli (anti-CD3, PHA, PMA/Ionomycin). We proposed if cells were senescent they may release cytokines in response to stimulation. Cells were therefore set up in triplicate alongside a well-established T-cell line. Cells were stimulated with anti-CD3, PHA or PMA+Ionomycin

on day 0 and day 6. ELISPot was then performed on day 7 to assess release of IFNγ in response to stimuli. DMSO was used as negative control (fig. 5.24).

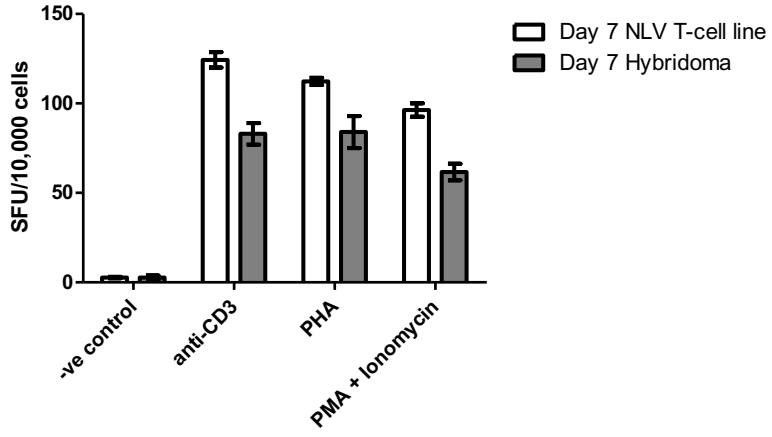

Fig. 5.24: Are hybridoma's able to mount a functional response to T-cell stimuli? Hybridoma cells were set up in triplicate alongside a well established viral T-cell line (termed NLV T-cell). All cells were stimulated with anti-CD3, PHA or PMA/ionomycin on day 0 and day 6, and analysed using ELISPOT kits specific for release of IFN-gamma. Negative control was cells treated with DMSO. Jurkat controls also used, however at day 7 the wells were completely confluent therefore unable to interpret number. Error bars represent SEM. Graph representative of 3 experimental repetitions performed in tripllicate.

This demonstrated that although the response was not the same as that seen in the T-cell line, the hybridoma line did become activated by these same stimuli and therefore could be considered as being able to mount a functional response. The evidence we have presented here suggests that hybridomas have been generated and they do appear to be functional, but in the absence of cell expansion, this clearly has limited potential as a mechanism for generating immortal expandable T-cells.

5.2.11 Can ionic forces lead to improved cell fusion?

Clearly for hybridoma formation to be successful there needs to be a method for allowing cells to be in close cell-to-cell contact and also a mechanism of cell membrane breach/fusion. In this chapter, it has been demonstrated that the most efficient method so far for generating a hybridoma was by harnessing electrical pulse (nucleofection) to either insert viral DNA (VSV-G) to aid fusion, or used after pre-treatment with anti-CD52 to the fusion partner allowing for

cross-linkage prior to application of electrical current which appeared to lead to cell membrane fusion.

Part of this PhD was spent at Harvard University, Boston, USA. As such we had access to equipment not previously available in UK. One such instrument was the Harvard ECM 2001 electroporator (BTXonline, Harvard Apparatus, MA, USA). This uses a AC current to draw cells together, followed by a pulse of DC current to breach the cell membranes and lead to fusion and proposed hybridoma formation. Because we had seen that nucleofection had been more efficient than standard protocols for fusion of fusion partner to target cells, we proposed that the ECM 2001 could also be used to fuse cells. This had not been attempted before and therefore required optimisation of suggested protocols. Cells were washed as described in chapter 2 and resuspended in BTXpress Cytofusion media. Electroporation is based on a simple process. Cells are suspended in a conductive solution (BTXpress Cytofusion media), and an electrical circuit is closed around the mixture using a modified tissue culture plate with electrodes connected to the base unit. An electrical pulse at an optimized voltage and only lasting a few microseconds to a millisecond is discharged through the cell suspension which disturbs the phospholipid bilayer which comprises the cell membrane. This leads to the formation of temporary pores. As a result, there is potential for charged molecules e.g. DNA to cross the membrane in a fashion similar to electrophoresis - or in this case allows for the cells to fuse by merging their cell membranes via the cell pores. A number of voltage combinations were attempted in order to allow enough time for target cells to come into close contact with the fusion partner cells, but not at the expense of cell viability. High voltage would lead to higher cell death (fig. 5.25).

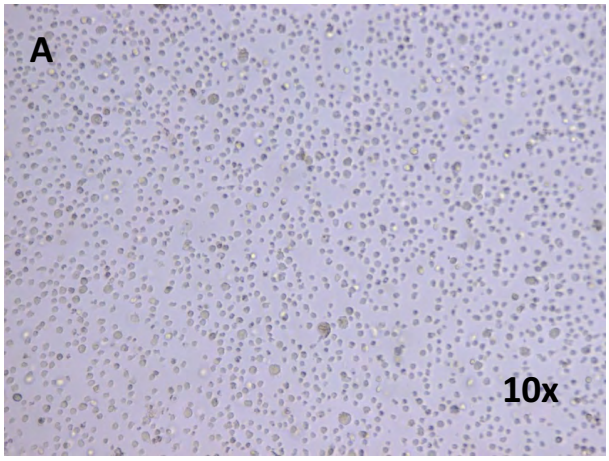

Pre-Electroporation

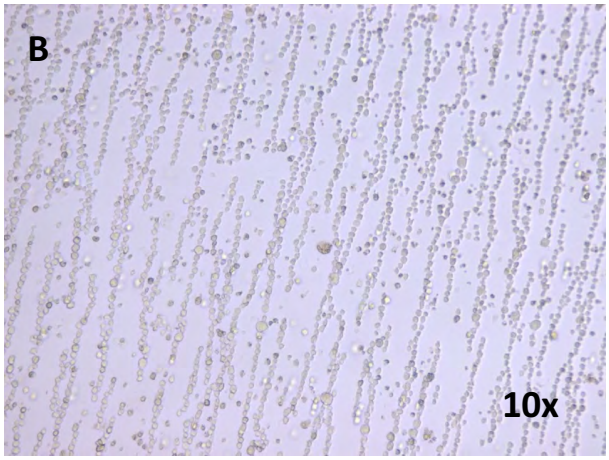

After AC pulse
Pre-DC pulse

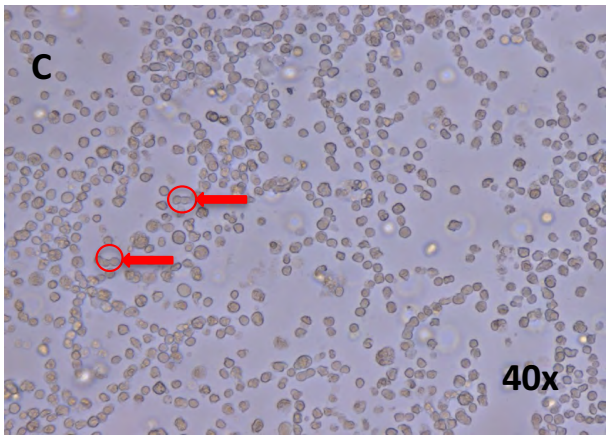

Post DC-pulse

Red circle/arrow shows fused cells

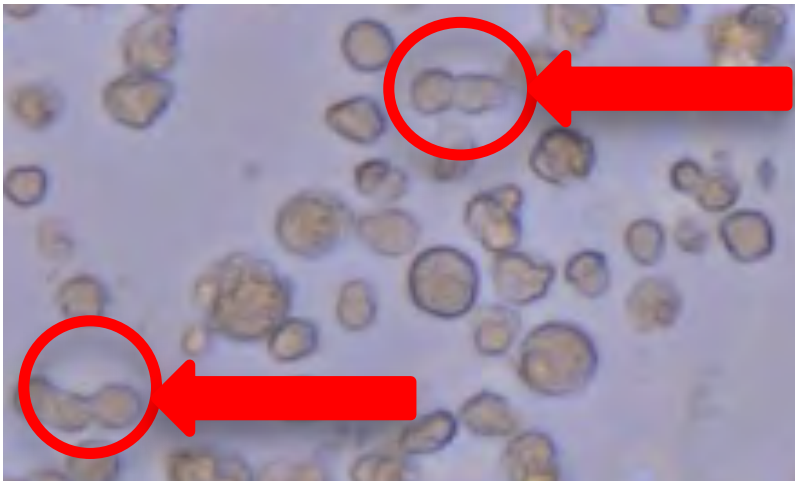

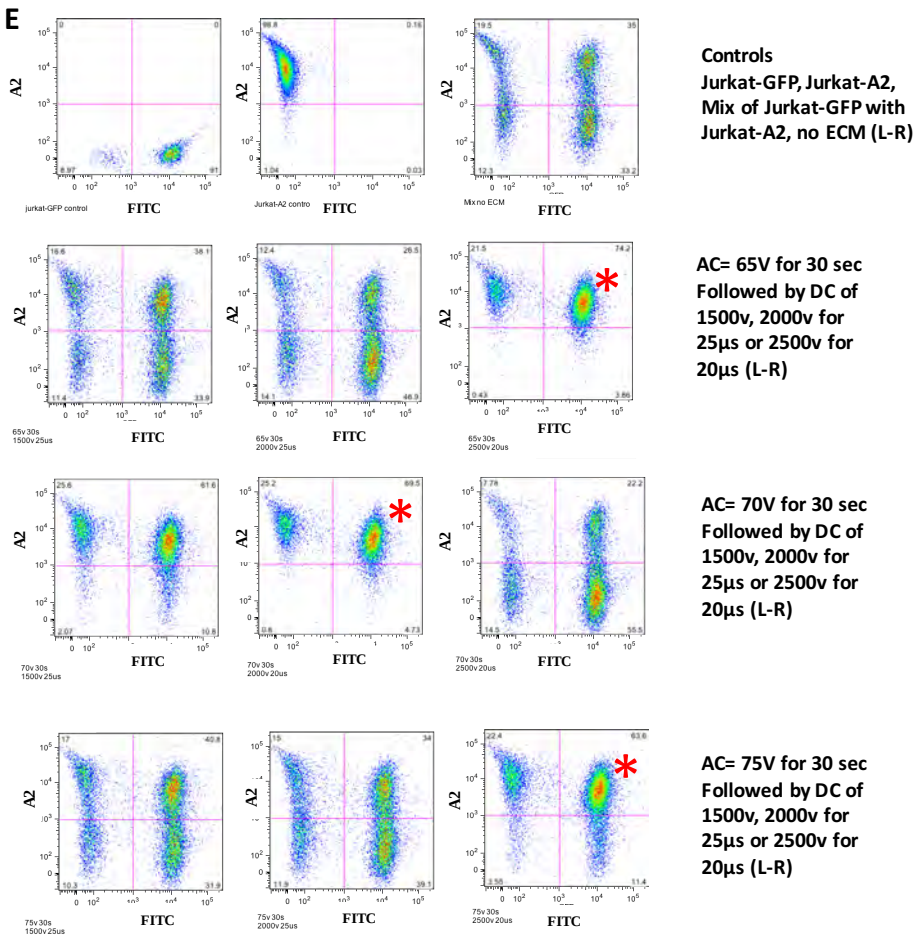

Fig. 5.25: Use of electroporation to generate hybridomas. Cell lines of interest were Jurkat-GFP and Jurkat-A2. (A) Cells were resuspended in BTXpress cytofusion media prior to application of an electrical pulse. AC pulse was applied and cells lined up due to their polarity (B) forming chains of cells. (C) Following application of DC pulse, fused cells (red circle/arrow) can be visualised using light microscope. (D) Panel C was further digitally magnified 100x to demonstrate possible fusion of cell membranes. Cells were allowed to rest at room temperature for 10 minutes prior to being transferred to appropriate tissue culture vessel and resuspended in RPMI/10% FCS supplemented with IL2 and IL21. (E) flow cytometry on day 3 following electroporation demonstrates good efficiency of hybridoma formation under a number of conditions – represented by red asterisk.Plots representative of 3 experimental repetitions performed in quadruplicate.

These data suggest that high DC pulses are needed to obtain efficient fusion of cells. In the control wells it can be seen that a relatively high proportion of cells are double positive without any intervention. It is assumed these are false positives, representing cell aggregation rather than true fusion. This was taken as the baseline DP for cells and therefore we focussed on conditions which led to higher percentages of DP cells. The most efficient combination of conditions, resulting in 74.2% DP cells was the lowest of AC voltages (65v) tested followed by the highest DC voltage (2500v). It is likely that higher AC voltages resulted in increased cell death when used in combination with high DC voltage (potentially there is an additive effect). Although 63.6% cells were DP when a combination of high AC (75v) is used with high DC (2500v), it can be seen that this is not a 'clean population of cells but more a smear of cells from single positive GFP^+ into the DP population (i.e. there is no clear distinction between the two as was seen in the mixture of cells in the absence of ECM, whereas the other tests which resulted in high DP cells – red asterisk – appeared distinct populations in a single quadrant only – not spanning two as a continuum. It is likely that this smear of cells is therefore a mixed population of cells spanning from single positive GFP into DP GFP/A2, and is likely a combination of hybridoma cells as well as aggregated cells. Due to cell line availability this experiment focussed on fusing two jurkat lines 'Jurkat-GFP' (obtained from Dr Millar, University of Biringham and previously modified to contain a GFP tag) to 'Jurkat-NLV' (obtained from Dr Bendle, University of Birmingham, a jurkat line modified to contain CMV peptide NLV-TCR) as these cells were readily available. This experiment represents a proof of principle that electroporation appears to be very efficient at generating hybridomas. Unfortunately, due to unforeseen circumstances these cells could not be analysed further as during transport from America to UK they were delayed in customs, leading to catastrophic cell loss.

In conclusion, T-cell hybridomas are not a new technology and the process of generating them is largely inefficient. By modifying the protocol either by nucleofection in the face of a fusogen, or application of electrical current in the form of electroporation we have shown that hybridoma formation could potentially be made more efficient than standard protocols using PEG as originally described. Unfortunately, although cells could be grown long term in culture they were not expandable, although did appear functional. Despite media modification we were unable to expand these cells and therefore it was concluded that hybridoma technology is not efficient enough or scaleable therefore is not useful as an experimental model that can be used in the investigation of antigen expression of T-cells and was not investigated further.

5.3 Viral transduction of T-cells

After concluding fusion and hybridoma formation is not efficient we chose to investigate viral transduction as a possible means to immortalising T-cells. This is also not a new technology, dating back to early 1990's, but more recently has again been the subject of yet another Nobel prize in 2012 for Shinya Yamanaka for Science and Technology, for his work in Induced Pluripotent Stem Cells (Takahashi and Yamanaka 2006, Takahashi, Tanabe et al. 2007, Nagata, Toyoda et al. 2009).

5.3.1 Herpesvirus saimiri transduction of human T-cells

We chose to start with the gammaherpes virus Herpesvirus saimiri (HVS) which naturally infects the Squirrel Monkey. It is non-pathogenic in this natural host (virtually all Squirrel Monkeys are carriers) but has the ability to produce T-cell lymphomas in other New World Monkeys. It is distantly related to Epstein Barr virus which has also been shown to immortalise B-cell lines in a similar fashion.

It was Biesinger et al in 1992 that first proposed the potential utility of HVS based on its ability to transform human T-cells into immortal culture lines (Biesinger, Mullerfleckenstein et al. 1992). In New World Monkeys, HVS can induce T-cell lymphomas as well as in rabbits. However Beisinger also demonstrated that it possessed the potential to immortalise primate T-cells *in vitro*. Sequences responsible for these effects have been localised to a region of the genome that varies significantly among the virus subgroups A, B, and C. Only HVS (subgroup C) has the ability to transduce a variety of human cell lines. Here the virus is seen to exist as a non-integrating circular episome, which has restricted gene expression and has a subsequent inability to produce virus particles. Of note, the transformed human cells do not allow viral reactivation despite the best efforts of a number of groups who have attempted to demonstrate this as being possible. The T-cells which are immortalized in culture are identical in phenotype as the mature activated T-cells from which they were derived, with normal CD4/CD8 expression. Also of benefit is that these cells will retain the parental cell's antigen specificity therefore leading to a potential use in immunotherapy due to this preservation of specificity (Grassmann, Biesinger et al. 1990, Biesinger, Mullerfleckenstein et al. 1992, Meinl, Hohlfeld et al. 1995, Meinl, Fickenscher et al. 1997, Hall, Giles et al. 2000).

Owl Monkey Kidney cells (OMK) were transfected with HVS as per standard protocols and the resultant supernatant used as a potent source of virus for infection of PBMC's (fig. 5.26).

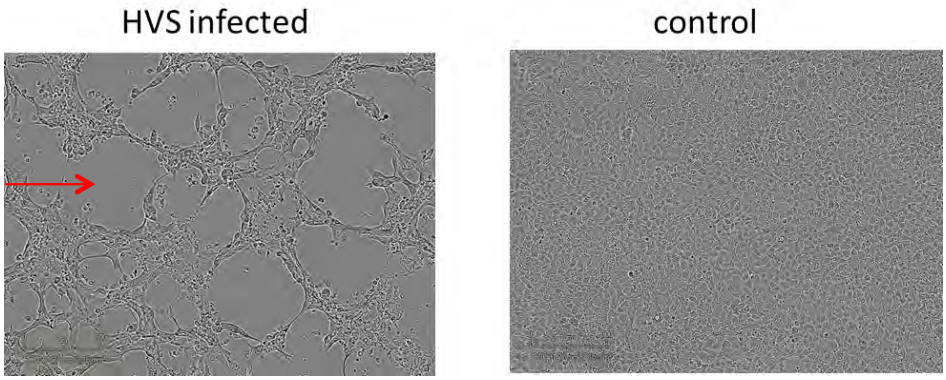

Fig. 5.26: Infection of OMK cells with HVS. Infection with virus results in areas of clearing (arrow) emerging on the once confluent adherent OMK cells. Virus particles are contained in the resultant supernatant. This supernatant is collected and titrated in order to identify optimal concentration for infection.

Following this we sought to investigate if we were able to maintain T-cells in culture and whether HVS could promote this. We hypothesised that based on previous authors' data, HVS should be able to immortalise T-cells. In order to test this, fresh healthy donor derived PBMC's were magnetically sorted and the $CD8^+$ fraction were set up in 24 well plates in triplicate ($1x10^6$/well) - fig 5.27. $CD8^+$ cells were selected as we proposed these cells as being the phenotype that would be most useful to this project as we have sought to identify technologies for immortalising tumour-specific T-cells which we predict would be CTL's.

Virus was diluted in RPMI/10% FCS and added to the sorted PBMC's. Cells were then incubated at 37c/5% CO2 overnight. On day 1, the media was supplemented with 100 units IL-2. On day 5 cells were washed and resuspended in fresh media containing 100units IL-2. On day 7, cells were stained for CD3 and CD8 and analysed using flow cytometry (fig. 5.27a). This initial data appears to suggest HVS is capable of supporting $CD8^+$ T-cell growth, with an optimum concentration of virus being 1:100 (see appendix for calculations). 41.3% of live cells were $CD8^+CD3^+$ T-cells, versus 30.3% in the non-infected cells. Using Student's paired t-test, this is a significant increase ($p<0.02$) when compared to non-infected cells. However, the number of live lymphocytes was drastically reduced as the amount of HVS increased by 50% (fig. 5.27b) suggesting that toxicity of HVS outweighs any benefit conferred by this to propagating $CD8^+$ cells, and the reality is these cells were all lost by day 21 in all wells, which we proposed was as a result of HVS toxicity.

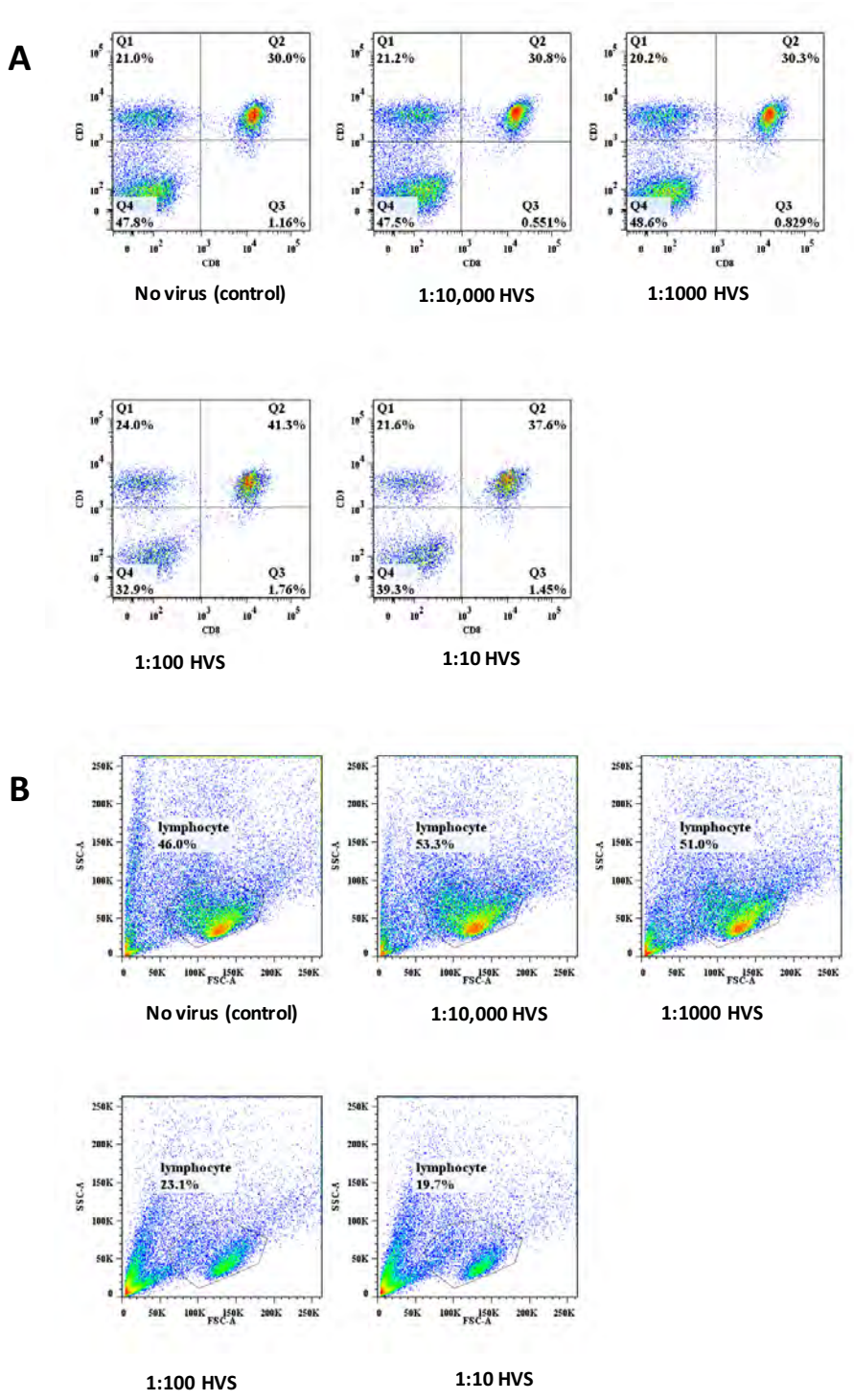

Fig. 5.27: Fresh healthy door-derived PBMC's were magnetically sorted and the CD8$^+$ fraction were infected with HVS on Day 0. Cells were incubated at 37c/5% CO_2 and (A) flow cytometry was used to assess CD8-positivity after 1 week incubation. (B) The number of live cells halved when comparing no virus control (46% lymphocyte) to 1:100 HVS (23.1% lymphocyte). Plots representative of 3 experimental repetitions.

5.3.2 Does cell number or media supplementation affect transduction efficiency?

We sought to identify a process that could support cells in this early period after viral infection and attempt to overcome the cell death which is due to viral toxicity. We hypothesised that lower cell numbers may lead to better outcome, as this was based on the observation that cells appeared overcrowded shortly after viral infection, and we wondered if this may affect outcome. Also, based on the previous observation that PBMC's and indeed T-cells grow better in the presence of IL-2 and IL-21, we proposed testing whether media supplementation may be able to maintain cells in culture following viral infection. Finally we questioned whether cells needed to be stimulated and therefore activated to be successfully infected. Activating the T-cells allows them to enter the cell cycle and we hypothesised that this may allow infection of the T-cells by HVS. In non-dividing cells, viral transduction doesn't work in all cases, so with retroviral transduction the cells need to be dividing to get the DNA into the genome. However, lentiviral transduction can be done in non-dividing cells so it is not the same for every virus. Biesinger described activating PBMC's with PHA yielding $CD8^+$ T-cells. These are the phenotype of choice to this arm of the project and therefore we proposed that this would be beneficial, as HVS transformation in the absence of PHA-stimulation appears to yield CD4 T-cell lines (Biesinger, Mullerfleckenstein et al. 1992).

5.3.3 Media supplementation with cytokines does not improve cell line longevity in culture.

Standard media for growth of PBMC's following HVS infection is RPMI/10% FCS supplemented on day 3 with 100 units IL-2. Having noted previously that higher concentrations of IL-2 and addition of IL-21 benefitted T-cell growth (figs. 5.21, 5.22), we proposed that this may benefit HVS-transformed cells also. Cells were set up in triplicate and supplemented with different concentrations of IL-2, IL-21 and a combination of both. PBMC's

were transformed with HVS at concentrations as previously determined (1:10,000, 1:1000, 1:100 and no virus) – fig 5.28. Following viral transformation they were resuspended in standard media (RPMI/10% FCS) and supplemented on day 3 as described previously.

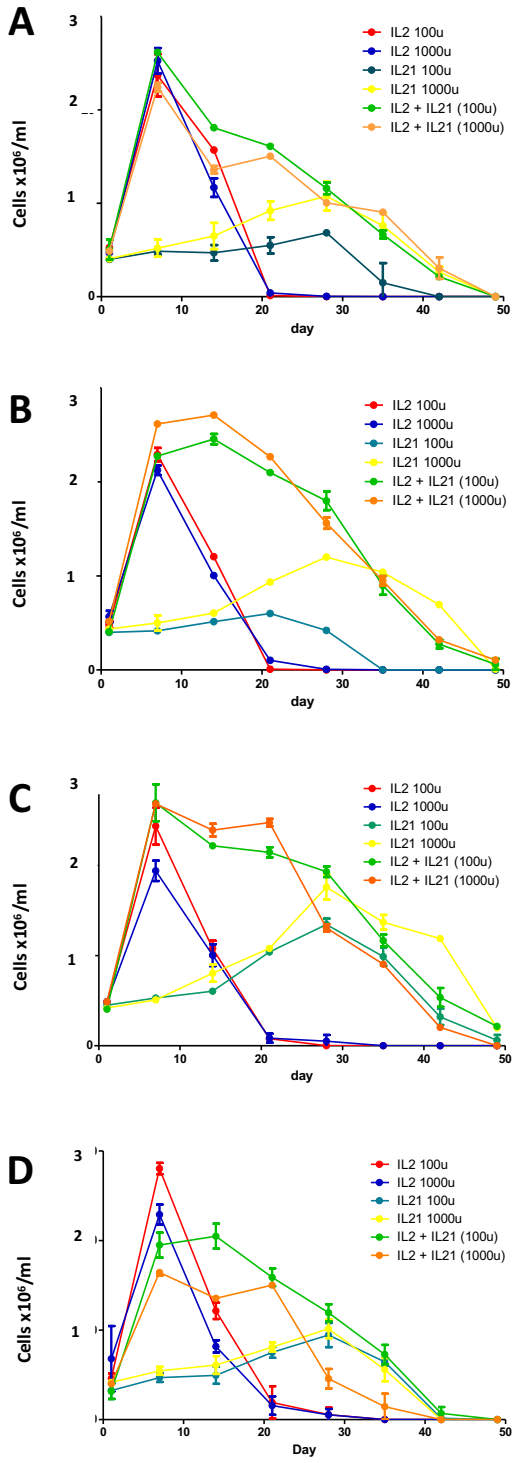

Fig. 5.28: Effect of cytokine supplementation to T-cell growth. It was proposed that as previously cytokine supplementation can help maintain cells in culture. This experiment assessed addition of IL2 and IL21, separately and in combination to check for a synergistic effect. Healthy donor derived PBMCs were counted at weekly intervals using coulter counter and microscope with trypan blue staining to assess dead:live ratio. (A) are control PBMC cells. (B) are cells infected with 1:10,000 HVS. (C) are PBMC cells infected with 1:1000 HVS. (D) are PBMC cells infected with 1:100 HVS.

Firstly when comparing control to the virally transformed wells there is little difference in overall longevity of cells in culture – with only 1:1000 still having live cells at day 50 (wells supplemented with IL-21 or IL-2+IL-21) – fig. 5.28c. When considering the cytokines separately it is clear that IL-2 supports cells in the short term – but there is no significant difference longer term, with all showing death of cells by day 21, suggesting IL-2 is stimulating growth of cells in PBMC's such as NK cells. It can be seen that the 1:100 transformed well did have a good response to IL-2 100units at day 7 with 28% cells live compared to 22% treated with 1000 units IL-2, but not sustained. These results indicated that 100 units of IL-2 was optimal as when 1000 units was added, more cell death was observed which could be the results of 'over-stimulation'. In contrast IL-21 1000 units was demonstrably better than 100 units at supporting cell growth in all wells except 1:100 HVS, this effect appeared to start around D15 peaking at day 30 before gradually tailing off again. We considered the synergistic effect of IL-2 with IL-21, and hypothesised IL-2 would support early growth and then the IL-21 would support latter growth of cells. This was observed up until around day 35, after which IL-21 1000units became the best at supporting cell growth (seen best in the 1:1000 wells – fig 5.28c). From these observations we can see that IL-2 and IL-21 do support growth and their effects do appear to be additive with regards to supporting growth/viability, however this is not sustainable long term. We concluded media supplementation with cytokines did not improve overall cell survival in the long term, although short term benefit can be seen. The caveat to this is that it is difficult to ascertain if addition of cytokines that promote cell viability of transformed cells, also promote this in non-transformed cells.

5.3.4 Cell density does not affect HVS viral transformation efficiency overall, however it does improve initial transformation

Previous observations of cells transformed by HVS appear to show that the cell number reaches a peak which is quickly followed by a rapid decline. In order to test whether this observation

was due to cell density within the culture plate becoming sub-optimal cells were set up in triplicate and starting cell number compared. Standard cell transformation prior to this was performed on $1x10^6$ cells/ml seeded. On this occasion we compared $5x10^5$ cells/ml, $1x10^6$ cells/ml $2x10^6$ cells/ml and $5x10^6$ cells/ml. Cells were transformed with virus as previously described at concentrations of 1:10,000, 1:1000 or 1:100 versus no virus. Cells were grown in RPMI/10% FCS and supplemented with IL-2 100units on day 3 (fig. 5.29 A-C).

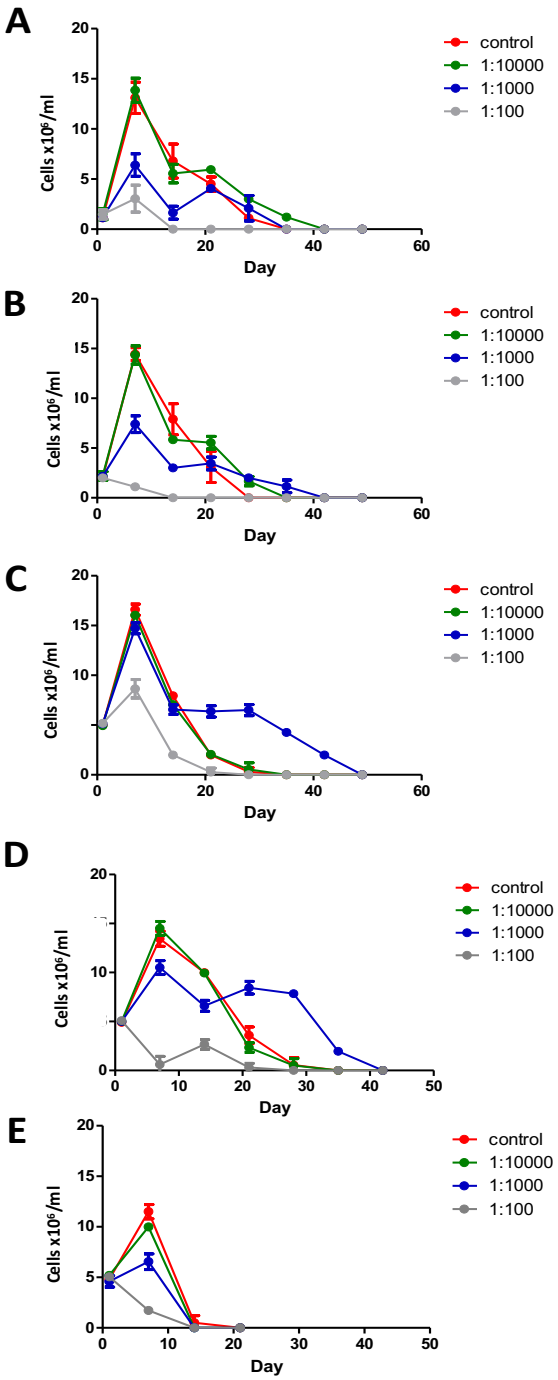

Fig. 5.29: Effect of number of cells transformed by HVS on overall longevity of line. Higher numbers of cells may result in higher transformation rate so initially we started with $5x10^5$/ml (data not shown as no cells viable at first timepoint), (A)$1x10^6$ cells/ml (B) $2x10^6$ cells/ml or (C) $5x10^6$ cells/ml. In these initial experiments cells were grown in 24w plates in RPMI/10% FCS supplemented with 100unit IL2 and split as necessary based on cell number (>$10x10^6$ cell/ml).

Higher cell numbers appeared to result in better survival therefore further experimental wells were set up starting with a cell number of $5x10^6$ cells/ml and compared either (D) not splitting the wells and allowing the cells to continue in 1x 24w or (E) splitting the cells at a set time point regardless of number on day 10 and resuspending in a 6w plate. NB cells received a media change on alternate days.

This demonstrates that starting with a higher number of cells leads to better transformation potential with cells seeded at a density of $5x10^6$ cell/ml and transformed with HVS at a concentration of 1:1000 appear to grow well, lasting longer than cells seeded at a lower density (cells start to decline between days 28 and 35 when seeded at density of $5x10^6$ cell/ml, compared with days 21-28 in cells seeded at lower concentrations. NB cells seeded at lower concentration ($5x10^5$/ml) were found to be non-viable following viral transformation (data not shown), suggesting that cells require at least a density of $1x10^6$/ml at the start of viral transformation in order to have enough cells remaining following toxic viral insult.

Based on the observation that cells initially grow well then appear to plateau we considered if this was as a result of over-confluence. In our initial experiments cells were split when they reached $1x10^6$ cell/ml. In order to investigate this further, cells were set up in triplicate and direct comparison was made between cells that were left to grow in the same 24 well plate they were seeded in (and therefore by definition became overconfluent) compared to cells which were split on day 10 regardless of cell number (fig 5.29 D,E). This demonstrated that cells left to grow and become confluent grow much better than those split early. Cells did appear to plateau again which suggested that the media components were being consumed, and following this cells rapidly declined in number between days 30 and 40 in those cells transformed with 1:1000 HVS (fig 5.29D). This led to the conclusion that there is an optimal concentration of cells above which cells are unable to be supported further. From the data collected over this experiment and observed previously this number would appear to be $10x10^6$ cells/ml, however as we have demonstrated previously, when cells are split when they reach this threshold that does not prevent them declining over time and therefore there remains the question as to how cells can be triggered to stay in culture over time.

5.3.5 Activation by media supplementation with PHA leads to increased numbers of $CD8^+$ T-cells, but does not affect long term survival

We hypothesised that supplementation with PHA would lead to better cell survival and longevity which would potentiate better virus infection and propagation. PHA (Phytohaemagluttinin) is a polyclonal T-cell activator, used as a mitogen to trigger T-cell activation and drive proliferation. It binds to the sugars on glycosylated cell surface proteins, including the TCR, and crosslinks them causing non-specific activation of the T-cells.

We hypothesised that stimulation before infection with HVS could lead to more efficient infection with HVS as the T-cells would be dividing and may be more receptive to HVS infection. We also considered whether stimulation after infection would lead to better cell longevity. It has been shown previously that stimulation with PHA could lead to preferential activation of $CD8^+$ T-cells (Reeve, Hewlett et al. 1974, Mercer and Schlegel 1979) which is the phenotype of choice for this project and therefore we predicted pre-stimulation prior to HVS transformation was the optimum condition for propagation of T-cells long term.

Fig 5.30 demonstrated that following stimulation T-cells are the predominant cell type in the previously heterogeneous soup of cells. In unstimulated cells there is a peak in T-cell number on day 14, which likely corresponds to IL-2 supplementation to the media on day 3 as previously described, however there is a rapid drop off in T-cells in the following week with numbers reduced to zero by day 21-28 (A). On assessing these cells further it was demonstrated that these cells are initially CD4 in phenotype (as demonstrated by CD4:CD8 ratio – fig 5.30E), but this ratio changes by day 14 coinciding with T-cell peak with at this stage predominantly CD8 T cells, which gradually tail off to zero by day 28 when most cells are also dead. Cells stimulated 1 day prior to HVS infection (fig 5.30B) demonstrate persistently high T-cell numbers in cells which have been infected with higher concentrations of HVS (1:100 and 1:1000), which would suggest that pre-stimulation of cells does appear to

confer some protection of cells, potentially as a result of them being activated and in the cell cycle leading to better transformation potential.

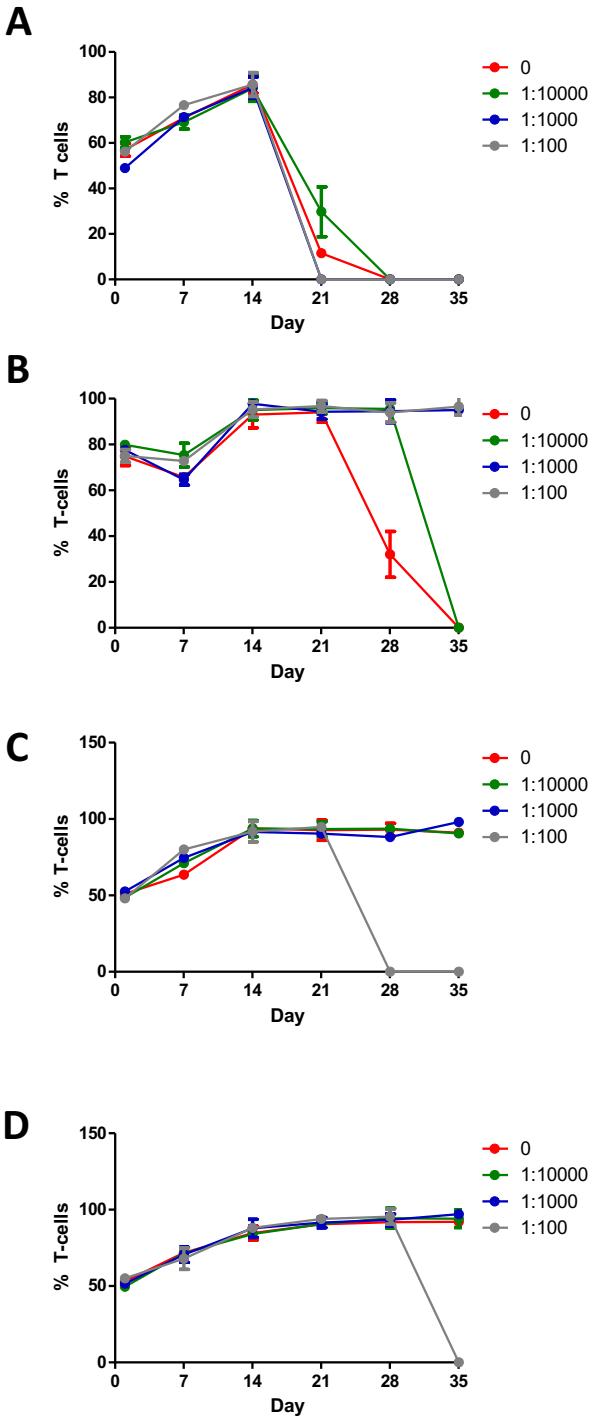

Fig. 5.30: Effect of stimulation of PBMC's on T-cell counts over time, as demonstrated by CD3$^+$ by flow cytometry. Based on previous studies suggesting PHA stimulates preferentially CD8$^+$ T-cells, it was proposed this could be beneficial in the long term to propagation and support of T-cells. PBMC's were either (A) non-stimulated, (B) stimulated 1 day prior to HVS transformation, (C) on day 3 after HVS transformation, or (D) on day 7 after HVS transformation. We first assessed total % T-cells as % of live cells which were CD3$^+$ by FACS analysis.

Further, a CD4:CD8 ratio for each experimental condition – (E) unstimulated, (F) stimulated 1 day prior to HVS transformation, (G) 3 days after HVS transformation or (H) 7 days after transformation – overleaf.

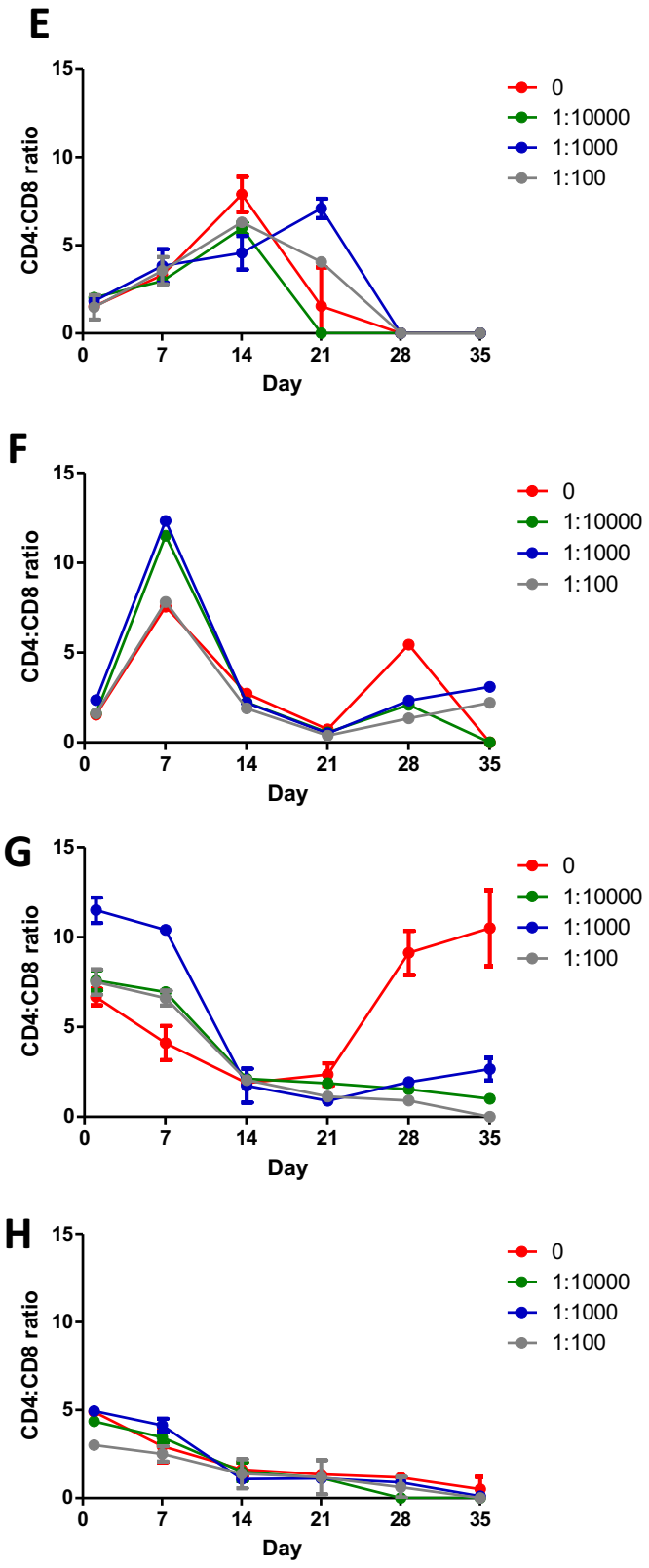

Uninfected and low concentration virus demonstrated rapid reduction of viable T-cells between Day 21 and 35 – the uninfected cell number falling off quicker than those with low

concentration HVS infection – suggesting there is a viral driven component to the T-cell survival. Perhaps more interesting is the CD4:CD8 ratio demonstrated by these pre-stimulated cells (fig 5.30F). Here it is demonstrated that initially there are higher numbers of CD8 cells : CD4 cells (as predicted by the observation that PHA predominantly stimulates CD8 cells). This rapidly changes by Day 7 post-viral transformation where the predominant phenotype are CD4 cells, followed by another switch in T-cell phenotype back to CD8 cells by Day14, which persists in all but the uninfected cells until all cells are dead. We proposed that CD4 cells proliferate following the initial expansion of CD8 T-cells (following stimulation with PHA) due to the subsequent increase in IFNγ levels, these are then exhausted leading to CD8 cells expanding as CD4 numbers drop.

We considered if stimulation of cells after infection may be beneficial with the hypothesis that stimulating cells will lead to increased cell division, which may also encompass those cells transformed by virus and therefore lead to propagation of virally transformed cells. Two time points were selected (day 3 and day 7 post viral transformation) – fig 5.30C and D. Here we show that prior to stimulation, cells are predominantly CD4, which after infection changes to CD8+ within 1 week (for instance when considering the wells infected with HVS at a concentration of 1:1000, CD4:CD8 ratio 10.34 prior to viral infection, 5.12 by day 10, and 1.98 by day 14) - fig 5.30E-H. NB the starting number of CD4 cells was higher than expected (usually in region of 3:2) and it is presumed this donor may be recovering from a recent illness. This trend of being predominantly CD8 cells continues in all virally transformed cells until the point that all cells are dead. Cells stimulated on day 7 with PHA showed a steady increase in CD8:CD4 suggesting $CD8^+$ cells are potentially increasing in number in response to viral infection. When the immune system first encounters a viral infection it is the CD8 T-cells that are first immobilised, this is then followed by a CD4 response, which is presumably the process occurring here in response to HVS. Cell numbers in these wells are similar to those seen under

the other conditions tested so it is not the case that these cells were at lower baseline numbers, therefore the only conclusion possible is that viral recognition leads to a predominantly CD8 phenotype due to antigen presentation with only CD8 peptides presented.

We concluded from this set of experiments that pre-stimulation with PHA did indeed lead to predominantly $CD8^+$ cells, which when infected with HVS, and we considered if this had any long term effect on cell number.

Fig. 5.31 demonstrates what effect PHA stimulation has on the length that cells can be maintained in culture. Stimulation 1 day prior to viral transformation appears to confer the greatest benefit (fig. 5.31B) with cells infected with virus at a concentration of 1:1000 peaking in number on day 21, however this is not sustainable with rapid decline in cell number and eventual loss by day 49. This is an improvement compared to cells not stimulated (fig. 5.31A) which shows loss of cells by between day 21-28. However, long term sustainability was not maintained. Stimulation of cells after viral transformation did not confer any benefit when stimulated on day 3 and appeared to be deleterious suggesting the initial viral insult lead to intolerance of the PBMC's to further stimulation leading to apoptosis (fig. 5.31C). Stimulation on day 7 conferred limited benefit (fig. 5.31D), and cells were sustained at high numbers for a shorter time compared to cells pre-stimulated 1 day prior to viral infection. Therefore, we concluded that pre-stimulation with PHA was beneficial to viral transformation, presumably as cells had entered the cell cycle and therefore were easier to transform as actively dividing, however this benefit was shortlived and we were unable to maintain cells longer than 49 days in culture.

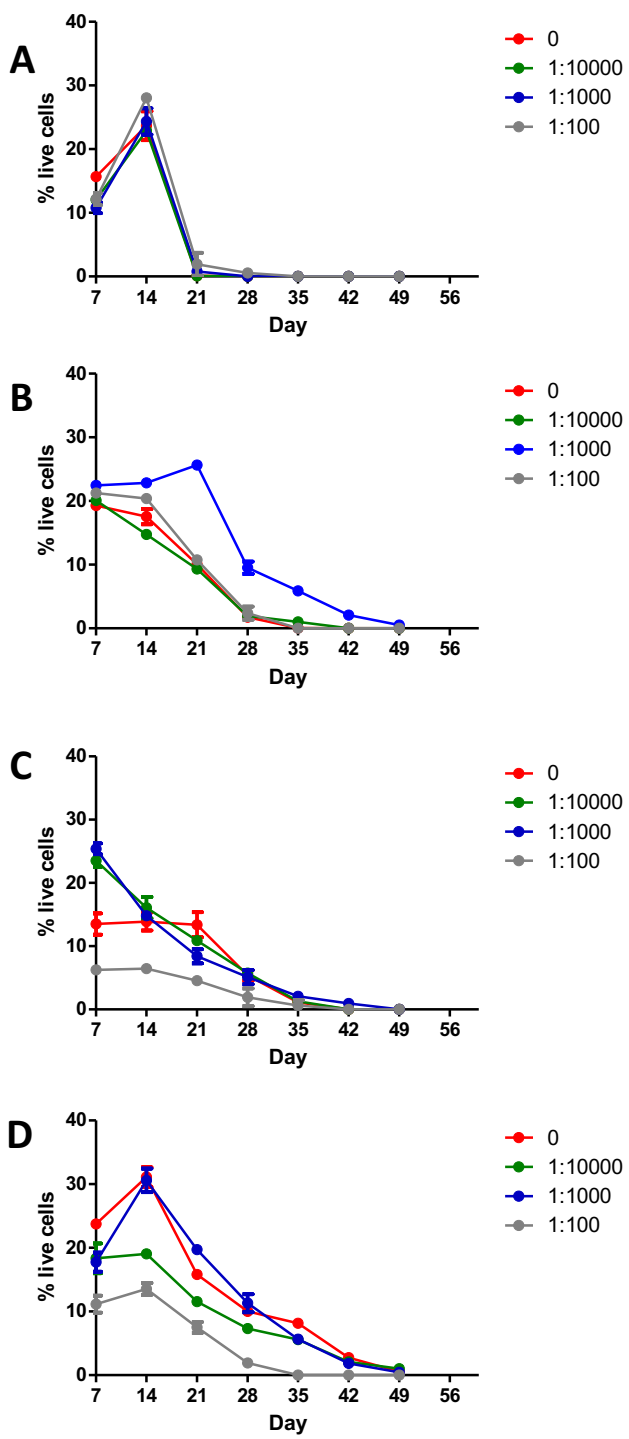

Fig. 5.31: Effect of stimulation of fresh healthy donor derived PBMC's by PHA.
Cells were set up in triplicate as previously described and grown in RPMI/10% FCS supplemented with IL2 100 units on day 3. (A) unstimulated cells were included as a control. (B) are cells stimulated on day 1with PHA prior to HVS transformation as described previously.
Stimulation after infection with HVS has a deleterious effect if stimulated on day 3 (C) with rapid decline in cell number already demonstrated by day 7 Stimulation at day 7 demonstrated a brief recovery in cell number (D).

From these experiments we concluded that cell transformation with HVS was unlikely to have use as an in vitro model for T-cell antigen recognition in the longer term and therefore no further time was dedicated to this process.

5.4 Human Induced Pluripotent Stem Cells (HIPSc) – are reprogrammed adult somatic cells a useful addition to the field of immunotherapy?

In the first few days after conception, an embryo consists of pluripotent cells which can develop into all cell types in the body. In 2006, Shinya Yamanaka found a new way to 'reprogramme' defined adult, specialized cells to turn them back into stem cells. He was able to do this following the observation of a number of different transcription factors which have been found in embryonic stem cells which were felt to contribute to this cell's pluripotency (Nichols, Zevnik et al. 1998, Niwa, Miyazaki et al. 2000, Chambers, Colby et al. 2003, Cartwright, McLean et al. 2005).

Following on from this initial discovery, there were questions raised as to clinical utility of hIPSCs, with doubts cast on our overall understanding of reprogramming and pluripotent potential (Okita, Ichisaka et al. 2007, Wu and Hothedlinger 2011). Since then much work has gone into investigating the potential clinical reach of IPSc and also the means by which the Yamanaka factors are transduced. Although initially retroviruses and lentiviruses were used to make IPSc, there has been a recent transition to use of sendai virus instead. The reasons for this are many but the main benefit is that this is a non-integrating parainfluenza-like virus and is easily cleared from the system, and does not lead to gene mutagenesis (fig. 5.1). For any system being considered for clinical utility, there needs to be no genomic footprint left behind and therefore this is a safe approach to consider (Cao, Loh et al. 2012, Rao and Malik 2012, Malik and Rao 2013).

In 2013, two groups described the use of IPSc in regenerating or rejuvenating exhausted T-cells, with clear clinical implications (Nishimura, Kaneko et al. 2013, Vizcardo, Masuda et al. 2013). Both groups described exhaustion of T-cells and the subsequent technology used to generate iPScs from reprogrammed mature cytotoxic T-cells. These were subsequently redifferentiated into "rejuvenated" expandable T-cells which clearly has very broad

applications for adoptive immunotherapy in both cancer and infections such as HIV. These two works have led to the belief that a focus on reprogramming of the immune system may provide a translational element to iPSc technology. Such an approach affords a potentially limitless supply of antigen-specific T-cells to target a range of diseases that could be delivered in a scalable manner to reach all patients in need and bypasses the issue of antigen-specific T cell exhaustion. These ‘‘rejuvenated’’ cells were shown to demonstrate killing potential on an antigen-specific basis with similar TCR rearrangements as seen in the parent cells from which they were derived.

hIPSc can be patient specific and therefore could negate the need for immunosuppression for instance in the right setting. Alternatively using donors who had a haploidentical genotype is a potential option; however it may be advantageous to consider some of the newer technologies currently under intense investigation internationally to potentially knock out multiple HLA alleles such as CRISPR technology.

Also in 2014 a number of controversial papers emerged revealing new techniques for making iPS cells, including a study where cells were exposed to extreme conditions (in this case acidity for a short period of minutes) and the emerging colonies 2 days later can be demonstrated to be iPS cells with the ability to be transformed into functional cells (Obokata, Wakayama et al. 2014, Obokata, Wakayama et al. 2014, Obokata, Wakayama et al. 2014). Although these papers were subsequently retracted, it does demonstrate the global enthusiasm for development of a novel technology which can revolutionise this field.

5.4.1 hIPSc can be derived from human T-cells

Most immunotherapies rely on activated CTL’s, with the resulting cells exhibiting only partial killing efficiency, and as a result this is not usually sufficient to result in cure. This is partly due to the short lifespan of activated $CD8^+$ T-cells, and this is hampered by antigen-induced

cell death (Willimsky and Blankenstein 2005, Mescher, Agarwal et al. 2007, Mescher, Popescu et al. 2007, Buschow, Charo et al. 2010). The idea of using hIPSc to expand antigen-specific T-cells is appealing as it could overcome this inactivation. Following the work by Nishimura et al and Vizcardo et al, where T-cells were rejuvenated by this method, we proposed that sendai viral transduction of the Yamanaka factors could be used to transduce antigen-specific T-cells with resultant cells demonstrated to have pluripotent potential and represent IPSc (Nishimura, Kaneko et al. 2013, Vizcardo, Masuda et al. 2013).

In order to test this hypothesis, a viral NLV-specific T-cell clone was chosen and cells were transduced with the Yamanaka factors using a commercially available Sendai virus kit (Invitrogen, Paisley, UK), by methods described in chapter 2. Using protocols as developed by Professor Ludovic Vallier at Cambridge University (Vallier 2015), cells were grown in media which allowed optimal transduction for 9 days, after which they were infected with virus as per the MOI recommended based on batch number and then transferred to appropriate culture vessels (pre-coated with 1% gelatin, and a monolayer of CF6 Mouse Embryonic Feeder cells (MEF's – Cambridge Biosciences, Cambridge UK) used to support emerging IPSc growth (fig. 5.32).

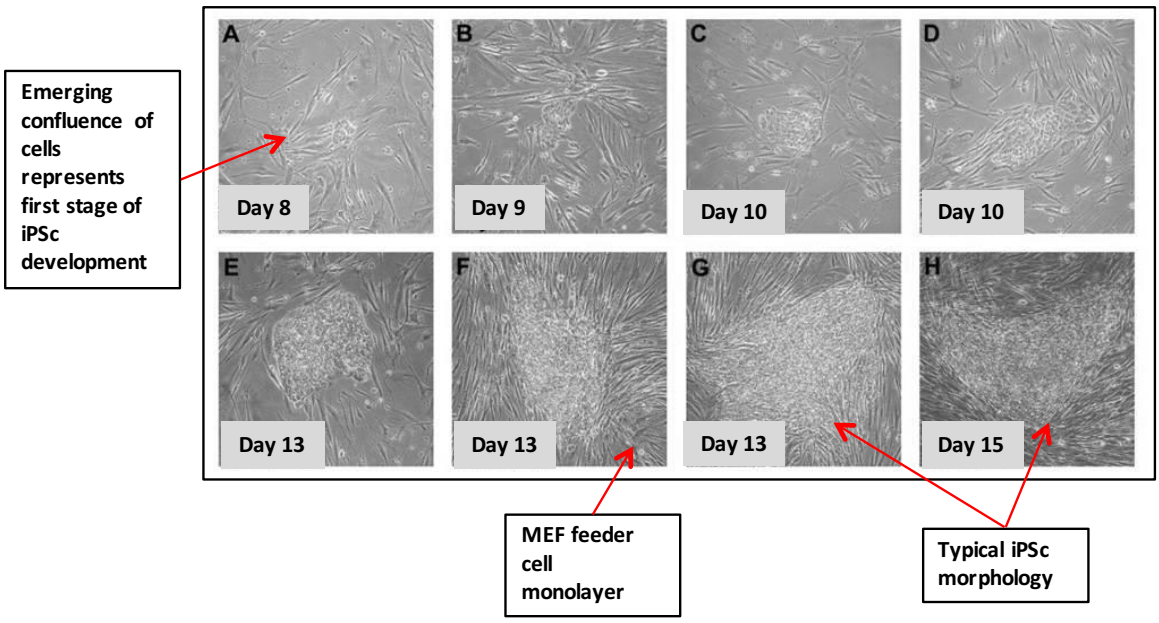

Fig. 5.32: Typical appearance demonstrating the progression in change of morphology of emerging iPSc. T-cells were transduced with sendai virus to incorporate the Yamanaka factors on day 0 and grown on a mouse embryonic feeder cell (MEF) monolayer. Typical first signs of an emerging iPSc colony are clumping of cells as seen in A and B. These become more confluent as colonies emerge forming the typical iPSc shape by day 13.

Following emergence of IPSc colonies, it was necessary to characterise them to confirm complete differentiation and thus confirm pluripotency. Pluripotent stem cells possess alkaline phosphatase on their cell surface when in the undifferentiated form. Therefore staining cells for this enzyme is used as a surrogate marker for pluripotent potential (fig. 5.33). Immunodetection is used to stain for stem cell markers, including c-myc, Oct-4, Sox-2 (fig. 5.34). IPSc colonies were selected based on morphology and stained for genes indicative of being a stem cell, and included the Yamanaka factors which were transduced into the cells using SeV. We proposed that if a cell had been adequately differentiated, then it would express alkaline phosphatase (a marker of pluripotent potential) as well as stem cell marker genes such as Oct-4, Sox-2, c-Myc. Visualisation was performed with 4', 6-diamidino-2-phenylindole (DAPI) a fluorescent stain that binds to DNA, providing a 'photofootprint'.

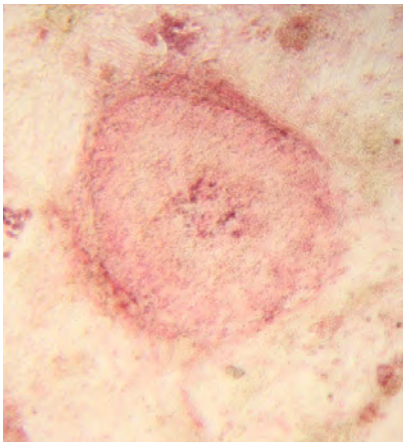

Fig. 5.33: Demonstration of pluripotent potential. iPSc colonies were stained for alkaline phosphatase a marker of pluripotency – a key feature of iPSc.

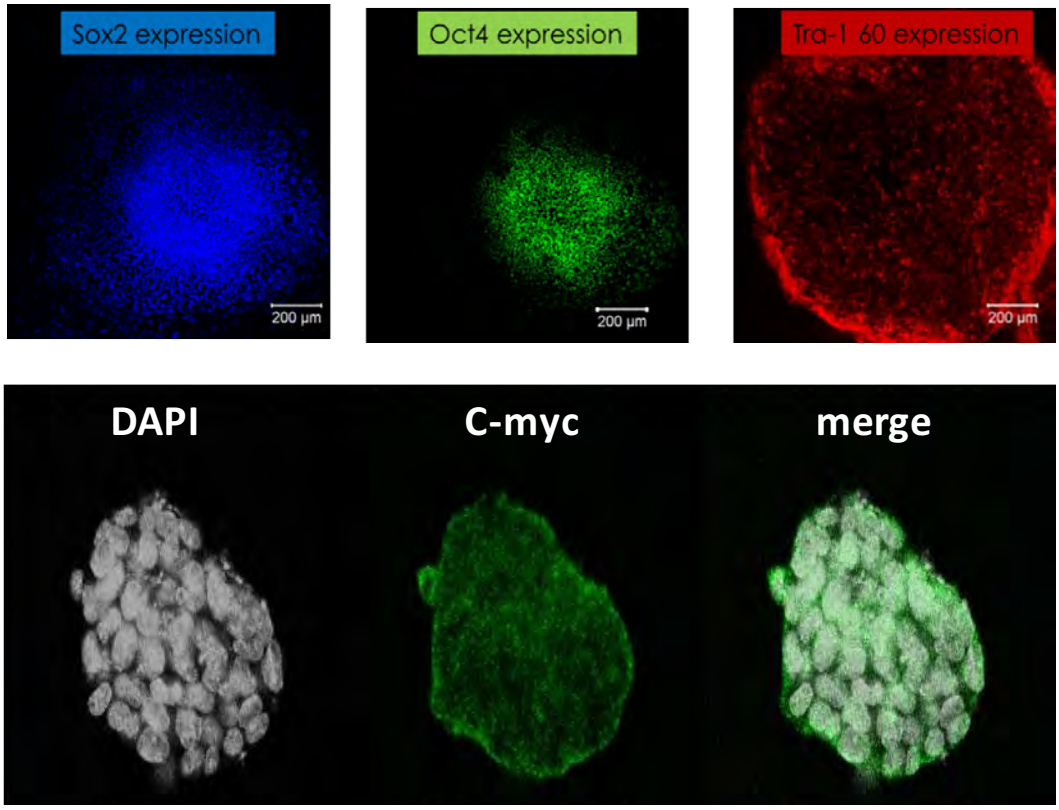

Fig. 5.34: Immunostaining for stem cell markers using confocal microscopy. iPSc colonies were selected out based on morphology and expanded from the pool of emerging cells. These colonies were grown on microscopic cover slips and stained as per standard protocols and fixed to microscope slide prior to analysis using confocal microscope. Imaging performed with the assistance of Dr Maelle Lorvellec.

Finally qPCR was used to validate clones against the standard Human Embryonic Stem Cell (hESc) line H1 (fig. 5.35). hIPSc lines were selected based on their pluripotent potential and stem cell gene expression when compared to hESc H1, with the optimal lines being those with as close as possible expression to H1.

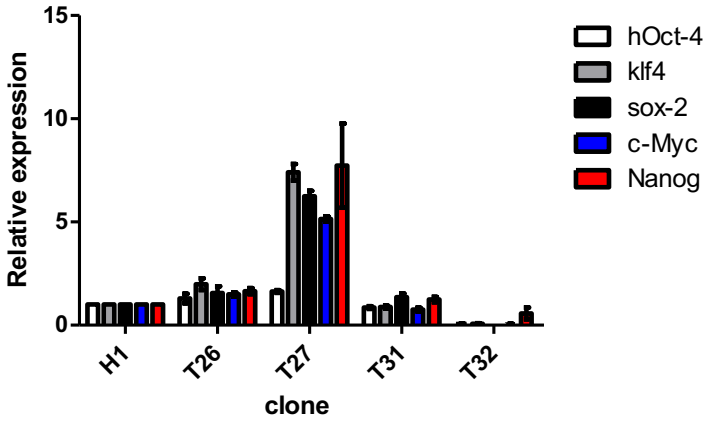

Fig. 5.35: Expression of Stem Cell marker genes by 4 hIPSc lines derived from an NLV-viral T cell clone (T26, T27, T31 and T32) compared to the hESc line H1. Ideally hIPSc colonies should have a similar expression of these stem cell marker genes (hOCT-4, Klf4, sox-2, c-Myc and Nanog) as the hESc. Too high expression suggests overexpression of markers as seen in T27, therefore this would be discarded as expression here is up to 10x that the standard set by hESc. Too low expression suggests incomplete transduction as seen in T32. Two lines were taken forward to further expand – T26 and T31 as expression is very close to that seen in hESc H1.

Finally cells were differentiated into the 3 germ cell layers to confirm pluripotent ability (fig. 5.36) by supplementing the growth media with various cytokines and growth factors (see also appendix 1 for scematic representation of germ layer differentiation) (fig. S1A-C):

1) **Mesoderm**: Activin (cell proliferation), FGF2 (fibroblast growth factor family). The FGF family of proteins have the ability to induce mitosis and angiogenesis. This is in part due to their binding of heparin. As a result of thiese activities, FGF has an obvious role in a number of key cancer pathways including tumour growth as well as being implicated in other key biological processes such as neurological development. BMP4 (a signalling molecule required for early embryonic differentiation and the establishment of a dorsal-ventral axis. BMP4 stimulates differentiation of overlying ectodermal tissue), Ly294002 (strong inhibitor of phosphoinositide 3-kinases (PI3Ks)), aminopyrimidine. Using CHIR99021, GSK-3β activity is blocked resulting in embryonic stem cell renewal). Differentiation was measured using relative protein expression for Brachyury (which is known to regulate mesoderm differentiation; and

Eomes (The Eomesodermin/Tbr2 gene), which is know to regulate a number of developmental processes) - fig S1A.

2) **Endoderm**: Activin, FGF2, BMP4, Ly294002, CHIR added at different time points in order to differentiate cells into endodermal germ layer. Bone morphogenetic protein-4 (BMP-4) has the ability to vary it effects based on the duration of exposure. For instance, short term it has been shown to induce mesoderm, whereas longer term it has been shown to differentiate endoderm. In order to measure its effects, the relative expression of FoxA2 was measured (due to its role indevelopment of endoderm systems). In addition to this we measured relative expression of hSox17 (This gene encodes a member of the SOX (SRY-related HMG-box) family of transcription factors, which plays a pivotal role in embryonic development and cell fate. It may act as a transcriptional regulator after forming a protein complex. It modulates transcriptional regulation via WNT3A and inhibits Wnt signalling. It is a probable transcriptional activator in premeiotic germ cells) - fig S1B.
3) **Ectoderm**: SB431542 (is an inhibitor of transforming growth factor-beta), FGF2, Noggin (Noggin is a signalling molecule that promotes somite patterning in embryonic development. It is released from the notochord and regulates bone morphogenic protein during development. The absence of BMP4 lead to the patterning of the neural tube and somites from the neural plate in the developing embryo). This was measured by comparing relative expression of Nestin (necessary for cell survival and regeneration of neural progenitor cells) and hSox1 which is involved in regulation of the developing embryo and cell fate - fig S1C.

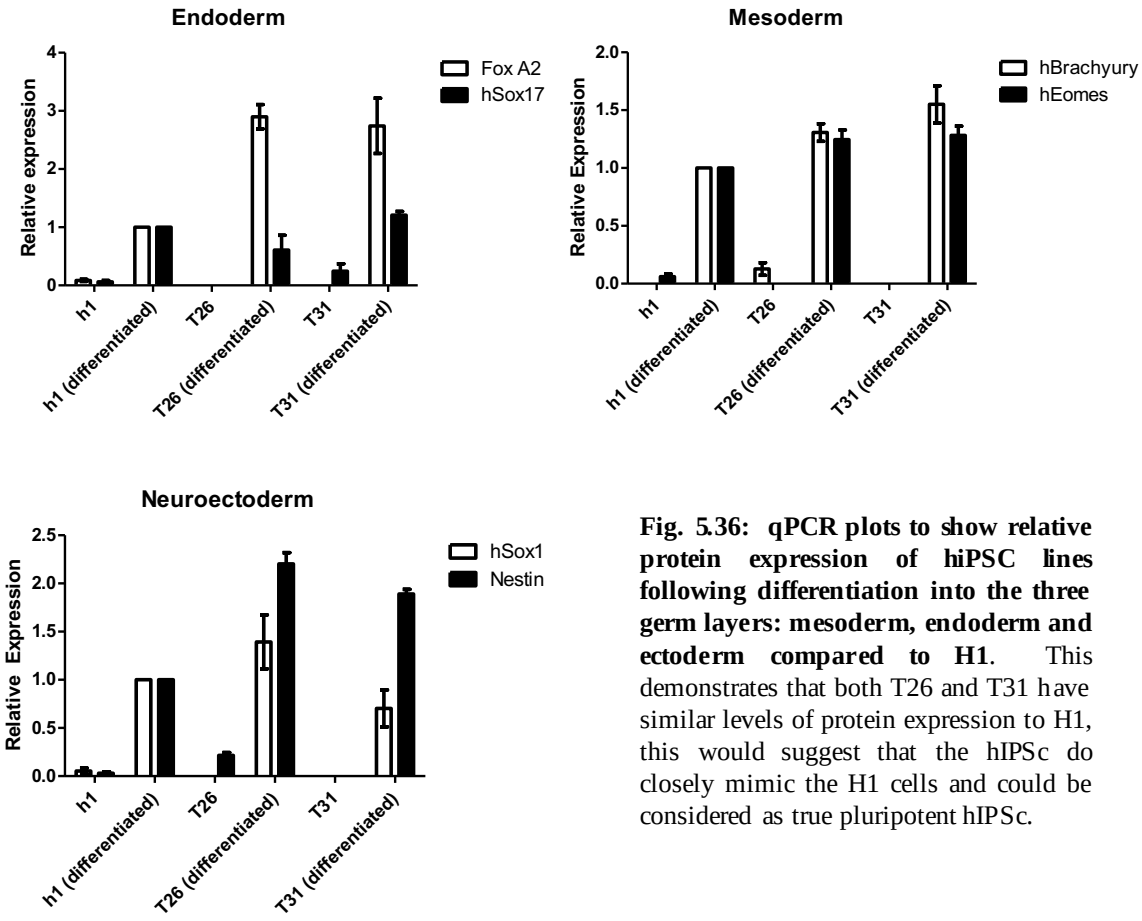

Fig. 5.36: qPCR plots to show relative protein expression of hiPSC lines following differentiation into the three germ layers: mesoderm, endoderm and ectoderm compared to H1. This demonstrates that both T26 and T31 have similar levels of protein expression to H1, this would suggest that the hIPSc do closely mimic the H1 cells and could be considered as true pluripotent hIPSc.

Pluripotent stem cell the lines should express protein at a similar level to the H1(fig 5.35, 5.36). From the clones tested, both T26 and T31 represent hIPSc that were closely resembling H1 in terms of protein expression, alkaline phosphatase secretion and the ability to be differentiated into the three germ layers (using paired t-test we demonstrated no significant differences between H1 and either T26 or T31) – fig 5.35. The clones were labelled T26, T27, T31 and T32 (T referring to them being derived from a T-cell and the number refers to the point they were selected from emerging colonies). Clones T26 and T31 were selected to be expanded further and differentiated into the different germ line layers (fig. 5.37).

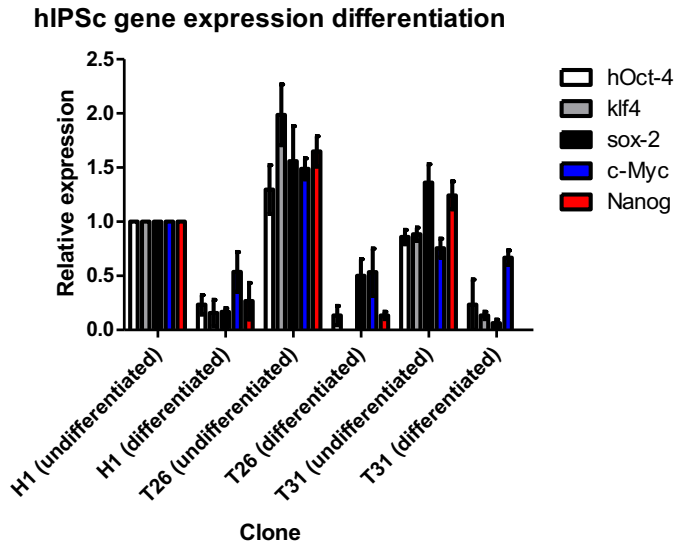

Fig. 5.37: Stem cell marker gene expression of hIPSc clones compared to the hESc clone H1. H1 was taken as the standard to which the hIPSc should be compared. Protein expression pre-differentiation was on the whole similar to the H1 cells. After differentiation expression reduced (which would be as expected) across both hIPSc lines and also the hESc line H1. This demonstrates loss of pluripotent potential following differentiation. In this case cells were differentiated into endoderm and the relative protein expression of each line compared to undifferentiated cells and H1. Similar plots were produced for the other germ layers.

Clones T27 and T32 were discarded as the protein expression suggested possible incomplete transduction. These cells were expanded exponentially in culture and intermittently sampled to check they still represented the early passages (data not shown). We concluded that differentiation of adult T-cells into hIPSc could be a valid method for expansion of T-cells *in vitro* of desired phenotype. This is proposed as a method for immortalising T-cells. Cells can be expanded exponentially, and with the right growth conditions this could continue indefinitely. We therefore proposed this as a method for the capture and expansion of desired T-cells. The next challenge was to induce these iPS cells to be differentiated back along the haematopoietic lineage.

5.4.2 OP9DL1 cell co-culture can support haematopoiesis in embryonic stem cells

Following the demonstration that we can transform T-cells into IPSc using sendai viral transduction, and thus potential to be converted into any developing cell in the body, we therefore proposed that these IPSc could be expanded in this fashion providing a limitless

supply of cells with which to work. Vizcardo and Takahashi both demonstrated it was possible, given the right growth conditions, to transform these IPSc into rejuvenated T-cells (Takahashi and Yamanaka 2013, Vizcardo, Masuda et al. 2013). Both studies discuss the use of OP9DL1 co-culture systems.

The OP9 stromal cell line is a well established line derived from the bone marrow of OP/OP Mice (Kodama, Nose et al. 1994), and found to be macrophage colony-stimulating factor (MCSF)-deficient. A number of studies have demonstrated its potential for lymphopoiesis from HSCs (Ueno, Sakita-Ishikawa et al. 2003) and ESCs (Nakano, Kodama et al. 1994). Stromal cells have also been implicated in diferentiation of haematopoietic cells, as a result of cytokine production. It is MCSF which is pivotal to myeloid differentiation. It is the inability to perform this role by OP9 cells which led to B-cell differentation from ESCs, due to a reduction in ESC-derived myeloid cells, which otherwise would have interrupted lymphopoiesis.

As a result of the observations above, OP9 cells have become a model system for the demonstration of lymphopoietic induction from a vast number of sources. One issue identified in this system is with the lack of T-cells generated using this system. It is however possible to do so in the presence of specialised cytokines, and it has been proposed that it is these that provide that missing link for supporting differentiation of T-cells from stem cells.

Notch signalling has been shown to regulate cell fate (Artavanis-Tsakonas, Rand et al. 1999) - fig. 5.38.

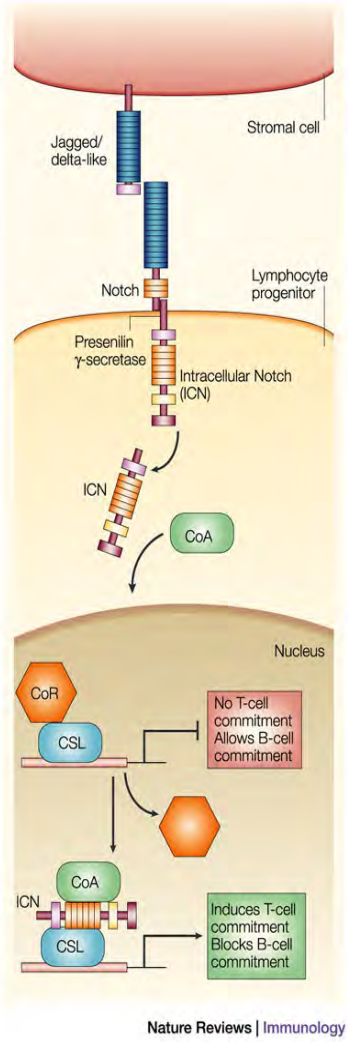

Fig. 5.38: The Notch-signalling pathway is an evolutionarily conserved pathway that controls many cell-fate decisions throughout ontogeny. Notch signalling is initiated by the interaction of Notch receptors with Notch ligands on neighbouring cells. In vertebrates, these ligands consist of two gene families, jagged and delta-like. Notch ligands that are expressed by stromal cells bind to Notch receptors on haematopoietic progenitors, inducing the presenilin-dependent gamma-secretase-mediated cleavage of intracellular Notch (ICN). ICN translocates to the nucleus, where it interacts with a transcriptional co-activator (CoA, mastermind-family member), which in turn displaces a co-repressor complex (CoR) containing silencing mediator of retinoid and thyroid hormone receptors (SMRT) and histone deacetylase 1 (HDAC1) from its association with the DNA-binding protein CSL (CBF1/RBP-Jkappa), to induce the transcriptional activation of T-cell-lineage-specific genes – taken from (Zuniga-Pflucker 2004).

There are a number of potential roles identified including cell survival and proliferation as well as having a role in cell fate of HSCs (Kondo, Weissman et al. 1997, Manz, Traver et al. 2001). Its role in acquired immunity is notable and it is thought that NOTCH signalling may influence the development of both B-cells and T-cells (Simpson 1998).

OP9-DL1 cells have been used as a system for the differentiation of mouse embryonic stem cells (ESCs) or hematopoietic stem cells (HSCs) into T-lymphocytes *in vitro*. This variant on the OP9 cell line is able to express ectopic Notch ligand Delta-like 1 (Dll1) (Robey, Chang et al. 1996, Fowlkes and Robey 2002, Schmitt and Zuniga-Pflucker 2002, Kutlesa, Zayas et al. 2009, Van De Wiele, Marino et al. 2010, Feng, Yang et al. 2012) - fig. 5.39.

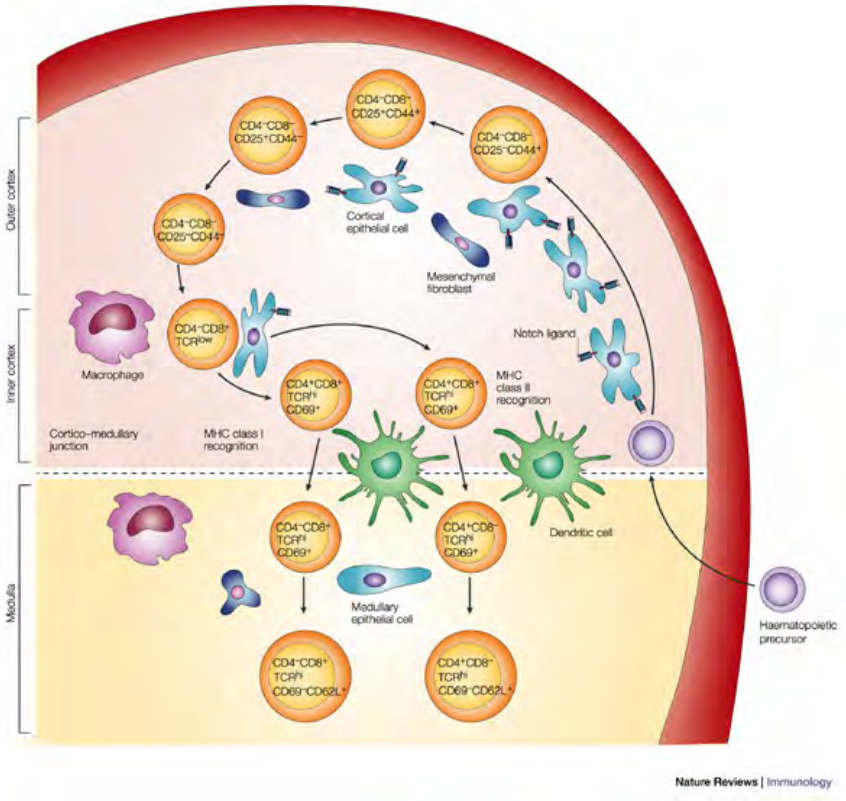

Fig. 5.39: Thymocyte Differentiation. The thymic architecture is organized into discrete cortical and medullary areas, each of which is characterized by the presence of particular stromal cell types, as well as thymocyte precursors at defined maturation stages. Thymocyte differentiation is characterized by the expression of well-defined cell-surface markers, including CD4, CD8, CD44 (or CD117) and CD25, as well as the status of the T-cell receptor (TCR). Interactions between Notch receptor-expressing thymocytes and thymic stromal cells that express Notch ligands induce a complex programme of T-cell maturation in the thymus, which ultimately results in the generation of self-tolerant CD4+ helper T cells and CD8+ cytotoxic T cells, which emigrate from the thymus to establish the peripheral T-cell pool. Taken from (Zuniga-Pflucker 2004).

Although it has lost the capacity to support active lymphopoiesis of B-cells, it is able to induce the differentiation of progenitors into T-cells (both single and double positive CD4 CD8 cells (Schmitt and Zuniga-Pflucker 2002) (Radtke, Wilson et al. 2004). As a result of early studies which showed both γδ-TCR$^+$ and αβ-TCR$^+$ T cells are generated, and that these cells could

secrete γ-interferon following stimulation, it was felt that this was good evidence that Delta-like-1 expression on stromal cells is necessary for the induction of T-cell lineage differentiation, and its associated functions such as progenitor expansion and TCR gene rearrangements *in vitro* (Deftos and Bevan 2000, Fowlkes and Robey 2002, Laky and Fowkes 2008). This has demonstrated a clear role for Delta-like-1/Notch interactions by the thymus confirming its ability to promote lymphopoietic differentiation and the generation of T-cells. How this is achieved is likely to represent the interplay between a number of intracellular cytokines. These roles have not however been well defined.

As previously described, T-cells undergo a series of well-documented differentiation steps, which relate to the cell surface expression of CD4 and CD8, with thymocytes progression from $CD4^-CD8^-$ double negative (DN), which go on to become $CD4^+CD8^+$ double positive given the right growth conditions (DP), and finally either $CD4^+$ or $CD8^+$ single positive (SP) T-cells. Based on expression of CD25 and CD44, these stages can be further investigated (Zuniga-Pflucker 2004) – fig. 5.39. Wang et al suggested that differentiation of cells from the DN stage to DP stage was provided for by IL-7 which originated from the stromal cells, however any further transformation required addition IL7 from alternative sources. SCF was also demonstrated to induce DN cell proliferation of DN and the inhibition of the DP stage in a largely a dose-dependent manner (Wang, Pierce et al. 2006). In addition to this, they observed that blocking endogenous SCF also blocked progenitor cell proliferation but led to increased differentiation of T-cells. They also showed that Flt3 ligand induced proliferation without having any noticeable effect on differentiation. They concluded that IL-7 SCF and Flt3-ligand were necessary for the promotion of efficient T-cell differentiation.

To test this suggestion, we proposed co-culturing developing mouse embryonic thymocytes harvested on day 13/14, which had not yet developed along any particular lineage with OP9DL1 cells (fig. 5.40).

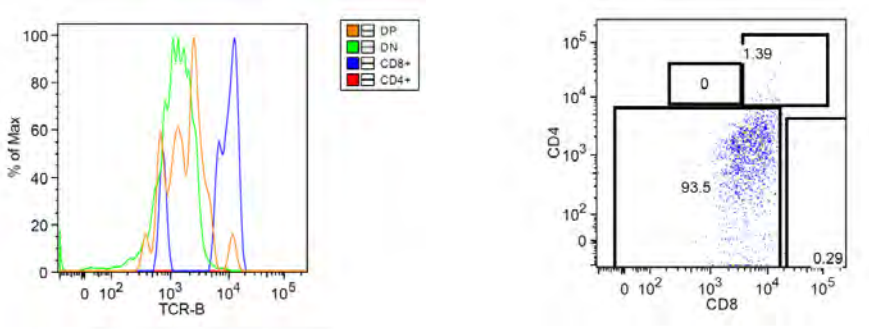

Fig. 5.40: Embryonic thymocytes were analysed using flow cytometry prior to co-culturing on OP9 cells. 93.5% of cells are in the DN state, which represents baseline at day 0. Following this cells were co-cultured either on OP9 cells or OP9-DL1 cells in standard cell media supplemented with Flt3L and IL7.

These cells are 93.5% $CD4^{-}CD8^{-}$, and this was taken as baseline. Previous observations suggested culturing on OP9-DL1 cells allowed differentiation of these cells down the haematopoietic lineage. Therefore we would expect transition of these cells through the various DN classes. Cells were therefore cultured in the presence of IL-7 and Flt3L on OP9DL1 cells, as well as OP9 cells (lacking DL1) to demonstrate the role of DL1 in lymphocyte development (fig. 5.41a, b).

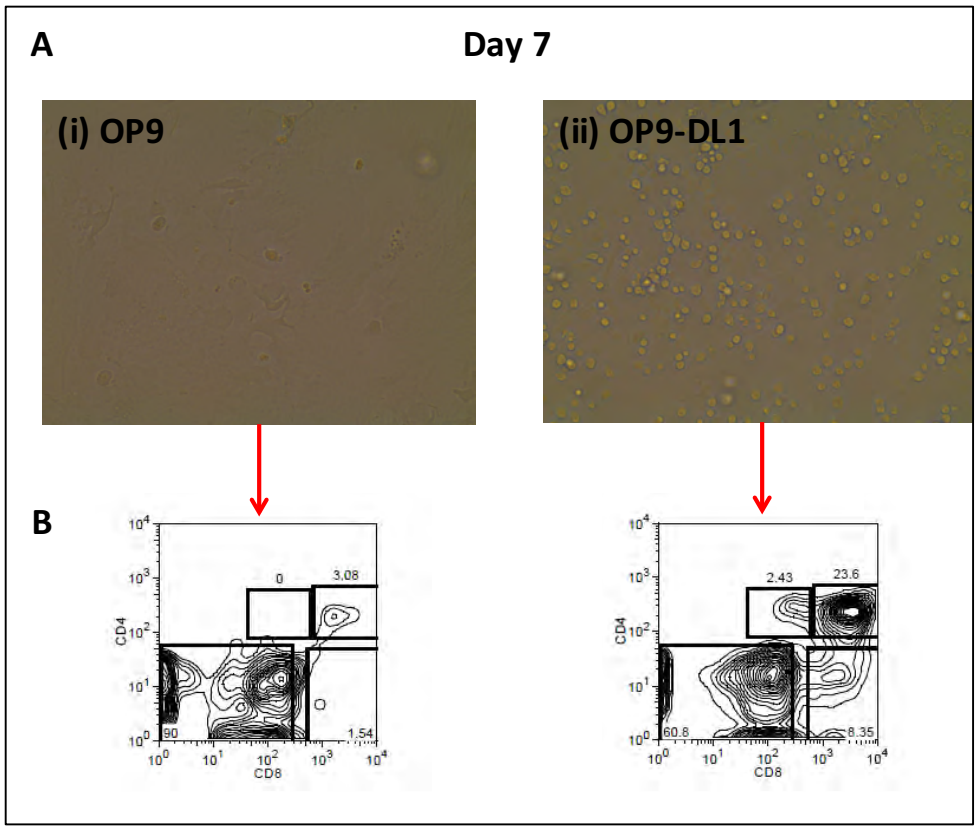

Fig. 5.41: Light microscope images (a) and Flow cytometry (b) plots of mouse thymocytes co-cultured on (i) OP9 cells or (ii) OP9-DL1 cells for 7 days in the presence of Flt3L and IL7. Those cells grown on the OP9-DL1 cells appear morphologically to look like lymphocyte cells (A) and have progressed from a largely DN state to 23.6% $CD4^{+}CD8^{+}$.

By day 14 (fig. 5.42) cells co-cultured with OP9-DL1 cells were predominantly $CD4^+CD8^+$. Cells grown on OP9 monolayer (in absence of DL1) did not survive.

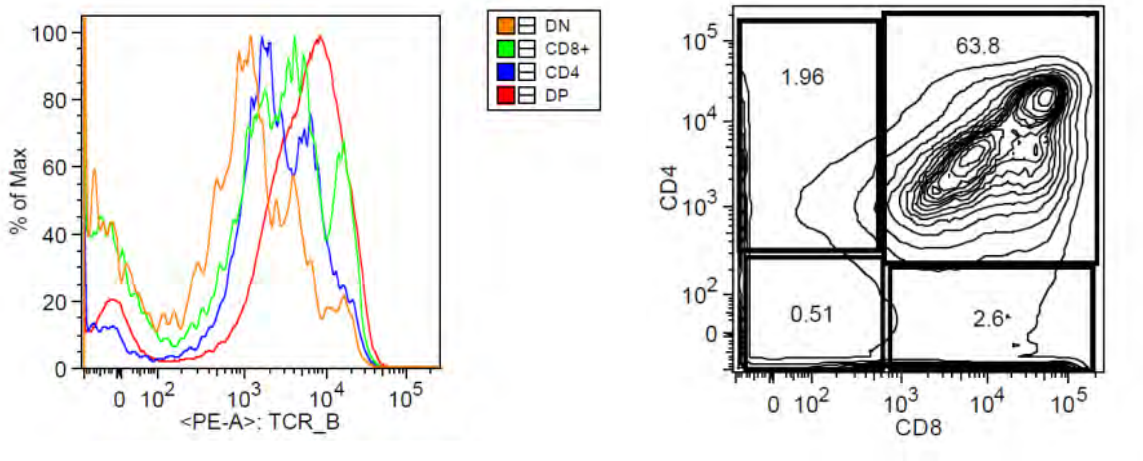

Fig. 5.42: Flow cytometry plots of mouse thymocytes co-cultured on OP9-DL1 cells for 14 days in the presence of Flt3L and IL7. Those cells grown on the OP9-DL1 cells have progressed from a 23.6% $CD4^+CD8^+$(DP) state to 63.8% DP. Those cells grown on an OP9 did not progress, and were lost at day 10. NB DN refers to $CD4^-CD8^-$, DP refers to $CD4^+CD8^+$

This preliminary experiment demonstrates the ability of OP9-DL1 cells to support differentiation of stem cells down the haematopoietic T-cell lineage. Having established this to be the case we proposed testing the system with IPSc.

5.4.3 OP9DL1 cell co-culture can support haematopoiesis in induced pluripotent stem cells leading to development of single positive $CD4^+$ and $CD8^+$ populations

We obtained a mouse IPSc line CD20.3, derived from a cross of C57BL/6 mice, generated using lentivirus with STEMCCA cassette (still being expressed) from Dr Carl Ward (Institute of Infection and Immunity, University of Birmingham). In order to confirm stem cell characteristic, this cell line was compared to the mouse Esc (line E4). Because the IPSc was still expressing the STEMCCA cassette protein markers were selected that were not on the cassette (fig. 5.43).

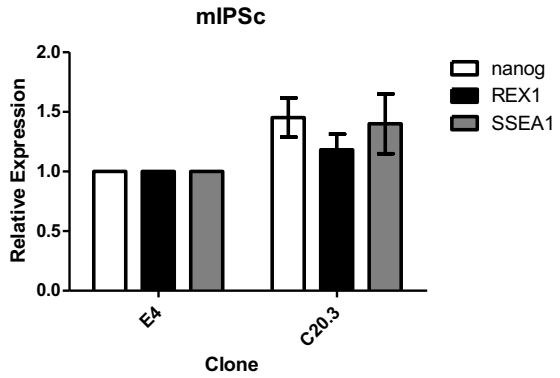

Fig. 5.43: qPCR plots showing relative expression of iPSc proteins NANOG, REX1 and SSEA1 in the mouse iPSc CD20.3 compared to the mouse ESc E4. qPCR performed as per standard protocols. Primers obtained from Dr Ward, School of INFECTION AND IMMUNITY, University of Birmingham. Expression of protein in both lines is relatively similar with no significant difference seen between the two, therefore confirming CD20.3 as a candidate iPSc. Chimeric transformation of mice injected with blastocysts was confirmed by Dr Ward's collaborators (data not shown). Error bars represent SEM.E4 taken as benchmark to which C20.3 was to be compared. Experiment repeated twice, these plots are representative of those obtained on both occasions.

Using methods as described by personal communication with Dr Kyoko Masuda (co-author of one of these previous studies) we aimed to develop a system for differentiating mIPSc into T-cells (Vizcardo, Masuda et al. 2013) – fig. 5.44.

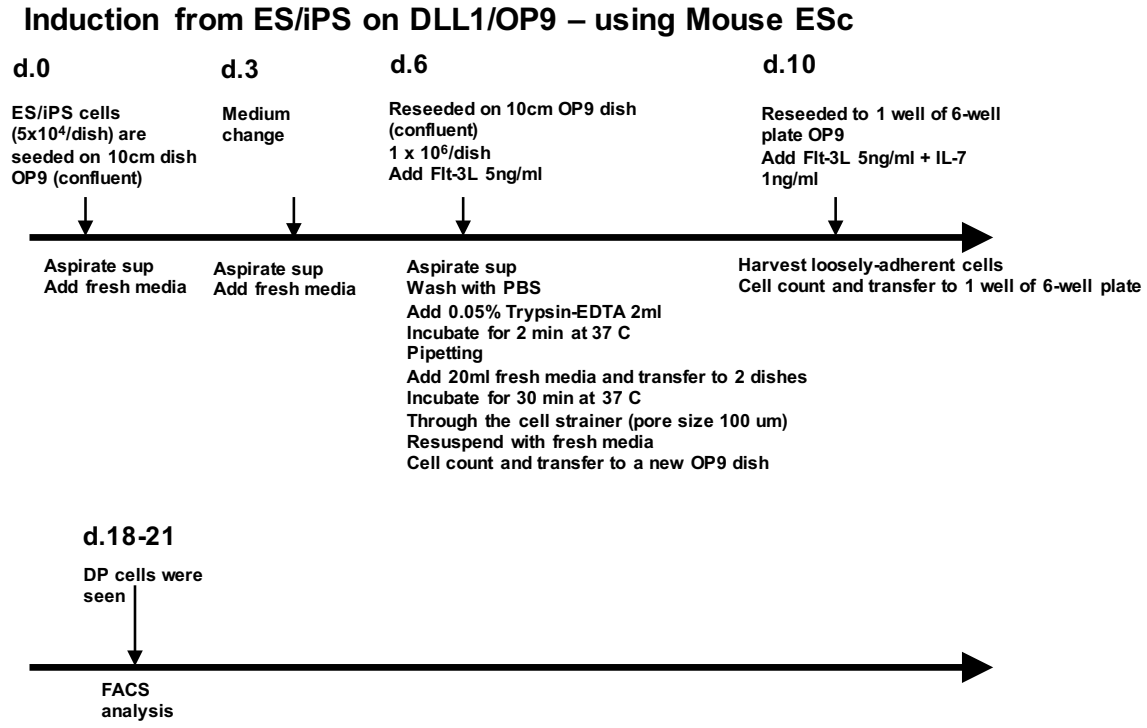

Fig. 5.44: Schematic representation of protocol for transformation of mouse iPSc to t-cells using OP9-DL1 co-culture system. This system was developed by Dr Matsuda and reproduced here with permission.

IPSc were cultured using standard techniques and transferred onto OP9 cells and OP9-DL1 cells to test this protocol. Media supplementation was as described and cells were observed and photographed at various time points. Morphologically it can be seen that cells co-cultured on OP9-DL1 cells do appear to be differentiated from typical rounded colony appearance (similar to that seen of cells cultured on OP9 cells) to single cell with a more typical lymphocyte-like morphological appearance - fig. 5.45.

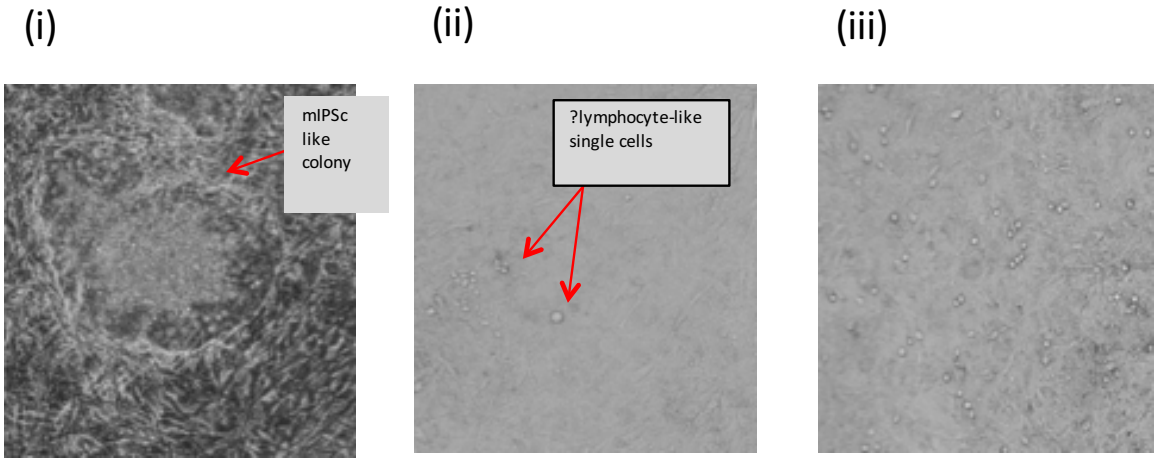

Fig. 5.45: Light microscope image of the mouse iPSc line CD20.3 grown on (i) OP9 cells and (ii) OP9-DL1 cells on day 14 and (iii) cells co-cultured on OP9-DL1 cells on day 21. This demonstrates minimal morphological change of the colonies grown on OP9 cells, however the typical colony formation is lost on cells co-cultured on OP9-DL1 cells, with the emergence of single cells at day 14 (ii) which have expanded in number by day 21 (iii). Morphologically these cells appear to be lymphocyte-like. (all cells viewed at same magnification x40).

These cells were analysed using flow cytometry. The control adult thymocytes show clear cell populations in each of the DN's (fig. 5.46A) demonstrating single positive cell populations which were $CD4^+$ or $CD8^+$. This compares to the mIPSc derived cells which had been co-cultured on OP9DL1's (fig. 5.46B), and were predominantly DN, suggesting that the system had not fully differentiated these cells. We had noted that initial experiments (fig 5.46c) had revealed a population that gated as 'lymphocyte-like' however were $CD45^-$ and therefore we considered that these cells possibly represented possible T-cell precursors. We therefore proposed that these cells had been insufficiently differentiated using the protocol described

previously. Moreover we hypothesised modifying this protocol, by increasing the IL-7 concentration 10 fold, and allowing cells to progress as previously with media changes as described, but harvested cells at varying time points for both ELISA (looking at TNFα and IFNγ) and also flow cytometry (fig. 5.47).

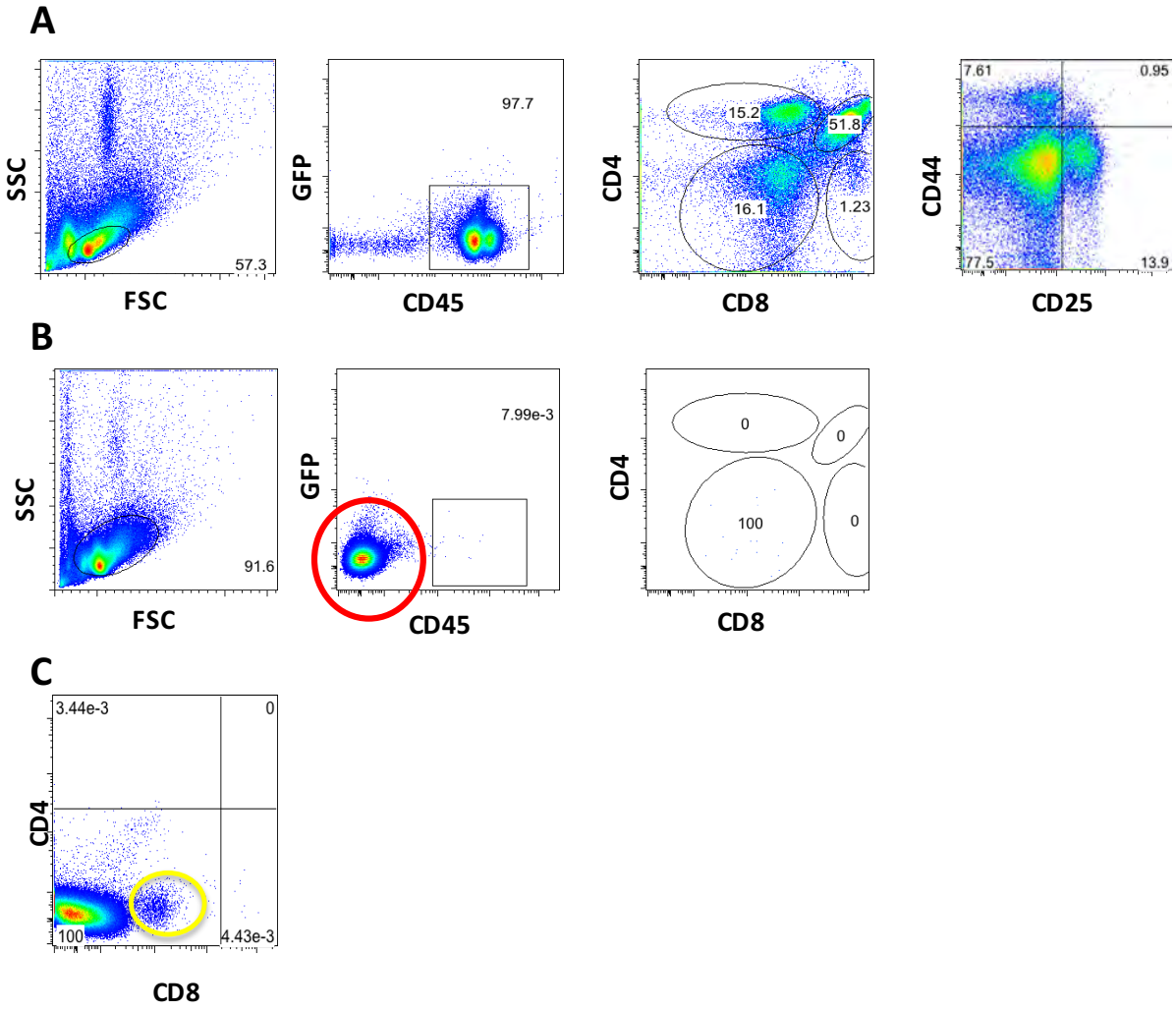

Fig. 5.46: Flow cytometry analysis of mIPSc-derived cells co-cultured on OP9-DL1 cells on day 17 compared to adult mouse thymocyte control cells. Here we can see progression of cells in the adult thymocyte control through the various DN's 1-4 (A). These cells show distinct populations, including single positive $CD4^+$ and $CD8^+$ populations (A). No CD20.3 (miPSc)-derived cells have progressed and remain in DN (B) . However, as denoted by the red circle in panel 2, row B, there is a population of cells which were gated as possible lymphocytes which are GFP negative (i.e. not OP9-DL1 cells which are GFP positive . Cells were re-gated on this population of cells (C). There appears to be a separate population of cells (yellow circle) which may represent CD8 positive cells as the gates were set up using adult thymocyte controls which is not a perfect match size wise for those cells derived from iPSc, but due to cell numbers we were unable to set gates using iPSc derived cells.

By modifying the protocol in this fashion we can see that cells derived from mIPSc can be differentiated into T-cell like cells by OP9-DL1 co-culturing. We assessed the cells at multiple timepoints (data not shown) and found cells cultured for 35 days on OP9-DL1 cells bore a very similar expression of markers to the adult mouse derived thymocyte control cells, with some subtle differences. For instance, in both adult thymus derived control cells and the mIPSc derived cells, DN4 predominated, but in the adult cells more cells are DN3 than DN2, which is the opposite to that seen in the mIPSc-derived cells. It is also noted that the mIPSc-derived cells showed a similar number of $CD45^{+}CD2^{+}$ cells (32.4%) versus 31.1% in the thymocyte control (NS), and higher $CD45^{+}$c-Kit^{+} (36.4%) versus 27.8% seen in the adult thymocyte controls (fig. 5.47).

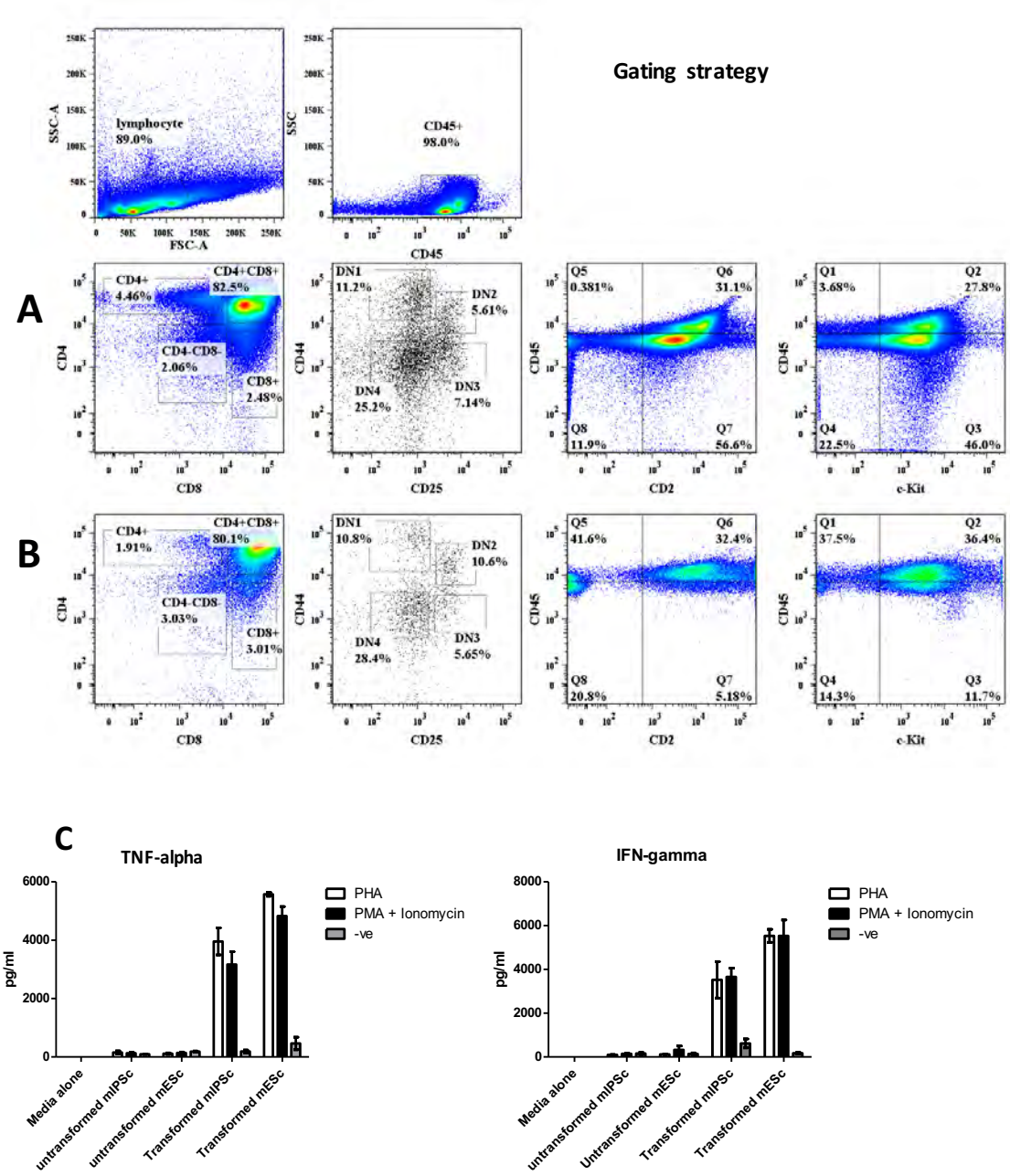

Fig. 5.47: Flow cytometry analysis of mouse iPSc derived cells (B) compared to adult thymocyte control cells (A) on day 35 of co-culture on OP9-DL1 cells. miPSc show a similar DN distribution to adult thymocyte controls with 80.1% $CD4^{+}CD8^{+}$ cells in the mISPc derived cells versus 82.5% in the control thymocytes. (C) ELISA data showing cytokine expression following stimulation with PHA or PMA/Ionomycin

This data is representative of n=4 repetitions of this protocol. This suggests therefore that these cells have not as efficiently been differentiated into lymphocytes as the adult thymus derived cells. This is unsurprising as no *in vitro* system can completely mimic an *in vivo* process like thymic control of cell fate. It was encouraging to see cells had started to differentiate and there was an increase in pre-cursors suggesting these cells could potentially become T-cells.

Unfortunately growing the cells for longer periods than this made no difference to the outcome (data not shown).

We considered if these cells were able to function like a T-cell. Therefore mIPSc-derived cell's media were sampled, at similar time points to when they were harvested for flow cytometry, and ELISA tests run to see what effect stimulation with PHA or PMA/ionomycin would have. When stimulated with PHA or PMA/Ionomycin, these transformed cells do express TNFα or IFNγ as measured using ELISA at the same time point (day 35), suggesting the majority of cells were activated as a result of stimulation with PHA or PMA/Ionomycin, with release of cytokine as a result. This preliminary data suggests that these cells functioned in a similar fashion to T-cells, although a limit of this assay is the inability to determine how many of the cells were capable of doing this (fig. 5.47C).

Therefore, we concluded, from these experiments, that co-culturing mIPSc with OP9-DL1 cells supplemented with Flt3 and IL-7 is a potential system for differentiating IPSc into T-cells. Moreover, this system could be used to differentiate IPSc derived from mature T-cells with defined immunogenic repertoire, and thus IPSc system could be a valid method for expanding defined T-cell populations, given we have a method for converting those cells back into T-cells again which are functional.

5.5 Discussion

One of the primary aims of this study was to generate a tumour-specific T-cell line. Following the identification of phosphopeptides exclusive to tumours, we selected a number for further investigation based on relative expression and HLA type. Phosphopeptide-specific T-cell lines were generated based on responses to phosphopeptide pulsing, with FACS data demonstrating T-cell activation. We proposed that these cells could be used as a cancer specific (and HLA specific) tumour therapy a so called 'off the shelf' cancer therapy which would be tumour and

HLA specific. A key finding was that a number of these phosphopeptide-specific T-cells were capable of killing which is clearly a key attribute, as there is no clinical utility to establishing a phosphopeptide-specific T-cell line which is not able to eliminate its target.

The follow-on to this is establishing the T-cells long term. It is widely accepted that tumour-specific T-cells are difficult to maintain in long term culture, with cells losing specificity or dying. Therefore, the other arm to this project was establishing a modality for expanding these cells exponentially and maintaining them long term. Having considered a number of techniques, we proposed that generating hIPSc from T-cells could represent a technology for overcoming this hurdle. Although a relatively new technique having first been described in 2013, we wanted to test the viability of this technique (Nishimura, Kaneko et al. 2013, Vizcardo, Masuda et al. 2013). Having established T-cell lines, we transfected cells using sendai virus with the Yamanaka factors as first described by Yamanaka and colleagues when generating IPSc initially in 2006 and further characterised by the same group on a number of occasions since using multiple different virus vehicles including retrovirus, lentivirus and most recently sendai virus (Takahashi and Yamanaka 2006, Takahashi, Tanabe et al. 2007, Nagata, Toyoda et al. 2009, Takahashi and Yamanaka 2013).

Our initial findings have shown that using a T-cell line we can establish a stable hIPSc clone which readily expands. This leads onto the obvious question of (1) how to transform an IPSc back into a T-cell, as hIPSc do not function like a T-cell and therefore expanding a cell line that is not functional is useless unless there is a way to transform it back and (2) will this T-cell be functional? Because of the relative novelty of this technique, the protocols for achieving this are still under development. Using methods as described by personal communication with Dr Kyoko Masuda (Kyoto University, and co-author of one of these previous studies) we aimed to develop a system for transforming mIPSc into T-cells (Vizcardo, Masuda et al. 2013) section

5.4.1. mIPSc that were co-cultured on OP9-DL1 cells to provide a source of Notch Ligand to trigger T-cell development, do appear to be transformed from typical rounded colony appearance (similar to that seen of cells cultured on OP9 cells) to single cells with a more typical lymphocyte-like appearance.

We can see that cells derived from mIPSc can be transformed into T-cell like cells by OP9-DL1 co-culturing. We assessed the cells at multiple timepoints (data not shown) and found cells cultured for 35 days on OP9-DL1 cells bore a very similar expression of markers to the adult mouse derived thymocyte control cells, with some subtle differences. For instance, in both adult thymus derived control cells and the mIPSc derived cells, DN4 predominated, but in the adult cells more cells are DN3 than DN2, which is the opposite to that seen in the mIPSc-derived cells. It is also noted that the mIPSc-derived cells show greater proportion $CD45^{+}CD2^{+}$ (32.4%) versus 31.1%, and higher $CD45^{+}$c-Kit+ (36.4%) versus 27.8% seen in the adult thymocyte controls. This suggests therefore that these cells have not as efficiently been transformed into lymphocytes as the adult thymus derived cells. This is unsurprising as no *in vitro* system can completely mimic an *in vivo* process like thymic control of cell fate. When stimulated with PHA or PMA/Ionomycin, these transformed cells do express TNFα or IFNγ as measured using ELISA), suggesting the majority of cells were functional T-cells.

Therefore, we concluded that co-culturing mIPSc with OP9-DL1 cells supplemented with Flt3 and IL7 is an efficient system for transforming IPSc into T-cells. We therefore concluded that this system could be used to transform IPSc derived from mature T-cells with defined immunogenic repertoire, and thus IPSc system could be a valid method for expanding defined T-cell populations, given we have a method for converting those cells back into T-cells again which are functional.

Chapter 6: DISCUSSION AND FUTURE WORK

Liver tumours (HB and HCC) and Post-transplantation lymphoproliferative disease (PTLD) pose a serious therapeutic challenge and novel approaches are being sought for the treatment of these tumours in the paediatric population. The immune system can specifically identify and eliminate tumour cells on the basis of their expression of tumour-associated antigens (TAA). This process is referred to as tumour immune surveillance, whereby the immune system identifies cancerous and/or precancerous cells and eliminates them before they can cause harm (Kaplan, Shankaran et al. 1998, Swann and Smyth 2007, Garrido, Perea et al. 2017). As a result of these observations, immunotherapy is considered a promising new treatment modality. A key aim of this project has been the identification of specific targets, which distinguishes the malignant cells from healthy cells. Very few immunogenic TAA have been characterised so far in general and even less for paediatric tumours in general, which is therefore a key outcome of this project.

Malignant transformation results from dysregulation of signalling pathways which is predicted to be as a result of accumulated cell mutations and epigenetic changes. One such change is deregulation of signalling pathways with altered and augmented phosphorylation of cellular proteins. Phosphoproteins involved in these signalling cascades can be degraded to phosphopeptides that are presented by major histocompatibility complex (MHC) class I and -II molecules and recognized by T cells (Zarling, Polefrone et al. 2006, Mohammed, Cobbold et al. 2008, Depontieu, Qian et al. 2009, Li, Depontieu et al. 2010, Cobbold, De La Pena et al. 2013, Abelin, Trantham et al. 2015). The contribution of phosphopeptide-specific T cells to immune surveillance in the development of liver cancer in chronic liver disease is unclear.

We hypothesised that phosphopeptides are presented by MHC molecules with increasing amounts on the surface of altered cells with progression of cellular change towards

malignancy. We further hypothesised that the immune system monitors the liver for malignant transformed hepatocytes and clears those cells with the help of phosphopeptide-specific cytotoxic T lymphocytes.

This project therefore had a number of key aims: (1) Identification of MHC class I-associated phosphopeptides that are presented on the surface of transformed cells using a mass spectrometry approach. (2) In order to show the immunogenicity of these novel identified tumour antigens, the second aim of this study was to characterise the T cell responses to these newly identified phosphoantigens in healthy individuals. (3) Finally we sought to identify a process for immortalising T-cells as a means of expanding a stable phosphopeptide specific T-cell line which has potential for in depth *in vitro* analysis of these phosphopeptide specific responses. Furthermore, the use of newer technologies such as iPSc technology, could benefit the development of a tumour-specific immunotherapy.

6.1 Identification of MHC class I-associated phosphopeptides as novel tumour-specific antigens for HB and PTLD

Several methods exist for identification of tumour antigens on the surface of cancer cells. In the past, most often a "reverse immunology" approach was used, in which the peptide sequences of the tumour antigens were predicted *in silico*. MHC presented peptides with low binding affinities or those carrying posttranslational modifications cannot be predicted with this approach. This project therefore implemented a more straightforward approach by directly isolating MHC-peptide-complexes from the surface of the tumour cells followed by sequencing of the peptides. The latter approach is necessary for the identification of posttranslational modified peptides. MHC class I-bound phosphopeptides were identified with the latter approach as described previously. This part was carried out in a collaboration with

the Department of Chemistry at the University of Virginia (laboratory of Prof. Donald Hunt).

To date, we have discovered in total 68 HB-associated MHC-I-phosphopeptides and nearly 200 PTLD-associated MHC-I-phosphopeptides. This data was acquired from 5 different HB samples and the corresponding adjacent healthy liver tissue and from a hepatoblastoma cell line (HepG2). In addition, we sampled the in vitro PTLD model (LCL) derived from healthy donors as well as some patient derived sample in order to understand phosphopeptide expression in this disease process. Sequence data from mass spectrometry is interpreted with the help of computer algorithms, but as no algorithm provided high enough confidence, the sequences had to be double-checked by hand, which led to limitations of this technique as it was as a result very time consuming to process each sample. This therefore limited the number of samples we were able to analyse for this current project.

Greater varieties of MHC-I-phosphopeptides and on an average greater expression were presented on malignant tissue than on healthy tissue. Some of the identified MHC-I-phosphopeptides have been previously found on other malignancies, e.g. colorectal and oesophageal cancers or on leukaemia (Zarling, Polefrone et al. 2006, Cobbold, Polefrone et al. 2007, Depontieu, Qian et al. 2009, Penny, Abelin et al. 2012, Cobbold, De La Pena et al. 2013, Abelin, Trantham et al. 2015), further highlighting the importance of this novel class of tumour antigens for cancer growths.

Many of the underlying proteins from the identified respective MHC-I-phosphopeptides can be directly linked to malignant signalling pathways, which highlight their importance as potential new immunotherapeutic targets. Several enriched clusters of proteins involved in transcriptional regulation, cell cycle regulation, regulation of metabolic processes, apoptosis, cell death, cell migration and many other biological processes, which have been associated with “hallmarks of cancer” have been identified in both the current study and also previous

studies by this group (Cobbold, Polefrone et al. 2007, Mohammed, Cobbold et al. 2008, Penny, Abelin et al. 2012, Cobbold, De La Pena et al. 2013, Abelin, Trantham et al. 2015). Several studies indicate a major role of the MAPK/RAF/MEK/ERK pathways in the tumorigenesis of liver tumours (Tomizawa and Saisho 2006, Hartmann, Kuechler et al. 2009, Armengol, Cairo et al. 2011, Esmaeili, Farimani et al. 2014, Mokkapati, Niopek et al. 2014, Wang, Lu et al. 2016, Leichter, Sullivan et al. 2017). However, due to the small sample size, the data does not represent a complete picture of the involvement of phosphopeptides into important biological functions and their pathways yet.

6.2 Characterisation of immune responses against MHC-I-phosphopeptides

Preliminary data from our the current project and other members of the Cobbold group have indicated that T cell responses against phosphoproteins can be found in healthy individuals and to a lesser extent in patients with malignant diseases (Zarling, Polefrone et al. 2006, Penny, Abelin et al. 2012, Cobbold, De La Pena et al. 2013, Abelin, Trantham et al. 2015). These results suggested that individuals with a functional immune system create T cell responses against aberrantly phosphorylated peptides in order to eliminate those cells with signs of transformation. This may prevent further alterations and malignant transformation of the cells.

According to our hypothesis we set out to identify $CD8^+$ T cell responses against the newly identified MHC class I- associated phosphopeptides in healthy individuals and patients with HB. A number of the newly identified PTLD and HB-associated HLA-A*02-restricted phosphopeptides, as well as HLA-B*07 were selected for further immunological testing in HLA-A*02 positive healthy individuals. Responses were assessed using intracellular cytokine staining (ICS) and several cytokines and surface markers were assessed in parallel. After 7 days of stimulation with the respective MHC-I-phosphopeptide and no other cytokines, CD3

and CD8 expressing T cells were stained for at least two different cytokines (IFN-γ, TNF-α). First peripheral blood mononuclear cells (PBMCs) from healthy donors were analysed (chapters 3,4).

We demonstrated phosphopeptide-specific responses, which were clear memory responses with the added capability of killing (section 3.2-3.4). We acknowledge that the number of healthy donors assessed was relatively small, and therefore in order to better understand the proportion of immune response targeting phosphopeptide, a larger cohort should be sought. We propose that this preliminary data, together with observations seen by other laboratory members, in their studies, suggest that these healthy donors have clear functional $CD8^+$ T-cell responses to these transformation-dependent epitopes (Zarling, Ficarro et al. 2000, Zarling, Polefrone et al. 2006, Mohammed, Cobbold et al. 2008, Penny, Abelin et al. 2012, Cobbold, De La Pena et al. 2013, Abelin, Trantham et al. 2015). This brings us back to the concept of tumour immunoediting (Meraz, White et al. 1996, Shankaran, Ikeda et al. 2001, Dunn, Old et al. 2004, Dunn, Old et al. 2004, Dunn, Bruce et al. 2005, Dunn, Koebel et al. 2006). Therefore, we concluded that it is probable that the memory T-cell responses are to epitopes which the T-cells have encountered before, and that these epitopes are likely to be phosphopeptides.

We found that phosphopeptides were displayed on MHC class I at significantly higher levels in hepatoblastoma and PTLD than the corresponding healthy tissues (Section 3.5, Section 4.2.1), an observation noted previously in other tumour types (Penny, Abelin et al. 2012). We identified 68 specific phosphopeptides associated with hepatoblastomas. Comparison of hepatoblastoma to healthy tissue and the cell line HepG2 shows that 41 phosphopeptides have been found unique to hepatoblastoma and not on healthy tissue or previously in the HepG2 cell line. There is an overlap of 16 phosphopeptides found on both tumour and cell line (HepG2). The colorectal adenocarcinomas as studied by Dr Sarah Penny, of this group, also had a subset

of patients with liver metastases, and on assessing phosphopeptides seen on these secondary malignancies a number were also identified on hepatoblastoma tumour samples, suggesting that these phosphopeptides may be involved in a hepatological development and tissue differentiation pathways. Their role could potentially be related to coding for proteins involved in hepatic tissue dysplasia for instance. It is also noted that there are a number of phosphopeptides identified on adult hepatocellular carcinoma samples (as studied by Dr Nico Büttner of this group), again bolstering this view of a role in hepatic dysplasia (Table 4.9).

A similar picture was identified when studying PTLD and the *in vitro* surrogate LCLs. Although obviously limited by lack of patient samples, we can identify a number of phosphopeptides which are presented exclusively on malignant or transformed cells, and not on healthy tissues. This has led to the suggestion that these tumour-associated phosphopeptides could be targets for immunotherapy.

Phosphopeptide-CTL-responses were compared with responses to immunodominant viral epitopes from cytomegalovirus (NLVPMATV) and Epstein-Barr virus (GLCTLVAML). In many cases T cell responses against MHC-I-phosphopeptide are comparable in quantity and quality to viral immune responses. This is in contrast to the "classic" TAA. Here immune responses are often nearly not detectable (< 0.1 % of $CD8^+$ T cells) and often show signs of exhaustion (Ramsay, Bates et al. 2008, Flecken, Schmidt et al. 2014).

Phosphopeptide-specific T-cells produce multiple cytokines, mainly IFNγ and TNFα. The production of multiple cytokines (IFNγ, TNFα and IL-2) by T lymphocytes is in general associated with better disease control. Phosphopeptide-specific T-cells were found to be mainly $CD27^+$ and $CD45RA^-$ and therefore most likely to reside in the memory compartment. This suggests that only individuals that have been previously exposed to the MHC-I-phosphopeptide establish an immunological memory against these antigens. If healthy donors

are too young, we proposed that they haven't had the chance yet to be exposed to MHC-I-phosphopeptide tumour antigens.

Finally, after establishing that healthy donor derived T-cells could mount a response to MHC-I-phosphopeptides, we considered if these phosphopeptide-specific (and thus potentially tumour-specific) cell lines could recognise tumours. This was performed on frozen tumour tissue as well as LCL-lines. From this series of experiments we were able to show that The Phosphopeptide-specific T-cell lines could recognise tumour and release cytokine as a result. Europium killing assay showed functionality of these cells. We therefore considered how to propagate these phosphopeptide-specific T-cells.

6.3 Establishing Phosphopeptide-specific T-cells

This arm of the project looked at methods of maintaining T-cells in culture long term without suffering the complications of loss of antigen-specificity, T-cell exhaustion and cell death. Initially we looked at methods for assessing T-cells *in vitro* with the aim of their use as a tool to probe phosphopeptide expression on both normal and transformed cell types. In order to do this, we explored the use of hybridoma-technology primarily with varying success. The main barrier to this technique was efficiency which despite extensive manipulation of experimental protocols remained relatively poor. This is perhaps unsurprising given the observation that T-cell hybridoma technology has largely fallen out of fashion as newer molecular biology techniques emerge.

Building on prior knowledge and skills gained from previous projects, iPSc technology was investigated as a means of expanding T-cells. This was based on two studies released in 2013, which showed success of iPSc technology in the rejuvenation of exhausted mature T-cells in

HIV and melanoma (Nishimura, Kaneko et al. 2013, Vizcardo, Masuda et al. 2013). Using Sendai virus, we were able to demonstrate differentiation of mature T-cells into induced pluripotent stem cells which demonstrated all the characteristics of a stem cell with regards to gene and protein expression. These cells have the potential to be differentiated into any cell type, and thus provide an ideal platform to be differentiated into a stable T-cell line. Preliminary data obtained during this project has demonstrated that iPSc cells derived from mature T-cells can be differentiated back into T-cell-like cells with the same cytokine expression and functionality as parent line. Although only reproduced twice and in mIPSc, it does demonstrate a proof of principal and a step towards generation of a phosphopeptide-specific T-cell line if a protocol could be established for hIPSc, given we have shown that we can generate an iPSc from mature T-cells.

6.4 Adoptive cell transfer – TiLs vs iPSc

It has been shown that adoptive cell transfer (ACT) of TILs can mediate cancer regression in patients with metastatic melanoma (Rosenberg 1984, Dudley, Wunderlich et al. 2003). In ACT autologous immune cells from a patient are removed, altered and/or expanded. A problem with this technique is that in order to generate a TiLs line from hepatoblastoma requires a large tissue sample, in order to get a sufficient number of lymphocytes to start a culture. That would mean that patients with HB or PTLD would need to have surgery before ACT in order to acquire enough tumour tissue. But that is not practical, considering the expected symptoms from liver disease, the need to initiate chemotherapy and time take to establish a culture. The only reasonable approach to obtain liver tissue before immunotherapy could be a liver biopsy. Protocols have to be optimised in the future in order to obtain suitable T cell populations from liver biopsies, which remains a challenge in the paediatric population as it requires general

anaesthesia and could delay initiation of chemotherapy. Also there is a risk of tumour seeding. The time taken to generate this line is also a key consideration when using autologous cells. Other members of the Cobbold group have attempted to investigate this in hepatocellular carcinoma but with very limited success. It was found that only very few and minor responses were detectable in all of the cultures. Background cytokine production was much higher in expanded lymphocyte cultures and therefore often genuine T cell responses were difficult to distinguish from background. Responses, which were demonstrated in the unexpanded cultures, were completely absent in the expanded T cell cultures (personal communication). Interestingly virus-specific T cell reactivity was not lost during expansion of T cells. This indicates that if expansion of T cells happens in a large scale and in an undirected way, virus-specific T cells and tumour-unspecific T cells overgrow tumour-specific T cells. This might be one reason why ACT with T cells failed to induce clinical responses on a regular basis. Overgrow of virus-specific cells could be due to the fact that these cells are less exhausted and express lower amounts of inhibiting receptors.

Recently iPSc have been proposed as a cell source for ACT (Minagawa and Kaneko 2014). Adoptive T-cell transfer is a potentially effective strategy for treating cancer and viral infections. However, previous studies of cancer immunotherapy have shown that T cells expanded *in vitro* fall into an exhausted state and, consequently, have limited therapeutic effect. One way to overcome this obstacle is to use induced pluripotent stem cells (iPSCs) as a cell source for making effector T cells. In recent years, there have been several reports on generating effector T cells suitable for adoptive immunotherapy. The reported findings suggest that using iPSC technology, it may be possible to stably derive large numbers of juvenile memory T cells targeted to cancers or viruses.

Adoptive T-cell transfer has been successful in treating many cancer patients (Grupp and June

2011). We have shown that there is tumour-resident immunity to the tumour-specific phosphopeptides in HB patients. Therefore, if patients have T cells targeting these phosphopeptides, it may be possible to select these from the patient blood, using HLA-phosphopeptide tetramers and selectively expand them, before adoptively transferring them back into the patient, as is done with viral specific T cells after stem cell transplants (Cobbold, Polefrone et al. 2007).This could potentially be a relatively inexpensive personalised therapy, performed at the bedside. However, for this we require robust phosphopeptide multimers and these have proved more difficult to refold than viral peptide tetramers.

6.5 Phosphopeptide-specific ImmTACs as potential immunotherapeutics

The value of the TCR transfer approach is underscored by the many patients with either cancer, viral infection, or other life-threatening diseases, for whom it is not possible to expand T cells of therapeutic value. For such patients, the successful transfer of TCR genes would undoubtedly be a significant step in the development of improved T cell-based therapies. TCR gene transfer has been facilitated by retroviral and more recently lentiviral transfer. Another potential therapeutic angle that could be used in targeting tumour-specific phosphopeptides is immune-mobilising monoclonal TCRs against cancer (ImmTACs). These are a set of new reagents engineered by Immunocore (Abingdon, UK). They comprise a tumour-specific TCR covalently linked to a CD3-specific single-chain antibody fragment (scFv). These thus engage specifically with tumour cells and induce responses from all of the $CD3^+$ T cells in the local environment. They can be used to target cells expressing fewer than 50 epitopes, but it is essential that these epitopes are completely tumour-specific. Therefore, we would need to assess MHC class I-associated expression of the tumour-specific phosphopeptides in a range of healthy tissues. However, if we could find a selection of HLA- phosphopeptides that were

tumour-specific, this could be a treatment covering all cancers in all patients. To this end, we are attempting to clone phosphopeptide-specific T cells to sequence their TCRs. Furthermore, these reagents could be used in conjunction with the sHLA biomarkers for early detection of cancer.

Cancer cells express MHC class I-associated phosphopeptides on their cell surface. ImmTACs specifically target these complexes with high affinity TCRs and stimulate all local T cells with the anti-CD3 scFv, redirecting T cell killing towards the cancer cells and clearing the cancer.

In the more distant future, if we could ensure that the HLA-phosphopeptides were completely tumour specific, and we could develop an effective vaccine strategy, they may have potential as preventative cancer vaccines, used in a similar way to HPV vaccination. However, this would need extensive development and validation in multiple animal models to ensure against toxicity.

6.6 The use of iPSC vs TCR gene transfer vs CAR-T

An alternative to the iPSc process is use of either autologous cells or alloreactive cells and manipulating them using gene-transfer technology (e.g. lentiviral/retroviral or use newer "gene-disruption" technologies e.g TALENs -developed by Cellectis or CRISPR/Cas9). The focus of this project is specifically about phosphopeptide responses which are recognised by T-cells, therefore a CAR cannot be constructed, and it would be necessary to construct an engineered TCR. This is because CAR-T cell therapies consist of an antigen binding region (usually drive from an antibody) which targets a surface protein on the tumour cell such as CD19 in B cell malignancies or MUC-1 on solid organ malignancies. It would be very difficult and impractical to generate CAR-T cells against multiple phosphopeptide-MHC complexes.

With tumour-specific peptides such as phophopeptides or NY-ESO, WT-1, MART-1, MAGE3, TCR constructs must be generated and transferred to T cells. These transfected T cells subsequently recognise peptides on the tumour cells. TCR constructs act through the MHC pathway and recognize a processed epitope presented by the target cell`s MHC complex and thus are HLA specific. However, one of the major limitations of TCR gene transfer is due to MHC restriction in patients. Those patients who express MHC class I alleles that can present a tumour-specific peptide may benefit from TCR gene transfer therapy but patients who do not express the correct MHC molecules cannot present the tumour-specific peptide and will therefore not benefit from this therapy.

As already alluded to, there are different methods of introducing or adoptively transferring T cell immunity against phosphopeptides to a given patient. iPSCs would give a potentially unlimited supply of T cells with the only manipulation being the T cell>iPSC>T cell modification. TCR gene transfer would require genetic manipulation of the patients harvested T cells, growth *ex vivo* and re-injection. Numbers of injected T cells would depend on transfection efficiency and *ex vivo* growth. Also, potential of new TCR alpha and beta chains pairing with the endogenous alpha and beta chains possibly altering T cell recognition. Potentially need to use non-autologous T cells for TCR transfer therapy meaning could have problems with Graft vs Host disease (GvHD) or host cells killing non-self T cells.

As already suggested, CAR-T cells would probably not work as a phosphopeptide immunotherapy as these use an antibody variable region to recognise a protein on the cell surface e.g. CD19. CAR-T likely would not easily recognise phophopeptide-MHC complex and would therefore not be useful in this setting. iPSc-based therapy would be tumour specific because of the restricted expression of the phosphopeptide so in theory it could target any tumour, haematological or solid organ. At the moment, CAR-T are very restricted in their

targeting because they kill all cells expressing the protein they are targeting. Therefore, they are mostly restricted to haematological malignancies because survival without their B cells or plasma cells is possible, but to specifically target liver cancer with a CAR-T therapy would be difficult as they would also kill healthy hepatocytes that express the CAR target antigen.

Making any of these theoretical processes into this a patient therapy is going to be expensive and require a lot of resources. For instance, with CAR-T, T cells are obtained from the patient, CAR-T construct is transfected in, subsequently the T cells are grown *ex vivo* and then re-infused after 14 days (Couzin-Frankel 2013). iPSC therapy would be similar, where phosphopeptide-specific T cells are selected and used to generate iPSC, cultured and then differentiated back into T cells prior to being re-infused. This is not dissimilar to CAR-T therapy so you could use that as a reasonable rationale for iPSC therapy moving forward. Many T cell therapies involve some sort of *ex vivo* T cell culture and a GMP facility facilitate this. Costs would be high for any of these therapies due to the rigorous controls necessary for a patient treatment, but would likely be comparable. Although costs will initially be high, there is significant investment in this area by a number of leading companies (Norvartis, Giliad acquiring Kite, Juno**)** and it would be predicted that costs will inevitably come down once the field has been established. In terms of where production is best achieved there are two options: Is it going to be centralised in big cell manufacture factories or will it be closely linked with University hospitals. The current view from the field is that it will be a mixture of the two. Maybe autologous therapies being hospital based using automated machines and allogenaic therapies being centralised is a sensible division.

6.7 The issue of HLA-restriction

Discovery of a phosphopeptide specific T cell response and generation of an iPSC therapy

from it, would either be suitable for that patient or at best patients with the same HLA allele. This project has identified a number of tumour-specific phosphopeptides, however as is already known, these are HLA-restricted. Although our focus here was on HLA A2 and HLA B7 (due to sample and time limitations), many other phosphopeptides were isolated on tumours which were of other HLA types. If this iPSc based therapy were to be adopted as a patient treatment, one way to overcome the issue of HLA restriction could be to generate banks of cells lines with different HLA restrictions. Alternatively, discovery of a phosphopeptide which binds to a non-classical HLA or similar may overcome this, but with the current phosphopeptides identified, MHC restriction is likely to prove an issue for the proposed therapy. This will therefore make this a more expensive therapy and potentially a move towards personalised therapy.

6.8 Summary

Although anti-host reactivity may lead to unacceptable toxicity, immune rejection of non-autologous T cells will most certainly reduce their efficacy. Therefore, critical to success of an 'off the shelf' adoptive T-cell therapy is escaping immune rejection, ensuring sufficient persistence and possibly long term engraftment. One fairly obvious and perhaps necessary approach to this is to bank cells with common HLA haplotypes. This is still however limited by HLA matching and donor availability. Establishment of iPSC banks is another option which could be explored, although this also requires the generation of multiple iPSC lines from multiple donors. This is not without its own limitations in terms of T-cell specificity, HLA restriction and the safety implications to name but a few.

Stem cell reprogramming is however an attractive option as it offers the potential for generation of an unlimited source of therapeutic T lymphocytes, as well as a cell source for

further genetic engineering (Themeli, Kloss et al. 2013). The combination of iPSC technology and immune engineering could potentially lead to generation of T-cells with favourable characteristics such as phosphopeptide/antigen specificity, histocompatibility or a lack of alloreactivity.

6.9 Future work

As a result of this project and other studies, there are of course a number of important questions to answer:

(1) Can phosphopeptide-specific T-cells be differentiated into hIPSc using the techniques described in Chapter 2?

(2) Can techniques be established for differentiating hIPSc back to T-cells?

(3) Will the resulting T-cells have the same specificity with regards to phosphopeptide as the parent T-cell?

(4) These cells will be HLA specific – can we identify a technique for overcoming this, as not all patients with a specific tumour will have the same HLA?

The answers to these questions form the basis of the future work. We have identified phosphopeptides present on tumours, and developed techniques to generate phosphopeptide specific T-cells. It would be useful to establish a larger cohort of tumours allowing for greater clarity of tumour-specific phosphopeptides identified. Can we narrow down more unique phosphopeptides for instance (novel phosphopeptides not identified on other tumours would be of particular interest as these could be truly considered ‘tumour-specific’, or ones which are expressed at much higher levels in tumour versus normal tissue. In the case of PTLD, a larger

patient cohort is key to our understanding of this disease, as much of what we have established is from an *in vitro* proxy, so essentially a theoretical model.

With regards to transforming hIPSc into T-cells, the protocol is constantly evolving, and as yet is not fully optimised. We chose not to investigate this further in the current project as the mouse protocol was closer to being fully optimised, and with further modification with regards to cytokine supplementation and duration of co-culture we believe we have established a reproducible protocol for transforming mIPSc into T-cells. The logical next step would be to do this in hIPSc and would be a key target of further work. The clear focus of this would therefore be to establish a T-cell line from hIPSc, and then to identify if it is functional (i.e. capable of activation following stimulation) but perhaps most important is establishing if the resultant T-cell line has the same phosphopeptide specificity as the T-cell from which it was originally derived. Again if the resultant T-cell is not phosphopeptide specific and therefore not tumour-specific then there will be no clinical utility. Finally, we acknowledge that the system we have used is very artificial and only specific to a limited number of HLA types. Therefore, if more tumours were investigated more HLA specific phosphopeptides could be identified. However as alluded to, not all patients have the same HLA type, and therefore focus could be to generate a non HLA specific T-cell line. Could we determine a mechanism for removing HLA TCR of a T-cell line so that it could have functionality in more patients? One obvious technique currently receiving a vast amount of research activity across the world is CRISPR/Cas9 technology, which may indeed overcome the issue of HLA restriction. It is the subject of much investment in terms of time and knowledge by the Cobbold laboratory and collaborators in Harvard University in relation to phosphopeptide specific T-cells and manipulation thereof. We propose the use of CRISPR/Cas9 technology to remove the endogenous TCR, overcome HLA restriction and thus the risk for GVHD, and therefore we propose this as a technology for removal of endogenous HLA alleles from the T-cell to avoid

interaction in this third party setting.

In summary, we have attempted to validate phosphopeptides as a potential new class of cancer antigen in a human cancer model. We showed that over half of the immune responses generated in healthy donors were directed towards phosphopeptides found on 'transformed-self'. We isolated tumour-specific phosphopeptides from paediatric hepatoblastoma tumours and PTLD patient samples as well as cell lines. We also found that a number of these phosphopeptides were also expressed on other tumours e.g. breast, melanoma, gastrointestinal tumours, and haematological malignancies. A key aim of this project was identifying what role phosphopeptide-specific T-cells played in the anti-tumour , which we achieved with the use of an *in vitro* model for PTLD which allowed us to assess the proportion of T-cell responses that are against phosphopeptides identified on LCLs as well as on paediatric liver tumour specimens. We found these T-cells did appear to use phosphopeptide to target tumour and displayed functional killing as a result. We assessed a number of techniques for immortalising specific T-cells so these could be expanded exponentially in culture. We established that generating induced pluripotent stem cells (IPSc) from T-cells appeared to be an efficient process for generating stable cell lines. Following on from this we explored methods for converting these IPSc back to functional T-cells. Using a mouse IPSc model we established that given the right growth conditions, co-culture with OP9 DL1 cells did allow for the IPSc to become T-cells which were capable of being activated following stimulation, leading us to believe that this method could be used to generate a stable T-cell line. This proof of principle has allowed us to explore various techniques, with the ultimate aim to repeat this using IPSc derived from phosphopeptide-specific T-cells.

References

(2010). "GlaxoSmithKline and Amplimmune join forces on targeting PD1." Nature Reviews Drug Discovery **9**(10).

Abdalla, E. K., et al. (2002). "The caudate lobe of the liver: implications of embryology and anatomy for surgery." Surgical oncology clinics of North America **11**(4): 835-848.

Abelin, J. G., et al. (2015). "Complementary IMAC enrichment methods for HLA-associated phosphopeptide identification by mass spectrometry." Nature Protocols **10**(9): 1308-1318.

Allan, B. J., et al. (2013). "Predictors of survival and incidence of hepatoblastoma in the paediatric population." Hpb **15**(10): 741-746.

Armeanu-Ebinger, S., et al. (2013). "Targeting EpCAM (CD326) for immunotherapy in hepatoblastoma." Oncoimmunology **2**(1).

Armengol, C., et al. (2011). "Wnt signaling and hepatocarcinogenesis: The hepatoblastoma model." International Journal of Biochemistry & Cell Biology **43**(2): 265-270.

Artavanis-Tsakonas, S., et al. (1999). "Notch signaling: Cell fate control and signal integration in development." Science **284**(5415): 770-776.

Ascierto, P. A., et al. (2010). "Clinical Experiences With Anti-CD137 and Anti-PD1 Therapeutic Antibodies." Seminars in Oncology **37**(5): 508-516.

Avilion, A.A., Nicolis, et al. (2003). "Functional expression cloning of nanog, a pluripotency sustaining factor in embryonic stem cells" .Genes Dev.; 17: 126–140

Babcock, G. J., et al. (2000). "The expression pattern of Epstein-Barr virus latent genes in vivo is dependent upon the differentiation stage of the infected B cell." Immunity **13**(4): 497-506.

Balkwill, F. and A. Mantovani (2001). "Inflammation and cancer: back to Virchow?" Lancet **357**(9255): 539-545.

Balkwill, F. R. and A. Mantovani (2012). "Cancer-related inflammation: Common themes and therapeutic opportunities." Seminars in Cancer Biology **22**(1): 33-40.

Barbee, M. S., et al. (2015). "Current Status and Future Directions of the Immune Checkpoint Inhibitors Ipilimumab, Pembrolizumab, and Nivolumab in Oncology." Annals of Pharmacotherapy **49**(8): 907-937.

Barnett, B., et al. (2005). "Depleting regulatory T cells is associated with improved immunity and tumor clearance in human cancer." Journal of Investigative Medicine **53**(1): S291-S291.

Berrington, J. E., et al. (2005). "Lymphocyte subsets in term and significantly preterm UK infants in the first year of life analysed by single platform flow cytometry." Clinical and Experimental Immunology **140**(2): 289-292.

Betts, M. R., et al. (2006). "HIV nonprogressors preferentially maintain highly functional HIV-specific CD8(+) T cells." Blood **107**(12): 4781-4789.

Bevan, M. J. (1976). "CROSS-PRIMING FOR A SECONDARY CYTOTOXIC RESPONSE TO MINOR H-ANTIGENS WITH H-2 CONGENIC CELLS WHICH DO NOT CROSS-REACT IN CYTOTOXIC ASSAY." Journal of Experimental Medicine **143**(5): 1283-1288.

Bex, A. (2016). "New options in treatment of advanced renal cancer." Lancet Oncology **17**(7): 850-852.

Bhaduri-McIntosh, S., et al. (2008). "Repertoire and frequency of immune cells reactive to Epstein-Barr virus-derived autologous lymphoblastoid cell lines." Blood **111**(3): 1334-1343.

Bhatia, S., et al. (2009). "Treatment of Metastatic Melanoma: An Overview." Oncology-New York **23**(6): 488-496.

Biesinger, B., et al. (1992). "STABLE GROWTH TRANSFORMATION OF HUMAN LYMPHOCYTES-T BY HERPESVIRUS SAIMIRI." Proceedings of the National Academy of Sciences of the United States of America **89**(7): 3116-3119.

Bogen, B., et al. (1995). "NAIVE CD4(+) T-CELLS CONFER IDIOTYPE-SPECIFIC TUMOR RESISTANCE IN THE ABSENCE OF ANTIBODIES." European Journal of Immunology **25**(11): 3079-3086.

Bollard, C. M., et al. (2010). "Administrations of Tumor-Specific Cytotoxic T Lymphocytes Engineered to Resist TGF-beta to Patients with EBV-Associated Lymphomas." Blood **116**(21): 248-248.

Bollard, C. M., et al. (2003). "Adoptive T-cell therapy for EBV-associated post-transplant lymphoproliferative disease." Acta Haematologica **110**(2-3): 139-148.

Burnet, M. (1957). "CANCER - A BIOLOGICAL APPROACH .1. THE PROCESSES OF CONTROL." British Medical Journal **1**(APR6): 779-786.

Burnet, M. (1957). "CANCER - A BIOLOGICAL APPROACH .3. VIRUSES ASSOCIATED WITH NEOPLASTIC CONDITIONS." British Medical Journal **1**(APR13): 841-846.

Buschow, C., et al. (2010). "In Vivo Imaging of an Inducible Oncogenic Tumor Antigen Visualizes Tumor Progression and Predicts CTL Tolerance." Journal of Immunology **184**(6): 2930-2938.

Cadranel, J., et al. (2006). "Lung cancer in HIV infected patients: facts, questions and challenges." Thorax **61**(11): 1000-1008.

Campesato, L. F., et al. (2015). "Comprehensive cancer-gene panels can be used to estimate mutational load and predict clinical benefit to PD-1 blockade in clinical practice." Oncotarget **6**(33): 34221-34227.

Cao, S., et al. (2012). "Overcoming barriers to the clinical utilization of iPSCs: reprogramming efficiency, safety and quality." Protein & Cell **3**(11): 834-845.

Cartwright, P., et al. (2005). "LIF/STAT3 controls ES cell self-renewal and pluripotency by a Myc-dependent mechanism." Development **132**(5): 885-896.

Castillo, F. J., et al. (1994). HYBRIDOMA STABILITY. Genetic Stability and Recombinant Product Consistency. F. Brown and A. S. Lubiniecki. **83:** 55-64.

Cattrini, C., et al. (2016). "Immunotherapy for genitourinary cancer: state of the art and new perspectives." Anti-Cancer Drugs **27**(7): 585-599.

Chambers, I., et al. (2003). "Functional expression cloning of Nanog, a pluripotency sustaining factor in embryonic stem cells." Cell **113**(5): 643-655.

Champiat, S., et al. (2014). "Exomics and immunogenics Bridging mutational load and immune checkpoints efficacy." Oncoimmunology **3**(1).

Cheever, M. A. and C. S. Higano (2011). "PROVENGE (Sipuleucel-T) in Prostate Cancer: The First FDA-Approved Therapeutic Cancer Vaccine." Clinical Cancer Research **17**(11): 3520-3526.

Chen, L. P. (2004). "Co-inhibitory molecules of the B7-CD28 family in the control of T-cell immunity." Nature Reviews Immunology **4**(5): 336-347.

Chen, W., et al. (2012). "The Advances in Molecular Biology of Hepatoblastoma: Implications for Diagnostic Pathology." N A J Med Sci **5**(4): 217-223.

Chen, X. H., et al. (2008). "Identification of tumor-associated antigens in human hepatocellular carcinoma by autoantibodies." Oncology Reports **20**(4): 979-985.

Chiereghin, A., et al. (2016). "Successful management of EBV-PTLD in allogeneic bone marrow transplant recipient by virological-immunological monitoring of EBV infection, prompt diagnosis and early treatment." Transplant Immunology **34**: 60-64.

Clevers, H. (2006). "Wnt/beta-catenin signaling in development and disease." Cell **127**(3): 469-480.

Cobbold, M., et al. (2013). "MHC Class I-Associated Phosphopeptides Are the Targets of Memory-like Immunity in Leukemia." Science Translational Medicine **5**(203).

Cobbold, M., et al. (2007). "Immune targeting of the phosphoproteome in lymphoma and leukemia." Blood **110**(11): 91A-91A.

Cohen, J. I. (2000). "Epstein-Barr virus infection." New England Journal of Medicine **343**(7): 481-492.

Coiffier, B., et al. (1998). "Rituximab (anti-CD20 monoclonal antibody) for the treatment of patients with relapsing or refractory aggressive lymphoma: A multicenter phase II study." Blood **92**(6): 1927-1932.

Couinaud, C. (1999). "Liver anatomy: portal (and suprahepatic) or biliary segmentation." Digestive Surgery **16**(6): 459-467.

Coulie, P. G., et al. (2014). "Tumour antigens recognized by T lymphocytes: at the core of cancer immunotherapy." Nature Reviews Cancer **14**(2): 135-146.

Couzin-Frankel, J. (2013). "Cancer Immunotherapy." Science **342**(6165): 1432-1433.

Crawford, D. H. (2001). "Biology and disease associations of Epstein-Barr virus." Philosophical Transactions of the Royal Society of London Series B-Biological Sciences **356**(1408): 461-473.

Curiel, T. J. (2007). "Regulatory T-cell development: is Foxp3 the decider?" Nature Medicine **13**(3): 250-253.

Curiel, T. J. (2007). "Tregs and rethinking cancer immunotherapy." Journal of Clinical Investigation **117**(5): 1167-1174.

Curiel, T. J., et al. (2004). "Specific recruitment of regulatory T cells in ovarian carcinoma fosters immune privilege and predicts reduced survival." Nature Medicine **10**(9): 942-949.

Cyranoski D (2014). "Stem cell scientist found guilty of misconduct". Nature News (01 Apr) doi:10.1038/nature.2014.14974

Czerkinsky, C. C., et al. (1984). "REVERSE ENZYME-LINKED IMMUNOSPOT ASSAY (RELISPOT) FOR THE DETECTION OF CELLS SECRETING IMMUNOREACTIVE SUBSTANCES." Journal of Immunological Methods **72**(2): 489-496.

Dang, T. O., et al. (2016). "Pembrolizumab for the treatment of PD-L1 positive advanced or metastatic non-small cell lung cancer." Expert Review of Anticancer Therapy **16**(1): 13-20.

Daubenberger, C. A., et al. (2001). "Herpesvirus saimiri transformed T cells and peripheral blood mononuclear cells restimulate identical antigen-specific human T cell clones." Journal of Immunological Methods **254**(1-2): 99-108.

Davis, T. A., et al. (1998). "Rituximab: First report of a phase II (PII) trial in NHL patients (pts) with bulky disease." Blood **92**(10): 414A-414A.

de Vries, E., et al. (2000). "Longitudinal survey of lymphocyte subpopulations in the first year of life." Pediatric Research **47**(4): 528-537.

Deftos, M. L. and M. J. Bevan (2000). "Notch signaling in T cell development." Current Opinion in Immunology **12**(2): 166-172.

Delves P, M. S., Burton D, Roitt I (2006). Essential Immunology, Blackwell.

Depontieu, F. R., et al. (2009). "Identification of tumor-associated, MHC class II-restricted phosphopeptides as targets for immunotherapy." Proceedings of the National Academy of Sciences of the United States of America **106**(29): 12073-12078.

Destgroth, S. F. and D. Scheidegger (1980). "PRODUCTION OF MONOCLONAL-ANTIBODIES - STRATEGY AND TACTICS." Journal of Immunological Methods **35**(1-2): 1-21.

Dharnidharka, V. R., et al. (2016). "Post-transplant lymphoproliferative disorders." Nature reviews. Disease primers **2**: 15088-15088.

Diehl, V., et al. (1968). "EFFECT OF A HERPES-TYPE (EBV) ON GROWTH OF PERIPHERAL LEUKOCYTE CULTURES." Federation Proceedings **27**(2): 682-&.

Domingues, D., et al. (2014). "Immunotherapy and lung cancer: current developments and novel targeted therapies." Immunotherapy **6**(11): 1221-1235.

Dranoff, G. (2004). "Cytokines in cancer pathogenesis and cancer therapy." Nature Reviews Cancer **4**(1): 11-22.

Dudley, M. E., et al. (2003). "Generation of tumor-infiltrating lymphocyte cultures for use in adoptive transfer therapy for melanoma patients." Journal of Immunotherapy **26**(4): 332-342.

Dunn, G. P., et al. (2005). "A critical function for type I interferons in cancer immunoediting." Nature Immunology **6**(7): 722-729.

Dunn, G. P., et al. (2006). "Interferons, immunity and cancer immunoediting." Nature Reviews Immunology **6**(11): 836-848.

Dunn, G. P., et al. (2004). "The immunobiology of cancer immunosurveillance and immunoediting." Immunity **21**(2): 137-148.

Dunn, G. P., et al. (2004). "The three Es of cancer immunoediting." Annual Review of Immunology **22**: 329-360.

Dunn, J. and S. Rao (2017). "Epigenetics and immunotherapy: The current state of play." Molecular Immunology **87**: 227-239.

Egawa, K. (2004). "Immuno-cell therapy of cancer in Japan." Anticancer Research **24**(5C): 3321-3326.

Emens, L. A., et al. (2012). "Toward integrative cancer immunotherapy: targeting the tumor microenvironment." Journal of Translational Medicine **10**.

Eshhar, Z. and G. Gross (1990). "CHIMERIC T-CELL RECEPTOR WHICH INCORPORATES THE ANTITUMOR SPECIFICITY OF A MONOCLONAL-ANTIBODY WITH THE CYTOLYTIC ACTIVITY OF T-CELLS - A MODEL SYSTEM FOR IMMUNOTHERAPEUTIC APPROACH." British Journal of Cancer **62**: 27-29.

Eshhar, Z., et al. (1996). "Targeting T-cells to cancer using chimeric receptors." Immunology **89**: SI114-SI114.

Eshhar, Z., et al. (1993). "SPECIFIC ACTIVATION AND TARGETING OF CYTOTOXIC LYMPHOCYTES THROUGH CHIMERIC SINGLE CHAINS CONSISTING OF ANTIBODY-BINDING DOMAINS AND THE GAMMA-SUBUNIT OR ZETA-SUBUNIT OF THE IMMUNOGLOBULIN AND T-CELL RECEPTORS." Proceedings of the National Academy of Sciences of the United States of America **90**(2): 720-724.

Esmaeili, M. A., et al. (2014). "Anticancer effect of calycopterin via PI3K/Akt and MAPK signaling pathways, ROS-mediated pathway and mitochondrial dysfunction in hepatoblastoma cancer (HepG2) cells." Molecular and Cellular Biochemistry **397**(1-2): 17-31.

Evan, G. I. and K. H. Vousden (2001). "Proliferation, cell cycle and apoptosis in cancer." Nature **411**(6835): 342-348.

Feng, F., et al. (2012). "OP9-DL1 cell co-culture enhances anti-tumour immunity of mouse bone marrow-derived dendritic cells." Cell Biology International **36**(3): 297-303.

Fickenscher, H., et al. (1996). "Regulation of the herpesvirus Saimiri oncogene stpC, similar to that of T-cell activation genes, in growth-transformed human T lymphocytes." Journal of Virology **70**(9): 6012-6019.

Fidler, I. J. and M. L. Kripke (1977). "METASTASIS RESULTS FROM PREEXISTING VARIANT CELLS WITHIN A MALIGNANT-TUMOR." Science **197**(4306): 893-895.

Flecken, T., et al. (2014). "Immunodominance and Functional Alterations of Tumor-Associated Antigen-Specific CD8(+) T-Cell Responses in Hepatocellular Carcinoma." Hepatology **59**(4): 1415-1426.

Fowlkes, B. J. and E. A. Robey (2002). "A reassessment of the effect of activated Notch1 on CD4 and CD8 T cell development." Journal of Immunology **169**(4): 1817-1821.

Fuchs, E. J. and P. Matzinger (1996). "Is cancer dangerous to the immune system?" Seminars in immunology **8**(5): 271-280.

Fulda, S., et al. (1998). "Chemosensitivity of solid tumor cells in vitro is related to activation of the CD95 system." International Journal of Cancer **76**(1): 105-114.

Galon, J., et al. (2012). "The Immune Score as a New Possible Approach for the Classification of Cancer." Journal of Translational Medicine **10**.

Garrido, F., et al. (2017). "The Escape of Cancer from T Cell-Mediated Immune Surveillance: HLA Class I Loss and Tumor Tissue Architecture." Vaccines **5**(1).

Gatti, R. A. and R. A. Good (1971). "OCCURRENCE OF MALIGNANCY IN IMMUNODEFICIENCY DISEASES - LITERATURE REVIEW." Cancer **28**(1): 89-&.

Gilboa, E. (2004). "Opinion - The promise of cancer vaccines." Nature Reviews Cancer **4**(5): 401-411.

Goldman, B. and L. DeFrancesco (2009). "The cancer vaccine roller coaster." Nature Biotechnology **27**(2): 129-139.

Gottesman, A., et al. (2010). "V-fusion: a convenient, nontoxic method for cell fusion." Biotechniques **49**(4): 747-+.

Grassmann, R., et al. (1990). "TRANSFORMING GENES TRANSDUCED BY THE T-LYMPHOTROPIC HERPESVIRUS SAIMIRI." Journal of Cancer Research and Clinical Oncology **116**(SUPPL. PART 2): 1182-1182.

Gregory, J. J. and J. L. Finlay (1999). "alpha-fetoprotein and beta-human chorionic gonadotropin - Their clinical significance as tumour markers." Drugs **57**(4): 463-467.

Gross, G., et al. (1989). "GENERATION OF EFFECTOR T-CELLS EXPRESSING CHIMERIC T-CELL RECEPTOR WITH ANTIBODY TYPE-SPECIFICITY." Transplantation Proceedings **21**(1): 127-130.

Gross, G., et al. (1989). "EXPRESSION OF IMMUNOGLOBULIN-T-CELL RECEPTOR CHIMERIC MOLECULES AS FUNCTIONAL RECEPTORS WITH ANTIBODY-TYPE SPECIFICITY." Proceedings of the National Academy of Sciences of the United States of America **86**(24): 10024-10028.

Grulich, A. E., et al. (2007). "Incidence of cancers in people with HIV/AIDS compared with immunosuppressed transplant recipients: a meta-analysis." Lancet **370**(9581): 59-67.

Grupp, S. A. and C. H. June (2011). "Adoptive Cellular Therapy." Cancer Immunology and Immunotherapy **344**: 149-172.

Gu, X., et al. (2015). "Genetic testing for sporadic hearing loss using targeted massively parallel sequencing identifies 10 novel mutations." Clinical Genetics **87**(6): 588-593.

Hall, K. T., et al. (2000). "Analysis of gene expression in a human cell line stably transduced with herpesvirus saimiri." Journal of Virology **74**(16): 7331-7337.

Hanahan, D. (2014). "Hallmarks of cancer: applications to cancer medicine?" European Journal of Cancer **50**: S21-S21.

Hanahan, D. and L. M. Coussens (2012). "Accessories to the Crime: Functions of Cells Recruited to the Tumor Microenvironment." Cancer Cell **21**(3): 309-322.

Hanahan, D. and R. A. Weinberg (2000). "The hallmarks of cancer." Cell **100**(1): 57-70.

Hanahan, D. and R. A. Weinberg (2011). "Hallmarks of Cancer: The Next Generation." Cell **144**(5): 646-674.

Haque, T., et al. (2011). "Long Term Clinical Outcome of Treating PTLD Patients with Epstein-Barr Virus (EBV)-Specific Cytotoxic T Cells (CTL)." American Journal of Transplantation **11**: 137-137.

Hartmann, W., et al. (2009). "Activation of Phosphatidylinositol-3 '-kinase/AKT Signaling Is Essential in Hepatoblastoma Survival." Clinical Cancer Research **15**(14): 4538-4545.

Henle, W., et al. (1967). "HERPES-TYPE VIRUS AND CHROMOSOME MARKER IN NORMAL LEUKOCYTES AFTER GROWTH WITH IRRADIATED BURKITT CELLS." Science **157**(3792): 1064-&.

Heslop, H. E., et al. (2010). "Long-term outcome of EBV-specific T-cell infusions to prevent or treat EBV-related lymphoproliferative disease in transplant recipients." Blood **115**(5): 925-935.

Higano, C. S. (2012). "New treatment options for patients with metastatic castration-resistant prostate cancer." Cancer Treatment Reviews **38**(5): 340-345.

Higano, C. S., et al. (2015). "Administration of sipuleucel-T (sip-T) infusions (infs) outside of the clinical trial setting: Data from the PROCEED registry." Journal of Clinical Oncology **33**(15).

Higano, C. S., et al. (2009). "Integrated Data From 2 Randomized, Double-Blind, Placebo-Controlled, Phase 3 Trials of Active Cellular Immunotherapy With Sipuleucel-T in Advanced Prostate Cancer." Cancer **115**(16): 3670-3679.

Higano, C. S., et al. (2010). "Sipuleucel-T." Nature Reviews Drug Discovery **9**(7): 513-514.

Hsiao, C. C., et al. (2013). "Toll-like receptor-4 agonist inhibits motility and invasion of hepatoblastoma HepG2 cells in vitro." Pediatric Blood & Cancer **60**(2): 248-253.

Hundhausen, T., et al. (1992). "NEW PARENTAL CELL-LINES FOR GENERATING HUMAN HYBRIDOMAS." Journal of Immunological Methods **153**(1-2): 21-29.

Hwu, P., et al. (1995). "IN-VIVO ANTITUMOR-ACTIVITY OF T-CELLS REDIRECTED WITH CHIMERIC ANTIBODY T-CELL RECEPTOR GENES." Cancer Research **55**(15): 3369-3373.

Jacobson, C. A. and A. S. LaCasce (2010). "Lymphoma: Risk and Response After Solid Organ Transplant." Oncology-New York **24**(10): 936-944.

Jager, E., et al. (1996). "Cytolytic T cell reactivity against melanoma-associated differentiation antigens in peripheral blood of melanoma patients and healthy individuals." Melanoma Research **6**(6): 419-425.

Jager, E., et al. (1996). "Inverse relationship of melanocyte differentiation antigen expression in melanoma tissues and CD8(+) cytotoxic-T-cell responses: Evidence for immunoselection of antigen-loss variants in vivo." International Journal of Cancer **66**(4): 470-476.

Joffre, O. P., et al. (2012). "Cross-presentation by dendritic cells." Nature Reviews Immunology **12**(8): 557-569.

Johnsen, A. K., et al. (1999). "Deficiency of transporter for antigen presentation (TAP) in tumor cells allows evasion of immune surveillance and increases tumorigenesis." Journal of Immunology **163**(8): 4224-4231.

Joseph, A. M., et al. (2000). "Cells expressing the Epstein-Barr virus growth program are present in and restricted to the naive B-cell subset of healthy tonsils." Journal of Virology **74**(21): 9964-9971.

Kamao, H., et al. (2014). "Characterization of Human Induced Pluripotent Stem Cell-Derived Retinal Pigment Epithelium Cell Sheets Aiming for Clinical Application." Stem Cell Reports **2**(2): 205-218.

Kaplan, D. H., et al. (1998). "Demonstration of an interferon gamma-dependent tumor surveillance system in immunocompetent mice." Proceedings of the National Academy of Sciences of the United States of America **95**(13): 7556-7561.

Keiff E, R. A. (2001). Epstein-Barr Virus and its replication, Lippincott, Williams and Wilkins.

Kiang, D. T. and B. J. Kennedy (1977). "TAMOXIFEN (ANTIESTROGEN) THERAPY IN ADVANCED BREAST-CANCER." Annals of Internal Medicine **87**(6): 687-690.

Klebe, R. J. and M. G. Mancuso (1981). "CHEMICALS WHICH PROMOTE CELL HYBRIDIZATION." Somatic Cell Genetics **7**(4): 473-488.

Klebe, R. J. and M. G. Mancuso (1982). "ENHANCEMENT OF POLYETHYLENE GLYCOL-MEDIATED CELL HYBRIDIZATION BY INDUCERS OF ERYTHROLEUKEMIA CELL-DIFFERENTIATION." Somatic Cell Genetics **8**(6): 723-730.

Klein, J. L., et al. (1996). "Herpesvirus saimiri immortalized gamma delta T cell line activated by IL-12." Journal of Immunology **156**(8): 2754-2760.

Kline, J. and T. F. Gajewski (2010). "Clinical development of mAbs to block the PD1 pathway as an immunotherapy for cancer." Current Opinion in Investigational Drugs **11**(12): 1354-1359.

Kodama, H., et al. (1994). "INVOLVEMENT OF THE C-KIT RECEPTOR IN THE ADHESION OF HEMATOPOIETIC STEM-CELLS TO STROMAL CELLS." Experimental Hematology **22**(10): 979-984.

Koh, K. N., et al. (2011). "Prognostic Implications of Serum Alpha-Fetoprotein Response During Treatment of Hepatoblastoma." Pediatric Blood & Cancer **57**(4): 554-560.

Kohler, G. and C. Milstein (1975). "CONTINUOUS CULTURES OF FUSED CELLS SECRETING ANTIBODY OF PREDEFINED SPECIFICITY." Nature **256**(5517): 495-497.

Kondo, M., et al. (1997). "Identification of clonogenic common lymphoid progenitors in mouse bone marrow." Cell **91**(5): 661-672.

Korinek, V., et al. (1998). "Two members of the Tcf family implicated in Wnt/beta-catenin signaling during embryogenesis in the mouse." Molecular and Cellular Biology **18**(3): 1248-1256.

Korswagen, H. C., et al. (1999). Activation and repression of wingless/Wnt target genes by the TCF/LEF-1 family of transcription factors. Signaling and gene expression in the immune system. **Volume 64:** 141-148.

Kotiranta-Ainamo, A., et al. (1999). "Mononuclear cell subpopulations in preterm and full-term neonates: independent effects of gestational age, neonatal infection, maternal pre-eclampsia, maternal betamethason therapy, and mode of delivery." Clinical and Experimental Immunology **115**(2): 309-314.

Kozyrskyj, A. L., et al. (2011). "Early life exposures: impact on asthma and allergic disease." Current Opinion in Allergy and Clinical Immunology **11**(5): 400-406.

Kutlesa, S., et al. (2009). "T-cell differentiation of multipotent hematopoletic cell line EML in the OP9-DL1 coculture system." Experimental Hematology **37**(8): 909-923.

Laky, K. and B. J. Fowkes (2008). "Notch signaling in CD4 and CD8 T cell development." Current Opinion in Immunology **20**(2): 197-202.

Lazebnik, Y. (2010). "What are the hallmarks of cancer?" Nature Reviews Cancer **10**(4): 232-233.

Lee, S.-G. (2015). "Twenty-year survival post-liver transplant: challenges and lessons." Hepatology International **9**(3): 342-345.

Leichter, A. L., et al. (2017). "MicroRNA expression patterns and signalling pathways in the development and progression of childhood solid tumours." Molecular Cancer **16**.

Li, K., et al. (2005). "Preclinical ex vivo expansion of G-CSF-mobilized peripheral blood stem cells: effects of serum-free media, cytokine combinations and chemotherapy." European Journal of Haematology **74**(2): 128-135.

Li, X. R., et al. (2010). "Efficient Treg depletion induces T-cell infiltration and rejection of large tumors." European Journal of Immunology **40**(12): 3325-3335.

Li, Y. L., et al. (2010). "Structural Basis for the Presentation of Tumor-Associated MHC Class II-Restricted Phosphopeptides to CD4(+) T Cells." Journal of Molecular Biology **399**(4): 596-603.

Liang, J., et al. (2013). "Expression pattern of tumour-associated antigens in hepatocellular carcinoma: association with immune infiltration and disease progression." British Journal of Cancer **109**(4): 1031-1039.

Liyanage, U. K., et al. (2002). "Prevalence of regulatory T cells is increased in peripheral blood and tumor microenvironment of patients with pancreas or breast adenocarcinoma." Journal of Immunology **169**(5): 2756-2761.

Lopez-Terrada, D., et al. (2014). "Towards an international pediatric liver tumor consensus classification: proceedings of the Los Angeles COG liver tumors symposium." Modern Pathology **27**(3): 472-491.

Lovvorn, H. N., III, et al. (2010). "Defining hepatoblastoma responsiveness to induction therapy as measured by tumor volume and serum alpha-fetoprotein kinetics." Journal of Pediatric Surgery **45**(1): 121-129.

Luo, L. Q., et al. (2004). "B7-H3 enhances tumor immunity in vivo by costimulating rapid clonal expansion of antigen-specific CD8(+) cytolytic T cells." Journal of Immunology **173**(9): 5445-5450.

Malik, N. and M. S. Rao (2013). "A review of the methods for human iPSC derivation." Methods in molecular biology (Clifton, N.J.) **997**: 23-33.

Maloney, D. G., et al. (1997). "IDEC-C2B8: Results of a phase I multiple-dose trial in patients with relapsed non-Hodgkin's lymphoma." Journal of Clinical Oncology **15**(10): 3266-3274.

Mann JR, K. N., Raafat F (1990). "Malignant hepatic tumours in children: incidence, clinical features and aetiology." Paediatr Perinat Epidemiol **4**: 276-289.

Mantovani, A., et al. (2008). "Cancer-related inflammation." Nature **454**(7203): 436-444.

Manz, M. G., et al. (2001). "Dendritic cell potentials of early lymphoid and myeloid progenitors." Blood **97**(11): 3333-3341.

Marchand, M., et al. (1999). "Tumor regressions observed in patients with metastatic melanoma treated with an antigenic peptide encoded by gene MAGE-3 and presented by HLA-A1." International Journal of Cancer **80**(2): 219-230.

Marmarelis, M. E., et al. (2016). "Tumor control with PD-1 inhibition in a patient with concurrent metastatic melanoma and renal cell carcinoma." Journal for Immunotherapy of Cancer **4**.

Matsuya, Y. and I. Yamane (1985). "CELL HYBRIDIZATION AND CELL AGGLUTINATION .2. ENHANCEMENT OF CELL HYBRIDIZATION BY POLYCATIONS." Journal of Cell Science **78**: 273-282.

Matsuya, Y. and I. Yamane (1985). "CELL-FUSION AND CELL AGGLUTINATION - ENHANCING EFFECT BY A COMBINED USE OF LECTIN AND POLYCATION." Somatic Cell and Molecular Genetics **11**(3): 247-255.

Meadows, L., et al. (1997). "The HLA-A*0201-restricted H-Y antigen contains a posttranslationally modified cysteine that significantly affects T cell recognition." Immunity **6**(3): 273-281.

Meinl, E., et al. (1997). "Growth transformation of antigen-specific T cell lines from rhesus monkeys by Herpesvirus saimiri." Virology **229**(1): 175-182.

Meinl, E., et al. (1995). "IMMORTALIZATION OF HUMAN T-CELLS BY HERPESVIRUS-SAIMIRI." Immunology Today **16**(2): 55-58.

Meraz, M. A., et al. (1996). "Targeted disruption of the STAT1 gene in mice reveals unexpected physiologic specificity in the JAK-STAT signaling pathway." Cell **84**(3): 431-442.

Mercer, W. E. and R. A. Schlegel (1979). "PHYTOHEMAGGLUTININ ENHANCEMENT OF CELL-FUSION REDUCES POLYETHYLENE-GLYCOL CYTOTOXICITY." Experimental Cell Research **120**(2): 417-421.

Mescher, M. F., et al. (2007). "Molecular basis for checkpoints in the CD8 T cell response: Tolerance versus activation." Seminars in immunology **19**(3): 153-161.

Mescher, M. F., et al. (2007). "Activation-induced non-responsiveness (anergy) limits CD8 T cell responses to tumors." Seminars in Cancer Biology **17**(4): 299-308.

Micheau, O., et al. (1997). "Sensitization of cancer cells treated with cytotoxic drugs to Fas-mediated cytotoxicity." Journal of the National Cancer Institute **89**(11): 783-789.

Milstein, C., et al. (1972). "POSSIBLE PRECURSOR OF IMMUNOGLOBULIN LIGHT CHAINS." Nature-New Biology **239**(91): 117-&.

Minagawa, A. and S. Kaneko (2014). "Rise of iPSCs as a cell source for adoptive immunotherapy." Human Cell **27**(2): 47-50.

Minn, A. J., et al. (2005). "Distinct organ-specific metastatic potential of individual breast cancer cells and primary tumors." Journal of Clinical Investigation **115**(1): 44-55.

Miyara, M. and S. Sakaguchi (2011). "Human FoxP3(+)CD4(+) regulatory T cells: their knowns and unknowns." Immunology and Cell Biology **89**(3): 346-351.

Miyashita, E. M., et al. (1997). "Identification of the site of Epstein-Barr virus persistence in vivo as a resting B cell." Journal of Virology **71**(7): 4882-4891.

Mizukoshi, E., et al. (2011). "Comparative Analysis of Various Tumor-Associated Antigen-Specific T-Cell Responses in Patients with Hepatocellular Carcinoma." Hepatology **53**(4): 1206-1216.

Moeini, A., et al. (2012). "Emerging signaling pathways in hepatocellular carcinoma." Liver cancer **1**(2): 83-93.

Mohammed, F., et al. (2008). "Phosphorylation-dependent interaction between antigenic peptides and MHC class I: a molecular basis for the presentation of transformed self." Nature Immunology **9**(11): 1236-1243.

Mokkapati, S., et al. (2014). "beta-Catenin Activation in a Novel Liver Progenitor Cell Type Is Sufficient to Cause Hepatocellular Carcinoma and Hepatoblastoma." Cancer Research **74**(16): 4515-4525.

Muller, M., et al. (1997). "Drug-induced apoptosis in hepatoma cells is mediated by the CD95 (APO-1/Fas) receptor/ligand system and involves activation of wild-type p53." Journal of Clinical Investigation **99**(3): 403-413.

Munn, D. H. (2009). "Th17 cells in ovarian cancer." Blood **114**(6): 1134-1135.

Murugaiyan, G. and B. Saha (2009). "Protumor vs Antitumor Functions of IL-17." Journal of Immunology **183**(7): 4169-4175.

Nagata, S., et al. (2009). "Efficient reprogramming of human and mouse primary extra-embryonic cells to pluripotent stem cells." Genes to Cells **14**(12): 1395-1404.

Nakano, T., et al. (1994). "GENERATION OF LYMPHOHEMATOPOIETIC CELLS FROM EMBRYONIC STEM-CELLS IN CULTURE." Science **265**(5175): 1098-1101.

Neitzel, H. (1986). "A ROUTINE METHOD FOR THE ESTABLISHMENT OF PERMANENT GROWING LYMPHOBLASTOID CELL-LINES." Human Genetics **73**(4): 320-326.

Nestle, F. O., et al. (1998). "Vaccination of melanoma patients with peptide- or tumor lysate-pulsed dendritic cells." Nature Medicine **4**(3): 328-332.

Nichols, J., et al. (1998). "Formation of pluripotent stem cells in the mammalian embryo depends on the POU transcription factor Oct4." Cell **95**(3): 379-391.

Nick, S., et al. (1993). "Herpesvirus saimiri transformed T cell lines: A new permissive system for HIV-1 and HIV-2." IXth International Conference on AIDS in affiliation with the IVth STD World Congress: 18-18.

NIH (2015). "What is Cancer."

Ninane, J., et al. (1991). "EFFECTIVENESS AND TOXICITY OF CISPLATIN AND DOXORUBICIN (PLADO) IN CHILDHOOD HEPATOBLASTOMA AND HEPATOCELLULAR-CARCINOMA - A SIOP PILOT-STUDY." Medical and Pediatric Oncology **19**(3): 199-203.

Nino, J. L. G., et al. (2016). "Antigen-specific T cells fully conserve antitumour function following cryopreservation." Immunology and Cell Biology **94**(4): 411-418.

Nishimura, K., et al. (2014). "Manipulation of KLF4 Expression Generates iPSCs Paused at Successive Stages of Reprogramming." Stem Cell Reports **3**(5): 915-929.

Nishimura, T., et al. (2013). "Generation of Rejuvenated Antigen-Specific T Cells by Reprogramming to Pluripotency and Redifferentiation." Cell Stem Cell **12**(1): 114-126.

Niwa, H., et al. (2000). "Quantitative expression of Oct-3/4 defines differentiation, dedifferentiation or self-renewal of ES cells." Nature Genetics **24**(4): 372-376.

Nowell, P. C. (1976). "CLONAL EVOLUTION OF TUMOR-CELL POPULATIONS." Science **194**(4260): 23-28.

Obokata, H., et al. (2014). "Retraction: Stimulus-triggered fate conversion of somatic cells into pluripotency." Nature **511**(7507): 112-112.

Obokata, H., et al. (2014). "Stimulus-triggered fate conversion of somatic cells into pluripotency (Retracted article. See vol. 511, pg. 112, 2014)." Nature **505**(7485): 641-+.

Obokata, H., et al. (2014). "Stimulus-triggered fate conversion of somatic cells into pluripotency (Retraction of vol 505, pg 641, 2014)." Nature **511**(7507): 112-112.

Ok, C. Y. and K. H. Young (2017). "Checkpoint inhibitors in hematological malignancies." Journal of Hematology & Oncology **10**.

Ok, C. Y. and K. H. Young (2017). "Targeting the programmed death-1 pathway in lymphoid neoplasms." Cancer Treatment Reviews **54**: 99-109.

Okimoto, T., et al. (2001). "VSV-G envelope glycoprotein forms complexes with plasmid DNA and MLV retrovirus-like particles in cell-free conditions and enhances DNA transfection." Molecular Therapy **4**(3): 232-238.

Okita, K., et al. (2007). "Generation of germline-competent induced pluripotent stem cells." Nature **448**(7151): 313-U311.

Otte, J.-B. (2010). "Progress in the surgical treatment of malignant liver tumors in children." Cancer Treatment Reviews **36**(4): 360-371.

Ozdemirli, M., et al. (1996). "Fas (CD95)/Fas ligand interactions regulate antigen-specific, major histocompatibility complex-restricted T/E cell proliferative responses." European Journal of Immunology **26**(2): 415-419.

Ozlu, N., et al. (2010). "Phosphoproteomics." Wiley Interdisciplinary Reviews-Systems Biology and Medicine **2**(3): 255-276.

Pages, F., et al. (2010). "Immune infiltration in human tumors: a prognostic factor that should not be ignored." Oncogene **29**(8): 1093-1102.

Pardoll, D. M. (2012). "The blockade of immune checkpoints in cancer immunotherapy." Nature Reviews Cancer **12**(4): 252-264.

Peifer, M. and P. Polakis (2000). "Cancer - Wnt signaling in oncogenesis and embryogenesis - a look outside the nucleus." Science **287**(5458): 1606-1609.

Penny, S. A., et al. (2012). "Identification of posttranslationally modified tumour antigens in colorectal carcinoma reveals functional tumour-resident immunity targeting phosphoantigens." Immunology **137**: 609-609.

Polakis, P. (2000). "Wnt signaling and cancer." Genes & Development **14**(15): 1837-1851.

Pritchard, J., et al. (2000). "Cisplatin, doxorubicin, and delayed surgery for childhood hepatoblastoma: A successful approach - Results of the first prospective study of the international society of pediatric oncology." Journal of Clinical Oncology **18**(22): 3819-3828.

Radtke, F., et al. (2004). "Notch signaling in T- and B-cell development." Current Opinion in Immunology **16**(2): 174-179.

Ramsay, A. D., et al. (2008). "Variable antigen expression in hepatoblastomas." Applied Immunohistochemistry & Molecular Morphology **16**(2): 140-147.

Rao, M. S. and N. Malik (2012). "Assessing iPSC reprogramming methods for their suitability in translational medicine." Journal of Cellular Biochemistry **113**(10): 3061-3068.

Rashin, A. A. and R. L. Jernigan (2016). "Clusters of Structurally Similar MHC I HLA-A2 Molecules, Found with a New Method, Suggest Mechanisms of T-Cell Receptor Avidity." Biochemistry **55**(1): 167-185.

Reeve, P., et al. (1974). "VIRUS-INDUCED CELL-FUSION ENHANCED BY PHYTOHEMAGGLUTININ." Nature **249**(5455): 355-356.

Reeves, E. and E. James (2017). "Antigen processing and immune regulation in the response to tumours." Immunology **150**(1): 16-24.

Reichert, J. M. (2014). "Antibodies to watch in 2014." Mabs **6**(1): 5-14.

Rellahan, B. L. and R. E. Cone (1990). "ONTOGENY AND EXPRESSION OF NON-MHC-RESTRICTED T-CELL ANTIGEN-BINDING MOLECULES BY THYMOCYTES AND PERIPHERAL T-CELL SUBSETS." Cellular Immunology **130**(1): 176-185.

Ricciardelli, I., et al. (2014). "Towards gene therapy for EBV-associated posttransplant lymphoma with genetically modified EBV-specific cytotoxic T cells." Blood **124**(16): 2514-2522.

Ricciardelli, I., et al. (2013). "Rapid Generation of EBV-Specific Cytotoxic T Lymphocytes Resistant to Calcineurin Inhibitors for Adoptive Immunotherapy." American Journal of Transplantation **13**(12): 3244-3252.

Robey, E., et al. (1996). "An activated form of notch influences the choice between CD4 and CD8 T cell lineages." Cell **87**(3): 483-492.

Roebuck, D. J., et al. (2007). "2005 PRETEXT: a revised staging system for primary malignant liver tumours of childhood developed by the SIOPEL group." Pediatric Radiology **37**(2): 123-132.

Romero, P. (1996). "Cytolytic T lymphocyte responses of cancer patients to tumor-associated antigens." Springer Seminars in Immunopathology **18**(2): 185-198.

Romero, V., et al. (2013). "Developmental programming for allergic disease: a secondary analysis of the Mothers, Omega-3 and Mental Health Study." American Journal of Obstetrics and Gynecology **208**(1): S24-S24.

Rosenberg, S. A. (1984). "ADOPTIVE IMMUNOTHERAPY OF CANCER - ACCOMPLISHMENTS AND PROSPECTS." Cancer Treatment Reports **68**(1): 233-255.

Rosenberg, S. A., et al. (1998). "Immunologic and therapeutic evaluation of a synthetic peptide vaccine for the treatment of patients with metastatic melanoma." Nature Medicine **4**(3): 321-327.

Ruth, N., et al. (2010). "IS REJECTION LESS COMMON IN CHILDREN UNDERGOING LIVER TRANSPLANTATION FOR HEPATOBLASTOMA?" Pediatric Blood & Cancer **55**(5): 904-904.

Sakaguchi, S., et al. (1995). "IMMUNOLOGICAL SELF-TOLERANCE MAINTAINED BY ACTIVATED T-CELLS EXPRESSING IL-2 RECEPTOR ALPHA-CHAINS (CD25) - BREAKDOWN OF A SINGLE MECHANISM OF SELF-TOLERANCE CAUSES VARIOUS AUTOIMMUNE-DISEASES." Journal of Immunology **155**(3): 1151-1164.

Salavoura, K., et al. (2008). "Development of cancer in patients with primary immunodeficiencies." Anticancer Research **28**(2B): 1263-1269.

Salmaninejad, A., et al. (2016). "Cancer/Testis Antigens: Expression, Regulation, Tumor Invasion, and Use in Immunotherapy of Cancers." Immunological Investigations **45**(7): 619-640.

Scaffidi, C., et al. (1998). "Two CD95 (APO-1/Fas) signaling pathways." Embo Journal **17**(6): 1675-1687.

Schabowsky, R. H., et al. (2007). "Targeting CD4(+)CD25(+)FoxP3(+) regulatory T-cells for the augmentation of cancer immunotherapy." Current Opinion in Investigational Drugs **8**(12): 1002-1008.

Schmitt, T. M. and J. C. Zuniga-Pflucker (2002). "Induction of T cell development from hematopoietic progenitor cells by delta-like-1 in vitro." Immunity **17**(6): 749-756.

Schneiderman, S., et al. (1979). "SIMPLE METHOD FOR DECREASING THE TOXICITY OF POLYETHYLENE-GLYCOL IN MAMMALIAN-CELL HYBRIDIZATION." Somatic Cell Genetics **5**(2): 263-269.

Schumacher, T. N. and R. D. Schreiber (2015). "Neoantigens in cancer immunotherapy." Science **348**(6230): 69-74.

Seliger, B. (2016). "Molecular mechanisms of HLA class I-mediated immune evasion of human tumors and their role in resistance to immunotherapies." Hla **88**(5): 213-220.

Senovilla, L., et al. (2012). "An Immunosurveillance Mechanism Controls Cancer Cell Ploidy." Science **337**(6102): 1678-1684.

Shankaran, V., et al. (2001). "IFN gamma and lymphocytes prevent primary tumour development and shape tumour immunogenicity." Nature **410**(6832): 1107-1111.

Shearer, W. T., et al. (2003). "Lymphocyte subsets in healthy children from birth through 18 years of age: The pediatric AIDS clinical trials group P1009 study." Journal of Allergy and Clinical Immunology **112**(5): 973-980.

Shreders, A., et al. (2016). "Prolonged Benefit from Ipilimumab Correlates with Improved Outcomes from Subsequent Pembrolizumab." Cancer Immunology Research **4**(7): 569-573.

Shrihari, T. G. (2017). "Dual role of inflammatory mediators in cancer." Ecancermedicalscience **11**.

Shukuya, T. and D. P. Carbone (2016). "Predictive Markers for the Efficacy of Anti-PD-1/PD-L1 Antibodies in Lung Cancer." Journal of Thoracic Oncology **11**(7): 976-988.

Siebenlist, U., et al. (2005). "Control of lymphocyte development by nuclear factor-kappa B." Nature Reviews Immunology **5**(6): 435-445.

Simpson, P. (1998). "Introduction: Notch signalling and choice of cell fates in development." Seminars in Cell & Developmental Biology **9**(6): 581-582.

Smyth, M. J., et al. (2001). "A fresh look at tumor immunosurveillance and immunotherapy." Nature Immunology **2**(4): 293-299.

Snyder, A., et al. (2014). "Genetic Basis for Clinical Response to CTLA-4 Blockade in Melanoma." New England Journal of Medicine **371**(23): 2189-2199.

Sonnenschein, C. and A. M. Soto (2013). "The aging of the 2000 and 2011 Hallmarks of Cancer reviews: A critique." Journal of Biosciences **38**(3): 651-663.

Staveley-O'Carroll, K., et al. (1998). "Induction of antigen-specific T cell anergy: An early event in the course of tumor progression." Proceedings of the National Academy of Sciences of the United States of America **95**(3): 1178-1183.

Stenner-Liewen, F., et al. (2000). "Definition of tumor-associated antigens in hepatocellular carcinoma." Cancer Epidemiology Biomarkers & Prevention **9**(3): 285-290.

Strebhardt, K. and A. Ullrich (2008). "Paul Ehrlich's magic bullet concept: 100 years of progress." Nature Reviews Cancer **8**(6): 473-480.

Stronen, E., et al. (2016). "Targeting of cancer neoantigens with donor-derived T cell receptor repertoires." Science **352**(6291): 1337-1341.

Stubbins, R. J., et al. (2015). "Morphologic Evolution in Post-Transplant Lymphoproliferative Disorders (PTLD): A Clinicopathologic Case Series." Blood **126**(23).

Stutman, O. (1974). "TUMOR DEVELOPMENT AFTER 3-METHYLCHOLANTHRENE IN IMMUNOLOGICALLY DEFICIENT ATHYMIC NUDE MICE." Science **183**(4124): 534-536.

Surh, C. D. and J. Sprent (2008). "Homeostasis of Naive and Memory T Cells." Immunity **29**(6): 848-862.

Swann, J. B. and M. J. Smyth (2007). "Immune surveillance of tumors." Journal of Clinical Investigation **117**(5): 1137-1146.

Syka, J. E. P., et al. (2004). "Peptide and protein sequence analysis by electron transfer dissociation mass spectrometry." Proceedings of the National Academy of Sciences of the United States of America **101**(26): 9528-9533.

Takahashi, K., et al. (2007). "Induction of pluripotent stem cells from adult human fibroblasts by defined factors." Cell **131**(5): 861-872.

Takahashi, K. and S. Yamanaka (2006). "Induction of pluripotent stem cells from mouse embryonic and adult fibroblast cultures by defined factors." Cell **126**(4): 663-676.

Takahashi, K. and S. Yamanaka (2013). "Induced pluripotent stem cells in medicine and biology." Development **140**(12): 2457-2461.

Taniguchi, M. and J. Miller (1978). "SPECIFIC SUPPRESSIVE FACTORS PRODUCED BY HYBRIDOMAS DERIVED FROM FUSION OF ENRICHED SUPPRESSOR T-CELLS AND A T-LYMPHOMA CELL LINE." Journal of Experimental Medicine **148**(2): 373-382.

Themeli, M., et al. (2013). "Generation of tumor-targeted human T lymphocytes from induced pluripotent stem cells for cancer therapy." Nature Biotechnology **31**(10): 928-+.

Thomas, J. A., et al. (1990). "IMMUNOHISTOLOGY OF EPSTEIN-BARR VIRUS-ASSOCIATED ANTIGENS IN B-CELL DISORDERS FROM IMMUNOCOMPROMISED INDIVIDUALS." Transplantation **49**(5): 944-953.

Thomson, J.A., Itskovitz-Eldor, J., et al (1998). “Formation of pluripotent stem cells in the mammalian embryo depends on the POU transcription factor Oct4”.Science. 282: 1145–1147.

Thorgeirsson, S. S. and J. W. Grisham (2002). "Molecular pathogenesis of human hepatocellular carcinoma." Nature Genetics **31**(4): 339-346.

Thorley-Lawson, D. A. (2001). "Epstein-Barr virus: exploiting the immune system." Nature Reviews Immunology **1**(1): 75-82.

Tikhonova, A. N., et al. (2012). "alpha beta T Cell Receptors that Do Not Undergo Major Histocompatibility Complex-Specific Thymic Selection Possess Antibody-like Recognition Specificities." Immunity **36**(1): 79-91.

Timms, J. M., et al. (2003). "Target cells of Epstein-Barr-virus (EBV)-positive post-transplant lymphoproliferative disease: similarities to EBV-positive Hodgkin's lymphoma." Lancet **361**(9353): 217-223.

Tomizawa, M. and H. Saisho (2006). "Signaling pathway of insulin-like growth factor-II as a target of molecular therapy for hepatoblastoma." World Journal of Gastroenterology **12**(40): 6531-6535.

Tsao, P. N., et al. (2002). "Longitudinal follow-up of lymphocyte subsets during the first year of life." Asian Pacific Journal of Allergy and Immunology **20**(3): 147-153.

Ueno, H., et al. (2003). "A stromal cell-derived membrane protein that supports hematopoietic stem cells." Nature Immunology **4**(5): 457-463.

Vallier, L. (2015). "Putting induced pluripotent stem cells to the test." Nature Biotechnology **33**(11): 1145-1146.

Van Allen, E. M., et al. (2015). "Genomic correlates of response to CTLA-4 blockade in metastatic melanoma." Science **350**(6257): 207-211.

Van De Wiele, C. J., et al. (2010). "Propagation of common lymphoid progenitors in OP9-DL1 co-culture results in generation of cells incapable of beta-selection." Journal of Immunology **184**.

Van Laethem, F., et al. (2012). "MHC restriction is imposed on a diverse T cell receptor repertoire by CD4 and CD8 co-receptors during thymic selection." Trends in Immunology **33**(9): 437-441.

Vella, C., et al. (2002). "Herpesvirus saimiri-immortalized human lymphocytes: Novel hosts for analyzing HIV type 1 in vitro neutralization." Aids Research and Human Retroviruses **18**(13): 933-946.

Viehl, C. T., et al. (2004). "Depletion of regulatory T cells promotes a tumor-specific immune response." Annals of Surgical Oncology **11**(2): S69-S69.

Vizcardo, R., et al. (2013). "Regeneration of Human Tumor Antigen-Specific T Cells from iPSCs Derived from Mature CD8(+) T Cells." Cell Stem Cell **12**(1): 31-36.

Waldmann, T. A. (2003). "Immunotherapy: past, present and future." Nature Medicine **9**(3): 269-277.

Wang, H. B., et al. (2016). "Coordinated Activities of Multiple Myc-dependent and Myc-independent Biosynthetic Pathways in Hepatoblastoma." Journal of Biological Chemistry **291**(51): 26241-+.

Wang, H. F., et al. (2006). "Distinct roles of IL-7 and stem cell factor in the OP9-DL1 T-cell differentiation culture system." Experimental Hematology **34**(12): 1730-1740.

Wang, L., et al. (2009). "IL-17 can promote tumor growth through an IL-6-Stat3 signaling pathway." Journal of Experimental Medicine **206**(7): 1457-1464.

Wang, S. D. and L. P. Chen (2004). "Co-signaling molecules of the B7-CD28 family in positive and negative regulation of T lymphocyte responses." Microbes and Infection **6**(8): 759-766.

Wang, W., et al. (1997). "A naturally processed peptide presented by HLA-A*0201 is expressed at low abundance and recognized by an alloreactive CD8(+) cytotoxic T cell with apparent high affinity." Journal of Immunology **158**(12): 5797-5804.

Weber, J. S., et al. (2016). "Sequential administration of nivolumab and ipilimumab with a planned switch in patients with advanced melanoma (CheckMate 064): an open-label, randomised, phase 2 trial." Lancet Oncology **17**(7): 943-955.

Wherry, E. J. (2011). "T cell exhaustion." Nature Immunology **12**(6): 492-499.

Wherry, E. J. and M. Kurachi (2015). "Molecular and cellular insights into T cell exhaustion." Nature Reviews Immunology **15**(8): 486-499.

Whiteside, T. L., et al. (2012). "Induced and natural regulatory T cells in human cancer." Expert Opinion on Biological Therapy **12**(10): 1383-1397.

WHO (2014). The WHO World Cancer Report 2014. W. C. Stweart BW, World Health Organisation**:** 16-17.

Willimsky, G. and T. Blankenstein (2005). "Sporadic immunogenic tumours avoid destruction by inducing T-cell tolerance." Nature **437**(7055): 141-146.

Wistinghausen, B., et al. (2013). "Post-Transplant Lymphoproliferative Disease in Pediatric Solid Organ Transplant Recipients." Pediatric Hematology and Oncology **30**(6): 520-531.

Wolf, D., et al. (2005). "The expression of the regulatory T cell-specific forkhead box transcription factor FoxP3 is associated with poor prognosis in ovarian cancer." Clinical Cancer Research **11**(23): 8326-8331.

Wu, S. M. and K. Hothedlinger (2011). "Harnessing the potential of induced pluripotent stem cells for regenerative medicine." Nature Cell Biology **13**(5): 497-505.

Xue, S. A., et al. (2013). "Human MHC Class I-restricted high avidity CD4(+) T cells generated by co-transfer of TCR and CD8 mediate efficient tumor rejection in vivo." Oncoimmunology **2**(1).

Yamamoto, N., et al. (1995). "REGULATORY MECHANISMS FOR PRODUCTION OF IFN-GAMMA AND TNF BY ANTITUMOR T-CELLS OR MACROPHAGES IN THE TUMOR-BEARING STATE." Journal of Immunology **154**(5): 2281-2290.

Yang, Q., et al. (2003). "Tumor-localization by adoptively transferred, interleukin-2-activated NK cells leads to destruction of well-established lung metastases." International Journal of Cancer **105**(4): 512-519.

Yokokawa, J., et al. (2008). "Enhanced functionality of CD4(+)CD25(high)FoxP3(+) regulatory T cells in the peripheral blood of patients with prostate cancer." Clinical Cancer Research **14**(4): 1032-1040.

Yoshii, F. and I. Kaetsu (1982). "EFFECT OF WATER-SOLUBLE POLYMER, POLYETHYLENEGLYCOL, AND GLASS-FORMING COMPOUNDS ON CELL-FUSION." Zeitschrift Fur Naturforschung C-a Journal of Biosciences **37**(11-1): 1234-1239.

Yoshikawa, M., et al. (1998). "Activation of NF-kappa B by TNF-alpha or IL-1 fails to suppresses Fas-mediated apoptosis in human hepatoblastoma (HepG2) cells." Gastroenterology **114**(4): A1369-A1369.

Zarling, A. L., et al. (2000). "Phosphorylated peptides are naturally processed and presented by major histocompatibility complex class I molecules in vivo." Journal of Experimental Medicine **192**(12): 1755-1762.

Zarling, A. L., et al. (2006). "Identification of class I MHC-associated phosphopeptides as targets for cancer immunotherapy." Proceedings of the National Academy of Sciences of the United States of America **103**(40): 14889-14894.

Zeh, H. J., et al. (1999). "High avidity CTLs for two self-antigens demonstrate superior in vitro and in vivo antitumor efficacy." Journal of Immunology **162**(2): 989-994.

Zhong, S., et al. (2013). "T-cell receptor affinity and avidity defines antitumor response and autoimmunity in T-cell immunotherapy." Proceedings of the National Academy of Sciences of the United States of America **110**(17): 6973-6978.

Zhu, J. F. and W. E. Paul (2008). "CD4 T cells: fates, functions, and faults." Blood **112**(5): 1557-1569.

Zou, W. P., et al. (2004). "Specific recruitment of regulatory T cells fosters immune privilege in ovarian carcinoma." Faseb Journal **18**(4): A67-A67.

Zsiros, J., et al. (2010). "Successful Treatment of Childhood High-Risk Hepatoblastoma With Dose-Intensive Multiagent Chemotherapy and Surgery: Final Results of the SIOPEL-3HR Study." Journal of Clinical Oncology **28**(15): 2584-2590.

Zuniga-Pflucker, J. C. (2004). "Innovation - T-cell development made simple." Nature Reviews Immunology **4**(1): 67-72.

Appendix 1

NB IPSc protocols were adapted from those provided by the Vallier Group, Cambridge University. All tissue culture vessels, media, supplements obtained from Sigma unless stated otherwise.

A1.1. Feeder-dependent IPScs protocols

*For media recipes, please see chapter 2 materials and methods.

Preparation of feeder plates

Commercially available irradiated MEFs (IRR MEFs, GlobalStem, Cambridge BioScience, UK) were used.

Tissue culture plates were pre-coated with 0.1% gelatin. One vial of CF1 IRR MEFs from GlobalStem contains 4-5 $x10^6$ cells. These were rapidly thawed cells in a 37°C water bath, and transferred to a 50ml conical tube containing 10ml MEF media * and centrifuge at 200g for 4 min. Cells were washed and resuspended in DMEM/10% FCS (GibCo, UK). Vessels were then transferred into an incubator set at 37°C, 5% CO_2, for at least 24 hours prior to usage, but can be stored for up to 2 weeks.

Table S1: Densities for MEFs on Different Culture Dishes

Cell culture vessel	Surface area in mm^2	# of MEFs	Optimum Volume For Plating (ml)
Dishes/plates			
35mm plate	962	0.15×10^6	2
60mm plate	2.827	0.4×10^6	3
100mm plate	7.854	1.0×10^6	10
Multi-well plates			
6-well plate	962	0.15×10^6	2-5
12-well plate	401	0.05×10^6	0.5-2
24-well plate	200	0.025×10^6	0.5-1

Picking hIPScs

Picking of single IPScs colonies enables separation of clonal population of cells for further culture and propagation.

MEF media (DMEM/10% FCS) was aspirated from the appropriate number of plates which were washed with PBS x2. 0.5ml IPSc media* containing 10μM ROCK inhibitor/Y-27632 was added to each well. Using 20μl pipette set to 15μl each colony was encircled. Subsequently, these were divided into clumps of 200-300 cells and transferred to the prepared feeder plates. Cells were subsequently incubated overnight, and media topped up after 24 hours (without ROCK inhibitor).

Passaging hIPScs

Human induced pluripotent stem cells need to be passaged in order to avoid overgrowth and to maintain them in undifferentiated state.

Plates were washed x1 with D-PBS, following which equal volumes of collagenase and dispase were applied (1ml of each per well of a 6w plate). Cells were returned to an incubator for up to 1 hour, but monitored for evidence of loosening (visible curling or thickening of colonies around edges). 15ml falcons were prepared with fresh DMEM/F12 =5ml per falcon (Gibco, UK). Colonies were aspirated and added to a falcon – one well per falcon. The lid was applied and the tube inverted x1. Colonies were allowed to sediment and the media layer was gently aspirated. Cells were washed x1 with 7ml DMEM/F12 and again colonies allowed to sediment. Feeder plates were washed with PBS and 1ml of IPSc media was added per well (6w plate). Colonies were resuspended in IPSc media and transferred to the feeder plates.

Non-integrating method of reprogramming PBMC with Sendai Virus (SeV)

This protocol allows generation of integration-free IPScs from peripheral blood. Peripheral blood mononuclear cells (PBMCs) are cultured to expand the erythroblast (EB) population. They are then used to derive IPScs using four recombinant Sendai viral vectors, expressing the four reprogramming factors: OCT4, SOX2, KFL4 and c-MYC. LifeTechnologies CytoTune 2.0 kits were used. Standard protocol as described below:

Day –9: Plate peripheral blood mononuclear cells (PBMCs) at 5×10^6/ml in a 12-well plate in complete PBMC medium*.

Day –8 to –1: Replace half of the medium per well with fresh PBMC media (with cytokines)*

Day 0: Transduce the cells using the appropriate MOI as per the batch number and calculation on product website. Cells incubated overnight.

Day 1: Media completely aspirated from the wells and replaced with fresh complete PBMC medium* to remove the 2.0 Sendai reprogramming vectors. MEF feeder plates prepared as described above.

Day 3: Plate the transduced cells on MEF culture dishes in complete PBMC media without cytokines*.

Day 4–6: Media replaced completely on alternate days.

Day 7: Cells transitioned gradually onto IPSc media* by initially replacing half the PBMC media with complete IPSc medium.

Day 8: Complete media change performed and complete IPSc media* added

Day 9–28: Media changed daily.

A1.2 Validation methods: Detection of expression of endogenous pluripotency markers versus transgenes by RT-PCR

Media was aspirated from IPScs and cells were pelleted from one confluent well of a 6-well plate and lyse with 250 lysis buffer. RNA isolation was performed as per manufacturers

protocols (GenElute mammalian total RNA miniPrep kit, Sigma, UK). 500ng of DNase treated RNA for reverse transcription according to SuperScript(R)II Reverse Transcriptase manufactures protocol (Life Tech., UK).

Table S2: MasterMix for Q-PCR was prepared according to the table below:

Reagent	**Volume per well**
F primer [5µM]	0.6µl
R primer [5µM]	0.6µl
Sensi Mix (2x]	7.5µl
Nuclease free water	1.3µl
Total volume of the MasterMix	10µl

cDNA was diluted 30x in sterile water and 5µl of this mixture cDNA was mixed with 10µl of the MasterMix. The Q-PCR was run with primers set for detection.

Table S3: Endogenous genes encoding pluripotency markers

Primers for detection Sendai virus transgenes	**Sequence**	**Annealing Temp**	**Product size**
Oct3/4 (p) F	CCC GAA AGA GAA AGC GAA CCA G	55°C	483bp
Oct3/4 (p) R	AAT GTA TCG AAG GTG CTC AA	55°C	
Sox2 (p) F	ATG CAC CGC TAC GAC GTG AGC GC	55°C	451bp
Sox2 (p) R	AAT GTA TCG AAG GTG CTC AA	55°C	
Klf4 (p) F	TTC CTG CAT GCC AGA GGA GCC C	55°C	410bp
Klf4 (p) R	AAT GTA TCG AAG GTG CTC AA	55°C	
c-Myc (p) F	TAA CTG ACT AGC AGG CTT GTC G	55°C	532bp
c-Myc (p) R	TCC ACA TAC AGT CCT GGA TGA TGA TG	55°C	
SeV F	GGA TCA CTA GGT GAT ATC GAG C	55°C	181bp

In vitro differentiation of IPScs into three germ layers

In order to validate differentiation capacity of IPScs, *in vitro* differentiation of IPScs into three germ layers: endoderm, mesoderm, neuroectoderm must be performed.

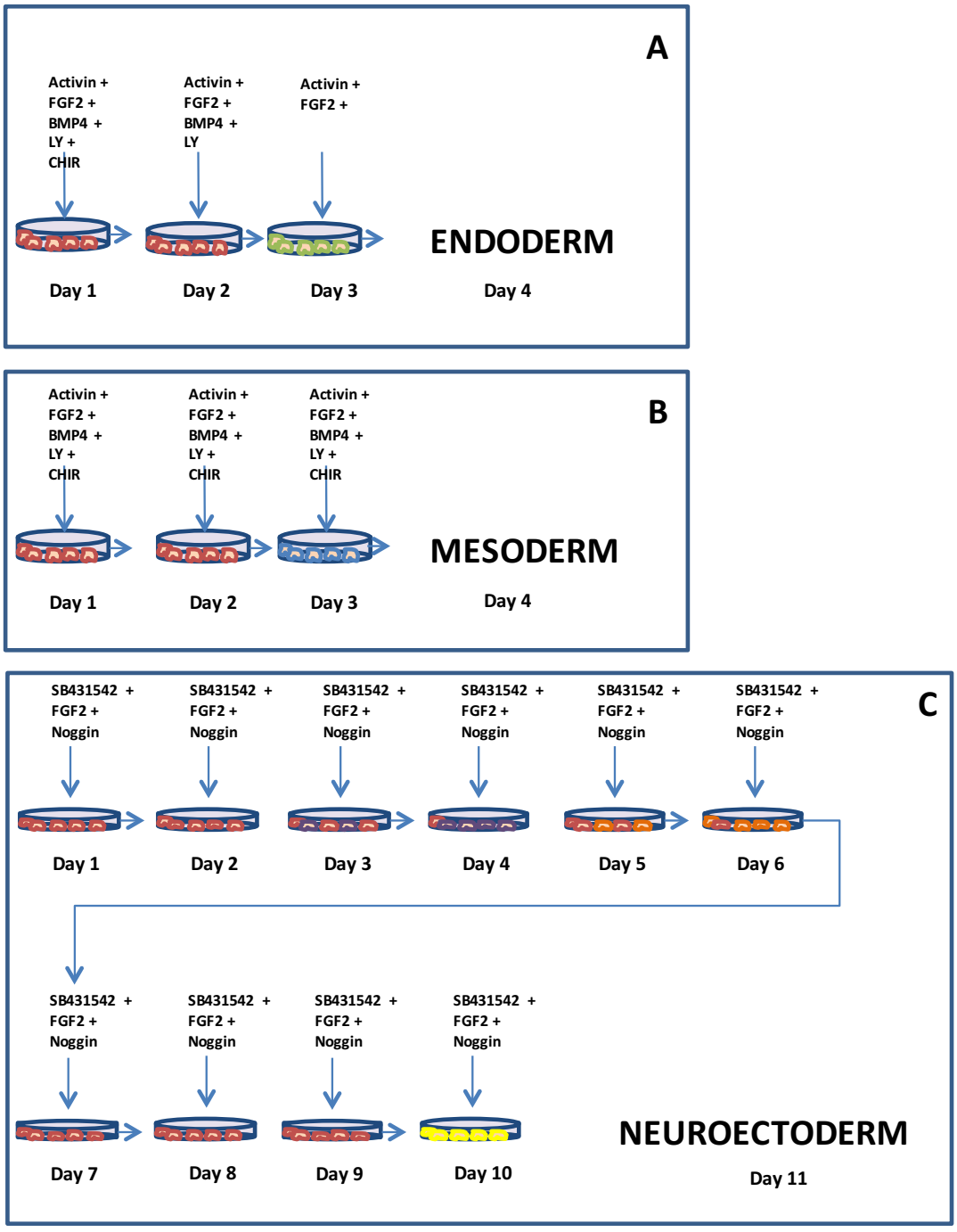

Fig.S1: Differentiation of iPSc into the three germ layers according to media supplementation. (A)Endoderm and (B)mesoderm have similar components but notably BMP4 is only required short term in endoderm but longer to differentiate cells to mesoderm. Mesoderm also requires the presence of LY and CHIR. (C)Neuroectoderm development is a lengthier process requiring 10 days of culturing in the presence of SB431542, FGF2 and Noggin in order to achieve differentiation.

Differentiation into Endoderm (fig. S1A)

Day 1 - after 24 hrs aspirate media and add 1ml per well of CDM-PVA containing:

10µl Activin [10µg/ml] /ml

20µl FGF2 [4µg/ml] /ml

1µl BMP4 [10µg/ml] /ml

1µl Ly [10mM] /ml

1µl CHIR [3mM] /ml

Day 2 - after 24 hrs aspirate media and add 1ml per well of CDM-PVA media containing:

10µl Activin [10µg/ml]/ml

20µl FGF2 [4µg/ml]/ml

1µl BMP4 [10µg/ml]/ml

1µl Ly [10mM]/ml

Day 3 - after 24 hrs aspirate medium and add 1ml per well of RPMI media containing:

10µl Activin [10µg/ml] /ml

20µl FGF2 [4µg/ml] /ml

After 24 hrs aspirate media and perform Q-PCR as described above.

Differentiation into Mesoderm (fig. S1B)

Day 1 - after 24 hrs aspirate media and add 1ml per well of 12-well plate of CDM-PVA containing:

10µl Activin [10µg/ml] /ml

5µl FGF2 [4µg/ml] /ml

1µl BMP4 [10µg/ml] /ml

1µl Ly [10mM] /ml

1.66µl CHIR [3mM] /ml

Change media daily for two more days

After 3 days of differentiation aspirate medium and validate with Q-PCR

Differentiation into Neurectoderm (fig. S1C)

After 24 hrs aspirate medium and add 1ml per well of 12-well plate CDM-PVA containing:

1µl SB [10µM]/ml

3µl FGF2 [4µg/ml] /ml

1.5µl Noggin [100µg/ml]/ml

Change medium daily for 10-12 days

After 10-12 days of differentiation aspirate medium and validate with Q-PCR

Detection of differentiation markers by immunostaining

Cells were fixed with 4% paraformaldehyde. Blocking solution was prepared by mixing 10ml D-PBS, 1ml Serum + 10µl Triton). Cells were covered with 0.5ml of D-PBS + 0.1% Triton X-100 per well of 12-well plate and incubated at room temperature for 20 minutes to one hour.

Primary Antibody Dilution was done in Dako Diluent (Cambridge, UK) according to the table below. 300µl of solution was added per well of 12-well plate (either 1% serum (or BSA), 0.1% Triton X-100 in D-PBS can be used for incubation with Primary Antibody). Blocking solution was aspirated and replaced by the Primary Antibody. Cells were incubated for 1 hour at room temperature. The Primary Antibody was removed and replaced by PBS. Cells were shaken for 5 minutes (gently) – table S4.

The Secondary Antibody Dilution was prepared as follows:

1-1000 > 4µl Ab - 4000µl (Dako Diluent) per 1well of 12-well plate and multiply by number of wells to be stained

1-2000 > 2µl Ab - 4000µl (Dako Diluent) per 1well of 12-well plate and multiply by number of wells to be stained

PBS was aspirated from the cells and the Secondary Antibody was added. Cells were incubated in the dark at room temperature for up to 2 hours.

The Secondary Antibody was aspirated and replaced with PBS. In order to visualize cells (DNA) DAPI was added in first wash (DAPI 1µl -10 000µl PBS). Cells were gently shaken for 2 minutes and PBS aspirated – this step was repeated x2. Cells were then visualized using confocal microscope.

Table S4: Antibodies used for pluripotency marker detection

Primary Ab	**Clonality/animal where Antibody raised**	**Dilution**	**Supplier/ Cat Number**
Pluripotency markers			
hNanog	PolyIgG Goat	1:100	R&D AF1997
hSox2	PolyIgG Goat	1:200	R&D AF2018
hTRA-1-60	MonoIgM Mouse	1:100	Santa Cruz sc-21705
hOct-3/4 (C-10)	MonoIgG Mouse	1:100	Santa Cruz sc-5279

Alkaline Phosphatase staining

10% neutral formalin buffer with formaldehyde was prepared (all reagents Sigma, UK unless stated otherwise)

Na2HPO4 16g

Na2HPO4:H2O 4g

In cold room as stock

Dist water 1l

Formaldehyde added to make final 4% solution.

Substrate solution was prepared as follows:

a) 0.0025g Napthol As Mx-PO4 (freezer) in 100ul N,N, DMF (dimethylforamide)
   12.5ml 0.2M pH8.3 Tris-HCl

b) 0.015g Fast red violet (freezer)
   12.5ml distilled water

'a' and 'b' were added together and filtered using Whatman Filter 1 paper.

The cells were washed x1 in cold PBS and fixed in 10% cold NFB for 15 minutes. They were washed x1 in distilled water (cold). Water was replaced and cells left on ice for 15 minutes. Following this the water was aspirated and the substrate solution added. Cells were incubated in the dark for up to 45 minutes. Following this substrate was aspirated and cells washed x1 with water. Cells visualised by light microscope.

A1.3. Additional figures for chapter 4

Figures S2-S7 represent FACS data obtained from healthy donors, showing response of T-cells to phosphopeptides. They supplement data presented in Fig. 4.7-4.10.

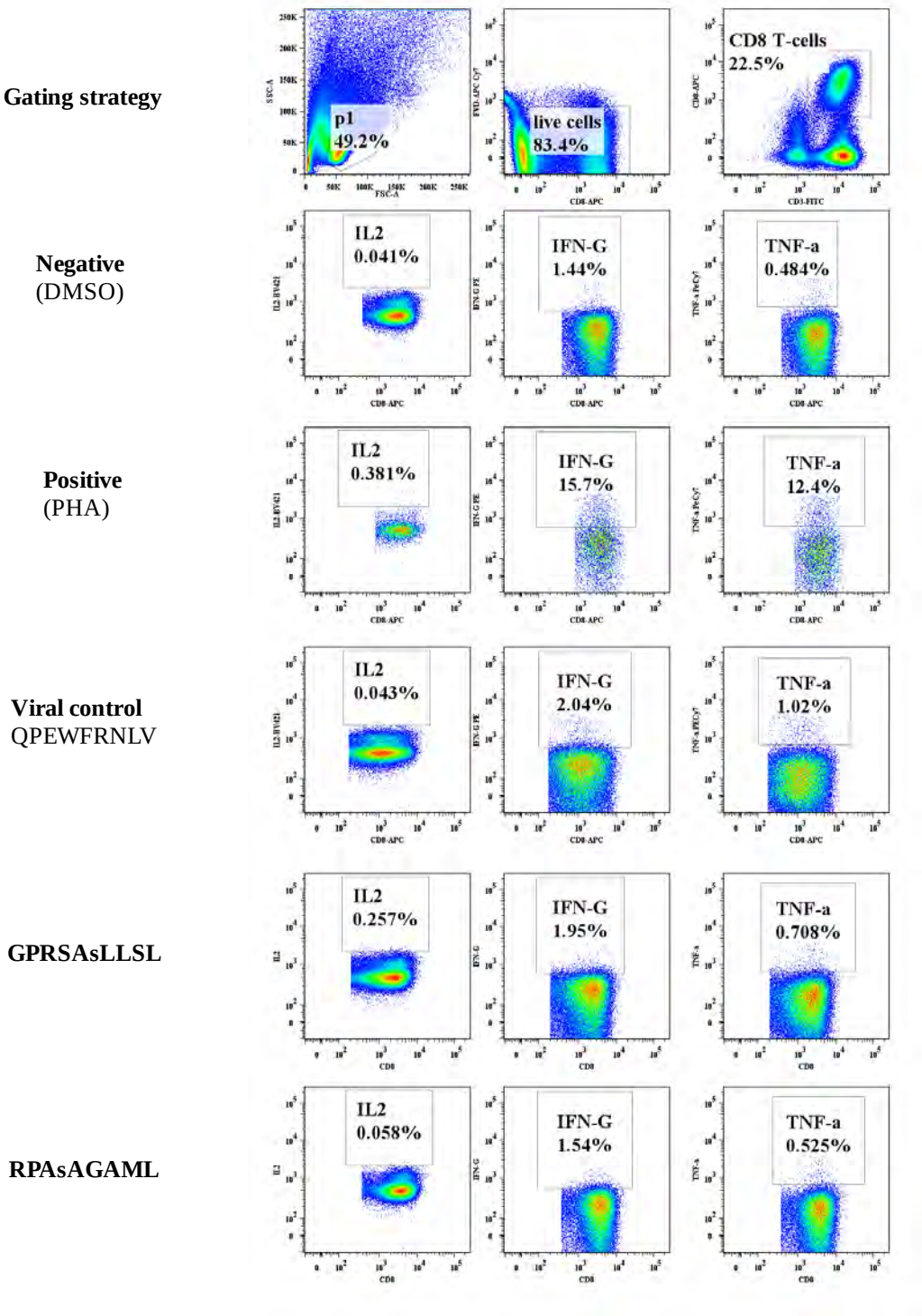

Fig. S2A: Phosphopeptide responses in Healthy Donor P(day 0)
PBMC's were generated from healthy donors and responses of these to tumour-associated phosphopeptides were then assessed using an ICS assay. The FACS plots depicted show the gating strategy employed and representative IFNγ ,TNFα, and IL-2 responses (from left to right). NB. IFN-G = IFNγ, TNF-a = TNFα,.

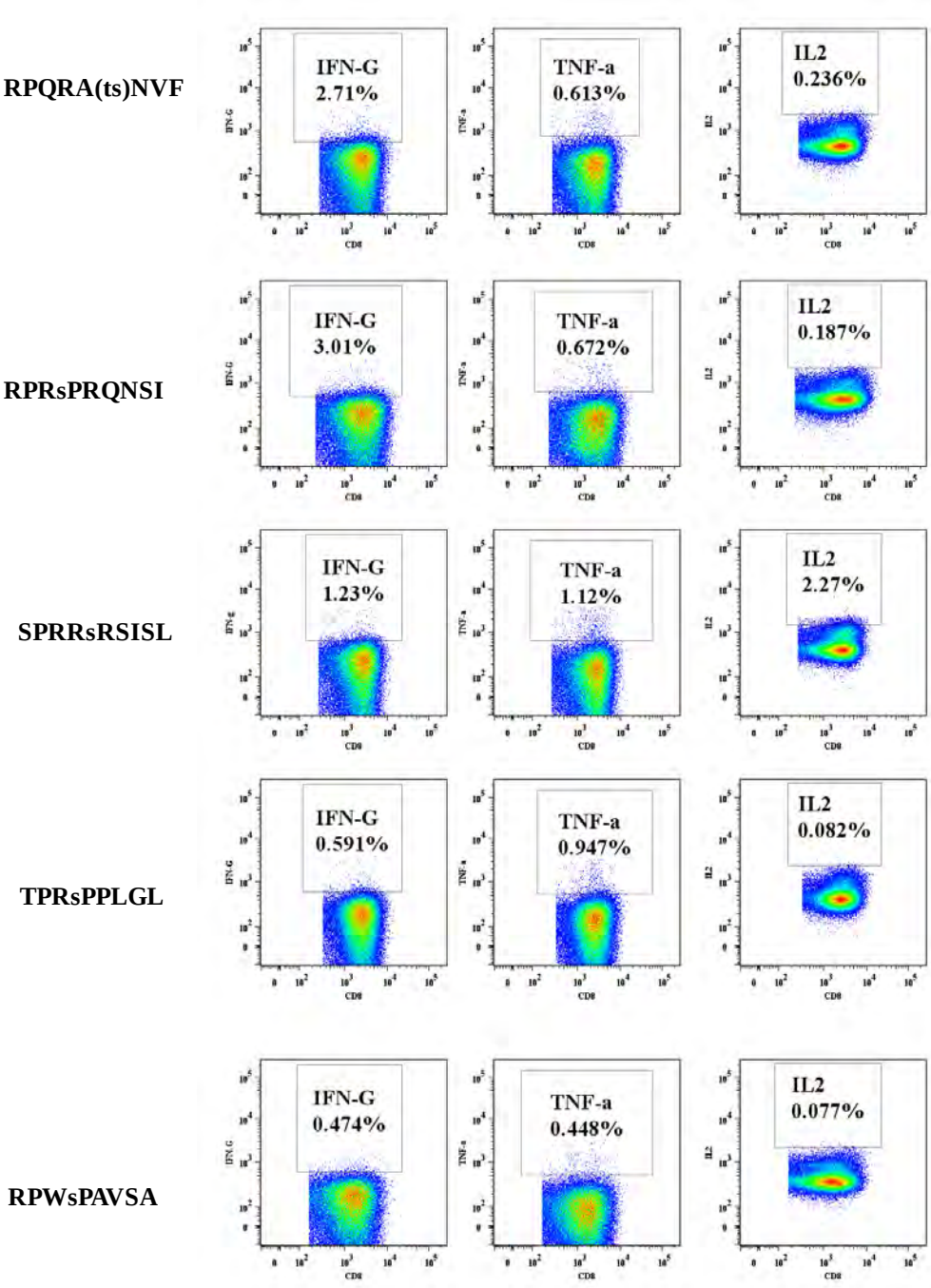

Fig. S2A:Phosphopeptide responses in Healthy Donor P(day 0) cont..
PBMC's were generated from healthy donors and responses of these to tumour-associated phosphopeptides were then assessed using an ICS assay. The FACS plots depicted show the gating strategy employed and representative IFNγ ,TNFα, and IL-2 responses (from left to right). NB. IFN-G = IFNγ, TNF-a = TNFα,

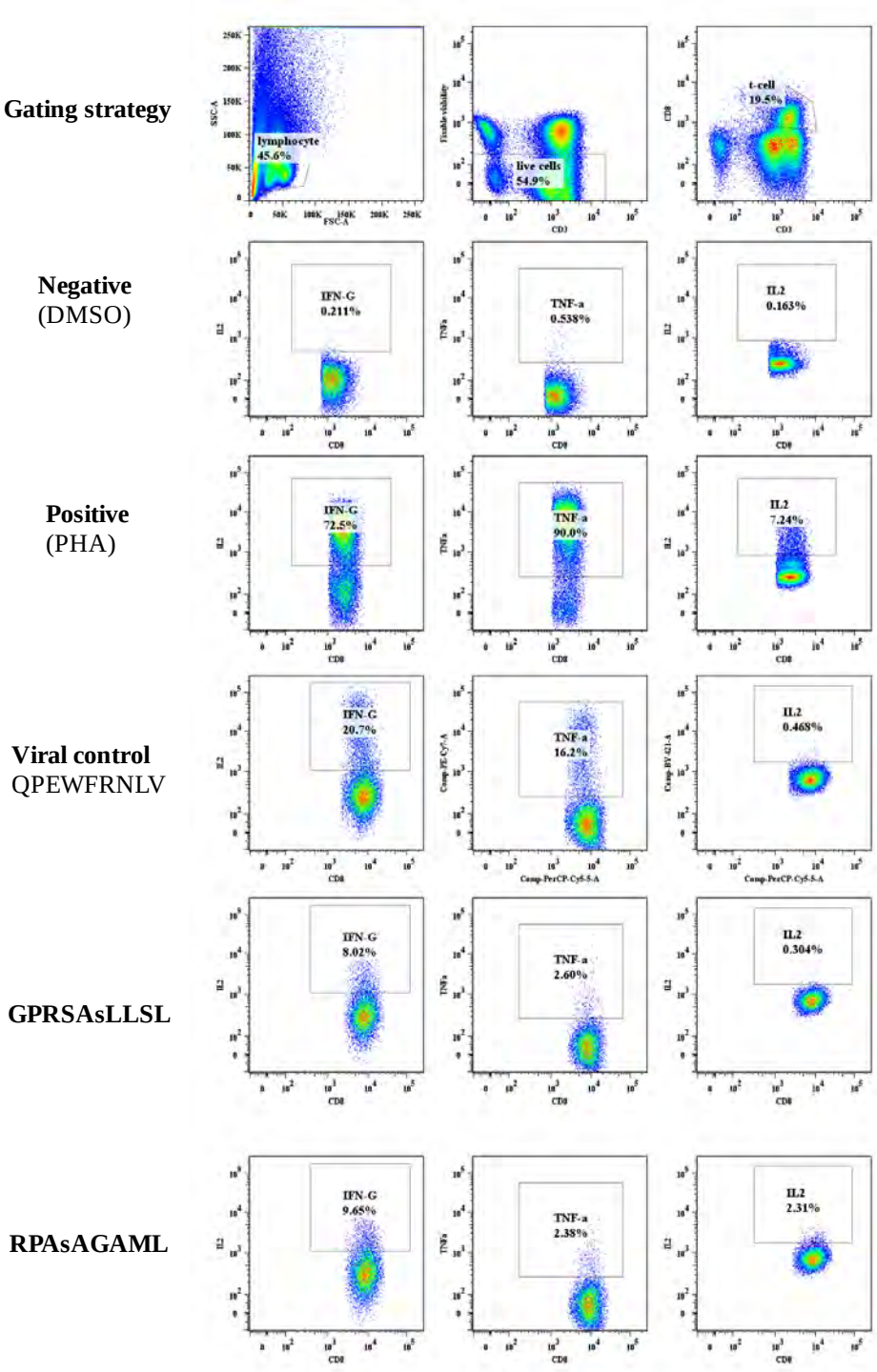

Fig. S2B:Phosphopeptide responses in Healthy Donor P (day 7)
PBMC's were generated from healthy donors and responses of these to tumour-associated phosphopeptides were then assessed using an ICS assay. The FACS plots depicted show the gating strategy employed and representative IFNγ ,TNFα, and IL-2 responses (from left to right). NB. IFN-G = IFNγ, TNF-a = TNFα,

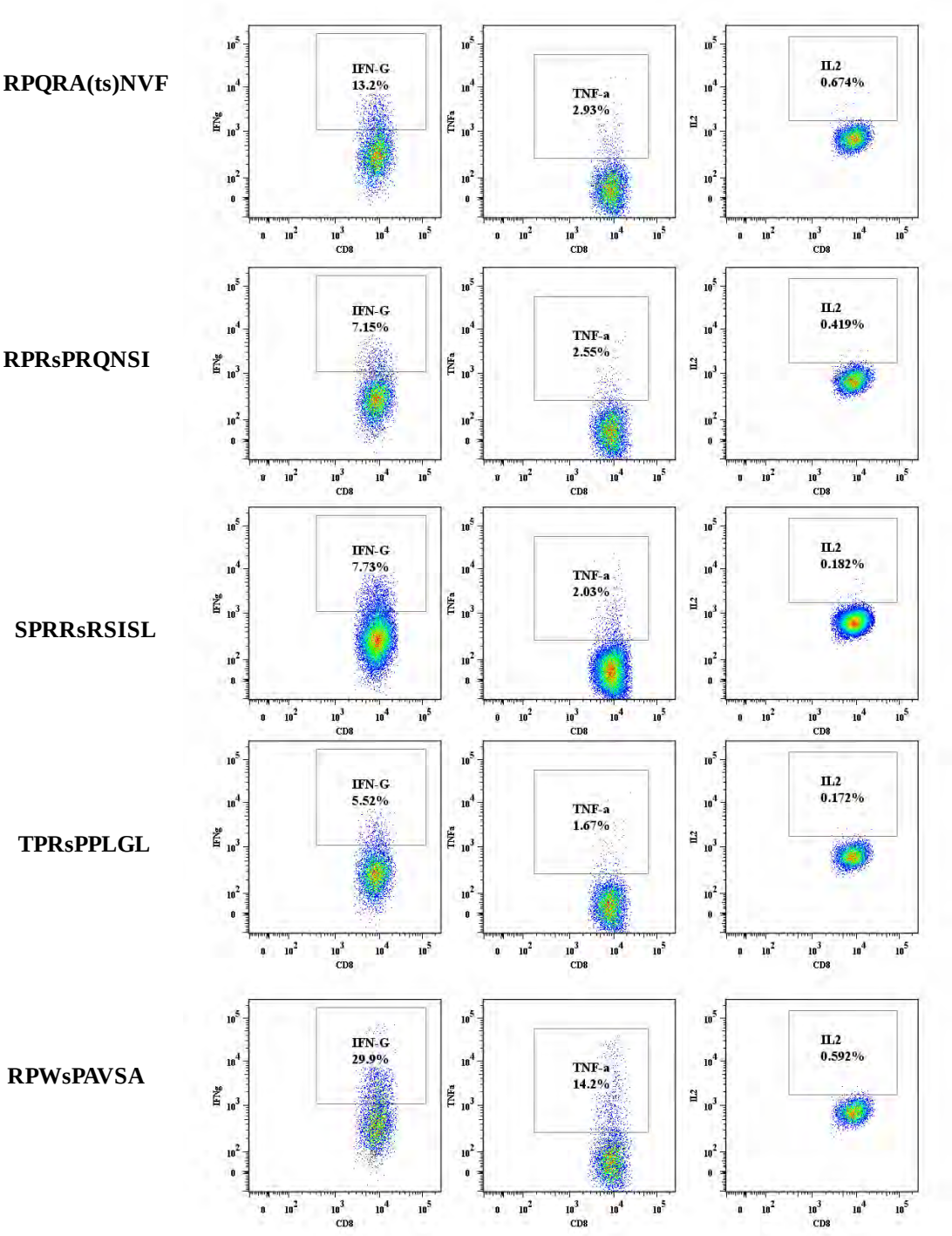

Fig. S2B:Phosphopeptide responses in Healthy Donor P(day 7) cont..
PBMC's were generated from healthy donors and responses of these to tumour-associated phosphopeptides were then assessed using an ICS assay. The FACS plots depicted show the gating strategy employed and representative IFNγ ,TNFα, and IL-2 responses (from left to right). NB. IFN-G = IFNγ, TNF-a = TNFα,

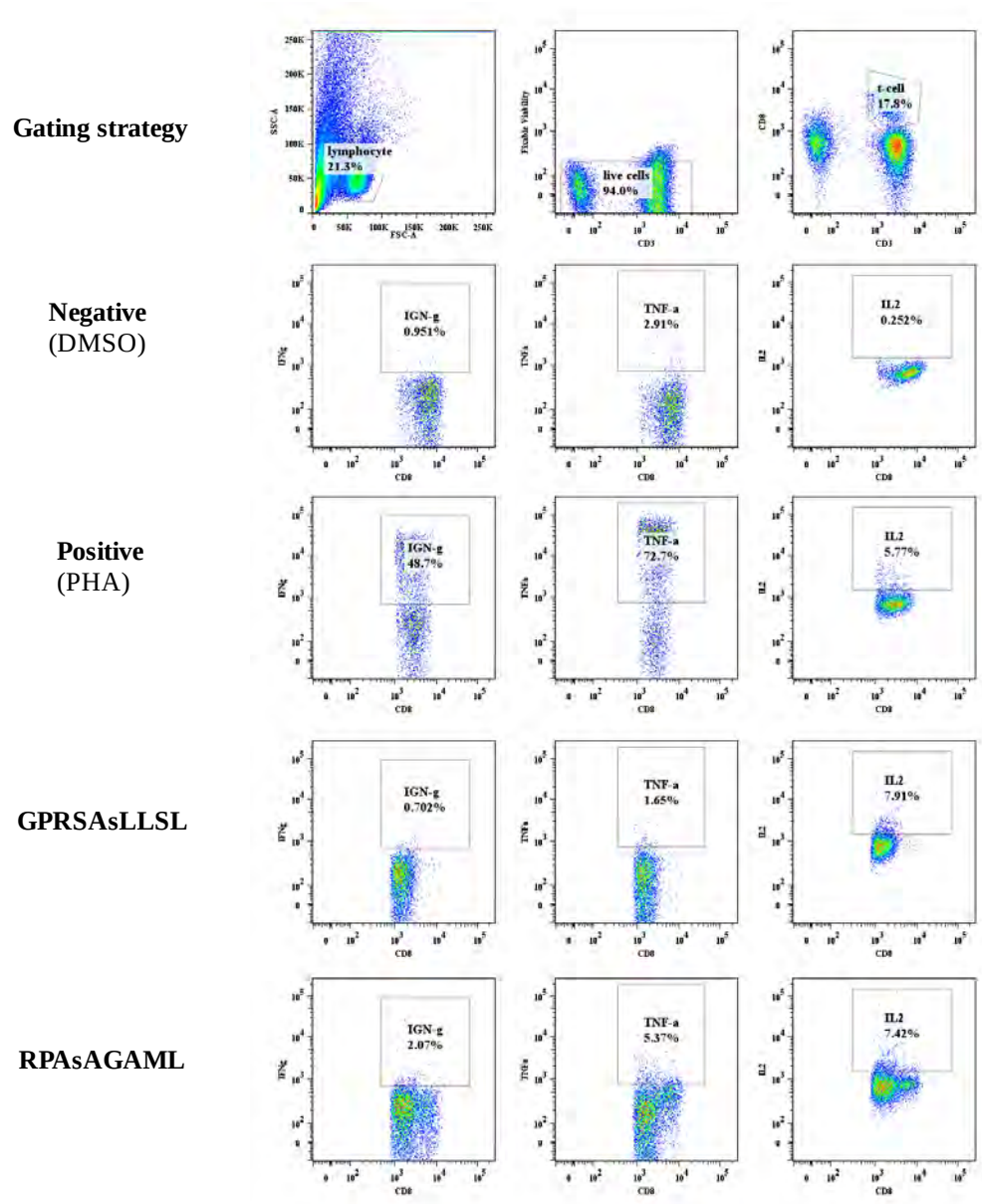

Fig. S3:Phosphopeptide responses in Healthy Donor C (day 7)
PBMC's were generated from healthy donors and responses of these to tumour-associated phosphopeptides were then assessed using an ICS assay. The FACS plots depicted show the gating strategy employed and representative IFNγ ,TNFα, and IL-2 responses (from left to right). NB no Viral response obtained. NB. IFN-G = IFNγ, TNF-a = TNFα.

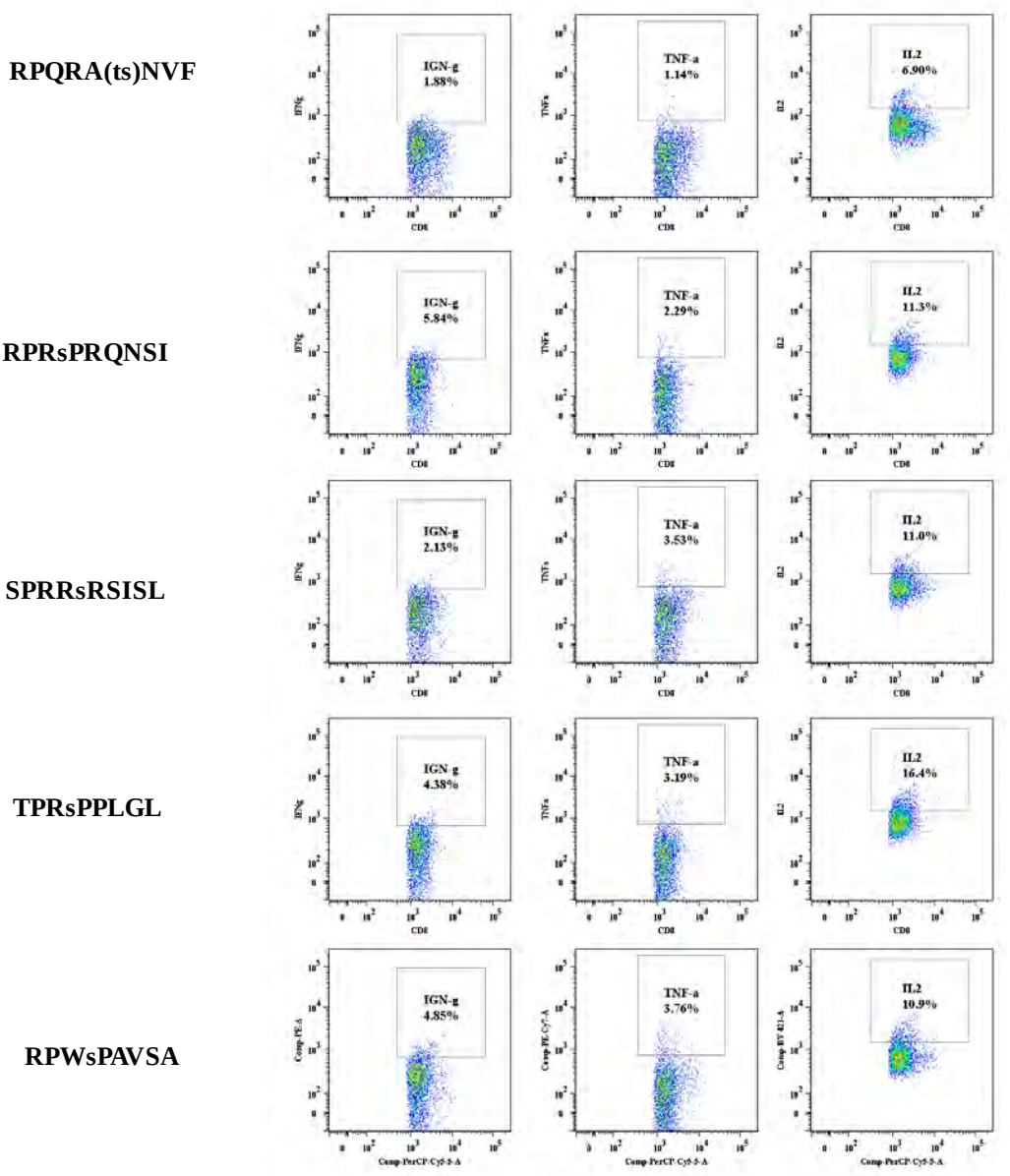

Fig. S3:Phosphopeptide responses in Healthy Donor C (day 7) cont..
PBMC's were generated from healthy donors and responses of these to tumour-associated phosphopeptides were then assessed using an ICS assay. The FACS plots depicted show the gating strategy employed and representative IFNγ ,TNFα, and IL-2 responses (from left to right). NB. IFN-G = IFNγ, TNF-a = TNFα.

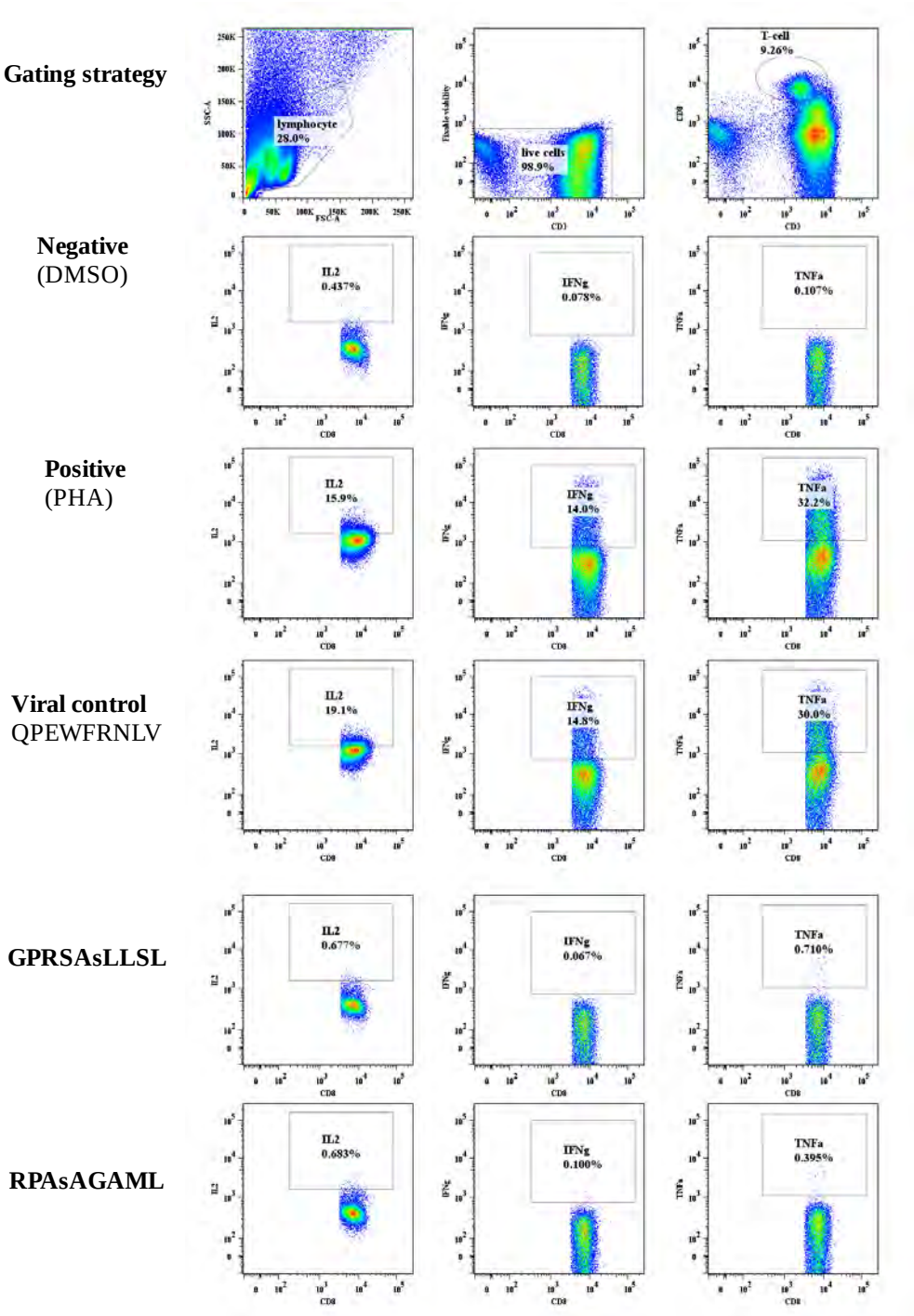

Fig. S4:Phosphopeptide responses in Healthy Donor O (day 7)
PBMC's were generated from healthy donors and responses of these to tumour-associated phosphopeptides were then assessed using an ICS assay. The FACS plots depicted show the gating strategy employed and representative IFNγ ,TNFα, and IL-2 responses (from left to right). NB. IFN-G = IFNγ, TNF-a = TNFα.

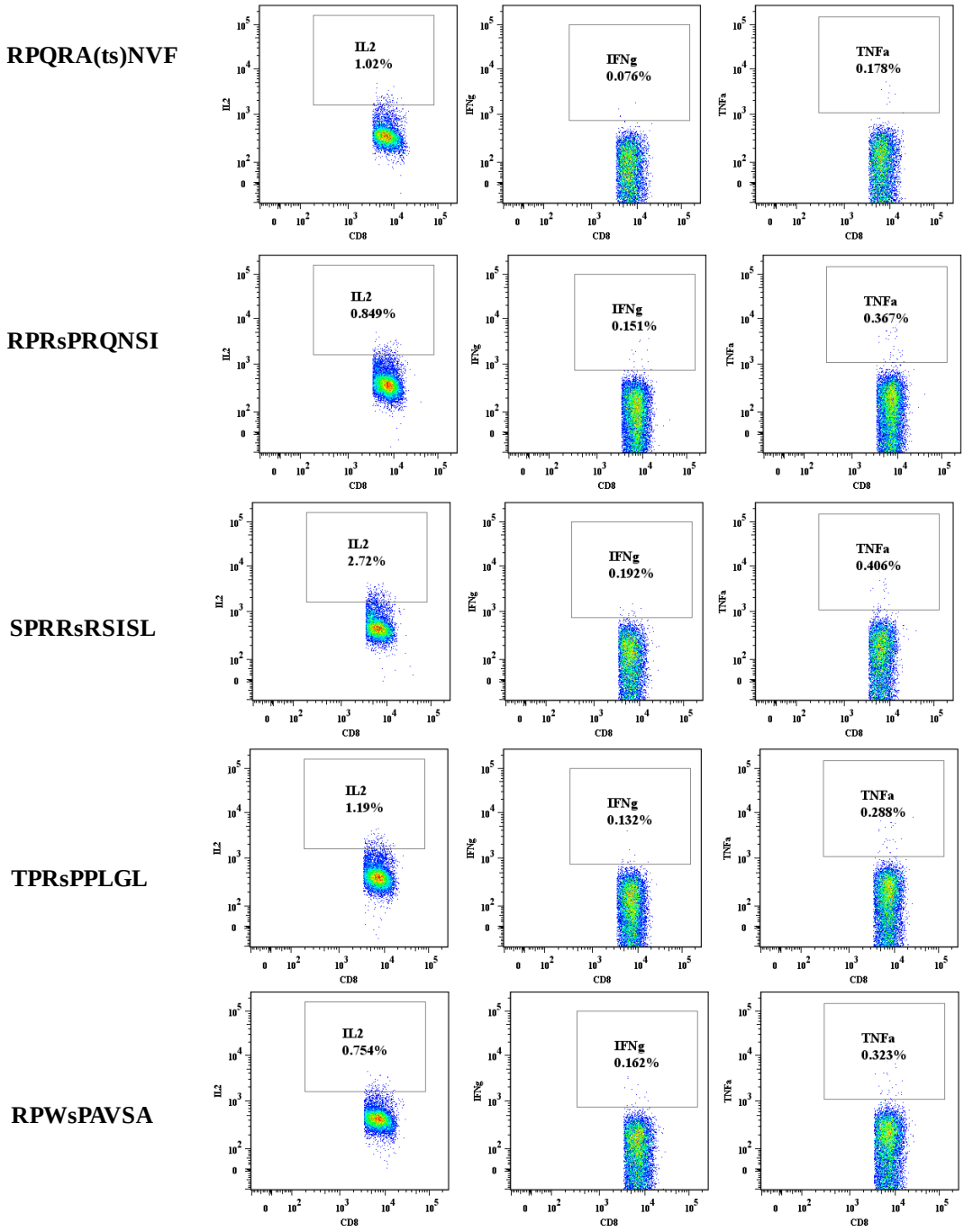

Fig. S4:Phosphopeptide responses in Healthy Donor O (day 7) cont..
PBMC's were generated from healthy donors and responses of these to tumour-associated phosphopeptides were then assessed using an ICS assay. The FACS plots depicted show the gating strategy employed and representative IFNγ ,TNFα, and IL-2 responses (from left to right). NB. IFN-G = IFNγ, TNF-a = TNFα.

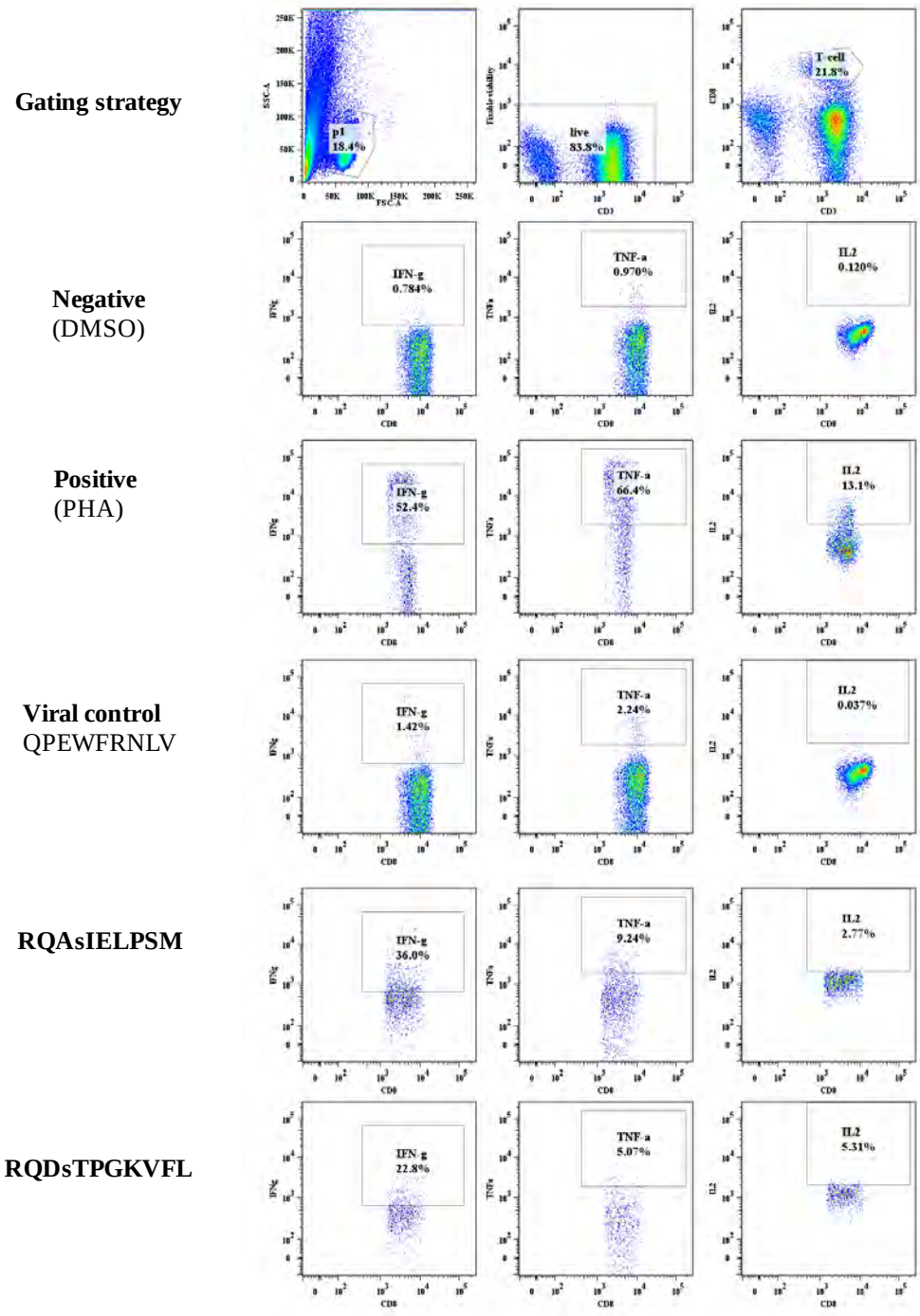

Fig. S5: Phosphopeptide A2 responses in Healthy Donor H (day 7)
PBMC's were generated from healthy donors and responses of these to tumour-associated phosphopeptides were then assessed using an ICS assay. The FACS plots depicted show the gating strategy employed and representative IFNγ ,TNFα, and IL-2 responses (from left to right). NB. IFN-G = IFNγ, TNF-a = TNFα.

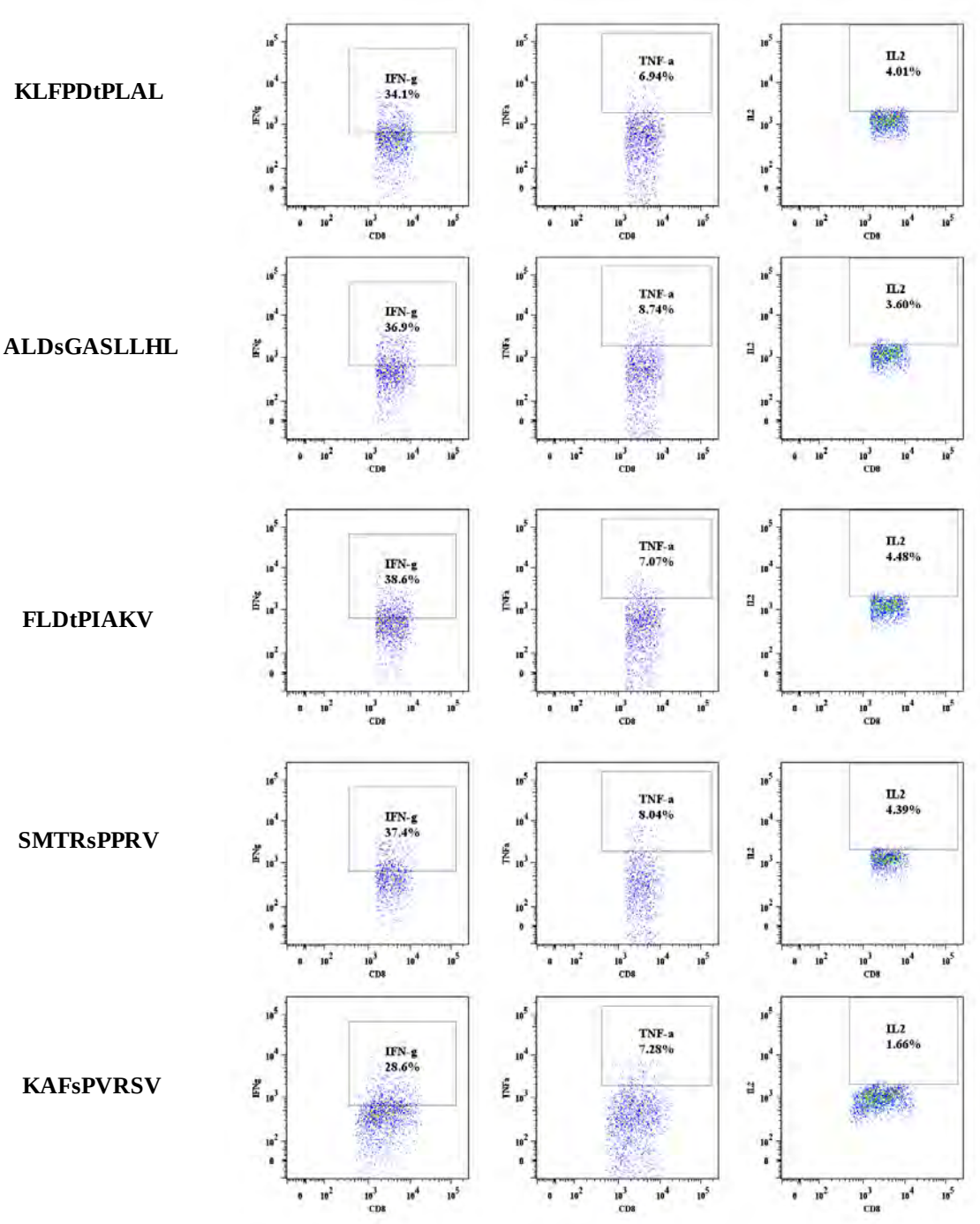

Fig. S5:Phosphopeptide responses in Healthy Donor H(day 7) cont..
PBMC's were generated from healthy donors and responses of these to tumour-associated phosphopeptides were then assessed using an ICS assay. The FACS plots depicted show the gating strategy employed and representative IFNγ ,TNFα, and IL-2 responses (from left to right). NB. IFN-G = IFNγ, TNF-a = TNFα.

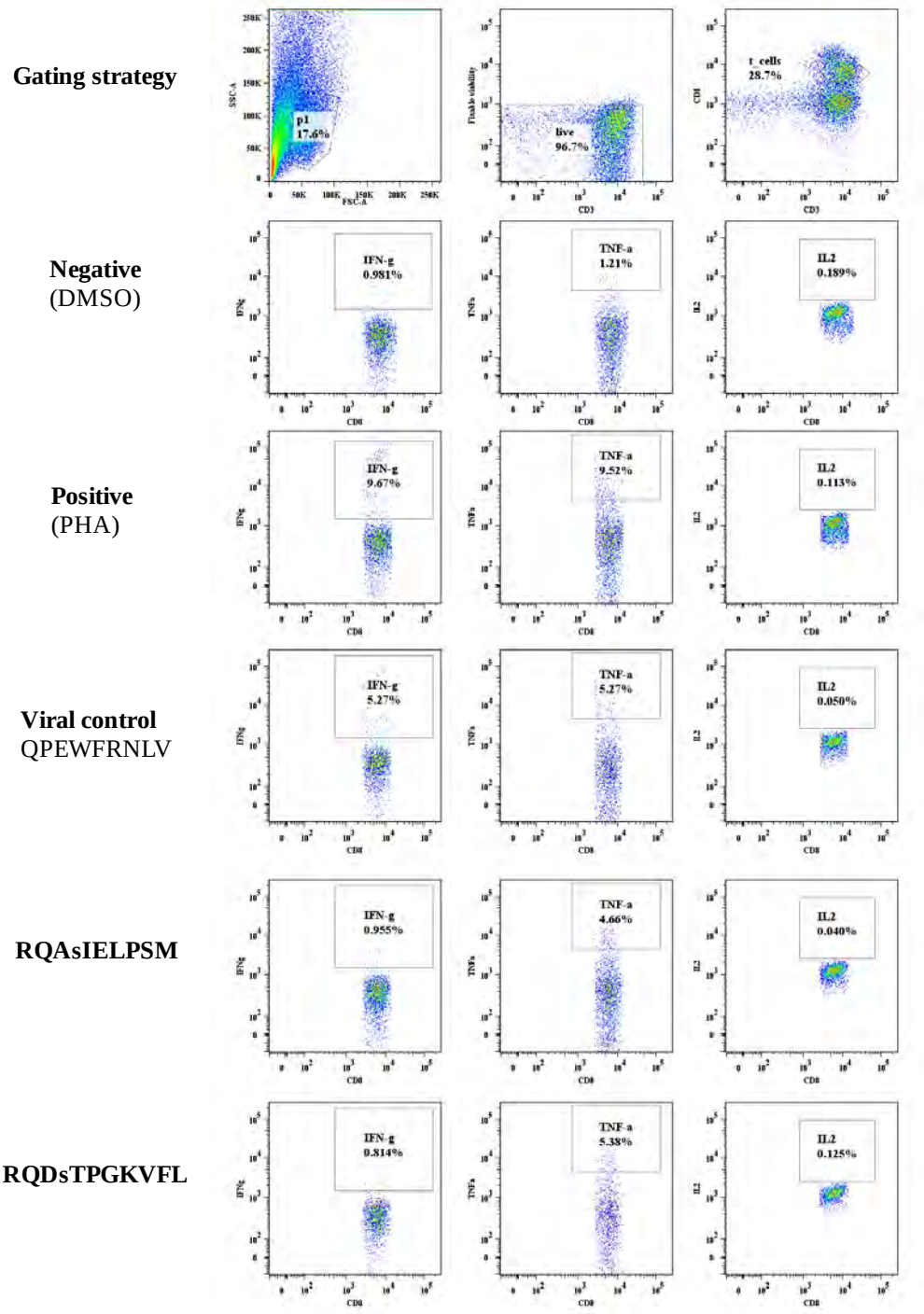

Fig. S6:Phosphopeptide A2 responses in Healthy Donor S (day 7)
PBMC's were generated from healthy donors and responses of these to tumour-associated phosphopeptides were then assessed using an ICS assay. The FACS plots depicted show the gating strategy employed and representative IFNγ ,TNFα, and IL-2 responses (from left to right). NB. IFN-G = IFNγ, TNF-a = TNFα.

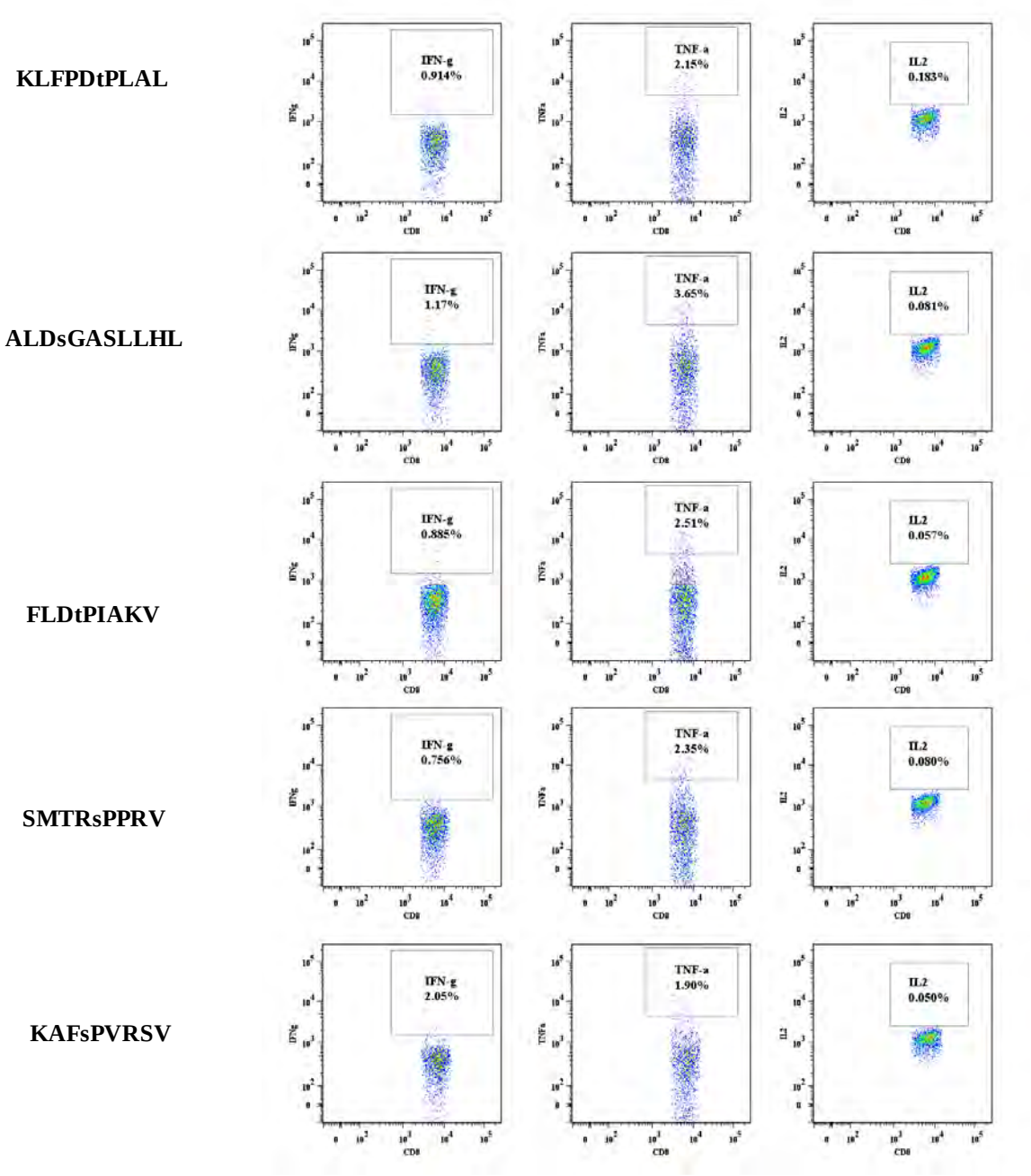

Fig. S6:Phosphopeptide responses in Healthy Donor S(day 7) cont..
PBMC's were generated from healthy donors and responses of these to tumour-associated phosphopeptides were then assessed using an ICS assay. The FACS plots depicted show the gating strategy employed and representative IFNγ ,TNFα, and IL-2 responses (from left to right). NB. IFN-G = IFNγ, TNF-a = TNFα.

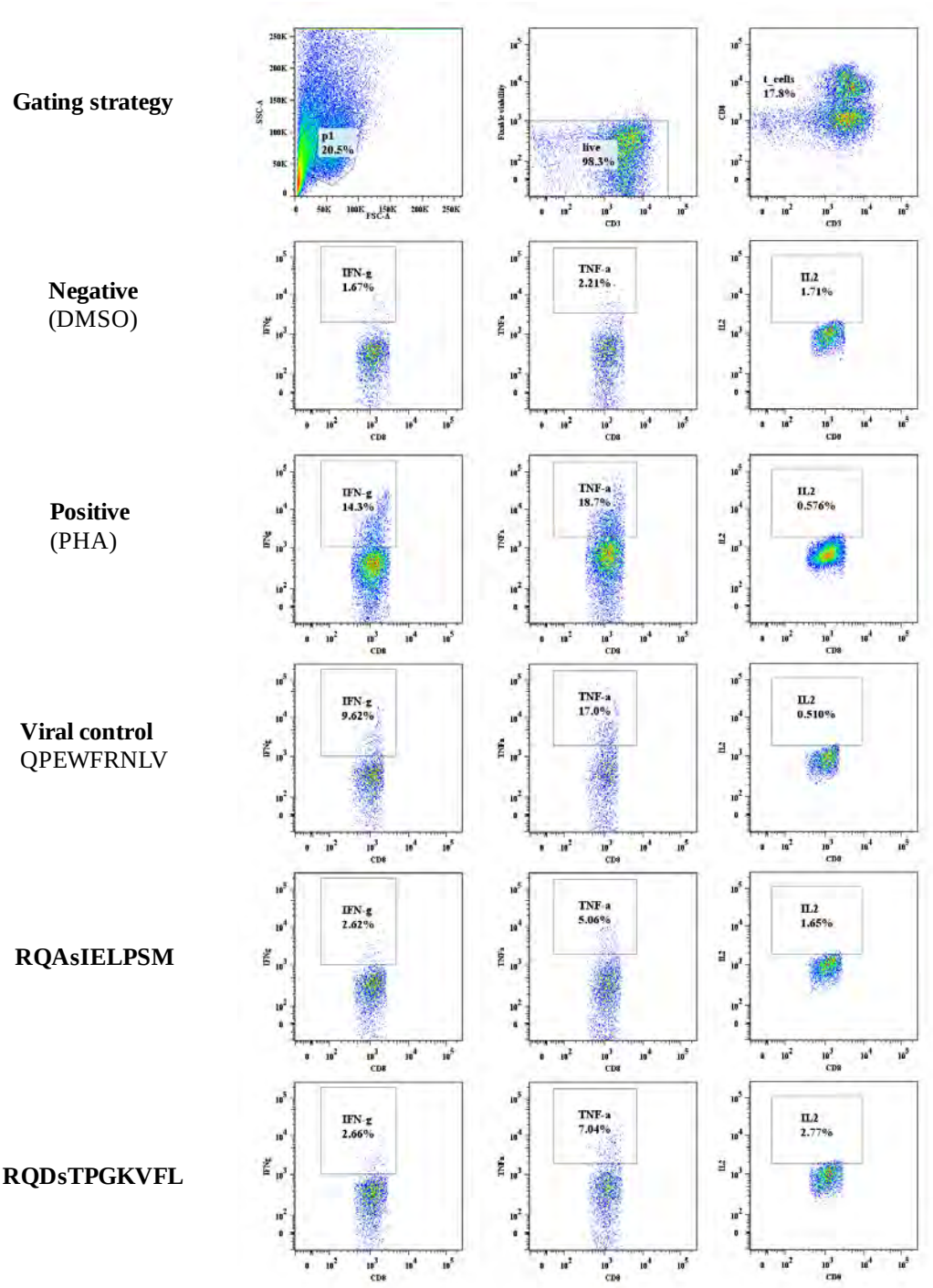

Fig. S7:Phosphopeptide A2 responses in Healthy Donor N (day 7)
PBMC's were generated from healthy donors and responses of these to tumour-associated phosphopeptides were then assessed using an ICS assay. The FACS plots depicted show the gating strategy employed and representative IFNγ ,TNFα, and IL-2 responses (from left to right). NB. IFN-G = IFNγ, TNF-a = TNFα.

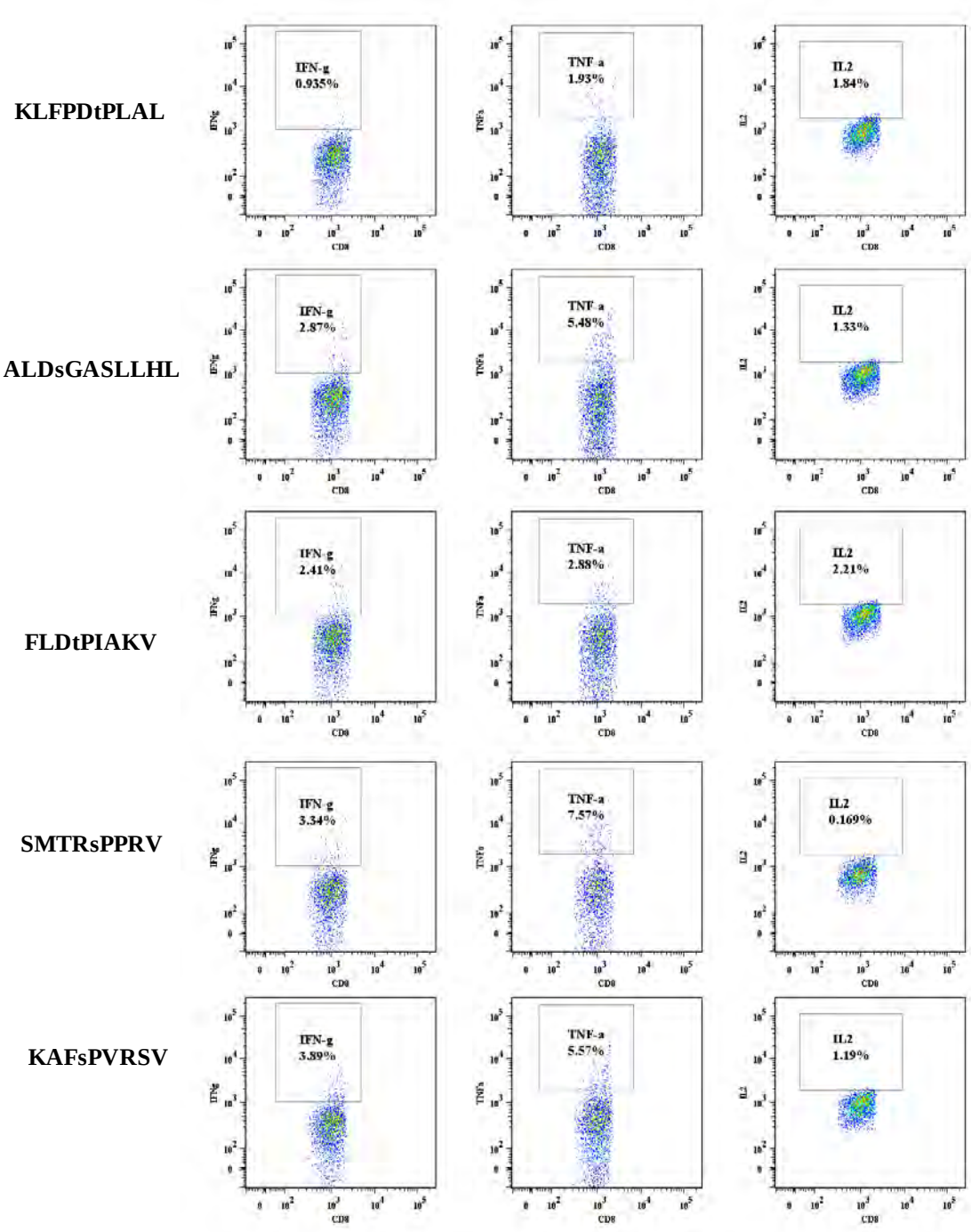

Fig. S7:Phosphopeptide responses in Healthy Donor N (day 7) cont..
PBMC's were generated from healthy donors and responses of these to tumour-associated phosphopeptides were then assessed using an ICS assay. The FACS plots depicted show the gating strategy employed and representative IFNγ ,TNFα, and IL-2 responses (from left to right). NB. IFN-G = IFNγ, TNF-a = TNFα.

A1.5. Calculation of TCID50

volume per well:	1000	µl
replicate wells per dilution:	3	
dilution factor:	1: 10	
dilution in the first well:	1: 100	

dilution	number of *wells with clearing >50%*
1:100 (10^-2)	3
1:1000 (10^-3)	3
1:10000 (10^-4)	3
1:100000 (10^-5)	2
1:1000000 (10^-6)	2
1:10000000 (10^-7)	2
1:100000000 (10^-8)	2
1:1000000000 (10^-9)	1
1:10000000000 (10^-10)	1
1:100000000000 (10^-11)	0
1:1000000000000 (10^-12)	0
1:10000000000000 (10^-13)	0

last complete infection at dilution: *10^-4*

TCID50/ml:		3.16E+05
	+sd	6.20E+05
	-sd	2.09E+05
FFU/ml (aprx.):		2.18E+05
	+sd	4.28E+05
	-sd	1.45E+05

with FFU aprx. 0.69 x TCID50

Excel calculator courtesy of Dr Marco Binder, Dept. Infectious Diseases, Molecular Virology, Heidelberg University. TCID50 is calculated by the Spearman & Kärber algorithm as described in Hierholzer & Killington (1996), Virology Methods Manual, p. 374.

$TCID50_{stock\ (Hugo)}$	$=3.16 \times 10^{6}$ /ml
$MOI_{stock\ (Hugo)}$	=2.24

Appendix 2: Research Outputs

Presentations/Posters

2017 **5000 Livers International Symposium**, Birmingham - Capturing T-cell Receptors. A potential new modality for targeting hepatic tumours and Post-Transplantation Lymphoproliferative Disease – poster presentation

2016 **BSPGHAN**, Bristol - Capturing T-cell Receptors. A potential new modality for targeting hepatic tumours and Post-Transplantation Lymphoproliferative Disease (PTLD) – oral presentation and award of Alex Mowatt Prize for hepatology

2016 **ESPGHAN**, Greece - Capturing T-cell Receptors. A potential new modality for targeting hepatic tumours and Post-Transplantation Lymphoproliferative Disease (PTLD) – poster Presentation and award of Young Investigator Award and Poster prize.

2015 **ESPGHAN**, Netherlands - Capturing T-cell Receptors. A potential new modality for targeting hepatic tumours and Post-Transplantation Lymphoproliferative Disease (PTLD) – poster Presentation

2014 **EASL** International Liver Congress 2014, London - GeneChip: Identifying Incidence Of Inherited Metabolic Disorders In Patients With Infantile Liver Disease – oral presentation

2013 **AASLD**, Washington, USA – Annual meeting – (1) Long term outcome of paediatric patients 15 years after liver transplantation – poster presentation. (2) The use of hIPSc in treatment of metabolic diseases affecting the liver – poster presentation. (3) GeneChip: Identifying Incidence Of Inherited Metabolic Disorders In Patients With Infantile Liver Disease – oral presentation.

Awards and Prizes

2017: ESPGHAN Transplant School prize, Bergamo, Italy

2016: Alex Mowatt Hepatology Prize BSPGHAN

2016: ESPGHAN Young Investigator Award

2016: ESPGHAN poster award

2014: EASL Young Investigator Award